

November 2020

## Methods for 1,2-Cis-Selective O-Glycosylation and Synthesis of an A. baumannii Lipooligosaccharide Core Disaccharide

Ashley Fulton

*Louisiana State University and Agricultural and Mechanical College*

Follow this and additional works at: [https://digitalcommons.lsu.edu/gradschool\\_dissertations](https://digitalcommons.lsu.edu/gradschool_dissertations)

 Part of the [Organic Chemistry Commons](#)

---

### Recommended Citation

Fulton, Ashley, "Methods for 1,2-Cis-Selective O-Glycosylation and Synthesis of an A. baumannii Lipooligosaccharide Core Disaccharide" (2020). *LSU Doctoral Dissertations*. 5396.  
[https://digitalcommons.lsu.edu/gradschool\\_dissertations/5396](https://digitalcommons.lsu.edu/gradschool_dissertations/5396)

This Dissertation is brought to you for free and open access by the Graduate School at LSU Digital Commons. It has been accepted for inclusion in LSU Doctoral Dissertations by an authorized graduate school editor of LSU Digital Commons. For more information, please contact [gradetd@lsu.edu](mailto:gradetd@lsu.edu).

# METHODS FOR 1,2-C/S-SELECTIVE O-GLYCOSYLATION AND SYNTHESIS OF AN *A. BAUMANNII* LIPOOLIGOSACCHARIDE CORE DISACCHARIDE

A Dissertation

Submitted to the Graduate Faculty of the  
Louisiana State University and  
Agricultural and Mechanical College  
in partial fulfillment of the  
requirements for the degree of  
Doctor of Philosophy

in

The Department of Chemistry

by  
Ashley Fulton  
B.S., Xavier University of Louisiana, 2011  
December 2020

*I dedicate this dissertation to my beautiful, sweet, smart, and feisty little girl, Tinsley Olivia. I do not know where I would be without you. You have given my life so much purpose, love and laughter. All that I do is for you and I am forever grateful that I was chosen to be your mother.*

## **ACKNOWLEDGEMENTS**

To my advisor, Dr. Justin Ragains, you have been such a patient, dedicated, and uplifting person to have in my corner. You have been a listening ear and an encouraging voice. In times of complete self-doubt, you were the person to restore my confidence as a chemist. Thank you for being the advisor I needed during this journey. Thank you to my committee members: Dr. Graça Vicente, Dr. George Stanley, and Dr. Yongchang Kwon for your encouragement during my time at LSU.

To my mentor, Dr. Gloria Thomas, you are not only my mentor, but my sister in Delta. I thank you for your guidance and for always being the person I can go to when times are at their hardest. I could never repay you for all the help you have given me with Tinsley. You were determined to see me through and I am forever grateful.

To my parents, Joanne and Wayne Lockhart. Pops, you are the greatest example of a go-getter and one of the reasons why I strive so high. Mommy, you are the most giving and loving person I know. I would not have made it without our daily talks. Thank you for believing in me even when I didn't believe in myself. I am not afraid to reach for the stars because I know you two will always have my back.

To my fiancé, Brady Skinner, I thank you for your reassurance and elaborate motivational talks. Your love brings me so much joy and your laughter is infectious. I am so thankful that I found you.

To the Ragains' group, past and present, thank you for practice talks, support and friendships. I appreciate all of you.

Thank you to my LSU family: Stephanie, Milcah, RJ, Justin, Shaniqua, Jamira, and Kendra. Thank you for being there for me no matter what. From babysitting to venting, I

am so grateful for what you all have done for me. Dr. Stephanie Vaughan, thank you for being my person, you constantly push me (because you're a pusher) and I appreciate all that you do for me and Tinsley. Thank you to my family and friends for being my cheerleaders when I needed it.

## TABLE OF CONTENTS

ACKNOWLEDGEMENTS .....	iii
LIST OF FIGURES .....	vii
LIST OF SCHEMES .....	ix
LIST OF ABBREVIATIONS.....	xii
ABSTRACT.....	xiv
CHAPTER 1. ORGANIC THIN FILM GROWTH ON AU(111) SURFACES USING PHOTOREDOX CATALYSIS.....	1
1.1. Introduction to Organic Thin Film Surface Modification .....	1
1.2. Methods of Surface Modification.....	2
1.3. The use of Fluoroarenes and Aryl Iodides for Thin Film Formation.....	3
1.4. Methods for Characterization .....	4
1.5. Research Significance.....	7
1.6. Results and Discussion .....	7
1.7. Conclusion .....	14
1.8. Experimental.....	15
CHAPTER 2. AN OVERVIEW OF O-GLYCOSYLATION .....	19
2.1. Importance of O-Glycosylation.....	19
2.2. Glycosylation Mechanistic Pathways and Stereochemical Factors .....	20
2.3. Anomeric Effect .....	22
2.4. Solvent Effect.....	23
2.5. Glycosyl Acceptors .....	25
2.6. Glycosyl Donors.....	26
2.7. Conclusion .....	33
CHAPTER 3. ORTHOGONALITY OF 4-(4-METHOXYPHENYL)-3- BUTENYLTHIOGLYCOSIDES IN O-GLYCOSYLATION.....	34
3.1. Introduction .....	34
3.2. Results and Discussion .....	37
3.3. Conclusion .....	41
3.4. Experimental.....	41
CHAPTER 4. NEW METHODS FOR 1,2-C/S-SELECTIVE O-GLYCOSYLATION .....	48
4.1. Introduction .....	48
4.2. Results and Discussion .....	49
4.3. Conclusion .....	58
4.4. Experimental.....	58

CHAPTER 5. NEW STUDIES ON THE TOTAL SYNTHESIS OF AN <i>ACINETOBACTER</i> <i>BAUMANNII</i> LIPOOLIGOSACCHARIDE CORE PENTASACCHARIDE .....	71
5.1. Introduction .....	71
5.2. Results and Discussion .....	73
5.4. Future Work .....	79
5.5. Experimental .....	80
APPENDIX A. COPYRIGHT RELEASE FOR CHAPTER 3.....	93
APPENDIX B. SPECTRAL DATA FOR COMPOUNDS FOUND IN CHAPTER 3 .....	94
APPENDIX C. SPECTRAL DATA FOR COMPOUNDS FOUND IN CHAPTER 4.....	101
APPENDIX D. SPECTRAL DATA FOR COMPOUNDS FOUND IN CHAPTER 5.....	116
LIST OF REFERENCES .....	134
VITA .....	146

## LIST OF FIGURES

1.1.	Face-centered Cubic Crystal (111) Index.....	2
1.2.	Photocatalysts Used .....	4
1.3.	Particle Lithography using a Mesosphere Mask .....	5
1.4.	Basic Schematic of Atomic Force Microscopy .....	6
1.5.	A thin film formed on Au(111) generated with an initial concentration of $10^{-1}$ M <b>2</b> after 30 minutes of irradiation. Nanopores were produced using immersion particle lithography .....	8
1.6.	A thin film formed on Au(111) generated with an initial concentration of $10^{-1}$ M <b>1</b> , after 30 minutes of irradiation. Nanopores were produced using immersion particle lithography .....	9
1.7.	Grazing-angle FT-IRRAS spectrum of pentafluorobenzene thin film. Strong peak at around 1300 nm indicates C-F stretching. ....	11
1.8.	XPS spectrum of pentafluorobenzene thin film. Shows binding energy with respect to intensity of gold, carbon, and oxygen peaks. ....	12
1.9.	TOF-SIMS Spectrum of Pentafluorobenzene Thin Film. ....	12
1.10.	A thin film formed on Au(111) generated with an initial concentration of $10^{-1}$ M <b>2</b> after 30 minutes of irradiation. Nanopores were produced using immersion particle lithography .....	14
1.11.	A Typical Au(111) Photografting Reaction Set-Up.....	17
2.1.	Dipole Moment Theory (DMT) and Molecular Orbital Theory (MOT) to explain the Anomeric Effect .....	23
2.2.	Nucleophilicity of Glycosyl Acceptors .....	26
2.3.	Protected Glycosyl Donors .....	26
3.1.	Structures of Glycosyl Donors .....	36
4.1.	Orientation of Glycosidic Linkages .....	48
4.2.	Desired Glycosyl Thioglycoside Donor.....	55
4.3.	Glycosylation Substrate Scope.....	58



5.1.	LOS Core Oligosaccharide of <i>A. baumannii</i> .....	73
5.2.	Retrosynthesis of LOS-Conjugate Vaccine .....	73
5.3.	Optimization of Disaccharide Synthesis .....	77
5.4.	Nap Ether Cleavage.....	78

## LIST OF SCHEMES

1.1	Proposed Hexafluorobenzene Grafting to Gold Substrate .....	3
1.2	Aryl Radicals from Aryl Iodides Grafting onto Gold Substrate .....	4
2.1	Glycosidic Linkages .....	20
2.2	Glycosylation Mechanistic Pathways .....	21
2.3	Neighboring Group Participation to Generate <i>beta</i> -Anomer .....	22
2.4	Solvent Effects of Acetonitrile and 1,4-dioxane .....	24
2.5	Solvent effects using QM and MD.....	25
2.6	TBAI-DIEA Activation of Glycosyl Iodide.....	28
2.7	Mechanism for Trichloroacetimidate Donor Activation Using <i>p</i> -Toluenesulfonic Acid.....	29
2.8	AgOTf promotion of Thioimidates.....	30
2.9	Thioglycoside Activation Using Methylating Compound.....	31
2.10	Visible-Light Promoted Activation of Selenoglycoside.....	31
2.11	Electrochemical Glycosylation Approach.....	32
2.12	Acid and Light Promoted O-Glycosylation .....	32
2.13	<i>In Situ</i> Formation of Glycosyl Sulfonates for the synthesis of $\beta$ -D-rhamnopyranosides .....	33
3.1	Chemoselective Activation Strategy and Selective Activation Strategy.....	35
3.2	Visible Light Promoted O-Glycosylation.....	36
3.3	Acid-Catalyzed O-Glycosylation.....	37
3.4	Synthesis of Tetraacetyl MBTG.....	37
3.5	Synthesis of Alkyl Iodide and Mercapto Glucose.....	38
3.6	Final Steps for Synthesis of C <sub>6</sub> MBTG Acceptor .....	39

3.7	Synthesis of TCAI Donor .....	40
3.8	Orthogonal Synthesis of Trisaccharide .....	40
4.1	Methods of 1,2- <i>cis</i> -O-Glycoylation .....	49
4.2	Hypothesized Mechanism of 1,2- <i>cis</i> -O-Glycoside Formation from MBTG .....	50
4.3	Benzylidenation and Benzylation of $\alpha$ -D-glucopyranoside .....	51
4.4	Benzylidene Removal and Acetylation.....	51
4.5	Direct Displacement of Bromine with Thiol .....	52
4.6	Synthesis of 3,4,6-triacetyl-2-O-benzyl MBTG .....	52
4.7	Glycosylations using 3,4,6-triacetyl-2-O-benzyl MBTG .....	53
4.8	Nifantiev Glycosylation using Acetate (EWG).....	53
4.9	Boons use of Lewis Base and EWG for 1,2- <i>cis</i> -selectivity .....	54
4.10	Strategy for 1,2- <i>cis</i> -Selectivity using EWG and LB.....	54
4.11	Synthesis of 2,3-di-O-benzyl Thioglycoside.....	55
4.12	Instillation of EWGs.....	56
4.13	Glycosylations Using Thioglycosides Containing EWGs.....	56
4.14	Turning Thioglycoside Donor to TCA Donor .....	56
4.15	Synthesis of PFT Containing Imidate Donors.....	57
5.1	Synthesis of Galactosamine Donors .....	75
5.2	Pilot Glycosylations using MBTG and MPTG .....	76
5.3	Synthesis of Thioglycoside Donor .....	76
5.4	Glycosylation of Disaccharide .....	78
5.5	Synthesis of Diol Acceptor.....	79
5.6	Glycosylation of Disaccharide .....	79

5.7	Future Route to Glycosyl Acceptor.....	80
-----	--	----

## LIST OF ABBREVIATIONS

$^1\text{H}$	Proton NMR
$^{13}\text{C}$	Carbon NMR
$^{19}\text{F}$	Fluorine NMR
AFM	Atomic Force Microscopy
DBU	1,8-Diazabicycloundec-7-ene
DDQ	2,3-Dichloro-5,6-dicyano-1,4-benzoquinone
DIPEA	<i>N,N</i> -Diisopropylethylamine
DMAP	4-Dimethylaminopyridine
DMF	<i>N,N</i> -Dimethylformamide
DMT	Dipole Moment Theory
DTBMP	2,6-di-tert-butyl-4-methylpyridine
EDA	Electron Donor Acceptor
FT-IRRAS	Fourier Transfer-Infrared Reflection-Absorption Spectroscopy
GlcNAcA	<i>N</i> -acetyl-D-glucosaminuronic acid
HRMS	High Resolution Mass Spectrometry
HSQC	Heteronuclear Single Quantum Coherence NMR
IR	Infrared
Kdo	3-deoxy-D-manno-oct-2-ulosonic acid
LED	Light Emitting Diode
LG	Leaving Group
LOS	Lipooligosaccharide
LPS	Lipopolysaccharide

MBTG	4-(4-methoxyphenyl)-3-butenylthioglycoside
MPTG	4-(4-methoxyphenyl)-4-pentenylthioglycoside
MOT	Molecular Orbital Theory
NGP	Neighboring Group Participation
NBS	<i>N</i> -bromosuccinimide
NIS	<i>N</i> -iodosuccinimide
NMR	Nuclear Magnetic Resonance
PFTA	<i>N</i> -Phenyl trifluoroacetimidate
PFP	Perfluoropropionate
PFT	Perfluorotoluene
PG	Protecting Group
SET	Single Electron Transfer
TBAF	Tetra- <i>n</i> -butylammonium fluoride
TBAI	Tetrabutylammonium Iodide
TCA	Trichloroacetimidate
TFA	Trifluoroacetate
TLC	Thin Layer Chromatography
TMSI	Trimethylsilyl Iodide
TOF-SIMS	Time-of-Flight Secondary Ion Mass Spectrometry
Troc-Cl	2,2,2-trichloroethyl chloroformate
XPS	X-Ray Photoelectron Spectroscopy

## ABSTRACT

This dissertation focuses on the formation of organic thin films on gold surfaces and synthesis of oligosaccharides. Chapter one, is a brief introduction on the utility of thin films, as well as ways to characterize thin films, as well as, a report on the attempt to form organic thin films on Au(111) surfaces using photoredox catalysis.

Glycoconjugates on cell surfaces serve as important mediators of intercellular recognition, adhesion, and viral infection. Due to the significant role that glycoconjugates play on the surface of cells, oligosaccharide synthesis is of great interest. Chapter two, is an extensive review of oligosaccharide synthesis, its importance, and glycosylation methods. There are several methods to form complex oligosaccharides; however, chapter three focuses on the orthogonal synthesis of a trisaccharide using temperature control.

The main challenge in the synthesis of biologically relevant oligosaccharides is the development of stereoselective glycosylation reactions. Methods to form the 1,2-*trans* glycosidic linkages (beta) have been developed with the help of neighboring group participation of acyl protecting groups in the C<sub>2</sub> position. However, protocols for selective synthesis of 1,2-*cis* glycosidic linkages (alpha) has proven to be difficult due to low yields and poor selectivity. To circumvent these difficulties, protecting group manipulation has been employed to form 1,2-*cis* glycosidic linkages through a S<sub>N</sub>2-like mechanism. Electron withdrawing groups have shown to play an important role in aiding in the formation of 1,2-*cis* linkages. Thus, in chapter four, methods to selectively form 1,2-*cis* linkages using thioglycosides and acetimidates armed with varying electron withdrawing groups is discussed.

Chapter five focuses on the application of oligosaccharide synthesis with the development of a glycoconjugate vaccine for *Acinetobacter baumannii*. *A. baumannii* is a common cause of infections associated with ICU residence, traumatic injury, mechanical ventilation, and neurosurgery. Vaccine development is an important preventative measure due to the increasing antibiotic resistance of *A. baumannii* strains. The proposed vaccine consists of a pentasaccharide portion of an *A. baumannii* lipooligosaccharide to be conjugated to a carrier molecule. Progress toward the synthesis of the pentasaccharide portion of the proposed glycoconjugate vaccine is discussed in this chapter.



# CHAPTER 1. ORGANIC THIN FILM GROWTH ON AU(111) SURFACES USING PHOTOREDOX CATALYSIS

## 1.1. Introduction to Organic Thin Film Surface Modification

The chemical modification of surfaces, or surface chemistry, has been a major topic of interest in materials science, medicine, and biotechnology since the 1990s.<sup>1</sup> Surface modification is the use of organic molecules as a protective layer to prevent the surface from changing adversely. A real world example of this is the coating on pots and pans where an organic thin film adheres to the metal surface to prevent sticking and corrosion.<sup>2</sup> Organic thin films are produced by molecules, with specific functionalities, that attach through various mechanisms to surfaces.

Organic thin films are common in surface chemistry as they prevent corrosion<sup>3</sup>, fouling<sup>4</sup>, and other oxidative processes<sup>5</sup> by providing a barrier at the surface. Both functionality and thickness of organic thin films can be modified, resulting in their implementation as important components of biosensors<sup>6</sup>, thin film transistors<sup>7</sup>, and medical devices<sup>8</sup>. For instance, chemically robust thin films can withstand physical and chemical stress aiding in the advancement of sensor technology.<sup>9</sup> Thin films that are resistant to oxidation, i.e. thin films on gold, aid in the advancement of corrosion and fouling resistant technologies.

Organic thin film growth has been studied on transition metals, carbon, and silicon surfaces.<sup>10</sup> The crystalline nature of gold makes it an advantageous surface on which to study organic thin film growth. Figure 1.1 depicts the (111) index arrangement within the plane. Au(111) is a well-defined gold surface with few defects, and is known to be the smoothest and most stable; therefore, it serves as an excellent substrate for organic thin films.

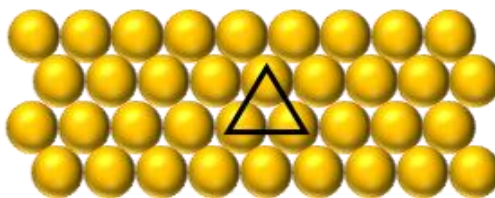


Figure 1.1. Face-centered Cubic Crystal (111) Index. The black triangle represents the (111) index.

## 1.2. Methods of Surface Modification

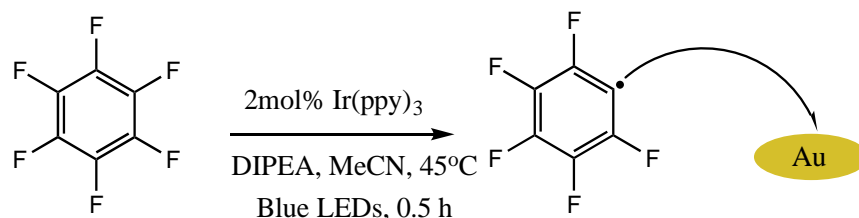
There are several techniques that can be used to generate thin films, such as self-assembled monolayer (SAM)<sup>11</sup> deposition and electrografting<sup>1</sup>. Although SAMs consist of a stable thin layer, they do not allow for multiple layers to be formed, which can increase the propensity for corrosion and fouling.<sup>12</sup> Electrografting allows for covalent bonding to the surface through single electron transfer (SET) from an organic molecule to an anode to form a radical that covalently binds to the surface.<sup>1</sup> To circumvent the use of invasive tools used in electrografting, visible-light photocatalysis can be used to achieve SET to the organic molecule. Visible-light photoredox catalysis can also allow for multiple layers to be formed.

Traditionally, visible-light photoredox catalysis has been used as a means to synthesize small organic molecules.<sup>13</sup> With this technique, metal complexes are used to convert visible light into chemical energy to induce single-electron or energy transfer to and from organic substrates. This process often induces the generation of carbon-centered radicals that can be used for the synthesis of organic compounds. These carbon-centered radicals have the ability to bond to a number of surfaces to form organic thin films.<sup>8</sup> In particular, Au(111) is used in the formation of thin films derived from aryl radicals.<sup>14</sup>

### 1.3. The use of Fluoroarenes and Aryl Iodides for Thin Film Formation

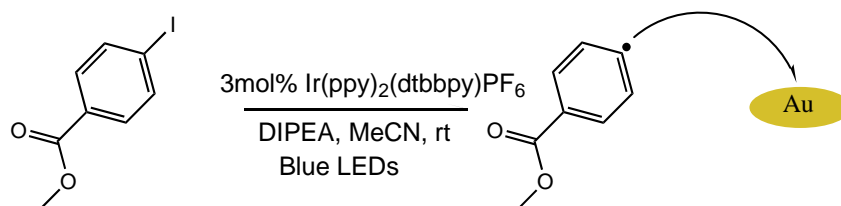
In 2014, the Ragains group demonstrated that aryl radicals produced from arenediazonium salts using visible-light photoredox catalysis could attach to gold surfaces to generate robust polyphenylene multilayered thin films.<sup>15</sup> Although the resultant thin films are robust, diazonium salts are unstable, unamenable to multistep synthesis, decompose over a period of days or weeks at low temperature, and graft spontaneously.<sup>16</sup> To by-pass these problems, this work focuses on fluoroarenes and aryl iodides due to their increased stability and amenability. Furthermore, photochemical approaches with fluoroarenes and aryl iodides have not been widely investigated for grafting organic thin films onto surfaces.

Weaver and coworkers have demonstrated the partial defluorination of arenes using visible light photoredox catalysis.<sup>17</sup> Based on this work, I hypothesized that polyfluoroaryl radical intermediates generated under these photoredox catalytic conditions can form covalent bonds with gold surfaces as a mechanism for thin film growth (Scheme 1.1). Fluorination of the benzene ring should prevent the further attachment of pentafluorophenyl radicals to already-grafted units, ensuring the formation of monolayers. Indeed, monolayer formation is rare in the areas of photografting and electrografting. According to my design, the photocatalyst, Ir(ppy)<sub>3</sub>, is excited by visible light. The excited photocatalyst then donates an electron to the polyfluoroarene to generate a radical that can attach to the gold surface.



Scheme 1.1 Proposed Hexafluorobenzene Grafting to Gold Substrate

Lee and coworkers have also demonstrated the formation of aryl radical intermediates from aryl iodides using visible-light photoredox catalysis.<sup>18</sup> Similar to the fluorinated arenes, I proposed that the aryl radicals formed from aryl iodides will graft onto gold (Scheme 1.2). In this instance, the photocatalyst that is used is Ir(ppy)<sub>2</sub>(dtbbpy)PF<sub>6</sub>. *N,N*-Diisopropylethylamine (DIPEA) transfers an electron to generate an Ir(II) species which then transfers an electron to the aryl iodide, which loses the iodide anion to give the aryl radical. This aryl radical can then interact with the gold surface to produce an organic thin film.



Scheme 1.2 Aryl Radicals from Aryl Iodides Grafting onto Gold Substrate

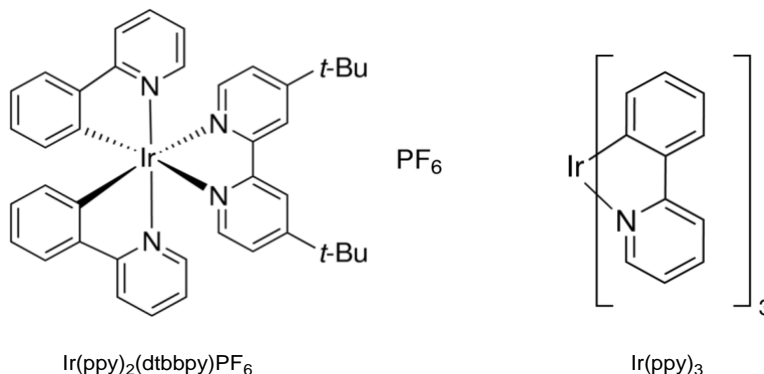


Figure 1.2. Photocatalysts Used

#### 1.4. Methods for Characterization

To determine structure and function of the organic thin films formed through photografting, several characterization techniques must be used. Verification of covalent bonding of the polyfluorinated arenes and aryl iodides can be determined using X-Ray Photoelectron Spectroscopy (XPS)<sup>19</sup> and Time-of-Flight Secondary Ion Mass

Spectroscopy (TOF-SIMS)<sup>20</sup>. Functional groups present in thin films can be determined using the Grazing-angle Infrared Reflection Absorption Spectroscopy (IRRAS) method in Fourier Transform Infrared (FTIR) spectroscopy. Also, determination of film thickness and robustness may be achieved using Atomic Force Microscopy (AFM) and particle lithography.<sup>21</sup>

Particle lithography enables control over the deposition of the thin film.<sup>22</sup> A SiO<sub>2</sub> mesosphere (d = 500 nm) surface mask is deposited on an area of the gold substrate preventing the thin film from covering areas blocked by the mask. Mesospheres cover the gold surface in a hexagonally close-packed manner (Figure 1.2). In nanofabrication, mesospheres are suspended in an aqueous solution and drop-cast onto the gold surface then allowed to dry in ambient conditions. The mask is then annealed onto the gold surface (**A**). The masked surface is then placed in the reaction solution containing the organic molecules that will produce the thin film (**B**). After grafting of the thin film, the mask is removed (**C**) leaving regions of bare gold substrate and a nanopattern of the deposited thin film (**D**) (Figure 1.3). These sites are called nanopores.<sup>23</sup>

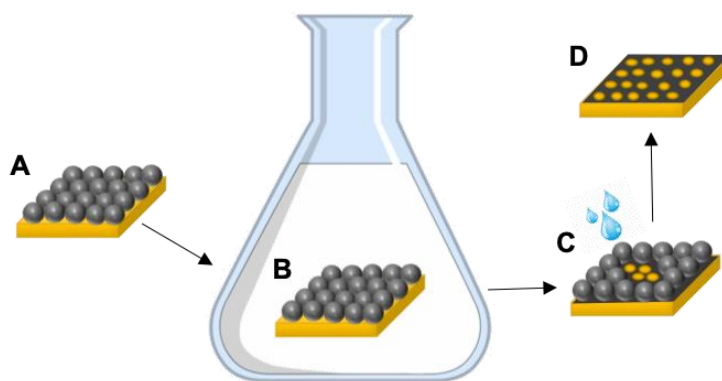


Figure 1.3. Particle Lithography using a Mesosphere Mask

Atomic Force Microscopy (AFM) in conjunction with particle lithography enables the depth of the thin film to be measured. AFM is used to measure surface morphological

properties through the scanning probe method (Figure 1.4). It is able to measure the topography and friction between the probe and the surface through the use of three modes: contact, tapping, and non-contact. These modes allow for imaging of the surface.

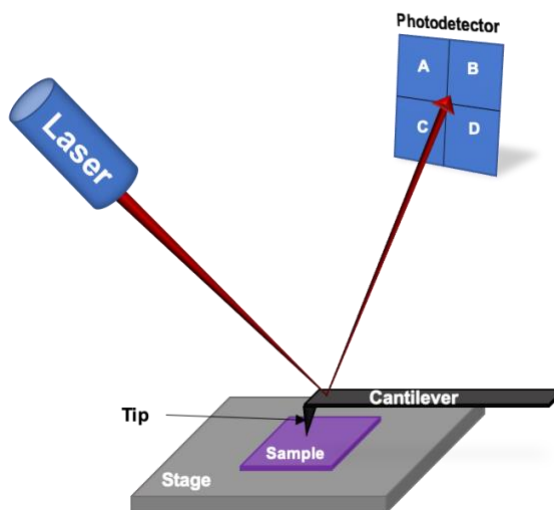


Figure 1.4. Basic Schematic of Atomic Force Microscopy

In contact mode, the tip is dragged along the surface while the deflection of the laser on the cantilever is kept constant.<sup>24</sup> In non-contact mode the tip does not have contact with the surface, instead it oscillates at a selected frequency above the surface and the surface is measured based on Van der Waals forces.<sup>21</sup> Contact and non-contact mode will give the same topography if the surface is dry. However, if the surface absorbs any moisture, then non-contact mode will be unable to differentiate the water from the actual surface. In contrast, contact mode can penetrate the moisture to give the surface topography. In tapping mode the cantilever oscillates up and down at a variable frequency.<sup>25</sup> Tapping mode is used in nanoshaving and nanografting experiments of thin films.<sup>26</sup> Nanoshaving is the use of high force on the cantilever as the tip sweeps across the surface.<sup>27</sup> This force is used to disrupt the thin film and expose the surface. The stability of the thin film can be determined by the force applied to the AFM tip to remove the thin film.

## 1.5. Research Significance

As mentioned previously, organic thin films, similar to the ones proposed in this dissertation, are important components of biosensors<sup>6</sup>, chemical sensors<sup>9</sup>, and corrosion/fouling-resistant coatings<sup>3</sup>. Since aryl iodides and fluoroarenes are more stable than diazonium salts, they could be manipulated with multistep synthesis prior to grafting on surfaces. This will enable the ability to functionalize thin films according to the substituents on the fluoroarenes and aryl iodides. Thin film formation using photochemical approaches with fluoroarenes and aryl iodides have not been widely investigated. Herein, I report my efforts of using photoredox catalysis for functionalization of Au(111) surfaces. Solutions of fluoroarenes and aryl iodides were irradiated at approximately 450 nm in the presence of a photoredox catalyst, which resulted in the deposition of thin films that we characterized using various methods.

## 1.6. Results and Discussion

### 1.6.1. Polyfluorinated Arene

To protect regions of Au(111) surface particle lithography was employed. A surface mask of silica mesospheres were drop-cast, dried, and annealed to the gold surface. The gold substrate was submerged in a solution of acetonitrile, polyfluorinated arenes, DIPEA, and an iridium photocatalyst (*fac*-Ir(ppy)<sub>3</sub>) contained in an Erlenmeyer flask with a nitrogen inlet. The solution was heated to 45°C and irradiated with blue LEDs for 30 minutes. Upon completion, the gold substrate was removed from the reaction solution and the mesosphere mask was removed via sonication by placing the gold substrate in a solution of water and ethanol. AFM revealed the formation, or lack thereof, of thin films through the hexagonal patterning of nanopores on the surface. The depths

of the nanopores were measured, and the presence of a thin film was identified. Figure 1.4 shows the formation of nanopores with a depth of approximately 6 nm using methyl pentafluorobenzoate **2**. One molecule of **2** is calculated to be 1 nm, so it was determined that the electron donating group allowed for formation of multiple layers.

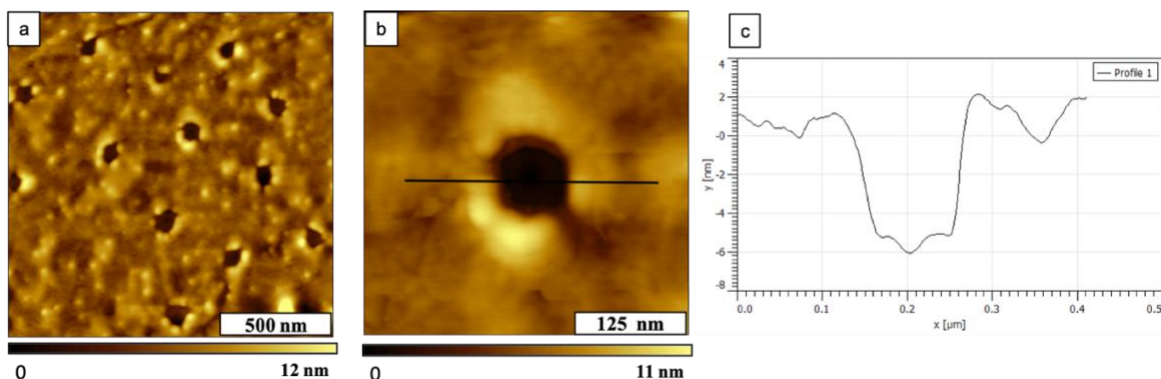


Figure 1.5. A thin film formed on Au(111) generated with an initial concentration of  $10^{-1}\text{M}$  **2** after 30 minutes of irradiation. Nanopores were produced using immersion particle lithography. (a) Topography image ( $5 \times 5 \mu\text{m}^2$ ) acquired in air; (b) a single nanopore ( $500 \times 500 \text{ nm}^2$ ); (c) cursor profile for the line in *b*.

This method was performed using other polyfluorinated arenes, hexafluorobenzene **1**, methyl-pentafluorobenzoate **2**, and pentafluorobenzonitrile **3**, under the same conditions (Table 1.1). The aim of testing materials **2** and **3** was to determine if electron donating groups or electron withdrawing groups would affect the formation of thin films. After determination of thin film formation, nanoshaving was used to identify the robustness of the thin film. The area containing the nanostructure and the surrounding organic thin film was subjected to a force of 10 nN. If the thin film remained after this force then it would be determined to be a robust film.<sup>28</sup> Figure 1.6 shows the formation of the monolayer generated from **1**. After the nanoshaving technique was used, nanopores remained intact.



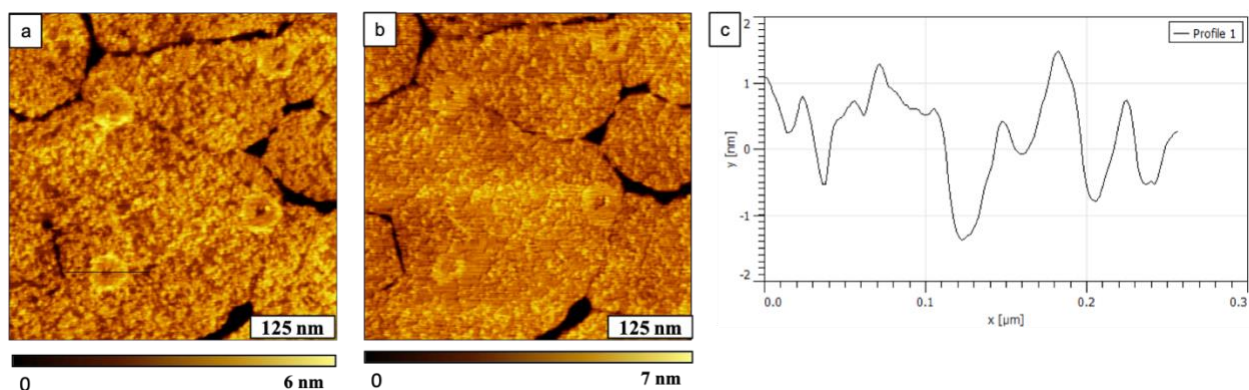
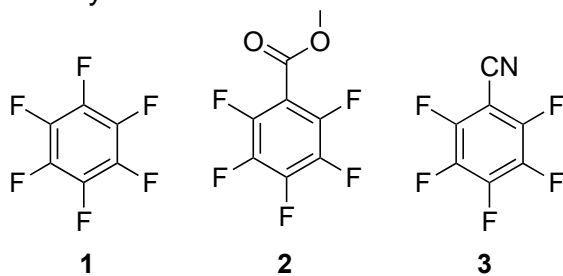


Figure 1.6. A thin film formed on Au(111) generated with an initial concentration of  $10^{-1}$  M **1**, after 30 minutes of irradiation. Nanopores were produced using immersion particle lithography, where (a) topography image ( $1.5 \times 1.5 \mu\text{m}^2$ ) acquired in air; (b) area after 10nN force applied using AFM tip (c) cursor profile for the line in a.

Table 1.1, below, outlines the outcome of each substrate. It was hypothesized that in entries 1 and 3 substrates that contain an electron withdrawing group did not allow for further radical attack as was determined from film thickness. All polyfluoroarenes survived nanoshaving experiments. With thin film formation and robustness of polyfluoroarenes confirmed by AFM, further characterization was carried out on **1**.

Table 1.1. AFM Results of Polyfluoroaranes Studied



Entry	Polyfluoroarene	Irradiation Time* (min)	Film Thickness	Nanoshave (at 10 nN)
<b>1</b>	<b>1</b>	30	1-2 nm	Not successful
<b>2</b>	<b>2</b>	30	4-6 nm	Not successful
<b>3</b>	<b>3</b>	30	1-2 nm	Not successful

\*Irradiation time remained the same for all polyfluoroarenes studied.

To determine organic structures on the surface of Au(111), grazing-angle IRRAS in FTIR was used. This enabled the functional groups present on the surface to be identified directly. The reported frequency for C-F stretching is within 1400-1000  $\text{cm}^{-1}$ .<sup>27</sup> For entry 1, the C-F stretching peak was apparent in the grazing-angle FT-IRRAS spectrum (Figure 1.7). We attribute the strong peak around 1300 nm to the presence of C-F bonds on the surface. However this did not confirm covalent attachment of pentafluorophenyl units to the Au(111) surface.

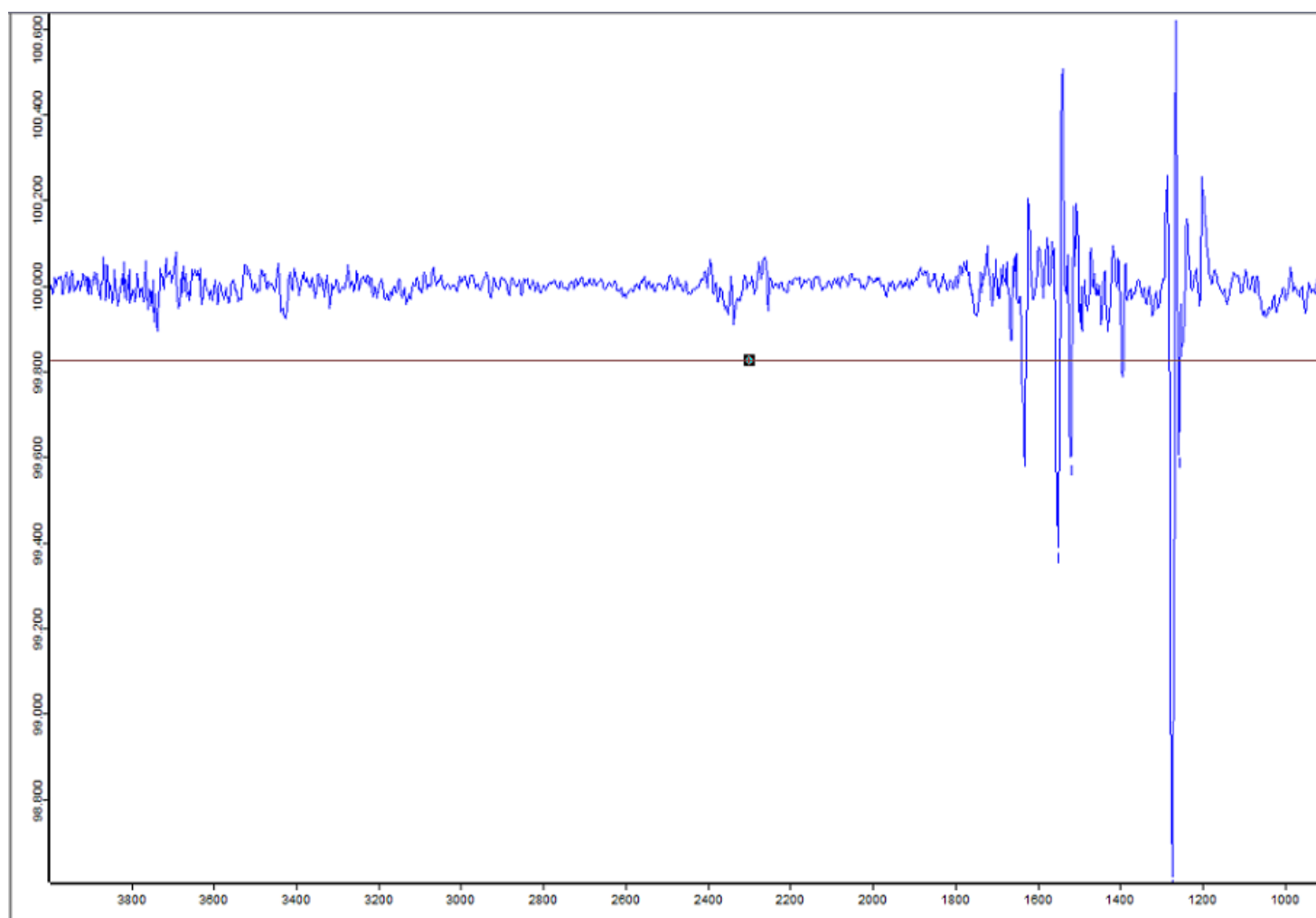


Figure 1.7. Grazing-angle FT-IRRAS spectrum of pentafluorobenzene thin film. Strong peak at around 1300 nm indicates C-F stretching.

To confirm the thin film was indeed generated from pentafluorobenzene, gold samples XPS and TOF-SIMS analysis was performed. XPS surveyed thin film surfaces, and elemental composition was determined (Figure 1.8). A survey of the binding energies from surface composition is displayed in the spectrum. It is determined that no fluorine was detected on the surface. The chemical and electronic state of the thin film on Au(111) was determined using TOF-SIMS (Figure 1.9). The TOF-SIMS analysis showed gold with some pentafluoroarene attached. This suggested that there was very little fluoroarene grafting on the surface. Although thin film formation using fluoroarenes was inconclusive, I was optimistic that my concurrent aryl iodide thin film grafting would be successful.

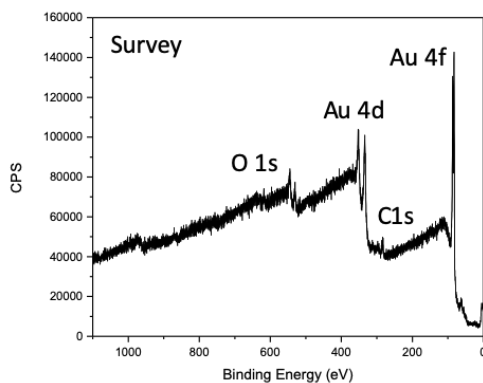


Figure 1.8. XPS spectrum of pentafluorobenzene thin film. Shows binding energy with respect to intensity of gold, carbon, and oxygen peaks.

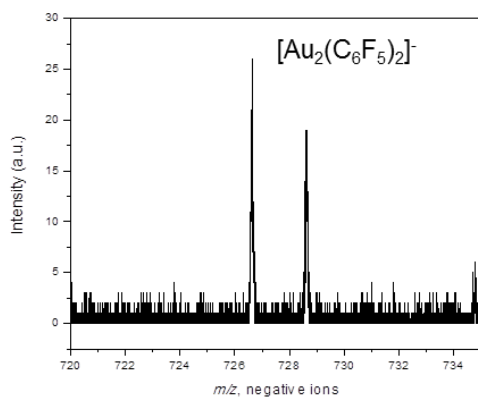
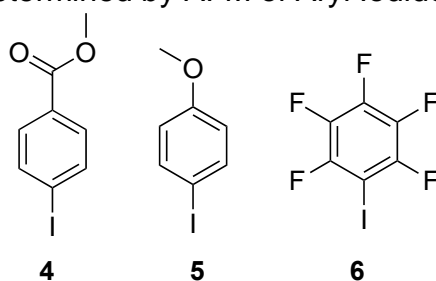


Figure 1.9. TOF-SIMS Spectrum of Pentafluorobenzene Thin Film. There is a peak showing the pentafluorobenzene on the surface of gold.

### 1.6.2 Aryl Iodides

Once again, particle lithography and Au(111) immersion in a photographing solution was used for a variety of aryl iodides. An iridium catalyst ( $\text{Ir}(\text{ppy})_2(\text{dtbbpy})\text{PF}_6$ ) was irradiated with blue LEDs in the presence of several solutions containing aryl iodides, DIPEA, and a submerged gold substrate. Formation of thin films was determined using AFM. 1-iodo-4-methoxybenzene (**5**), pentafluoriodobenzene (**6**), and methyl 4-iodobenzoate (**4**) were studied and the outcomes are outlined in Table 1.2. Monolayer thickness was achieved with compounds (**4**) and (**6**) using standard conditions. With compound (**5**), concentration of substrate and irradiation time determined the thickness of the thin film. Higher concentration at longer irradiation times yielded multilayer thickness as shown in entry 7.

Table 1.2. Film Thickness determined by AFM of Aryl Iodides Studied



Entry	Aryliodides	Concentration	Irradiation Time (min)	Film Thickness
1	4	0.1 M	30	1 nm
2	5	0.01 M	15	1 nm
3	5	0.01 M	30	1-2 nm
4	5	0.01 M	45	1-2 nm
5	5	0.01 M	60	1-2 nm
6	5	0.1 M	30	1 nm
7	5	0.1 M	60	4-6 nm
8	6	0.1 M	30	1 nm

Unfortunately, when nanoshaving was employed, none of the thin films survived the 10 nN force. Figure 1.10 shows the formation of 1 nm nanopores of **1** and the disruption caused by nanoshaving. Thus, aryl iodide thin films were found to not be robust.

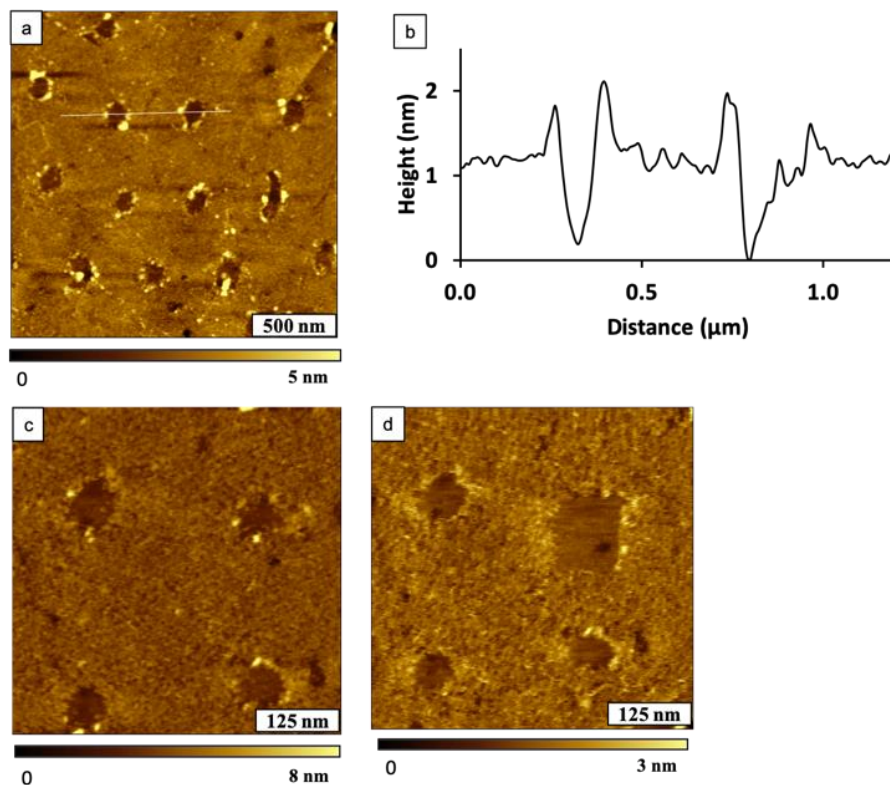


Figure 1.10. A thin film formed on Au(111) generated with an initial concentration of  $10^{-1}$  M **2** after 30 minutes of irradiation. Nanopores were produced using immersion particle lithography. (a) Topography image ( $5 \times 5 \mu\text{m}^2$ ) acquired in air; (b) cursor profile for the line in a; (c) zoom-in view ( $1.5 \times 1.5 \mu\text{m}^2$ ); (d) the shaved area after 10 nN force applied using AFM tip.

## 1.7. Conclusion

Interpretation of polyfluoroarene and aryl iodide thin films characterization results, made it evident that our hypothesis to form organic thin films in this manner was inconclusive. Although we were able to form strongly bound thin films using polyfluoroarenes in the reaction mixture, the amount of fluorinated compound on the surface of the substrate was not significant enough to explore further. Nanoshaving

experiments of aryl iodide thin films showed that they were not robust. For these reasons, we concluded investigation on this area of surface chemistry.

## **1.8. Experimental**

### **1.8.1. Materials and Reagents**

Hexafluorobenzene (99%), methyl pentafluorobenzoate (99%), and pentafluorobenzonitrile (99%), 1-iodo-4-methoxybenzene (98%), pentafluoriodobenzene (98%), methyl 4-iodobenzoate (97%), Ir(ppy)<sub>2</sub>(dtbbpy)PF<sub>6</sub>, *fac*-Ir(ppy)<sub>3</sub> (99%), and diisopropylethylamine (99.5%) were purchased from Sigma-Aldrich and used without further purification. 500 nm size sorted silica mesospheres were purchased from Thermo Scientific. Glassware was flame dried under vacuum and backfilled with dry nitrogen prior to use. The irradiation source for photografting reactions of aryl iodides were two 4 W sapphire blue LED flex strips from Creative Lighting Solutions (Cleveland Ohio). Irradiation source for photografting reactions of fluoroarenes were 4 pre-mounted rebel star royal-blue LEDs from the Luxeon Star LEDs by Quadica.

### **1.8.2. Preparation of Gold Surfaces with a Mesosphere Mask**

Template-stripped, ultraflat gold substrates were prepared by a previously reported procedure.<sup>29</sup> Gold films were prepared on mica(0001) by evaporative deposition. Glass discs were glued to freshly prepared gold films using an epoxy (EPO-TEK, Billerica, MA). Pieces of ultraflat gold/glass were stripped from mica to expose a clean, atomically flat Au(111) surface. 500 nm size-sorted silica mesospheres were cleaned by centrifugation and suspension in deionized water (three cleaning cycles). A 40  $\mu$ L drop of the silica mesosphere suspension was placed onto the template-stripped gold substrates, dried in air for 24h, and then oven dried at 150°C for at least 48h. The final heating step

was used to temporarily anneal the silica spheres to the substrate to prevent displacement during immersion in solutions. After completing the chemical reactions, removal of the surface mask was accomplished by sonication in ethanol/water solutions.

### **1.8.3. General Photografting Procedure for Fluoroarenes**

Acetonitrile (MeCN) from a solvent purification system was dried over 3Å molecular sieves for 24h. Fluoroarene (0.2 mmol), *fac*-Ir(ppy)<sub>3</sub> (0.004 mmol), anhydrous MeCN (2 mL) and diisopropylethylamine (DIEA) (0.66 mmol) were added to a dry 20 mL test tube and sealed with a septum. The test tube was placed in an ice bath. A needle connected to the nitrogen line was used to purge the solution for 15 min. A 125 mL Erlenmeyer flask was flame dried and charged with a flat stir bar and the silica masked gold substrate. The flask was sealed with a rubber septum and nitrogen purged. The deoxygenated solution was added via syringe to the Erlenmeyer flask containing masked gold and stir bar. The reaction flask was placed in an oil bath at 45°C and irradiated using blue LED lights. The solution was magnetically stirred taking care that the stir bar did not touch the gold substrate. After irradiation for the desired period of time, the solution was decanted. The masked gold substrate was washed twice with 2 mL of deionized water and twice with 2 mL of ethanol to remove extraneous material. The gold substrate was sonicated in ethanol for >1 min to remove the mesospheres.

### **1.8.4. General Photografting Procedure for Aryliodides**

Acetonitrile (MeCN) from a solvent purification system was dried over 3Å molecular sieves for 24h. Aryliodide (0.02 mmol or 0.2 mmol) and Ir(ppy)<sub>2</sub>(dtbbpy)PF<sub>6</sub> (0.0006 mmol or 0.006 mmol) were added to a flame dried 125 mL Erlenmeyer flask charged with a stir bar. The gold substrate was added and the flask was sealed with a rubber septum



equipped with nitrogen inlet. Anhydrous MeCN (2 mL) and DIEA were added to the flask via syringe. The solution was magnetically stirred, ensuring that the stir bar did not touch the gold substrate, and irradiated with blue LEDs. After irradiation for the desired period of time, the solution was decanted. The masked gold substrate was washed twice with 2 mL of deionized water and twice with 2 mL of ethanol to remove extraneous material. The gold substrate was sonicated in ethanol for >1 min to remove the mesospheres.

#### **1.8.5. Experimental Set-up**



Figure 1.11. A Typical Au(111) Photografting Reaction Set-Up

#### **1.8.6. Atomic Force Microscopy (AFM)**

The samples were imaged using a model 5500 or model 5420 atomic force microscope with Pico View v.1.12 software (Agilent Technologies, Chandler, AZ). Non-conductive imaging probes from Bruker (MSCT, 0.01 – 0.6 N/m) were used to acquire contact-mode images. Images were processed and analyzed using Gwyddion (v. 2.22), an open-access processing software designed for AFM images, supported by the Czech Metrology Institute.

### 1.8.7. Photografting Procedure for Preparation of Samples for PM-IRRAS

Polycrystalline 100 nm Au-film-coated glass slides obtained from PlatypusTechnologies (catalog number Au.1000.SL1) and approximately cut into 1x1 inch sections then cleaned using UV/ozone for 24 hours. Arene (0.2 mmol), photocatalyst (0.004 mmol), and diisopropylethylamine (DIEA) (0.66 mmol) were added to a 125 mL Erlenmeyer flask charged with a stirbar. The freshly-cleaned Au film-coated glass was then added and the flask was sealed with a rubber septum in an N<sub>2</sub> environment. Anhydrous MeCN (4 mL) was added and the reaction mixture was stirred at room temperature (18°C). The reaction mixture was irradiated with blue LEDs for 3 hours. The gold substrate was removed from the reaction mixture and washed with deionized water (10 mL) and ethanol (10 mL) before analysis.

## CHAPTER 2. AN OVERVIEW OF O-GLYCOSYLATION

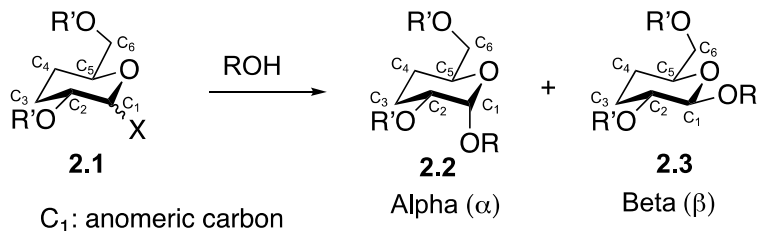
### 2.1. Importance of O-Glycosylation

Glycoscience, the study of simple and complex carbohydrates as free-standing species or as they are attached to lipids and proteins, is of great interest across chemical and biological sciences<sup>1</sup> Oligosaccharide-modified proteins and lipids are called glycoproteins and glycolipids, respectively, and they belong to the class of molecules known as glycoconjugates.<sup>2-3</sup> Glycoconjugates on cell surfaces serve as important mediators of intercellular recognition<sup>4</sup>, adhesion<sup>5</sup>, and viral infection<sup>6</sup> among many other things. Because of the role glycoconjugates play on the surface of cells, carbohydrates-based therapeutics can be used to target specific diseases by mimicking or disrupting (for example) the molecular recognition events in disease that are dependent on carbohydrates.<sup>1</sup>

O-linked glycosylation, or O-glycosylation, is the attachment of the anomeric center of a monosaccharide or the reducing-end anomeric center of an oligosaccharide to an oxygen atom. O-Glycosidic compounds are the most abundant carbohydrates in nature. Isolating these oligosaccharides from natural sources provides small amounts of often complex mixtures.<sup>7</sup> Unfortunately, synthesis of oligosaccharides has proven to be difficult due to the abundance of glycosidic linkages which are often hard to install in high yield stereoselectively.<sup>8</sup> To overcome difficulties associated with stereoselectivity, yields, and harshness of the reaction conditions, several procedures have been developed with the goal of facile O-glycosylation.<sup>6</sup> Several factors must be considered in the development of new O-glycosylation procedures such as, glycosyl donor stability, glycosyl acceptor reactivity, solvent properties, protecting group choice, and mode of activation.

## 2.2. Glycosylation Mechanistic Pathways and Stereochemical Factors

Disaccharides are made through the formation of glycosidic bonds, which are formed when a glycosyl acceptor (typically an alcohol, ROH) attaches to the anomeric carbon of the glycosyl donor **2.1**. In O-glycosylation, acceptor replaces a leaving group (X) on the anomeric carbon of the glycosyl donor either through associative or dissociative mechanisms (Scheme 2.1). The resulting glycosidic linkage could be either an *alpha* (1,2-*cis*) **2.2** or *beta* (1,2-*trans*) **2.3** configuration. If the glycosidic C-O bond is *trans* with the C<sub>5</sub>-C<sub>6</sub> bond then the configuration is said to be *alpha*. If these same bonds are *cis* to each other then the configuration is said to be *beta*. An activator is often used in either catalytic or stoichiometric quantities to promote and drive the formation of the glycosidic linkage.

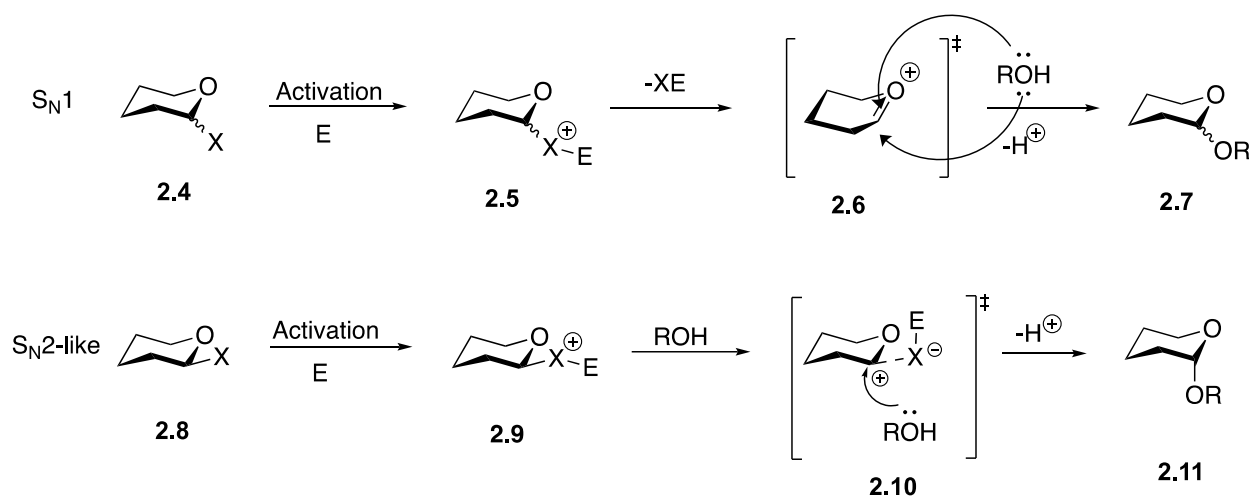


Scheme 2.1 Glycosidic Linkages

### 2.2.1. S<sub>N</sub>1 (Dissociative) or S<sub>N</sub>2-Like (Associative) Mechanistic Pathways

Two commonly proposed chemical O-glycosylation mechanisms are the S<sub>N</sub>1 and S<sub>N</sub>2-like mechanisms (Scheme 2.2). In the S<sub>N</sub>1 pathway, the glycosyl donor's leaving group is activated by an electrophilic promoter "E" to generate **2.5**. After loss of the now-activated leaving group, there is a formation of an oxocarbenium ion **2.6**. The glycosyl acceptor attacks the glycosyl donor at either face to form the glycosidic bond, which results in a mixture of *alpha* and *beta* linkages designated by structure **2.7**. The S<sub>N</sub>2-like mechanism proceeds through the activation of the leaving group "X" by an electrophile "E" resulting in **2.9**. This then enables direct backside attack of the acceptor on the

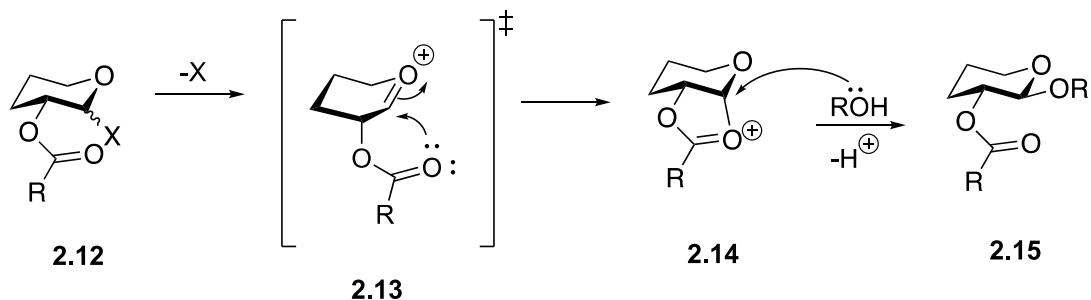
anomeric carbon of the donor **2.9**. This proceeds through the caged pair transition state **2.10** resulting (for instance) in the *alpha* anomer **2.11**. Partitioning between the S<sub>N</sub>1 and S<sub>N</sub>2-like mechanisms can be highly dependent on protecting groups (electron-withdrawing groups favor S<sub>N</sub>2-like by destabilizing **2.6**), solvent dielectric constant (high  $\epsilon$  favors S<sub>N</sub>1 by stabilizing **2.6**), and the nucleophilicity of ROH (poor nucleophiles result in more S<sub>N</sub>1 whereas stronger nucleophiles result in more S<sub>N</sub>2-like mechanism).



Scheme 2.2 Glycosylation Mechanistic Pathways

### 2.2.2. Neighboring Group Participation

*Beta* glycosyl linkages can be synthesized easily using neighboring group participation (NGP), which follows the S<sub>N</sub>1 mechanism as shown in Scheme 2.3. Acyl protecting groups (*i.e.* benzoyl-, acetyl-, pivaloyl-) in the C<sub>2</sub> position facilitate the formation of a *beta* linkage. After loss of the leaving group and formation of the oxocarbenium ion, the lone pair on the carbonyl **2.13** adds to the anomeric carbon forming the dioxolenium ion **2.14**. This only allows equatorial attack by the acceptor forming the *beta* linkage **2.15**. Methods to form *alpha* glycosidic linkages have been developed, but are not as universal as NGP.



Scheme 2.3 Neighboring Group Participation to Generate *beta*-Anomer

### 2.3. Anomeric Effect

The term anomeric effect, also known as the Edward-Limeux effect, was first introduced in 1958 at a meeting of the American Chemical Society. It is the tendency of an electronegative atom to assume the axial orientation rather than equatorial at the C<sub>1</sub> position on a pyranoid ring.<sup>9</sup> Molecular orbital theory (MOT)<sup>10</sup> and dipole moment theory (DMT) have been used to explain this effect<sup>11</sup> (Figure 2.1). The electrostatic repulsion between the ring oxygen and the C—X bond is lessened when the C—X bond is axial as in **2.16**. This is due to the dipole moments opposing each other making it more stable and preferred to **2.17**. The MOT further explains the anomeric effect. Through hyperconjugation, lone pairs on the heteroatom add to the aligned sigma\* antibonding orbital of the C—X bond and provide stability as in **2.18**. The anomeric effect is important when interpreting glycosylation outcomes, but it is also important to mention that O-glycosylation frequently occurs under kinetic control whereas the anomeric effect is explained using thermodynamic arguments.<sup>12</sup>

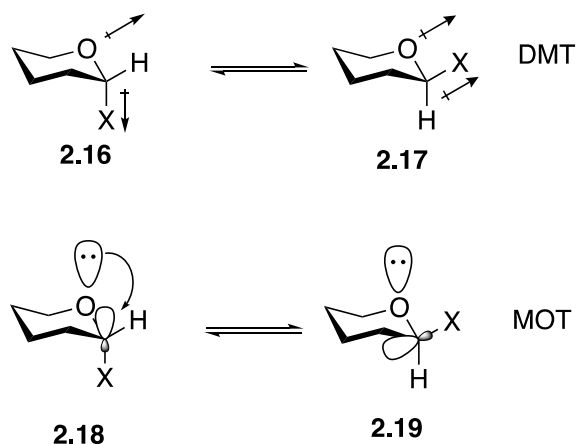
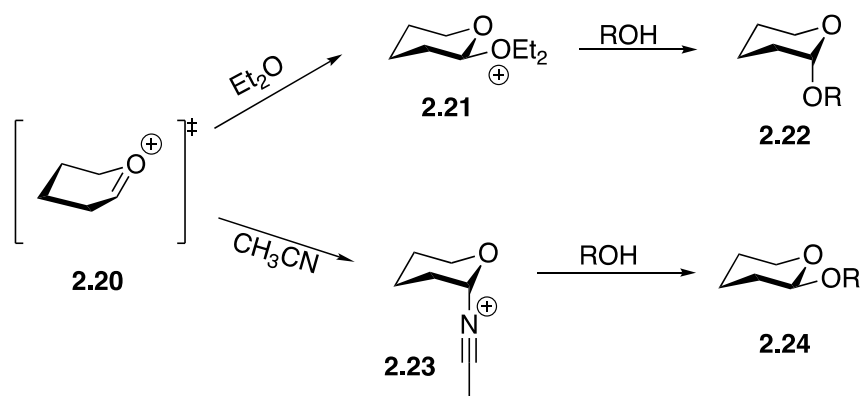


Figure 2.1. Dipole Moment Theory (DMT) and Molecular Orbital Theory (MOT) to explain the Anomeric Effect

## 2.4. Solvent Effect

The solvent used in a glycosylation reaction can affect the stereochemical outcome. In the absence of neighboring group participation, solvent effects can dominate the stereochemical outcome of chemical glycosylation. In general, nonpolar solvents such as toluene, dichloromethane, and dichloroethane are non-participating solvents, meaning that their interaction with oxocarbenium ions like **2.6** in Scheme 2.2 is minimal. Due to their nucleophilicity and tendency to interact with oxocarbenium ions, ether and nitrile solvents can have a profound effect on stereochemical outcome (Scheme 2.4).

Weakly polar and participating solvents such as dioxane<sup>13</sup>, diethyl ether<sup>14</sup> (Et<sub>2</sub>O), and tetrahydrofuran<sup>13</sup> (THF) **2.21** drive the formation of *alpha*-glycosidic linkages. Coordination of the solvent to the oxocarbenium ion via its  $\beta$ -face to generate intermediates like **2.21** (Scheme 2.4) forces the glycosyl acceptor to attack the  $\alpha$ -face.<sup>15</sup>

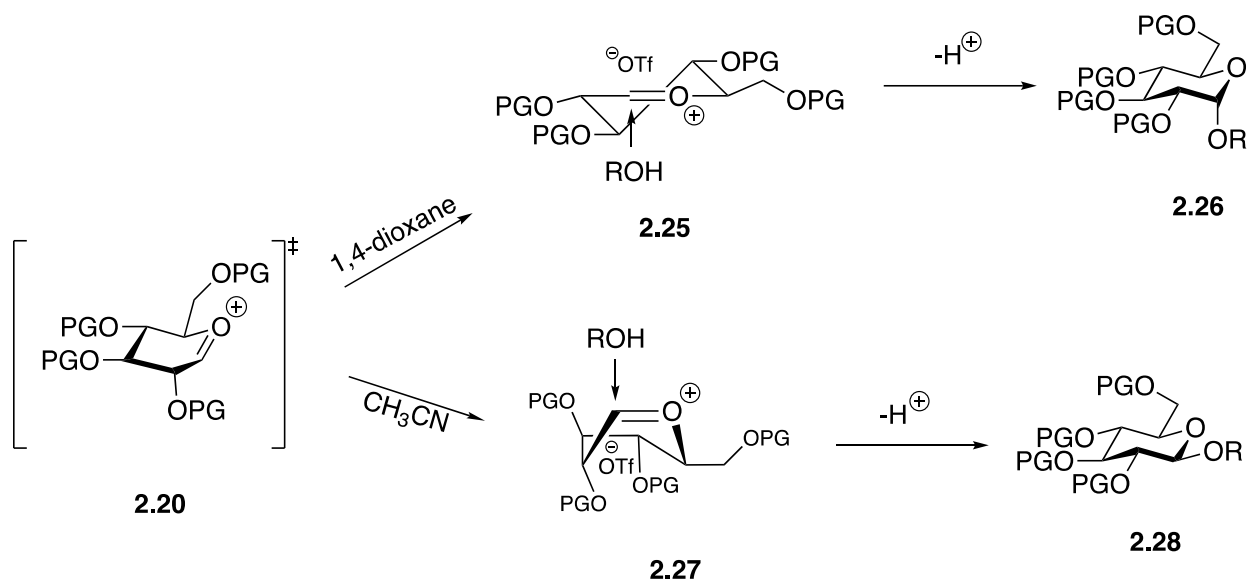


Scheme 2.4 Solvent Effects of Acetonitrile and 1,4-dioxane

The use of participating polar solvents like acetonitrile and propionitrile to promote formation of  $\beta$ -glycosidic linkages has been widely studied. In 1990, Fraser-Reid and coworkers studied the formation of  $\alpha$ -nitrilium ion intermediate **2.23** which is kinetically favored upon generation of **2.20**.<sup>16</sup> This forces the glycosyl acceptor to attack from the  $\beta$ -face.<sup>17</sup>

A more recent theory on solvent effect, proposed by Satoh and Hünenberger, used quantum mechanical (QM) and molecular dynamic (MD) simulations to probe the mechanism of solvent effect. In a concept termed the “conformer and counterion distribution” hypothesis<sup>18</sup>, it is suggested that the solvents are not actively participating in the glycosylation mechanism (Scheme 2.5). Instead, the conformation of the oxocarbenium ion is determined by the polarity of the solvent.<sup>18</sup> In addition, the position of the counterion determines which face the acceptor attacks. In ethereal solvents, the oxocarbenium ion assumes a  $^4\text{H}_3$  conformation **2.25**, where the counterion is situated at the  $\beta$ -face. This only allows for nucleophilic attack of the glycosyl acceptor from the  $\alpha$ -face. In acetonitrile the oxocarbenium ion adopts the  $\text{B}_{2,5}$  conformation **2.27**. The triflate counterion is located on the  $\alpha$ -face allowing for attack on the  $\beta$ -face.





Scheme 2.5 Solvent effects using QM and MD

The use of toxic solvents such as ether, acetonitrile and dichloromethane has grown increasingly prohibitive. Thus, more environmentally friendly approaches to solvent choice are being investigated. Toshima and coworkers studied the use of ionic liquids as a green solvent for glycosylation.<sup>19</sup> In their study, the protic acid counterion ( $-\text{NTf}_2$ ) for the ionic liquid ( $\text{C}_6\text{mim}[\text{NTf}_2]$ ) salt was used to promote glycosylation. These authors were able to achieve moderate to good yields with no stereoselectivity observed.

## 2.5. Glycosyl Acceptors

Glycosyl acceptors play an important role in the stereochemical outcome of a glycosylation reaction. As previously mentioned, the glycosyl acceptor is an alcohol that acts as the nucleophile in the reaction. The nucleophilicity of the acceptor can effect the mechanistic pathway of the glycosylation. Less reactive nucleophiles follow the  $\text{S}_{\text{N}}1$  pathway while more reactive nucleophiles follow the  $\text{S}_{\text{N}}2$  pathway.<sup>20</sup> Primary alcohols are more reactive than secondary, because they are stronger nucleophiles. Due to steric hinderance and nucleophilicity, the  $\text{C}_4$  glycosyl acceptor is especially unreactive. Equatorial alcohols are more nucleophilic than axial, thus making them more reactive.

The nucleophilicity of glycosyl acceptors can also be modulated based on the protecting groups. Acyl (PG = Bz, Piv) protecting groups located within an acceptor are deactivating due to electron withdrawing effects. On the other hand, electron donating groups (PG = Bn, Me) increase nucleophilicity while the bulkiness of protecting groups decreases reactivity.

To better illustrate the hierarchy of acceptor nucleophilicity, an example is given in Figure 2.2. The primary alcohol at the left is the most nucleophilic while the least nucleophilic C<sub>4</sub> acceptor at the far right is greatly hindered by the bulky tert-butyldimethylsilyl group. Electron-withdrawing effects and steric effects modulate the reactivity of the three acceptors in the middle.

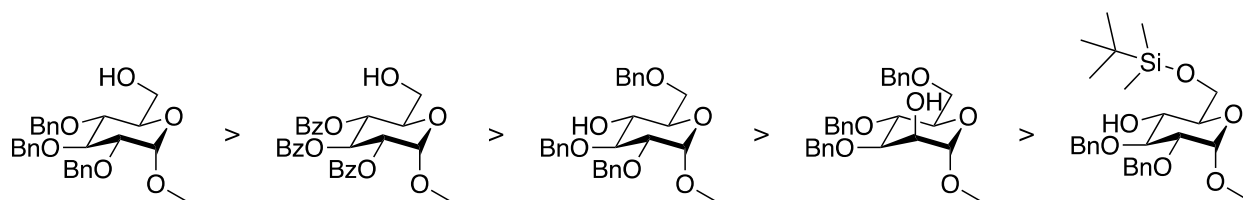


Figure 2.2. Nucleophilicity of Glycosyl Acceptors

## 2.6. Glycosyl Donors

### 2.6.1. Protecting Groups

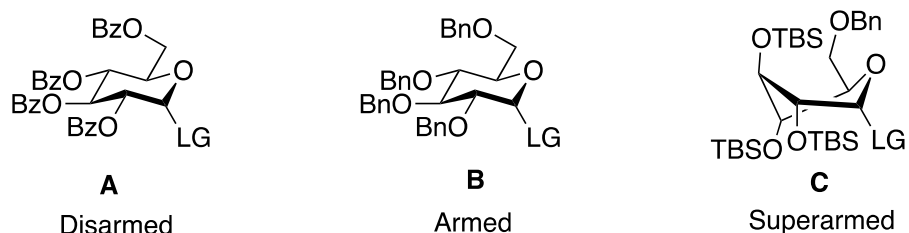


Figure 2.3. Protected Glycosyl Donors

In carbohydrate chemistry, protecting groups are often used to mask the multiple sites of reactivity in a sugar molecule. Similar to glycosyl acceptors, protecting groups can have a profound effect on reactivity in O-glycosylation. Fraser-Reid stated it best: “Protecting groups do more than protect”.<sup>21</sup> The most notable example of this is the use

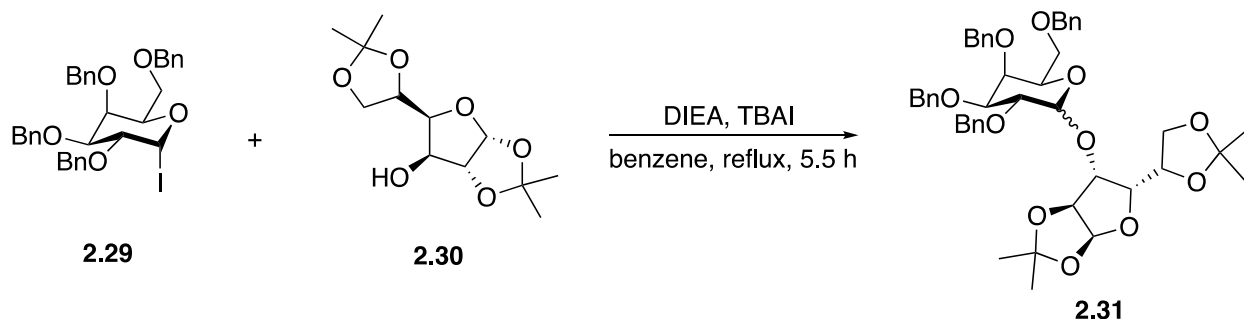
of an acyl group in the C<sub>2</sub> position for NGP.<sup>22</sup> Considering the role of protecting groups more deeply, Fraser-Reid was the first to classify protecting groups by their ability to stabilize oxocarbenium ions generated from glycosyl donors.<sup>23</sup> He categorized ester protecting groups as “disarming” and alkyl protecting groups as “arming” (**A** and **B**, Figure 2.3). It was found that the reactivity of donors exhaustively protected with disarming protecting groups was decreased compared to donors exhaustively protected with arming protecting groups due to the electron withdrawing effects of the acyl group. This is because the formation of oxocarbenium ions (S<sub>N</sub>1 mechanism) or contact ion pairs (S<sub>N</sub>2-like mechanism) is more facile with electron-releasing arming groups and less facile with electron-withdrawing disarming groups. Protecting groups that confer higher reactivity than perbenzylation (arming groups) of donors are called “superarming.” Bols and coworkers observed a conformational change in glucose donors when persilylating with the *tert*-butyldimethylsilyl (TBS) group. The resulting conformational shift from <sup>4</sup>C<sub>1</sub> to a skew-boat confirmation<sup>24</sup> (Figure 2.3) resulted in the pseudoaxial disposition of “OTBS” at positions 2, 3, and 4. The resulting proximity of pseudoaxial oxygens stabilizes the as-formed oxocarbenium to an extent much greater than that of benzyl groups. As a result, persilylated donors like **C** in Figure 2.3 are more reactive than their perbenzylated counterparts. As a result, Bols and co-workers classified systems like **C** as “superarmed”.<sup>25</sup>

### 2.6.2. Glycosyl Halides

The stability of glycosyl halides is as follows: fluoride > chloride > bromide > iodide. Bromides and chlorides have been the most used and widely studied of the glycosyl halides.<sup>26</sup> Keonigs and Knorr were the first to report glycosyl halides as viable donors in

1901.<sup>27</sup> A range of heavy metal (mercury and silver) salts were used to activate glycosyl bromides and chlorides.<sup>28</sup> These salts are considered halophiles and include: AgOTf, AgClO<sub>4</sub>, HgCl<sub>2</sub>, and HgI<sub>2</sub>.<sup>29</sup> In 1975, Lemieux and coworkers introduced a mild and metal-free way to catalyze glycosyl bromides and chlorides.<sup>30</sup>

Glycosyl iodides were studied as a way around the use of heavy metals due to their increased reactivity.<sup>31</sup> Iodides are very unstable, but their reactivity is tunable through varying the protecting groups on the donor.<sup>31</sup> Activation is achieved through non-metals such as tetrabutylammonium iodide - N,N-diisopropylethylamine (TBAI-DIEA)<sup>32</sup> and N-iodosuccinimide - Iodine - Trimethylsilyl trifluoromethanesulfonate (NIS-I<sub>2</sub>-TMSOTf).<sup>33</sup> Gervay-Hague and coworkers demonstrated the utility of TBAI-DIEA to activate glycosyl iodides,<sup>31</sup> and this approach is particularly mild and user-friendly (Scheme 2.6).

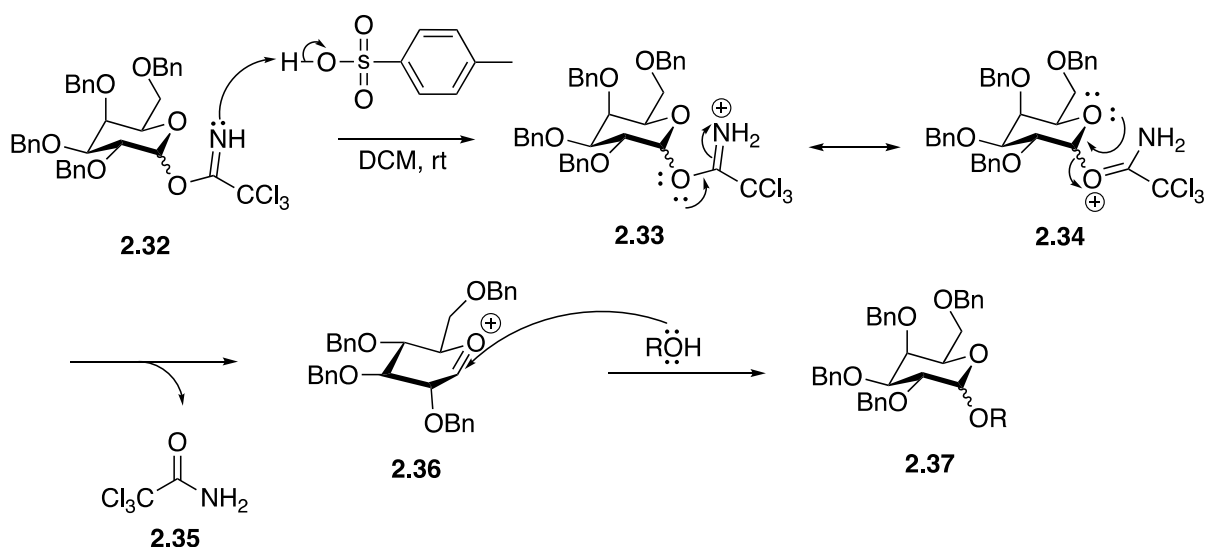


Scheme 2.6 TBAI-DIEA Activation of Glycosyl Iodide

The stability of glycosyl halides drastically improves when using glycosyl fluorides. In 1981, Mukaiyama and coworkers showed that the glycosyl fluorides could be activated by AgClO<sub>4</sub> and SnCl<sub>2</sub>.<sup>34</sup> Although glycosyl fluorides have a longer shelf life and are easily purified, they require special conditions for activation.<sup>35</sup> Glycosyl halides have proven to be a useful tool in glycosylation; however, the instability of these compounds make other glycosyl donors more desirable.

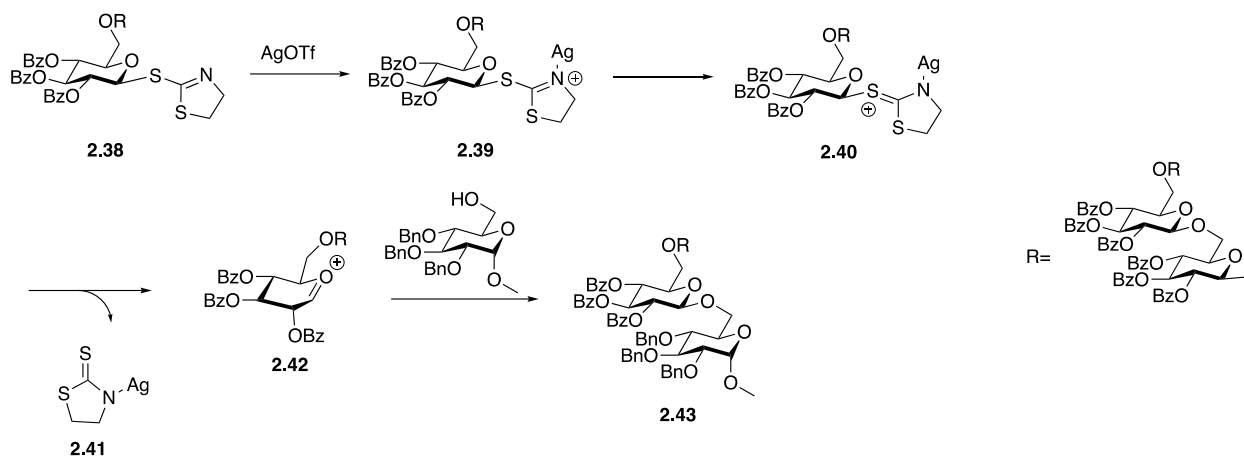
### 2.6.3. Glycosyl Imidates

Glycosyl imidates are a group of highly reactive donors that are widely used and very versatile. Trichloroacetimidates were the first glycosyl imidate introduced to chemical glycosylation in 1980 by Schmidt and coworkers.<sup>36</sup> This group of donors can use a range of promoters such as the mild *p*-toluenesulfonic acid (TsOH)<sup>37</sup> or the more popular activators TMSOTf<sup>38</sup> and  $\text{BF}_3 \cdot \text{Et}_2\text{O}$ <sup>39</sup>. Yu and coworkers found that when phenol is the acceptor  $\text{BF}_3 \cdot \text{Et}_2\text{O}$  is the better promoter, giving only the  $\beta$  anomer.<sup>40</sup> Some methods that have been developed use mild lanthanide salts such as  $\text{Yb}(\text{OTf})_3$  demonstrating that activation does not require harsh protic or lewis acids.<sup>41</sup> Trichloroacetimidates are activated by protonation of (or Lewis-acid coordination to) the nitrogen in **2.32**. This prompts the imido group to leave **2.34** and generates the trichloroacetamide by-product **2.35** along with the glycosyl product **2.37**. Although trichloroacetimidates are highly useful, they are very unstable and require use within two days or storage of  $-30^\circ\text{C}$  or less. They also readily decompose in solution.



Scheme 2.7 Mechanism for Trichloroacetimidate Donor Activation Using *p*-Toluenesulfonic Acid

Thioimidates have been used by Demchenko and coworkers in their one-pot strategy for oligosaccharide synthesis.<sup>42</sup> Two classes of thioimidoyl derivatives, *S*-benzoxazolyl (SBox) and *S*-thiazolyl (STaz) glycosides, were used to synthesize a tetrasaccharide. Using AgOTf as the activator, these investigators were able to alkylate the STaz group **2.39**, facilitating the departure of the thioimidoyl group **2.41** along with the glycosyl product **2.43**.

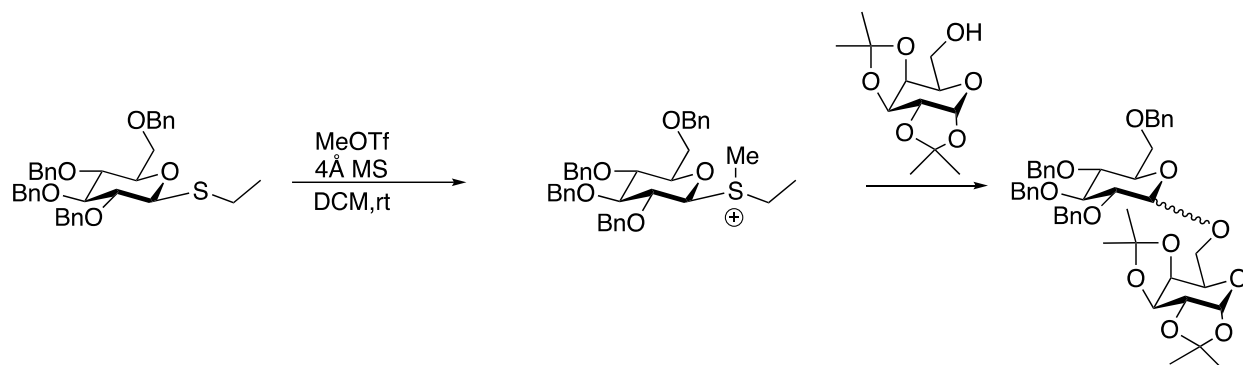


Scheme 2.8 AgOTf promotion of Thioimides

#### 2.6.4. Chalcogenoglycosides

Chalcogenoglycosides, including thioglycosides and selenoglycosides, are popular among synthetic chemists, due to their easy synthesis and handling. Chalcogenoglycosides are very stable and can undergo several synthetic manipulations. Due to their stability, chalcogenoglycosides need strong promoters to facilitate the loss of the leaving group. Mercury and silver salts such as PhHgOTf and AgOTf<sup>43</sup> were used in glycosylation using simple sugars. In later years, thiophilic and selenophilic promoters<sup>44-45</sup> (*i.e.* MeOTf, NIS/TfOH, IDCP) were used to generate the selenonium and sulfonium ions from sulfides and selenides. These are better leaving groups and allow for the

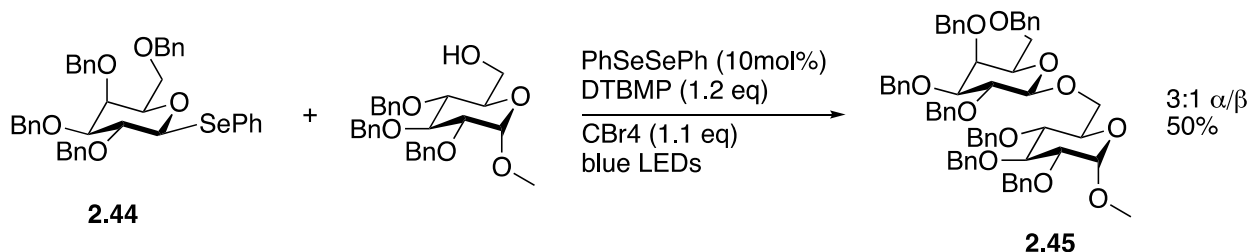
formation of the oxocarbenium ion intermediate. In 1987, Lönn demonstrated the use of the methylating compound MeOTf as a facile activating agent (Scheme 2.9).<sup>49</sup>



Scheme 2.9 Thioglycoside Activation Using Methylating Compound

#### A. Selenoglycosides

To form selenonium ions under milder conditions, selenoglycosides have been activated using a variety of methods. One method is using photochemistry to promote thioglycosides. Spell and coworkers found that irradiation via visible light resulted in  $\alpha$ -selective formation of O-glycosylation products<sup>46</sup> (Scheme 2.10).

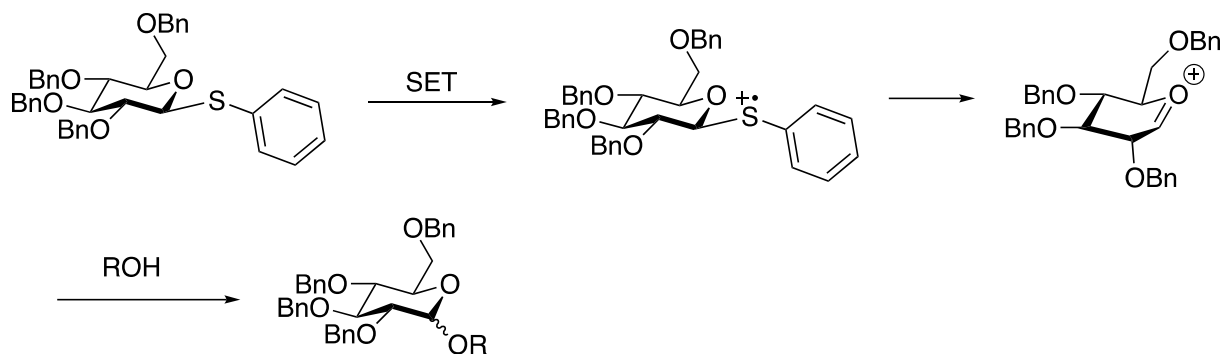


Scheme 2.10 Visible-Light Promoted Activation of Selenoglycoside

#### B. Thioglycosides

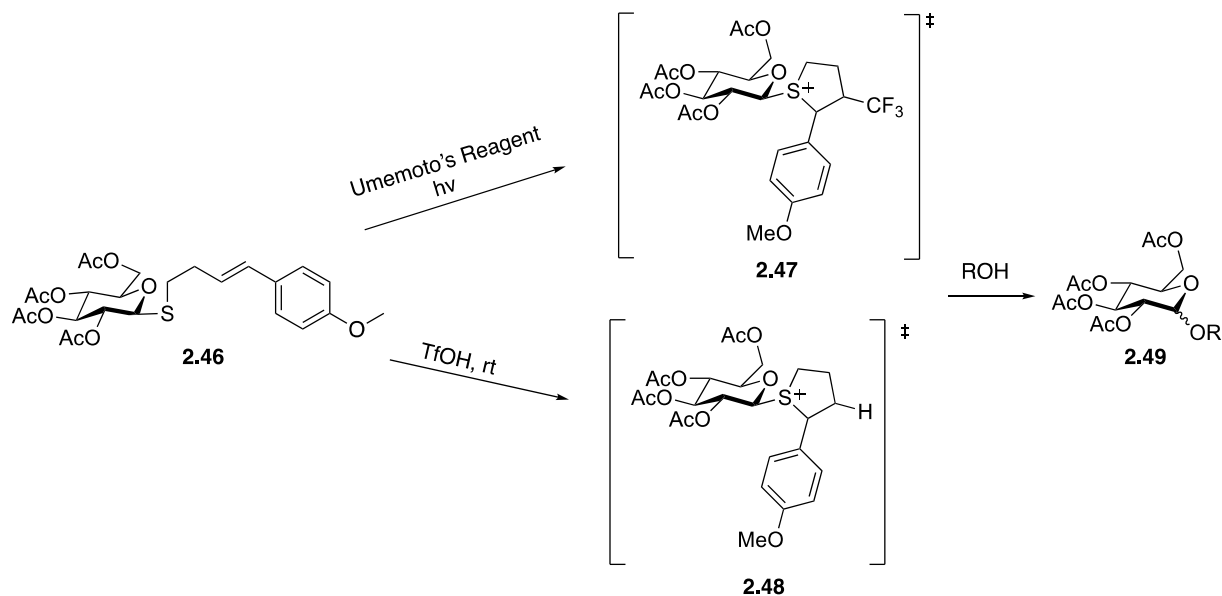
Thioglycosides were first introduced in 1973 by Ferrier and coworkers.<sup>47</sup> In the facile generation, of thioglycosides, a thiol nucleophile is used to attack the anomeric carbon of 1,2-trans-diacetates, glycosyl halides, or trichloroacetimidates to produce the target product.<sup>48</sup>

Sinay and coworkers used an electric current to activate thioglycosides<sup>50</sup> through single electron transfer (SET) resulting in the formation of a sulfur radical cation. After the radical cations were irreversibly fragmented, the oxocarbenium ion is generated (Scheme 2.11).



Scheme 2.11 Electrocemical Glycosylation Approach

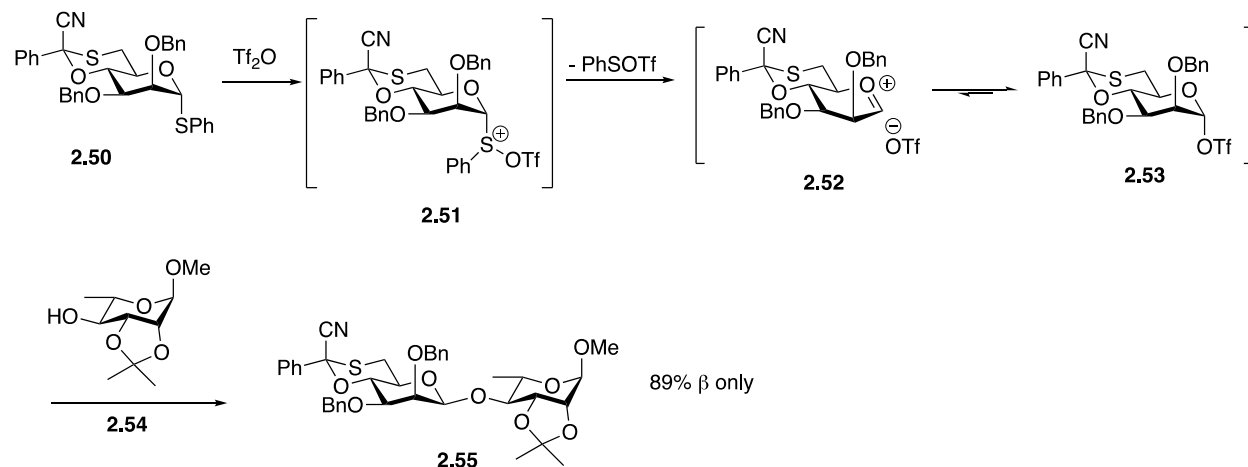
Photochemical and acid promotion have been used in the activation of thioglycosides. Spell and coworkers were able to show that pi stacking with the glycosyl donor and Umemoto's reagent allowed for glycosylation to occur during light promoted glycosylation.<sup>51</sup> Lacey and coworkers were able to develop mild glycosylation conditions using catalytic amounts of TfOH, in DCM at room temperature (Scheme 2.12).<sup>52</sup>



Scheme 2.12 Acid and Light Promoted O-Glycosylation



*In situ* sulfonate formation from thioglycosides is another glycosylation method. A widely used application of sulfonates was discovered by Crich and Sun.<sup>53</sup> Their 4,6-O-benzylidene-directed  $\beta$ -manno-sylation has been used in the synthesis of many mannose-containing glycans. One example from the Crich group is their synthesis of  $\beta$ -D-rhamnopyranosides<sup>54</sup> (Scheme 2.13).



Scheme 2.13 *In Situ* Formation of Glycosyl Sulfonates for the synthesis of  $\beta$ -D-rhamnopyranosides

Overall, chalcogenoglycosides provide for stable glycosidic precursors that can withstand multiple synthetic manipulations. They can also be activated in a multitude of ways, which allows for mild glycosylation conditions.

## 2.7. Conclusion

Oligosaccharides have proven to be a vital component in nature. Stereoselective glycosylation methods are of great interest in glycoscience. The parameters mentioned in this chapter have to be considered in the development of a stereoselective glycosylation protocol. Development of glycosyl donors that are stable and tunable, so that they follow the desired mechanistic pathway, is of growing interest in carbohydrate chemistry. Efforts towards the development of selective glycosylation methods will be discussed in the upcoming chapters.

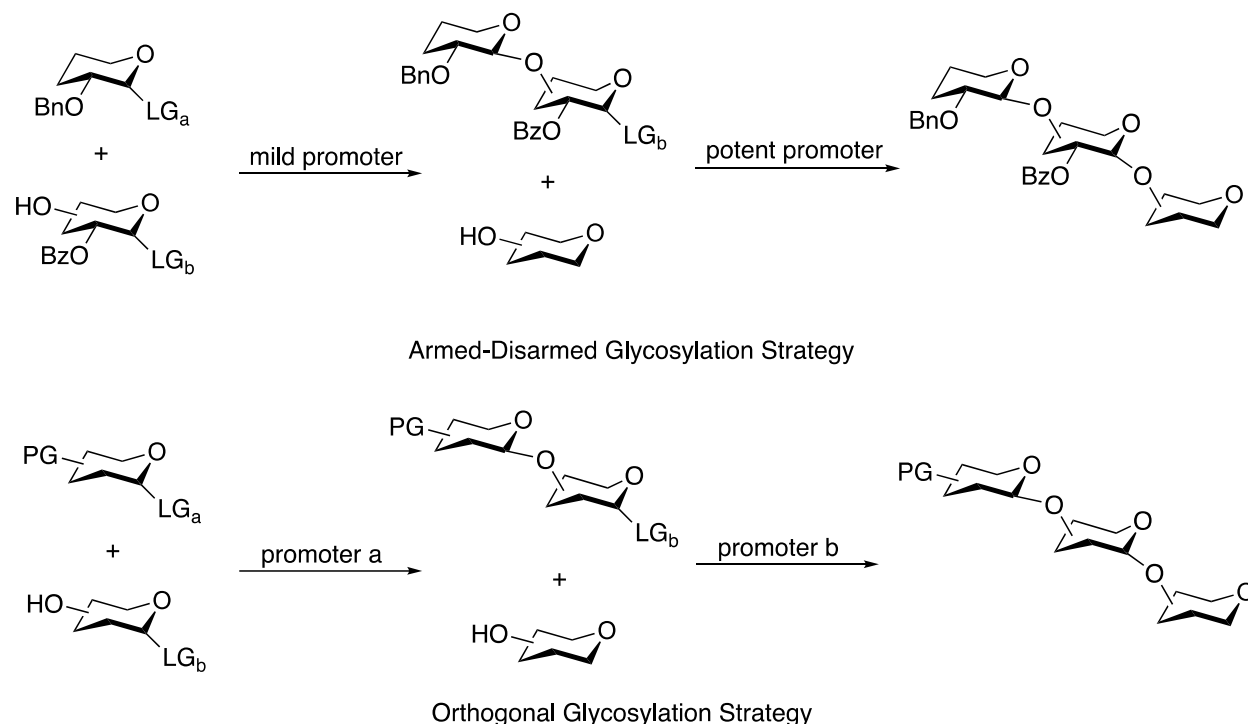
## CHAPTER 3. ORTHOGONALITY OF 4-(4-METHOXYPHENYL)-3-BUTENYLTHIOGLYCOSIDES IN O-GLYCOSYLATION

### 3.1. Introduction

Oligosaccharides have proven to be important in biological processes.<sup>1</sup> Their post-translational conjugation to proteins is ubiquitous in nature, and their attendant roles in (among many other things) molecular recognition events suggests that they are an important target for therapeutics.<sup>1</sup> However, isolation of oligosaccharides in pure, serviceable quantities for biochemical characterization has proven to be very difficult. To overcome this problem, synthetic chemistry has been used for the *de novo* preparation of these oligosaccharides. There are numerous synthetic and purification steps to prepare a targeted oligosaccharide. O-glycosylation, the reaction of alcohol acceptor with the anomeric center of a glycosyl donor, is arguably the most important reaction in this process. To improve the synthetic efficiency of O-glycosylation, an array of approaches have been employed, which include arming/disarming<sup>2</sup> strategies, latent-active strategies<sup>3</sup>, one-pot strategies<sup>4</sup>, and orthogonal/semi-orthogonal<sup>5-6</sup> approaches. Each have a specific purpose in oligosaccharide synthesis, but the orthogonal technique is employed to assemble oligosaccharides selectively. For instance, the armed-disarmed strategy is the condensation of an armed donor with a disarmed acceptor (Scheme 3.1). As stated in Chapter 2, “armed” and “disarmed” are terms for the reactivity conferred by electron-withdrawing and electron-donating protecting groups on glycosyl units. This allows for a chemoselective method of glycosylation. In orthogonal glycosylation strategy,

\* This chapter was adapted with permission from a portion of the article, Lacey, K.; Quarels, R.; Du, S.; Fulton, A.; Reid, N.; Firesheets, A. “Acid-Catalyzed O-Glycosylation with Stable Thioglycoside Donors”, *Org. Lett.* 2018, 20, 5181-5185, Copyright 2020 American Chemical Society.

one leaving group is activated while the other remains intact (Scheme 3.1). This enables oligosaccharide synthesis independent of the reactivities of the components.



Scheme 3.1 Chemoselective Activation Strategy and Selective Activation Strategy

To construct oligosaccharides orthogonally we must first look at the glycosyl units. Thioglycosides and trichloroacetimidates (TCAs) are two main workhorses in *O*-glycosylation (Figure 3.1). As stated in Chapter 2, TCAs are activated by protonation or coordination to the nitrogen group of the imidate by a range of promoters. TCAs are highly reactive, and are activated even under mildly Brønsted- or Lewis-acidic conditions.<sup>7</sup> Unfortunately, TCAs are unstable, and the imidate functionality does not survive multistep synthesis. Thioglycosides, on the other hand, are very stable with the sulfide moiety surviving a host of strongly acidic and basic conditions. As a result, thioglycosides are amenable to multistep synthesis.<sup>8</sup> As of 2018, an unmet goal in the area of carbohydrate synthesis was development of a donor that combined the stability of

thioglycosides with relative ease of activation associated with TCAIs. To achieve this elusive combination, the Ragains group developed a new class of donor.

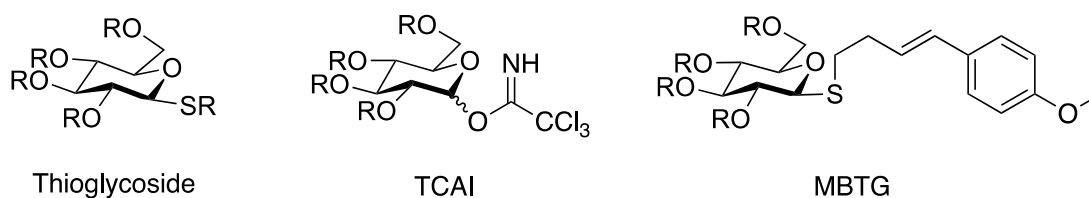
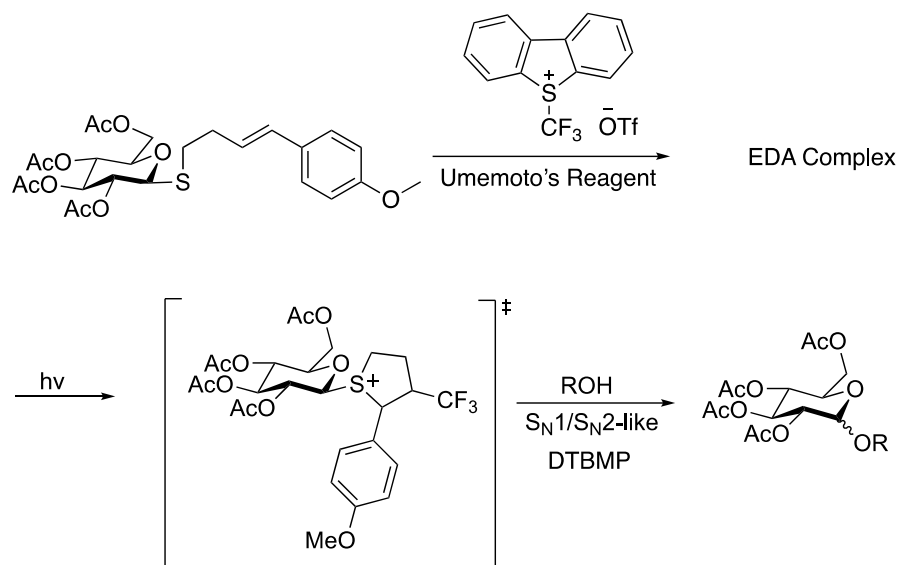
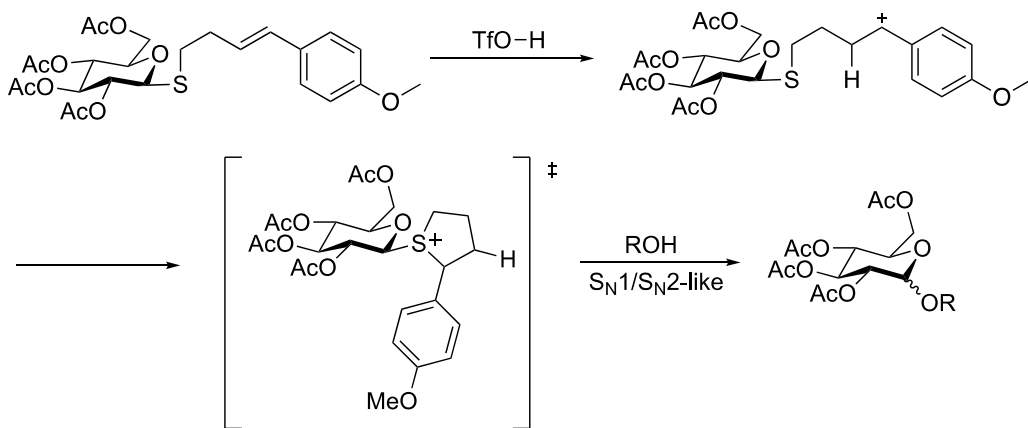


Figure 3.1. Structures of Glycosyl Donors

The Ragains group has developed a new class of thioglycosides: 4-(4-methoxyphenyl)-3-butenylthioglycosides (MBTGs)<sup>9</sup> (Figure 3.1). MBTGs are stable, amenable to multistep synthesis, and activated using mild conditions. These thioglycosides have been activated through visible-light irradiation in the presence of Umemoto's reagent<sup>10</sup> (Scheme 3.1) and by using catalytic amounts of acid at room temperature<sup>9</sup> (Scheme 3.2). In optimization studies for acid catalyzed glycosylation of MBTGs the donor was unreactive at low temperatures. Due to TCAIs high reactivities they are reactive at low temperatures such as -20°C. This prompts the question: can controlling the temperature enable orthogonal activation of TCAIs in the presence of MBTGs? Herein, I report my efforts toward developing an orthogonal glycosylation with a TCAI in the presence of MBTG using temperature control.



Scheme 3.2 Visible Light Promoted O-Glycosylation



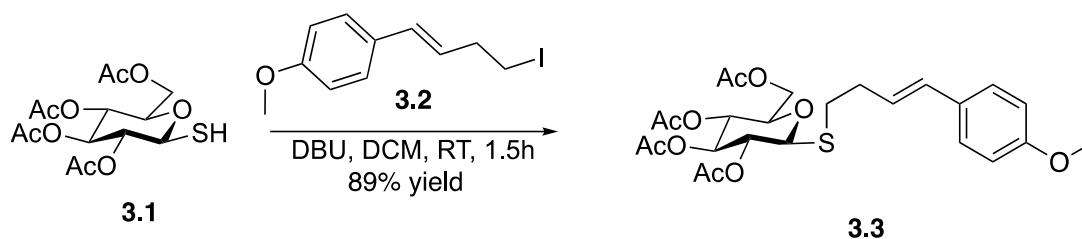
Scheme 3.3 Acid-Catalyzed O-Glycosylation

## 3.2. Results and Discussion

### 3.2.1. Synthesis of MBTG Glycosyl Acceptor

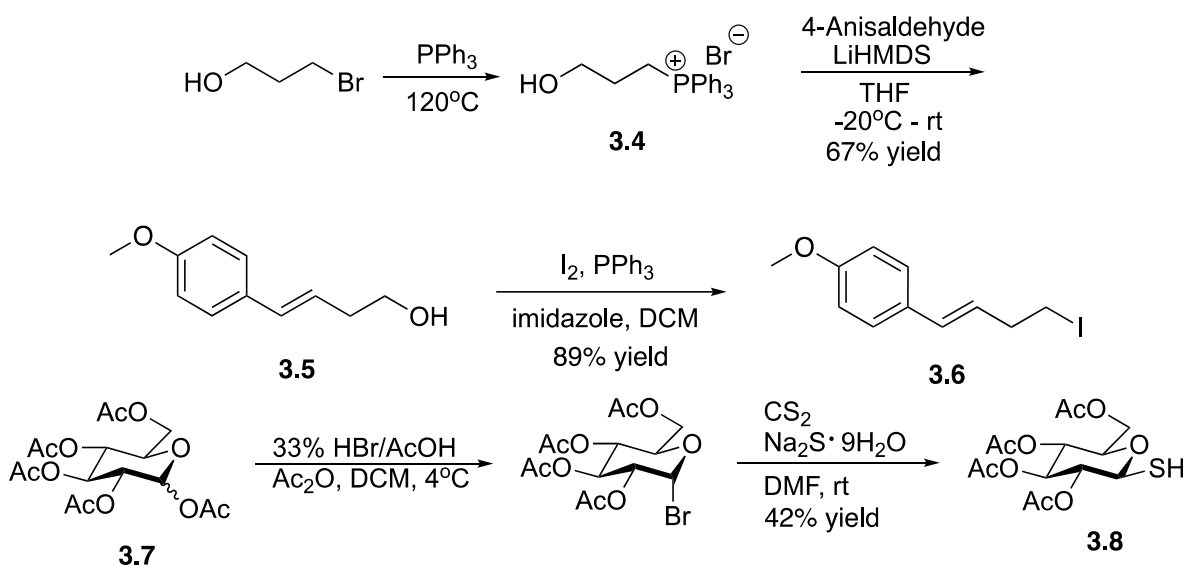
To test my of orthogonality hypothesis, the acceptor being synthesized must be an MBTG with a free hydroxyl that will act as an acceptor in O-glycosylation with a TCAI. The C<sub>6</sub> position was chosen for glycosylation because of its high reactivity as a 1° alcohol acceptor. Also, benzoyl (Bz) protection was implemented because of synthetic practicability (Figure 3.2). The synthesis of 2,3,4-benzoylated MBTG C<sub>6</sub> acceptor starts with the coupling of mercapto glucose **3.1** and alkyl iodide **3.2** using 1,8-

Diazabicyclo[5.4.0]undec-7-ene (DBU) to obtain the tetraacetylated MBTG **3.3** (Scheme 3.4).<sup>11</sup>



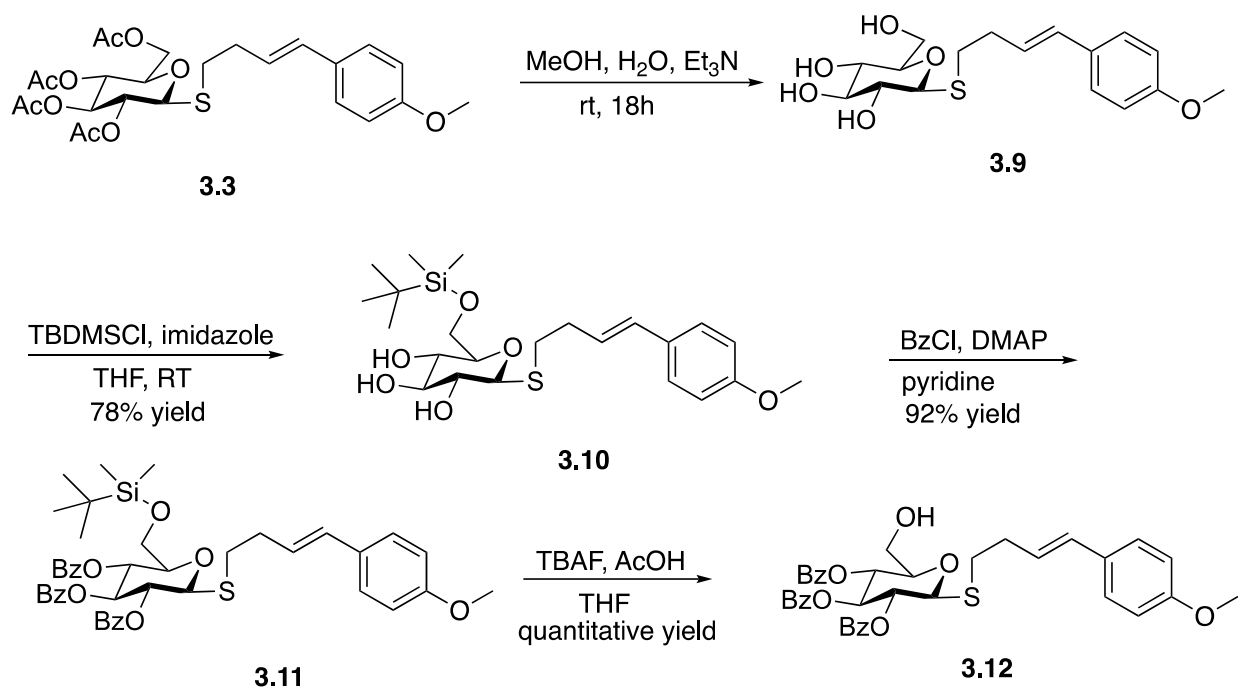
Scheme 3.4 Synthesis of Tetraacetyl MBTG

Synthesis of the alkyl iodide **3.2** begins with generation of the phosphonium salt **3.4** by melting triphenylphosphine at 120°C and adding 3-bromopropanol.<sup>12</sup> Next, a Wittig reaction using the phosphonium salt and p-anisaldehyde in the presence of lithium bis(trimethylsilyl)amide (LHMDS) forms the alcohol **3.5** in 67% yield.<sup>13</sup> Iodination of alcohol under Appel conditions using iodine, triphenylphosphine, and imidazole in dichloromethane to generates alkyl iodide **3.6** in 89% yield to finalize the synthesis.<sup>14</sup> Synthesis of the 1-mercapto glucose **3.8** is straightforward starting with the pentaacetate glucose **3.7**. First, bromination of the C<sub>1</sub> position followed by sulfur displacement of the bromide generates the mercapto glucose **3.8** in a 42% 2-step yield.<sup>15</sup>



Scheme 3.5 Synthesis of Alkyl Iodide and Mercapto Glucose

After coupling, tetraacetylated MBTG **3.3** was then globally deprotected using triethylamine, water, and methanol.<sup>9</sup> Without purification, tetraol **3.9** was subjected to *tert*-butyldimethylsilyl chloride (TBDMSCl) to protect the C<sub>6</sub> position selectively, which resulted in **3.10** in a 78% 2-step yield.<sup>9</sup> Benzoyl protection was employed on the remaining free hydroxyl groups (**3.11**). Tetra-*n*-butylammonium fluoride (TBAF) and acetic acid were used to remove the TBDMS group to afford the desired acceptor **3.12** in quantitative yield.

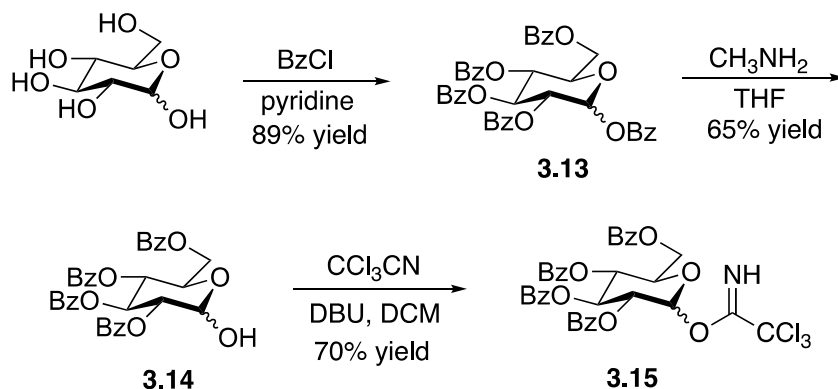


Scheme 3.6 Final Steps for Synthesis of C<sub>6</sub> MBTG Acceptor

### 3.2.2. Synthesis of TCAI Donor

Due to the high reactivity of TCAIs, they must be used as soon as possible after preparation in order to achieve optimal yields.<sup>16</sup> To ensure the *beta* anomer is generated preferentially Bz esters were installed on all free hydroxyls of the donor. To begin the synthesis of tetrabenzoyl TCAI **3.14**, glucose was globally protected using benzoyl chloride in pyridine to afford **3.13** in 89% yield. Next, the C<sub>1</sub> position was selectively

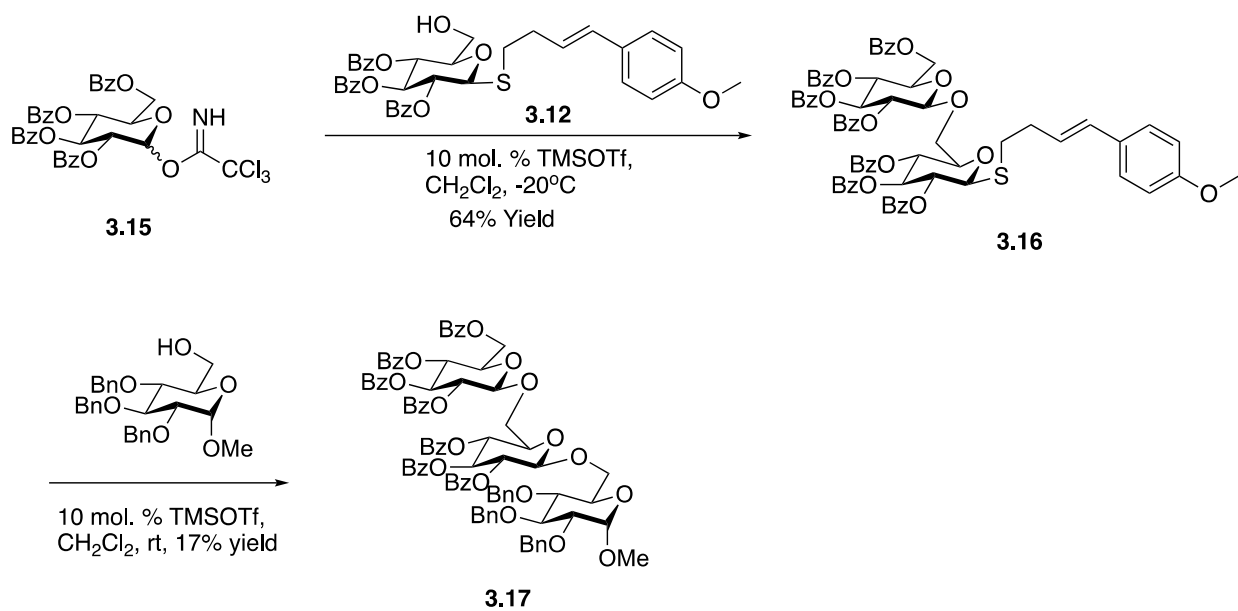
deprotected using methyl amine in THF **3.14**. Lastly, using trichloroacetonitrile in the presence of DBU in DCM, the desired TCAI donor **3.15** was synthesized in 70% yield.<sup>17</sup> Glycosylation of acceptor with donor was conducted within 24h of synthesis of the donor.



Scheme 3.7 Synthesis of TCAI Donor

Glycosylation of the MBTG acceptor **3.12** with the TCAI donor **3.15** with 10 mol% TMSOTf at -20°C in DCM provided 64% yield of disaccharide **3.16** (Scheme 3.7). Activation of the TCAI was accomplished without unwanted activation of the MBTG at -20°C. To further demonstrate the utility of this approach, the disaccharide underwent an additional glycosylation of the alcohol acceptor 2,3,4-tri-O-benzyl- $\alpha$ -D-glucopyranoside with 10 mol% of TMSOTf in DCM. The trisaccharide **3.17** was synthesized in 17% yield at room temperature (18°C) (Scheme 3.7). This supports my hypothesis that the second activation of the MBTG sidechain could occur at room temperature but not at -20°C.





Scheme 3.8 Orthogonal Synthesis of Trisaccharide

### 3.3. Conclusion

Orthogonal glycosylation to generate a trisaccharide product was accomplished through temperature control. Although MBTGs cannot be activated at low temperatures, TCAs can. This enables the selective activation of TCAs in the presence of MBTGs. Further optimization must be conducted for the synthesis of the trisaccharide to increase yield. The scope of this study will be expanded by using common donors for trisaccharide synthesis.

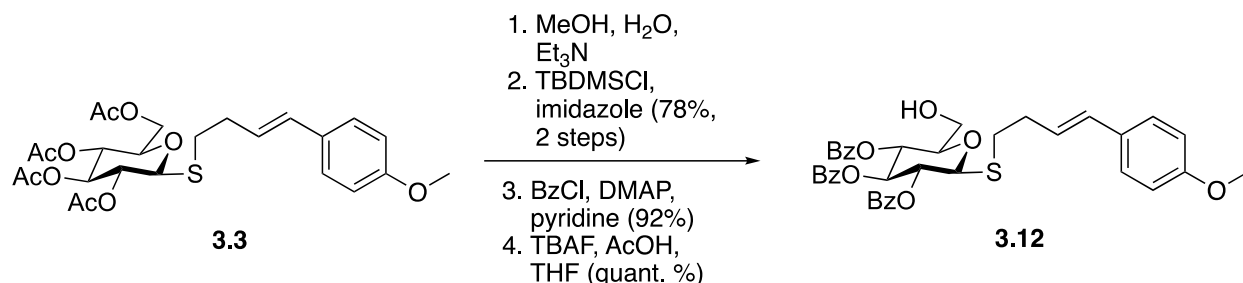
### 3.4. Experimental

#### 3.4.1. General Methods

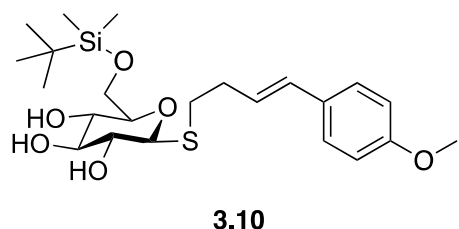
<sup>1</sup>H NMR and <sup>13</sup>C NMR spectroscopy was conducted using a Bruker AV-400 spectrometer or a Bruker AV-500 spectrometer. Mass spectra were attained using an Agilent 6210 electrospray time-of-flight mass spectrometer. All materials were received from commercial suppliers and used without further purification. Flash column chromatography was accomplished using high purity grade 60 Å silica gel (Fluka® Analytical). Qualitative

TLC was performed on aluminum sheets (Merck, silica gel, F254) and observed via UV absorption (254 nm) and staining with anisaldehyde.

### Synthesis of MBTG Acceptor **3.12**:



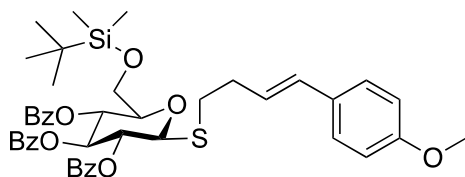
### Synthesis of (*E*)-4-(4-methoxyphenyl)-3-butenyl-β-D-1-thio-6-*O*-*tert*-butyldimethylsilylglucopyranoside **3.10**:



To a solution of MeOH (2.4 mL), H<sub>2</sub>O (0.30 mL), and Triethylamine (0.30 mL) was added to **3.3** (0.36 mmol, 0.19 g) and allowed to stir at room temperature (17°C) overnight (18h). The solution was concentrated to yield the deacetylated thioglycoside and then co-evaporated with toluene (3 x 10 mL) to afford the tetraol (0.160 g) as a white solid. The tetraol was taken forward without further purification. The tetraol (0.102 g, 0.286 mmol) was dissolved in THF (3.8 mL) in a round bottom flask. TBSCl (0.127 g, 0.841 mmol) was added followed by imidazole (0.095 g, 1.20 mmol). The reaction was allowed to stir at room temperature until complete according to TLC analysis (1.5h). The reaction was then diluted with EtOAc (50 mL), and washed with H<sub>2</sub>O (2x15mL). The organic layer was dried over Na<sub>2</sub>SO<sub>4</sub>, and concentrated. Purification by silica gel chromatography (gradient run

from 30% EtOAc in hexanes to 100% EtOAc). Purification yielded 0.102 g (78%) of **3.10** as a colorless oil.  $^1\text{H}$  NMR (500 MHz,  $\text{CDCl}_3$ )  $\delta$  7.27 (d,  $J$  = 9.0 Hz, 2H), 6.84 (d,  $J$  = 8.3 Hz, 2H), 6.38 (d,  $J$  = 15.8 Hz, 1H), 6.12 – 5.99 (m, 1H), 4.36 (d,  $J$  = 9.7 Hz, 1H), 3.94 (dd,  $J$  = 10.4, 4.9 Hz, 1H), 3.85 – 3.80 (m, 1H), 3.80 (s, 3H), 3.59 (m, 2H), 3.52 (s, 1H), 3.40 (m, 2H), 3.15 (br s, 1H), 2.81 (td,  $J$  = 12.0, 5.1 Hz, 2H), 2.71 (br s, 1H), 2.57 – 2.46 (m, 2H), 0.90 (s, 9H), 0.10 (s, 6H).  $^{13}\text{C}$  NMR (126 MHz,  $\text{CDCl}_3$ )  $\delta$  159.1, 131.2, 130.2, 127.4, 125.8, 114.2, 86.0, 78.1, 77.8, 73.0, 72.3, 64.9, 55.4, 33.9, 30.1, 26.0, 18.3, -5.33, -5.34. HRMS  $m/z$  Calcd for  $\text{C}_{23}\text{H}_{38}\text{O}_6\text{SSiNa}$  ( $\text{M}+\text{Na}$ ) $^+$  493.2070, found 493.2075.  $[\alpha]_{\text{D}}^{25}$  = -15.3 ( $c$  = 0.92, DCM). IR ( $\text{cm}^{-1}$ ): 3390, 2927, 2855, 1743, 1607, 1511, 1463, 1247, 1175, 1146, 1069, 1036, 965, 836, 779, 576.

Synthesis of (*E*)-4-(4-methoxyphenyl)-3-butenyl)-2,3,4-tri-*O*-benzoyl-6-*O*-tert-butyltrimethylsilyl- $\beta$ -D-1-thioglucopyranoside **3.11**:

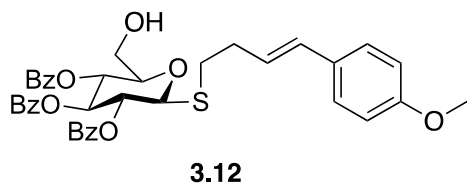


**3.11**

**3.10** (0.42 g, 0.85 mmol) was dissolved in pyridine (3 mL) in a round bottom flask and allowed to stir at room temperature (18°C). BzCl (0.44 mL, 3.8 mmol) was then added and allowed to stir until complete according to TLC analysis (16h). The solution was then diluted with EtOAc (6 mL). The organic layer was washed with sat.  $\text{NaHCO}_3$  (aq.) (2mL) then dried over  $\text{Na}_2\text{SO}_4$ , and concentrated. Silica gel chromatography (isocratic run 5% EtOAc in hexanes) yielded 0.612 g (92%) of benzoylated thioglucopyranoside as a white foam.  $^1\text{H}$  NMR (500 MHz,  $\text{CDCl}_3$ )  $\delta$  7.93 (m, 4H), 7.81 (d,  $J$  = 7.3 Hz, 2H), 7.54 – 7.47 (m, 2H), 7.41 (t,  $J$  = 7.5 Hz, 1H), 7.39 – 7.33 (m, 4H), 7.30 – 7.24 (m, 2H), 7.22 (d,  $J$  = 8.7

Hz, 2H), 6.81 (d,  $J = 8.7$  Hz, 2H), 6.36 (d,  $J = 15.9$  Hz, 1H), 6.11 – 5.99 (m, 1H), 5.86 (t,  $J = 9.5$  Hz, 1H), 5.53 (dt,  $J = 9.6, 4.1$  Hz, 2H), 4.80 (d,  $J = 9.9$  Hz, 1H), 3.90 – 3.81 (m, 3H), 3.80 (s, 3H), 2.95 (ddd,  $J = 12.3, 8.4, 6.4$  Hz, 1H), 2.91 – 2.82 (m, 1H), 2.60 – 2.45 (m, 2H), 0.86 (s, 9H), 0.03 (s, 3H), 0.02 (s, 3H).  $^{13}\text{C}$  NMR (126 MHz,  $\text{CDCl}_3$ )  $\delta$  166.1, 165.4, 165.2, 159.0, 133.8, 133.4, 133.4, 133.3, 131.0, 130.4, 130.3, 130.0, 129.9, 129.9, 129.4, 129.3, 129.1, 128.6, 128.5, 128.49, 128.4, 127.3, 126.1, 114.0, 83.5, 79.7, 74.6, 70.8, 69.6, 62.3, 55.4, 33.3, 29.5, 26.0, 18.5, 0.1, -5.2, -5.3. HRMS  $m/z$  Calcd for  $\text{C}_{44}\text{H}_{50}\text{O}_9\text{SSiNa}$  ( $\text{M}+\text{Na}$ ) $^+$  805.2830, found 805.2838.  $[\alpha]_{\text{D}}^{25} = -14.1$  ( $c = 1$ , DCM). IR ( $\text{cm}^{-1}$ ): 2952, 2929, 2855, 1727, 1603, 1511, 1451, 1246, 1176, 1087, 1067, 1026, 968, 836, 779, 707, 687, 558.

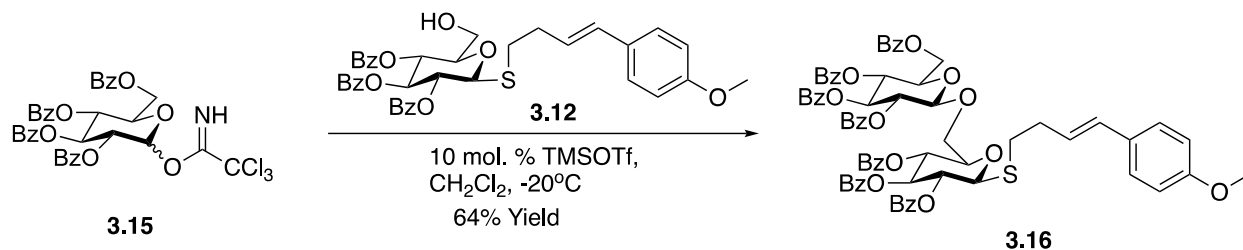
Synthesis of (E)-4-(4-methoxyphenyl)-3-butenyl)-2,3,4-tri-O-benzoyl- $\beta$ -D-1-thioglucofuranoside **3.12**:



1 mL of TBAF (1 M in THF) was acidified to pH 6 by dropwise addition of acetic acid with and carefully monitoring by pH paper. 0.47 mL of the premixed AcOH/TBAF solution was added to **3.11** (0.112 g, 0.143 mmol) in a 10 mL round bottom flask and allowed to stir at room temperature for 6h. The reaction was then diluted with EtOAc (2 mL). The organic layer was washed with sat.  $\text{NH}_4\text{Cl}$  (aq., 2 mL) and sat. NaCl (aq., 3 mL) then dried over  $\text{Na}_2\text{SO}_4$ , and concentrated. Silica gel chromatography (isocratic run 25% EtOAc in hexanes) yielded 0.0957 g (quantitative) of **3.12** as a white solid.  $^1\text{H}$  NMR (500 MHz,  $\text{CDCl}_3$ )  $\delta$  7.94 (d,  $J = 7.7$  Hz, 4H), 7.82 (d,  $J = 7.4$  Hz, 2H), 7.56 – 7.48 (m, 2H), 7.45 –

7.34 (m, 5H), 7.28 (d,  $J = 7.8$  Hz, 2H), 7.21 (d,  $J = 8.7$  Hz, 2H), 6.81 (d,  $J = 8.7$  Hz, 2H), 6.36 (d,  $J = 15.8$  Hz, 1H), 6.04 (dt,  $J = 15.7, 6.9$  Hz, 1H), 5.95 (t,  $J = 9.5$  Hz, 1H), 5.56 (t,  $J = 9.7$  Hz, 1H), 5.50 (t,  $J = 9.7$  Hz, 1H), 4.85 (d,  $J = 10.0$  Hz, 1H), 3.90 – 3.80 (m, 2H), 3.79 (s, 3H), 3.74 (dd,  $J = 12.6, 4.6$  Hz, 1H), 2.98 – 2.83 (m, 2H), 2.58 – 2.44 (m, 2H).  $^{13}\text{C}$  NMR (126 MHz,  $\text{CDCl}_3$ )  $\delta$  166.13, 165.95, 165.33, 159.05, 133.83, 133.44, 133.41, 131.14, 130.22, 130.08, 130.00, 129.85, 129.28, 128.97, 128.70, 128.65, 128.53, 128.45, 127.35, 125.79, 114.05, 83.96, 79.11, 74.10, 70.67, 69.57, 61.71, 55.42, 33.28, 29.94. HRMS  $m/z$  Calcd for  $\text{C}_{38}\text{H}_{36}\text{O}_9\text{SNa}$  ( $\text{M}+\text{Na}$ ) $^+$  691.1972, found 691.1975.  $[\alpha]_{\text{D}}^{25} = -25.4$  ( $c = 1$ , DCM). IR ( $\text{cm}^{-1}$ ): 3513, 3065, 2935, 2836, 1725, 1603, 1510, 1451, 1246, 1176, 1086, 1068, 1026, 969, 849, 802, 736, 707, 500.

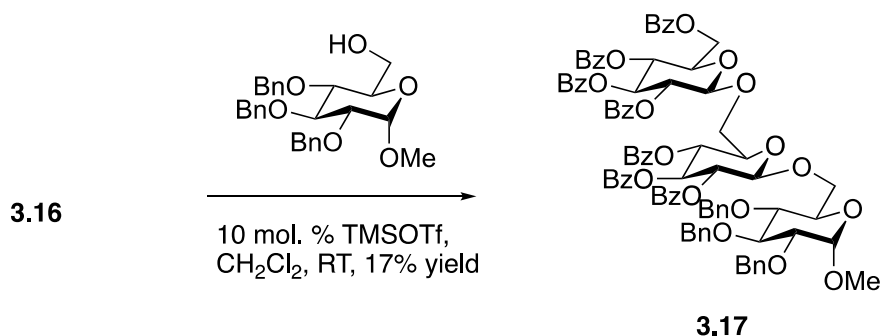
Synthesis of 2,3,4,6-Tetra-*O*-benzoyl- $\beta$ -D-glucopyranosyl-1 $\rightarrow$ 6-(*E*)-4-(4-methoxyphenyl)-3-butenyl)-2,3,4-tri-*O*-benzoyl-6- $\beta$ -D-thioglucopyranoside **3.16**:



(*E*)-4-(4-methoxyphenyl)-3-butenyl)-2,3,4-tri-*O*-benzoyl- $\beta$ -D-1-thioglucopyranoside (**3.12**, 0.1007 g, 0.1506 mmol) and 2,3,4,6-tetra-*O*-benzoyl-D-glucopyranose trichloroacetimidate (**3.15**, 0.1105 g, 0.1491 mmol) were added to a 5mL round bottom flask. The flask was sealed, nitrogen was introduced, and vacuum-purge-backfilled was performed two times before final backfilling with nitrogen. Anhydrous  $\text{CH}_2\text{Cl}_2$  (0.86 mL) was then added to the reaction vessel and the resulting solution was cooled to  $-20^\circ\text{C}$  in a dry ice/MeOH-water bath and allowed to stir for 10 minutes. TMSOTf (2.7  $\mu\text{L}$ , 0.015 mmol)

was added to the solution at -20°C. The reaction solution was allowed to stir at -20°C for 1 h, after which triethylamine (5.4  $\mu$ L, 0.038 mmol) was added to the solution and allowed to stir for 5 minutes. The resulting mixture was concentrated in vacuo. The product **3.16** was obtained as a white solid (0.1184 g, 64%) following purification by column chromatography using 1:1:8 EtOAc/ CH<sub>2</sub>Cl<sub>2</sub>/hexanes to 1:3:6 EtOAc/CH<sub>2</sub>Cl<sub>2</sub>/hexanes gradient solvent system. <sup>1</sup>H NMR (400 MHz; CDCl<sub>3</sub>)  $\delta$ : 8.03-7.98 (m, 4H), 7.91-7.84 (m, 6H), 7.80 (d,  $J$  = 7.0Hz, 2H), 7.76 (d,  $J$  = 7.1Hz, 2H), 7.56-7.21 (m, 23H), 6.79 (d,  $J$  = 8.8Hz, 2H), 6.34 (d,  $J$  = 15.8Hz, 1H), 6.01 (dt,  $J$  = 15.8Hz, 6.9Hz, 2.1Hz, 1H), 5.88 (t,  $J$  = 9.7Hz, 1H), 5.80 (t,  $J$  = 9.5 Hz, 1H), 5.62 (t,  $J$  = 9.7Hz, 1H), 5.50 (dt,  $J$  = 7.8Hz, 2.0Hz 1H), 5.41 (t,  $J$  = 9.7Hz, 1H), 5.36-5.31 (m, 1H), 4.99 (d,  $J$  = 7.8Hz, 1H), 4.67 (d,  $J$  = 9.9Hz, 1H), 4.60 (dd,  $J$  = 12.1Hz, 3.2Hz 1H), 4.44 (dd,  $J$  = 12.2Hz, 5.0Hz 1H), 4.09-3.98 (m, 3H), 3.89-3.85 (m, 1H), 3.77 (s, 3H), 2.77-2.71 (m, 1H), 2.66-2.59 (m, 1H), 2.44-2.33(m, 2H); <sup>13</sup>C NMR (101 MHz, CDCl<sub>3</sub>)  $\delta$  166.05, 165.77, 165.66, 165.36, 165.14, 165.10, 158.83, 133.46, 133.40, 133.23, 133.20, 133.14, 130.89, 130.28, 129.90, 129.84, 129.77, 129.74, 129.69, 129.57, 129.30, 129.22, 128.89, 128.83, 128.80, 128.74, 128.43, 128.40, 128.38, 128.34, 128.27, 128.23, 127.27, 125.90, 113.91, 101.36, 83.45, 78.14, 74.06, 72.87, 72.30, 71.91, 70.58, 69.74, 69.59, 68.59, 62.90, 55.25, 33.03, 29.67. HRMS  $m/z$  Calcd for C<sub>72</sub>H<sub>62</sub>O<sub>18</sub>SNa (M+Na)<sup>+</sup> 1269.3555, found 1269.3556.  $[\alpha]_D^{25}$  = +2.7 ( $c$  = 0.73, DCM). IR (cm<sup>-1</sup>): 3065, 2956, 1725, 1602, 1511, 1451, 1257, 1177, 1091, 1068, 1027, 851, 708, 687.

Synthesis of Methyl 2,3,4-tri-O-benzyl-6-O-(2,3,4-tri-O-benzoyl-6-O-(2,3,4,6-tetra-O-benzoyl- $\beta$ -D-glucopyranosyl)- $\beta$ -D-glucopyranosyl)- $\alpha$ -D-glucopyranoside **3.17**:



**3.16** (0.200 g, 0.160 mmol) and methyl 2,3,4-tri-*O*-benzyl- $\alpha$ -D-glucopyranoside (75.3 mg, 0.160 mmol) were added to a 5 mL round bottom flask. The system was then vacuum-purge-backfilled 2 times and DCM was added (1.05 mL). TMSOTf (1.41  $\mu$ L, 0.016 mmol) was then added to the reaction and set to stir at room temperature until complete according to analysis with TLC (2h). To quench the reaction, triethylamine (20  $\mu$ L) was added and allowed to stir for 2 min. Purification was completed using preparatory TLC with a 2:2:6 EtOAc/DCM/hexane mixture to afford 0.041g (17%) **3.17** as a white solid. Spectral data matched that previously reported in the literature.<sup>17</sup>

## CHAPTER 4. NEW METHODS FOR 1,2-*CIS*-SELECTIVE O-GLYCOSYLATION

### 4.1. Introduction

O-glycosylation has been a topic of great interest for over one hundred years.<sup>1</sup> Development of methodology for efficient, high yielding, and stereoselective O-glycosylations is of great importance.<sup>2</sup> Formation of 1,2-*trans* glycosidic linkages has been accomplished through installation of an acyl protecting group in the C<sub>2</sub> position of the glycosyl donor (Figure 4.1). Development of methodology for 1,2-*cis* glycosidic linkages has not been as straightforward and is a topic of great interest. Oligosaccharides containing 1,2-*cis* glycosides are of high interest due to their biological importance and use in therapeutics.<sup>3</sup>

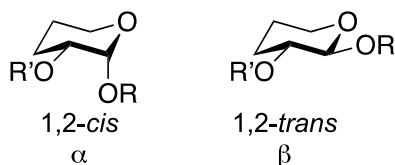
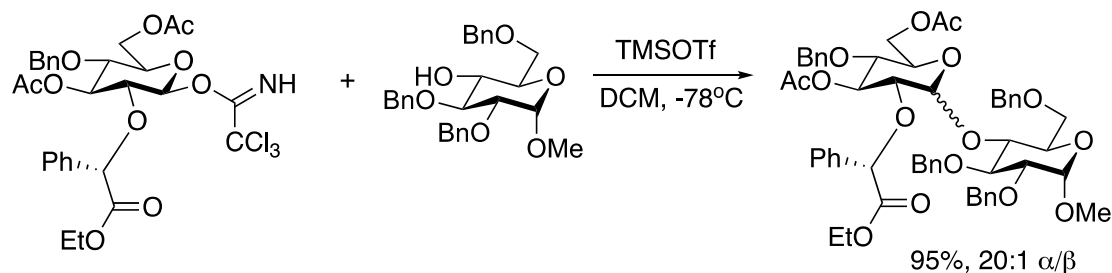


Figure 4.1. Orientation of Glycosidic Linkages

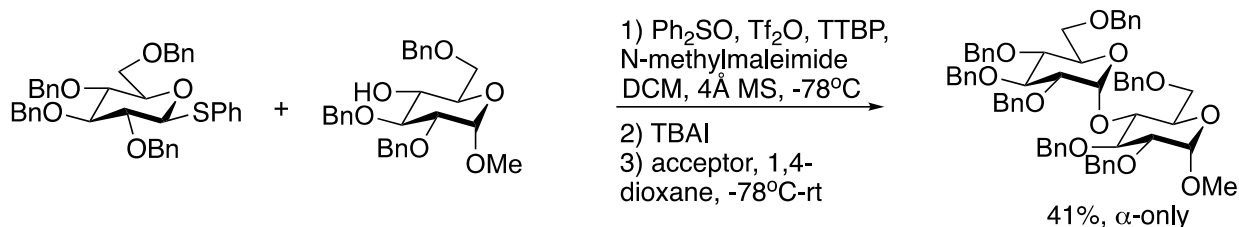
There have been many advances in the formation of 1,2-*cis* glycosidic linkages. Some methods have been effected through protecting group manipulations, activators of glycosyl donor, or the use of additives. Boons and coworkers used a chiral auxiliary on C<sub>2</sub> position of glucose to form 1,2-*cis* linkages (Scheme 4.1a).<sup>4</sup> An auxiliary containing a (*S*)-stereochemistry favors 1,2-*cis* linkages while (*R*)-stereochemistry favors 1,2-*trans* linkages.<sup>4</sup> Bennett and coworkers saw that with pre-activation of the glycosyl donor using Ph<sub>2</sub>SO/Tf<sub>2</sub>O followed by treatment of TBAI enables the formation of 1,2-*cis* linkages (Scheme 4.1b).<sup>5</sup> Ye and coworkers demonstrated that Lewis acid additive favored 1,2-*cis* linkages after pre-activation (Scheme 4.1c).<sup>6</sup>



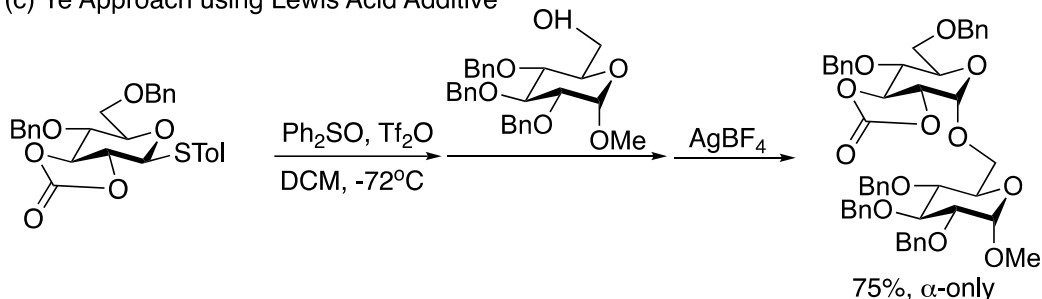
(a) Boons Approach using Chiral Auxiliary<sup>4</sup>



(b) Bennett Approach using Preactivation<sup>5</sup>



(c) Ye Approach using Lewis Acid Additive<sup>6</sup>



Scheme 4.1. Methods of 1,2-*cis*-O-Glycoylation

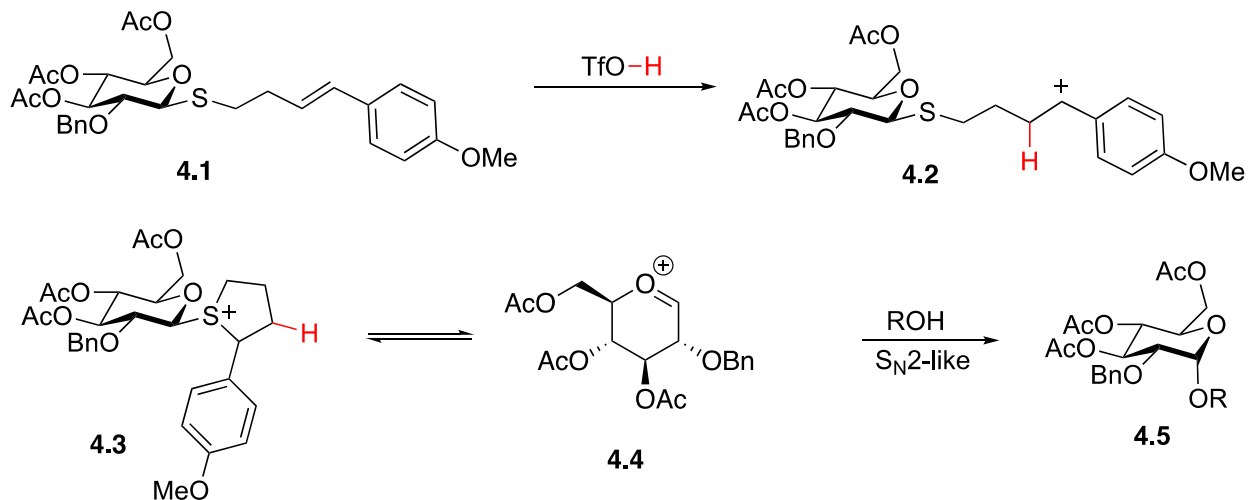
Although these approaches are valuable, they require extra synthetic steps and lack a generalized approach to 1,2-*cis*-selectivity. There is also a lack of a general approach and theory for 1,2-*cis*-selectivity. In this chapter I discuss my efforts for a generalized formation of 1,2-*cis*-glycosidic linkages.

## 4.2. Results and Discussion

### 4.2.1. 4-(4-methoxyphenyl)-3-butenylthioglycosides

Thioglycosides are a major workhorse in oligosaccharide synthesis. These highly stable glycosides can be activated by a wide range of promoters.<sup>7</sup> The Ragains group began investigating 4-(4-methoxyphenyl)-3-butenylthioglycosides (MBTGs) as a new class of thioglycoside donors for oligosaccharide synthesis in 2016.<sup>8</sup> These thioglycosides

are amenable to manipulation, are stable, and can be activated with triflic acid.<sup>9</sup> The question of how to promote *alpha*-selective O-glycosylation using MBTGs then arose. I hypothesized that, by stabilizing the sulfonium ion **4.3**, displacement via backside attack on **4.3** would generate 1,2-*cis*-glycosidic linkages stereospecifically (Scheme 4.2). To contrast, the oxocarbenium **4.4** enables attack on both sides, which results in low selectivity. To prevent neighboring group participation, the protecting group, benzyl, is selectively added to the C<sub>2</sub> alcohol while electron withdrawing Ac groups are placed at C<sub>3</sub>, C<sub>4</sub>, and C<sub>6</sub> to prevent oxocarbenium formation. Benzyl groups are non-participating and less activating, which will favor the S<sub>N</sub>2-like mechanism (Scheme 4.2). This method proves promising to provide a simple protocol for 1,2-*cis*-glycosidic linkages.



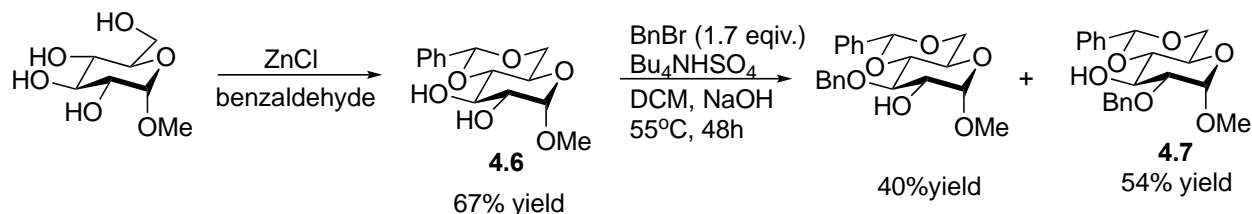
Scheme 4.2 Hypothesized Mechanism of 1,2-*cis*-O-Glycoside Formation from MBTG

#### 4.2.2. Synthesis of 3,4,6-triacetyl-2-O-benzyl MBTG

The synthesis of (*E*)-4-(4-methoxyphenyl)-3-butenyl- $\beta$ -D-1-thio-3,4,6-tri-O-acetyl-2-O-benzylglucopyranoside **4.1** (Scheme 4.2) was performed in 12 steps. Herein, I report the synthesis of this 4-(4-methoxyphenyl)-3-butenylthioglycoside.

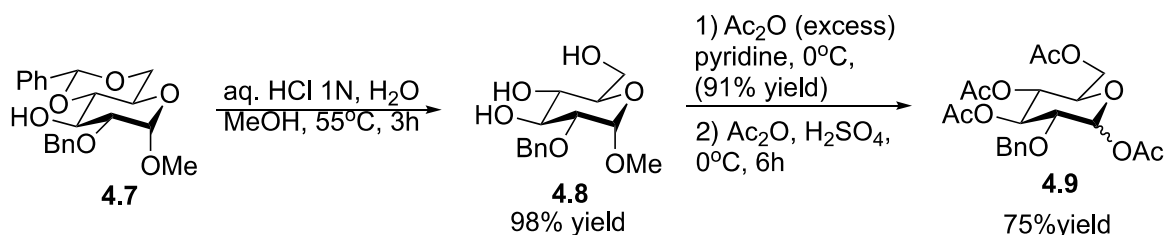
First, protection of C<sub>6</sub> and C<sub>4</sub> alcohols of  $\alpha$ -D-glucopyranoside as the cyclic benzylidene yields **4.6**.<sup>15</sup> A biphasic reaction of **4.6** with BnBr, aqueous 5% NaOH, and

Bu<sub>4</sub>NHSO<sub>4</sub> in DCM enables benzylation of the alcohols in the C<sub>2</sub> and C<sub>3</sub> positions (Scheme 4.3).<sup>16</sup> The purification of these isomers required several attempts to perfect at the cost a substantial amount of product.



Scheme 4.3 Benzylation and Benzylation of  $\alpha$ -D-glucopyranoside

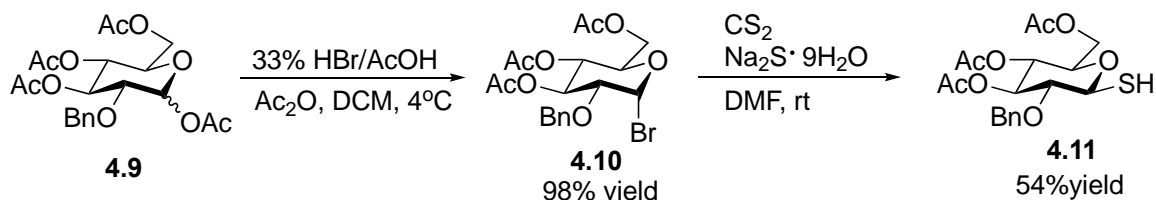
The benzyl protection of the C<sub>2</sub> position is desired to prevent neighboring group participation. Benzyl group at the C<sub>2</sub> position is also less activating than acyl groups at the C<sub>2</sub> position and enables the S<sub>N</sub>2-like mechanism according to Scheme 4.2. Removal of the benzylidene from **4.7** using acidic hydrolysis yielded **4.8** (Scheme 4.4). Acyl groups are electron-withdrawing which destabilizes the oxocarbenium ion. Acetylation of free hydroxyls produced a mixture of equatorial and axial acetates **4.9** (Scheme 4.4).



Scheme 4.4 Benzyldiene Removal and Acetylation

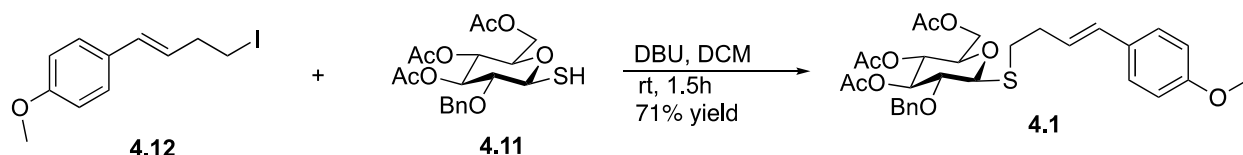
The acetylated sugar was then converted to the  $\alpha$ -bromide **4.10** by treatment with HBr/HOAc and Ac<sub>2</sub>O. Conducting the reaction at room temperature caused over removal of the Bn protecting group in the C<sub>2</sub> position. I hypothesized that the reaction needed to be conducted at a lower temperature. At 0°C the reaction proceeded too slowly (12 h), but by placing the reaction in the refrigerator at 4°C allowed for the reaction to complete

without loss of Bn group (Scheme 4.5). Displacement of the  $\alpha$ -bromide with mercapto generated the thiol **4.11** (Scheme 4.4).



Scheme 4.5 Direct Displacement of Bromine with Thiol

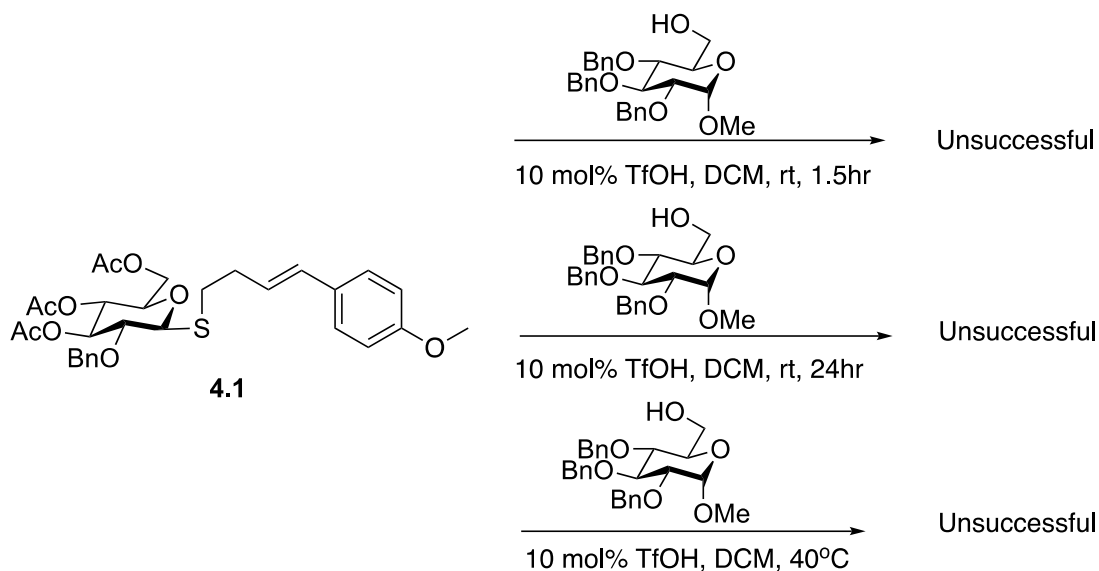
Finally, the thiolate generated by deprotonation of **4.11** attacked iodide **4.12** to produce the desired product **4.1** (Scheme 4.6).



Scheme 4.6 Synthesis of 3,4,6-triacetyl-2-O-benzyl MBTG

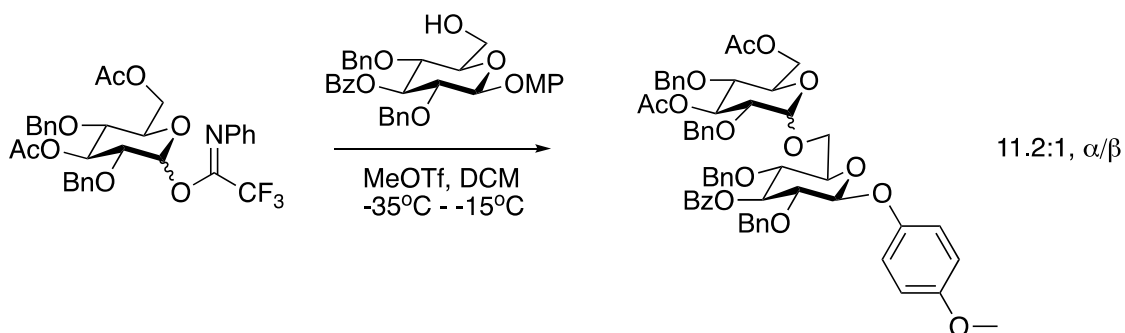
### 4.2.3. Glycosylations Using 3,4,6-triacetyl-2-O-benzyl MBTG

Under standard conditions developed in the Ragains group, I sought to obtain 1,2-*cis* glycosidic linkages. Catalytic amounts of triflic acid were used in an effort to form the stable sulfonium ion for backside attack. Allowing the reaction to stir at room temperature for 1.5 hr did not result in activation of the MBTG. Next, the reaction was allowed to stir for 24 hrs in the hope of activation, but still there was no reaction. Lastly the reaction was heated to 40°C with some donor activation but no desired product (Scheme 4.7).



Scheme 4.7 Glycosylations using 3,4,6-triacetyl-2-O-benzyl MBTG

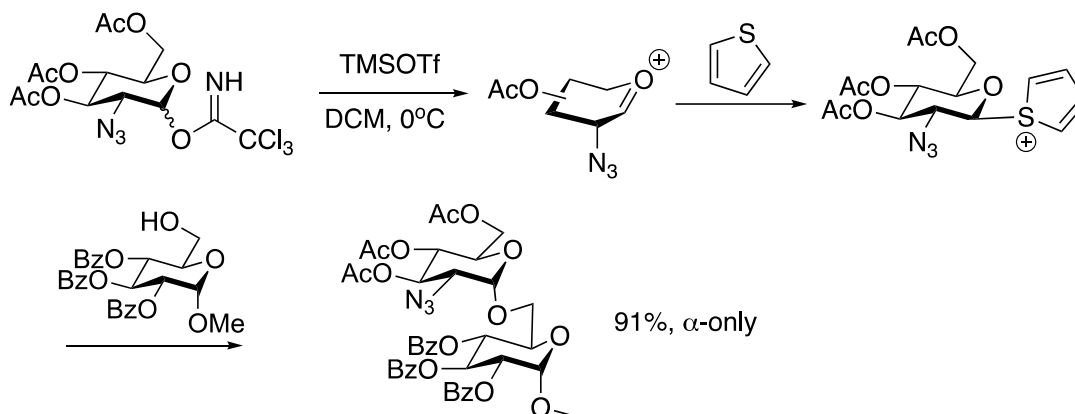
Unfortunately, 1,2-*cis*-glycosidic linkages using MBTGs were not formed due to the inability to activate the donor. This did spark an interest in the role of electron withdrawing groups (EWGs) and their ability to promote 1,2-*cis* glycosidic linkages. It has been demonstrated that EWG have increased 1,2-*cis* selectivity. Nifantiev and coworkers observed 1,2-*cis* selectivity by installing EWGs (Ac) in the C<sub>3</sub> and C<sub>6</sub> positions of an *N*-phenyl trifluoroacetimidate (PTFA) donor (Scheme 4.8).<sup>10</sup> An increase in selectivity was accomplished when the C<sub>6</sub> position was changed to a stronger EWG (Bz).



Scheme 4.8 Nifantiev Glycosylation using Acetate (EWG)

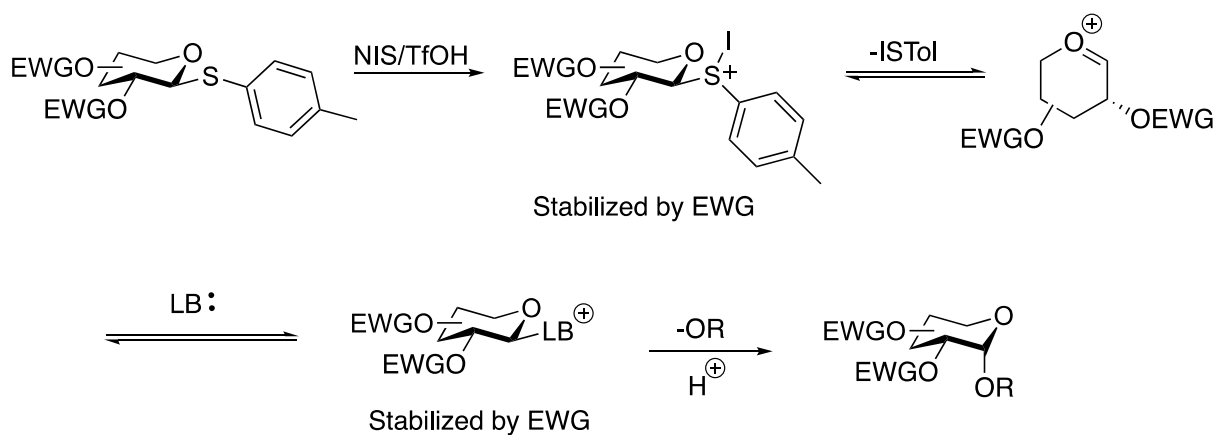
There is also strong evidence of Lewis base (LB) additives aiding in 1,2-*cis* selectivity. Triphenylphosphine oxide (TPPO)<sup>11</sup>, DMF<sup>12</sup>, and thiophene<sup>13</sup> have all been used to

promote 1,2-*cis* selectivity. Boons and coworkers have shown that an excess of thiophene increased 1,2-*cis* selectivity for donors with EWGs (Ac and azido groups). Formation of a sulfonium ion occurs after loss of the leaving group due to the excess of thiophene. The electron withdrawing groups stabilize the sulfonium ion and enable backside attack of the acceptor (Scheme 4.9).



Scheme 4.9 Boons use of Lewis Base and EWG for 1,2-*cis*-selectivity

With this evidence in hand, a new hypothesis arose: the synergy of EWGs and LBs could promote 1,2-*cis*-selective glycosylation in a generalized manner (Scheme 4.10).



Scheme 4.10 Strategy for 1,2-*cis*-Selectivity using EWG and LB

#### 4.2.4. Synthesis of EWG Containing Donor

To test this hypothesis, began with synthesizing a thioglycoside with EWGs installed in the C<sub>4</sub> and C<sub>6</sub> positions. To prevent neighboring group participation Bn groups were installed in the C<sub>2</sub> and C<sub>3</sub> positions (Figure 4.2).

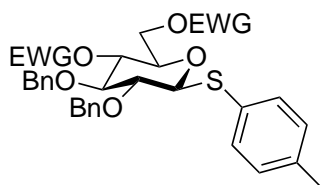
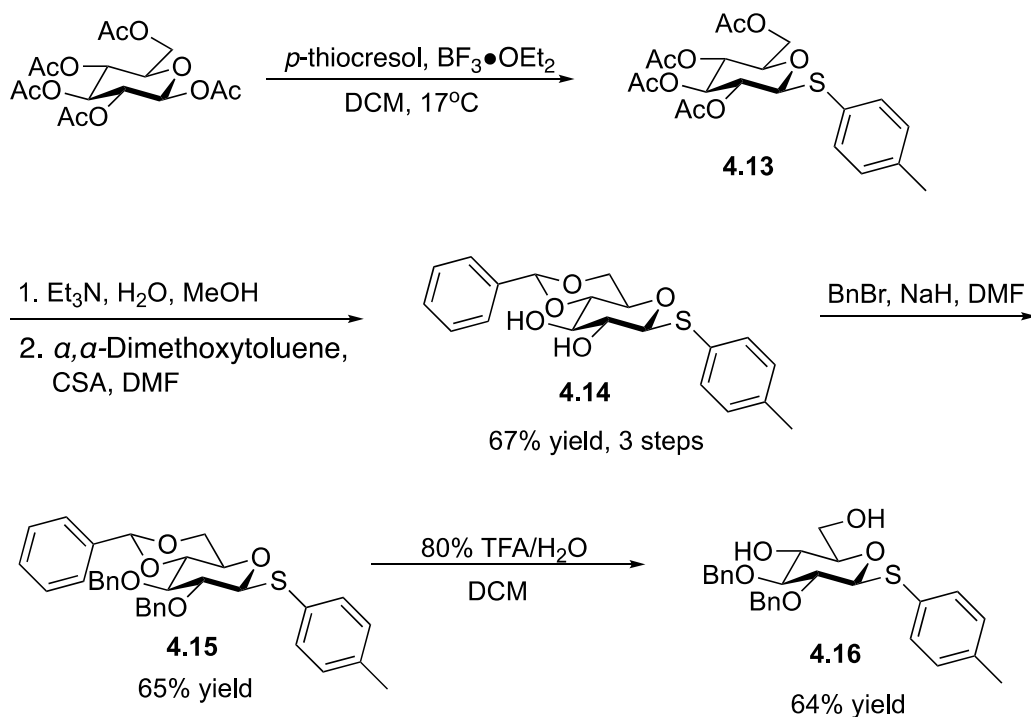


Figure 4.2. Desired Glycosyl Thioglycoside Donor

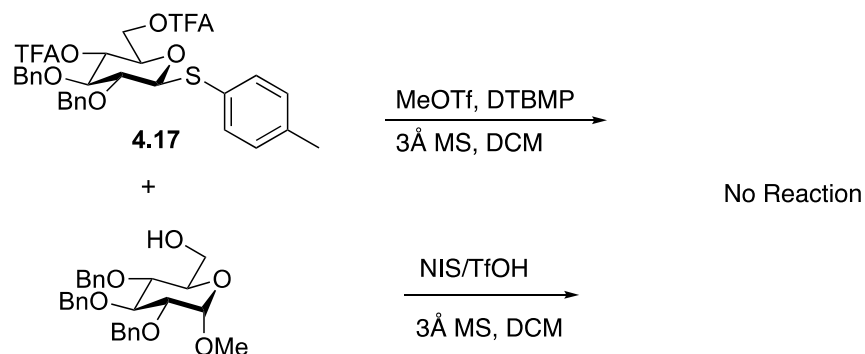
First, *p*-thiocresol was used to make the thioglycoside donor **4.13** followed by deacetylation and installation of benzylidene to give thioglycoside **4.14** in 3 steps with a yield of 67%. Next, benzylation of C<sub>2</sub> and C<sub>4</sub> was accomplished in 65% yield to afford **4.15**. Finally, removal of the benzylidene afforded thioglycoside **4.16** in 64% yield (Scheme 4.11). From here, the EWGs were installed.



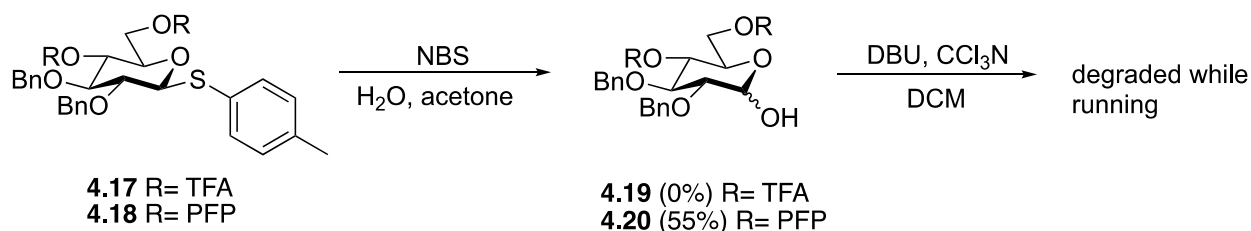
Scheme 4.11 Synthesis of 2,3-di-O-benzyl Thioglycoside

**4.17** (quantitative) R= TFA  
**4.18** (quantitative) R= PFP

Glycosylations using thioglycoside **4.17** were conducted to test the hypothesis. Using a reactive thiophilic promoter (MeOTf) in the presence of 6 eq of thiophene, no reaction was observed. The promoter was switched to a highly reactive thiophile and again no reaction was observed. (Scheme 4.13). To increase the reactivity of the glycosyl donor,



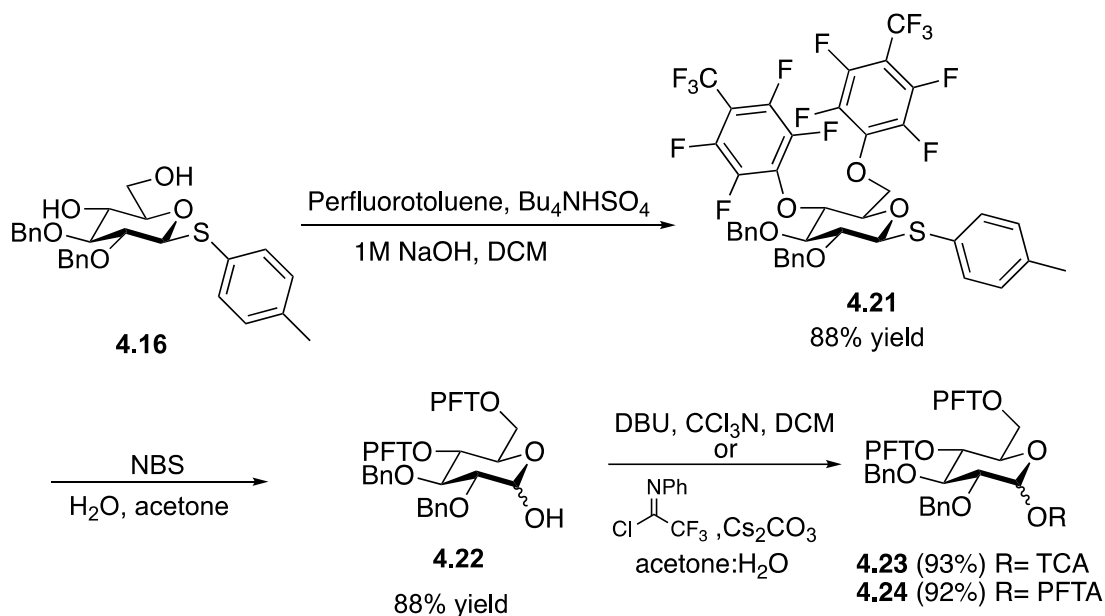
the thioglycoside was changed to a trichloroacetimidate (TCA). Unfortunately, the EWG did not withstand *p*-thiocresol removal and TCA installation (Scheme 4.14).



56



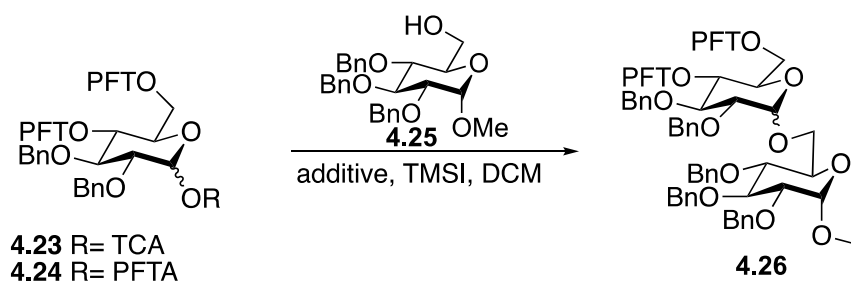
To circumvent the loss of EWG during TCA synthesis, the groups were changed to perfluorotolyl (PFT). Addition of PFT groups was completed in one step (**4.21**, Scheme 4.12). Next, removal of the *p*-thiocresol group (**4.22**), and generation of TCA (**4.23**), as well as the more stable PFTA (**4.24**) were performed (Scheme 4.15).



Scheme 4.15 Synthesis of PFT Containing Imidate Donors

#### 4.2.5. Experiments Using PFP Glycosyl Donors

Trimethylsilyl iodide (TMSI) and LB additive triphenylphosphine oxide (TPPO) has shown to be an effective system for promoting 1,2-*cis* selectivity<sup>11</sup> and was chosen as the standard reaction conditions for this study. Glycosylations with **4.23** and **4.24** of acceptor **4.25** were successful, giving a *cis/trans* ratio of 15:1 and 14:1, respectively (Table 4.1, entries 1 and 3). Entry 2 conditions were used to synthesize the 1,2-*trans* product. Just by adding two EWGs to the donor increased the selectivity.



Entry	Donor	additive	Promoter	Crude <i>cis/trans</i> ( $\alpha/\beta$ )	Yield	<i>cis/trans</i> ( $\alpha/\beta$ )
1	4.23	Ph <sub>3</sub> PO	TMSI	<i>cis</i> only	69%	15:1
2	4.23	(CH <sub>3</sub> O) <sub>3</sub> PO <sub>4</sub>	TfOH	1.10:1	91%	1.13:1
3	4.24	Ph <sub>3</sub> PO	TMSI	14:1	99%	12:1

Figure 4.3. Glycosylation Substrate Scope

### 4.3. Conclusion

Unfortunately, 1,2-*cis*-selectivity using the 3,4,6-triacetyl-2-O-benzyl MBTG was not tested due to its recalcitrance. After long fought battles with the synthesis of the donor the desired product was not obtained after many trials. Fortunately, this study sparked an interest the role of EWGs in 1,2-*cis*-selectivity. We noticed a trend in the synergy between EWGs and LBs for 1,2-*cis*-selectivity. 1,2-*cis*-selectivity was accomplished by exploiting that synergy. Increase in 1,2-*cis*-selectivity was established by incorporating two EWGs into the glycosyl donor. Overall, this study shows the effectiveness of EWGs to obtain 1,2-*cis*-selectivity.

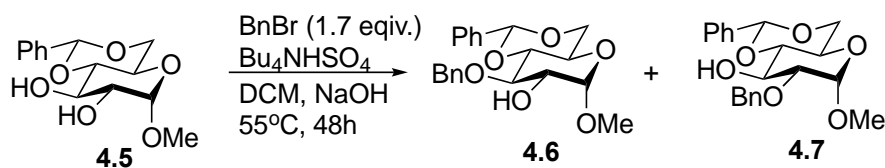
### 4.4. Experimental

#### 4.4.1. General Methods

<sup>1</sup>H NMR and <sup>13</sup>C NMR spectroscopy was conducted using a Bruker AV-400 spectrometer. Mass spectra were attained using an Agilent 6210 electrospray time-of-flight mass spectrometer. All materials were received from commercial suppliers and used without

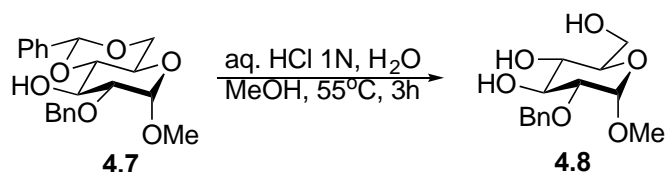
further purification. Flash column chromatography was accomplished using high purity grade 60 Å silica gel (Fluka® Analytical). Qualitative TLC was performed on aluminum sheets (Merck, silica gel, F254) and observed via UV absorption (254 nm) and staining with anisaldehyde.

Synthesis of methyl 2-O-benzyl-4,6-O-benzylidene- $\alpha$ -D-glucopyranoside (**4.6**) and methyl 3-O-benzyl-4,6-O-benzylidene- $\alpha$ -D-glucopyranoside (**4.7**):



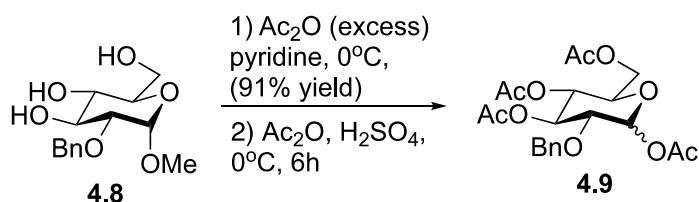
Methyl 4,6-O-benzylidene- $\alpha$ -D-glucopyranoside (9.03 g, 31.9 mmol, 1 equiv.) was added to a 1000mL round bottom flask equipped with stir bar and reflux condenser. Benzyl bromide (6.45 mL, 54.2 mmol, 1.7 equiv.) and tertbutylammonium hydrogensulfate (2.16 g, 6.38 mmol, 0.20 equiv.) was added via syringe at room temperature. The reaction was diluted with dichloromethane (387 mL) and 5% w/w sodium hydroxide (45 mL). The reaction was heated in an oil bath to 55°C until complete (48hrs). The aqueous layer was extracted with dichloromethane (3 x 40 mL). The organic layers were combined and washed with brine, dried over Na<sub>2</sub>SO<sub>4</sub>, filtered and concentrated. The crude product was purified with flash chromatography using a gradient solvent system (20%-50% EtOAc/hexanes). The desired product methyl methyl 2-O-benzyl-4,6-O-benzylidene- $\alpha$ -D-glucopyranoside (**4.7**) was collected and evaporated to dryness (white powder) 6.43g (54%). The spectral data matches that of previously reported.<sup>14</sup>

Synthesis of methyl 2-O-benzyl- $\alpha$ -D-glucopyranoside **4.8**:



Methyl 2-O-benzyl-4,6-O-benzylidene- $\alpha$ -D-glucopyranoside (3.12 g, 8.38 mmol, 1 equiv.) was added to a 250 mL round bottom flask equipped with stir bar and reflux condenser. Methanol (84 mL) was added to dilute. 1N HCl (8.4 mL) and water (4.2 mL) was added simultaneously and the reaction mixture was heated to 55°C. The reaction was monitored by TLC and was allowed to cool to room temperature when the starting material was consumed. The reaction mixture was then evaporated to dryness. The material was purified using flash column chromatography using a mixture of 20% EtOAc/Hexanes to flush benzaldehyde byproduct, and the product was eluted using 100% EtOAc. The purified product was evaporated to dryness resulting in a white powder (2.03 g, 86%). The spectral data matches that of previously reported.<sup>14</sup>

Synthesis of 1,3,4,6-tetra-O-acetyl-2-O-benzyl- $\alpha$ - and  $\beta$ -D-glucopyranose **4.9**:

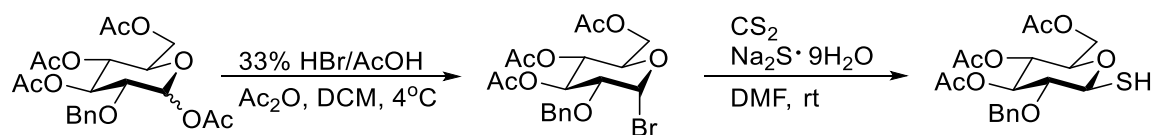


methyl 2-O-benzyl- $\alpha$ -D-glucopyranoside (3.05 g, 10.6 mmol, 1 equiv.) and Pyridine (106 mL) was added to a round bottom flask and set to stir. The reaction was cooled to 0°C and acetic anhydride (66 mL). The reaction stirred at 0°C until complete. The reaction was evaporated then redissolved with ethyl acetate. The organic layer was washed with 10% citric acid (3 x 50 mL), sodium bicarbonate (2 x 40 mL), and brine (1 x 40 mL). The

organic layer was dried with sodium sulfate, filtered and concentrated. The tabulated data is similar to those previously reported.<sup>14</sup>

To a round bottom flask that was flame dried and nitrogen flushed methyl 3,4,6-tri-O-acetyl-2-O-benzyl- $\alpha$ -D-glucopyranoside (3.80 g, 9.26 mmol, 1 equiv.) was added and diluted with acetic anhydride (32 mL, 0.23 M). the reaction was cooled to 0°C. A solution of acetic anhydride (38 mL) and sulfuric acid (1.4 mL) was made and added dropwise over the course of 45 min. The reaction was allowed to stir at 0°C until complete. While the reaction was stirring at 0°C saturated NaOAc (8 mL) was slowly added. Chloroform was added (25 mL). Sodium bicarbonate was added dropwise until no effervescence was seen. The solution was then transferred to a separatory funnel and the organic layer was washed with water (2 x 40 mL), and brine (1 x 40 mL). The organic layer was dried over sodium sulfate, filtered, and concentrated. The crude material was purified using column chromatography using a gradient solvent system (20%-30% Ethyl Acetate/ Hexanes) resulting in 2.35 g (58% yield) of pure product. The tabulated data is similar to those previously reported.<sup>14</sup>

Synthesis of 3,4,6-tri-O-acetyl-2-O-benzyl-1-mercapto- $\beta$ -D-glucopyranoside **4.11**:

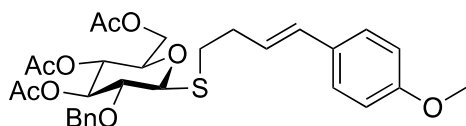


1,3,4,6-tetra-O-acetyl-2-O-benzyl- $\alpha$ - and  $\beta$ -D-glucopyranose (309.9 mg, 0.68 mmol, 1 equiv.) was added to a dry round bottom flask equipped with a stir bar. Dichloromethane (10 mL) was added to dilute. The reaction was cooled to 0°C in ice bath. A 10:1 mixture of 33% hydrobromic acid (1.18 mL) and acetic anhydride (0.12 mL) was made and added dropwise to the reaction. The reaction was taken out of the ice bath and quickly store in

the refrigerator at 4°C. The reaction was monitored by TLC until starting material was consumed. The reaction was quenched with cold water (20 mL). The layers were separated and extracted with dichloromethane (20 mL). The organic layer was washed with sodium bicarbonate (3 x 10 mL), dried over sodium sulfate, filtered, and concentrated resulting in 0.3123 g of product that was carried on to the next step without purification. <sup>1</sup>H NMR (400 MHz, Chloroform-d) δ, 2.02, 2.37, 2.06 (3s, 9H), 3.57 (dd, 1H, *J* = 9.6, 3.92 Hz), 4.06 (dd, 1H, *J* = 12.4, 1.88 Hz), 4.27 (m, 1H), 4.33 (dd, 1H, *J* = 12.48, 4.16 Hz), 4.63 (q, 2H, 12.3 Hz), 5.06 (t, 1H, *J* = 9.6 Hz), 5.48 (t, 1H, *J* = 9.6 Hz), 6.33 (d, 1H, *J* = 3.9 Hz), 4.37 (m, 5H). Sodium sulfide nonahydrate (0.18 g, 1.34 mmol, 2 equiv.) was added to 10 mL of *N,N*-dimethylformamide in a round bottom flask and allowed to stir at room temperature. Carbon disulfide (60 μL, 1.005 mmol, 1.5 equiv.) was added dropwise to the reaction. 3,4,6-Tri-*O*-acetyl-2-*O*-benzyl-α-D-glucopyranosyl bromide was (0.31 g, 0.67 mmol, 1 equiv.) was added in one portion, 5 mL of DMF was used to wash remaining bromide. Solution stirred for 5 min then acidified using hydrochloric acid until yellow color appeared. The solution was diluted with water (25 mL), then extracted with ethylacetate (2x10 mL), dried over sodium sulfate, filtered and concentrated. The product was purified by flash chromatography using a gradient system (20-40% EtOAc/Hexanes) and afforded 0.13g (46% yield) pure product (white solid). <sup>1</sup>H NMR (400 MHz, Chloroform-d) δ 1.92, 2.00, 2.08 (3s, 9H), 2.36 (d, 1H, *J* = 8.12 Hz), 3.45 (t, 1H, *J* = 9.28 Hz), 3.70 (ddd, 1H, *J* = 10.08, 5.16, 2.2 Hz), 4.10 (m, 2H), 4.24 (dd, 1H, *J* = 4.96, 12.4 Hz), 4.56 (t, 1H, *J* = 8.2 Hz), 4.65 (d, 1H, *J* = 11.04 Hz), 4.89 (d, 1H, *J* = 11.08 Hz), 5.01 (t, 1H, *J* = 9.72 Hz), 5.18 (t, 1H, *J* = 9.28 Hz), 7.31 (m, 5H). <sup>13</sup>C NMR (126MHz, CDCl<sub>3</sub>) δ 62.21, 68.47, 76.11,

79.80, 82.26, 128.08, 128.52, 137.35, 169.69, 169.97, 170.64. HRMS (m/z): [M+Na]<sup>+</sup> calcd. For C<sub>19</sub>H<sub>24</sub>O<sub>8</sub>NaS 435.1084, found 435.1094.

Synthesis of (*E*)-4-(4-methoxyphenyl)-3-butenyl-β-D-1-thio-3,4,6-tri-O-acetyl-2-O-benzylglucopyranoside **4.1**:

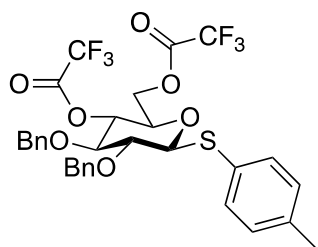


3,4,6-tri-O-acetyl-2-O-benzyl-1-mercapto-β-D-glucopyranoside (0.133 g, 0.315 mmol, 1 equiv.) and toluene (20 mL) was added to a 100 mL round bottom flask charged with a stir bar under nitrogen atmosphere at -10°C. 1,8-Diazabicyclo[5.4.0]undec-7-ene (0.06 mL, 0.41 mmol, 1.3 equiv.) was added. A solution of (*E*)-1-iodo-4-(4-methoxyphenyl)-3-butene (137.3 mg, 0.473 mmol, 1.5 equiv.) and 5 mL of toluene was made and added to the reaction. After consumption of starting material as observed by TLC (1.5hrs), the reaction was quenched with water (20 mL). The solution was then extracted with DCM (2 x 20 mL) followed by dilution with 50 mL of DCM. The organic layer was then washed with 50 mL each of 1M sulfuric acid, saturated sodium bicarbonate, and brine.<sup>4</sup> The organic layer was then dried over sodium sulfate, filtered and concentrated to give 0.21g of crude material. Purified by gradient silica gel chromatography 20%-40% (ethyl acetate/hexanes) to give 0.129 mg (72% yield, need further purification) white solid. <sup>1</sup>H NMR (400 MHz, Chloroform-d) δ 1.90, 2.00, 2.06 (3 s, 9H), 2.55 (m, 2H), 2.86 (m, 2H), 3.49 (t, 1H, *J* = 9.44 Hz), 3.67 (ddd, 1H, *J* = 2.28, 5.24, 10.04 Hz), 3.80 (s, 3H), 4.10 (dd, 1H, *J* = 2.32, 12.28 Hz), 4.24 (dd, 1H, 5.28, 12.28 Hz), 4.56 (t, 2H, *J* = 9.68 Hz), 4.86 (d, 1H, *J* = 11.12 Hz), 4.99 (t, 1H, *J* = 9.68 Hz), 5.19 (t, 1H, *J* = 9.24 Hz), 6.08 (m, 1H), 6.39

(d, 1H,  $J = 15.8$  Hz), 6.83 (d, 2H,  $J = 8.76$ Hz), 7.27 (m, 7H). HRSM ( $m/z$ ):  $[M+H]^+$  calcd.

For  $C_{30}H_{37}O_9S$  573.2153, found 573.2144

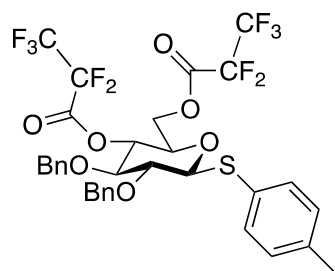
Synthesis of 4-methylphenyl 2,3-di-O-benzyl-4,6-di-O-trifluoroacetyl-1-thio- $\beta$ -D-glucopyranoside **4.17**:



4-methylphenyl 2,3-di-O-benzyl-1-thio- $\beta$ -D-glucopyranoside (0.501 g, 1.07 mmol) was dissolved in  $CH_2Cl_2$  (10.0 mL) and Pyridine (0.17 mL, 2.1 mmol) and allowed to stir at under nitrogen atmosphere. The reaction was cooled to  $0^\circ C$  and Trifluoroacetic anhydride (1.49 mL, 10.7 mmol) was added dropwise to the solution. The solution was allowed to warm to room temperature and stirred overnight (16h). The reaction was quenched using ice. EtOAc was used to dilute and the organic layer was washed with ice water (10 mL), followed by 0.2 N HCl (10 mL), and brine (2 x 20 mL). The organic layer was then dried over  $Na_2SO_4$ , filtered and concentrated to afford 0.704 g (quantitative) of pure product.  $^1H$  NMR (400 MHz,  $CDCl_3$ )  $\delta$  7.44-7.29 (m, 10H), 7.26, 7.16 (dd,  $J = 1.84$  Hz, 7.68 Hz, 2H), 7.11 (d,  $J = 7.84$  Hz, 2H), 5.9 (t,  $J = 9.68$  Hz, 1H), 4.95 (d,  $J = 10.28$  Hz, 1H), 4.80 (d,  $J = 10.8$  Hz, 1H), 4.70 (d,  $J = 10.3$  Hz, 1H), 4.61 (dd,  $J = 1.28$  Hz, 9.76 Hz, 2H), 4.43 (d,  $J = 4$  Hz, 3.80 (m, 2H), 3.54 (t,  $J = 8.68$  Hz, 1H), 2.35 (s, 3H).

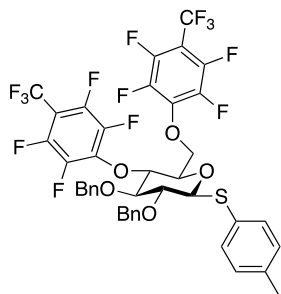
Synthesis of 4-methylphenyl 2,3-di-O-benzyl-4,6-di-O-pentafluoropropionyl-1-thio- $\beta$ -D-glucopyranoside **4.18**:





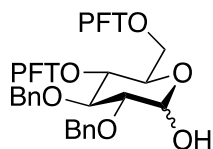
4-methylphenyl 2,3-di-O-benzyl-1-thio- $\beta$ -D-glucopyranoside (0.102 g, 0.214 mmol) was dissolved in  $\text{CH}_2\text{Cl}_2$  (2 mL) and Pyridine (0.03 mL, 0.4 mmol) allowed to stir at under nitrogen atmosphere. The reaction was cooled to  $0^\circ\text{C}$  and Pentafluoropropionic anhydride (0.42 mL, 2.1 mmol) was added dropwise to the solution. The solution was allowed to warm to room temperature and stirred overnight (16h). The reaction was quenched using ice. Ethyl acetate was used to dilute and the organic layer was washed with ice water (10 mL) followed by 0.2N HCl (10 mL), and brine (2 x 20 mL). The solution was then dried over  $\text{Na}_2\text{SO}_4$ , filtered and concentrated to afford 0.16 g (quantitative) pure product.  $^1\text{H}$  NMR (400 MHz,  $\text{CDCl}_3$ )  $\delta$  7.43-7.27 (m, 10H), 7.15 (dd,  $J = 2.48$  Hz, 5.24 Hz, 2H), 7.10 (d,  $J = 8.06$  Hz, 2H), 5.15 (t,  $J = 9.96$ ), 4.94 (d,  $J = 10.28$  Hz, 1H), 4.82 (d,  $J = 10.76$  Hz, 1H), 4.67 (d,  $J = 10.32$  Hz, 1H), 4.61 (dd,  $J = 7.6$  Hz, 2.12 Hz, 2H), 4.51 (dd,  $J = 2.2$  Hz, 14.4 Hz, 1H), 4.36 (dd,  $J = 4.84$  Hz, 12.2 Hz, 1H), 3.82-3.75 (m, 2H), 3.54 (t,  $J = 8.72$  Hz, 1H), 2.35 (s, 3H).

Synthesis of 4-methylphenyl 2,3-di-O-benzyl-4,6-di-O-perfluorotolyl-1-thio- $\beta$ -D-glucopyranoside **4.21**:



4-methylphenyl 2,3-di-O-benzyl-1-thio- $\beta$ -D-glucopyranoside (32.5 mg, 0.07 mmol) and Tetrabutylammonium bisulfate (36.3 mg, 0.107 mmol) were added to a dry round bottom flask.  $\text{CH}_2\text{Cl}_2$  (0.61 mL) was added followed by NaOH (0.61 mL) in a 1:1 ratio. Perfluorotoluene (0.15 mL, 1.1 mmol) was added to the reaction solution and allowed to stir at room temperature (17°C) until completed according to TLC analysis (10 min). The organic phase was then separated from the aqueous phase via separatory funnel. The aqueous phase was acidified with 1N HCl then extracted with DCM (10 mL). Organic phases were then combined and dried over  $\text{Na}_2\text{SO}_4$  and concentrated. Purification by silica gel chromatography (gradient run from 10% EtOAc in hexanes to 20% EtOAc in hexanes). Purification afforded 38.8 mg (88%) of **4.21** as a white solid.  $^1\text{H}$  NMR (500 MHz,  $\text{CDCl}_3$ )  $\delta$  7.38-7.27 (m, 7H), 7.22-7.19 (m, 3H), 7.12 (d,  $J$  = 6.32 Hz, 2H), 6.92-6.89 (m, 2H), 5.00 (d,  $J$  = 8.56, 2H), 4.77-4.70 (m, 3H), 4.64 (d,  $J$  = 8.36 Hz, 2H), 4.37 (d,  $J$  = 9.04 Hz, 1H), 3.93-3.86 (m, 2H), 3.54 (t,  $J$  = 7.34 Hz), 2.36 (s, 3H).  $^{13}\text{C}$  NMR (126 MHz,  $\text{CDCl}_3$ )  $\delta$  138.45, 137.34, 137.09, 132.68, 129.87, 128.86, 128.55, 128.25, 128.16, 128.13, 127.79, 126.21, 88.14, 85.64, 80.87, 78.55, 75.24, 75.20, 72.50, 21.15.  $^{19}\text{F}$  NMR (471 MHz,  $\text{CDCl}_3$ )  $\delta$  -56.23 (td, 3F), -141.96 (m, 2F), -155.35 (m, 1F), -155.89 (td, 1F). HRMS  $m/z$  Calcd for  $\text{C}_{41}\text{H}_{28}\text{F}_{14}\text{KO}_5\text{S}$  ( $\text{M}+\text{K}$ ) $^+$  937.10655, found 937.10667.

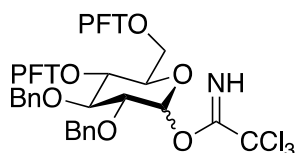
Synthesis of 2,3-di-O-benzyl-4,6-di-O-perfluorotolyl-D-glucopyranose **4.22**:



**4.21** (2.37 g, 2.64 mmol) was dissolved in an 8:1 mixture of acetone (13.5 mL) and  $\text{H}_2\text{O}$  (1.67 mL) at room temperature. N-bromosuccinimide (1.88 g, 10.56 mmol) was added and the reaction was allowed to stir until complete according to TLC analysis (reaction

solution color change from red to colorless). The reaction was then cooled to 0°C and neutralized to pH 7 and concentrated. The crude material was then purified by silica gel column (gradient run 0% to 20% EtOAc in hexanes) to afford pure 1.83 g (88%) of pure **4.22**. <sup>1</sup>H NMR (400 MHz, CDCl<sub>3</sub>) δ 7.34-7.31 (m, 5H), 7.23-7.18 (m, 3H), 6.94-6.88 (m, 2H), 5.19 (t, *J* = 3.08 Hz, 1H), 5.06-4.98 (m, 1H), 4.76- 4.59 (m, 5H), 4.47- 4.32 (m, 2H), 4.17 (t, *J* = 9.04 Hz), 3.62 (dd, *J* = 3.36 Hz, 5.92 Hz, 1H) 3.03 (d, *J* = 2.8 Hz, 1H). <sup>13</sup>C NMR (126 MHz, CDCl<sub>3</sub>) δ 137.69, 137.37, 137.23, 137.10, 128.71, 128.54, 128.36, 128.23, 128.20, 128.13, 127.99, 127.74, 126.42, 126.35, 97.61, 90.91, 83.58, 82.75, 80.50, 80.20, 78.90, 78.77, 78.74, 75.19, 75.08, 74.58, 73.26, 73.06, 72.91, 69.04, 52.92, 45.80, 29.71, 7.91. <sup>19</sup>F NMR (471 MHz, CDCl<sub>3</sub>) δ -56.74 (td, 3F), -141.53 (m, 2F), -154.81 (m, 1F), -155.11 (dd, 1F). HRMS *m/z* Calcd for C<sub>34</sub>H<sub>22</sub>BrF<sub>14</sub>O<sub>6</sub> (M+Br)<sup>-</sup> 871.03817, found 871.03309.

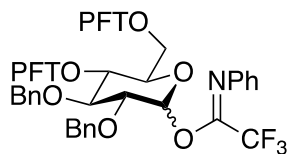
Synthesis of 2,3-di-O-benzyl-4,6-di-O-perfluorotolyl-D-glucopyranosyl trichloroacetimidate **4.23**:



**4.22** (0.317 g, 0.379 mmol) was dissolved in dichloromethane (5 mL) at room temperature (17°C) under nitrogen. DBU (6.8 μL, 0.045 mmol) was added followed by trichloroacetylnitrile (0.38 mL, 3.79 mmol) and allowed to stir until complete according to TLC analysis. The reaction was concentrated and the crude material was purified by silica gel chromatography (isocratic run of 8% EtOAc in hexanes) to afford 0.313 g (93%) of **4.23**. <sup>1</sup>H NMR (400 MHz, CDCl<sub>3</sub>) δ 8.68 (s, 1H), 7.30- 7.26 (m, 8H), 7.22- 7.17 (m, 3H), 6.91 (dd, 2.04 Hz, 5.76 Hz, 2H), 6.45 (d, 3.4 Hz, 1H), 4.76- 4.62 (m, 5H), 4.41 (d, *J* = 11.2

Hz, 2H), 4.21 (t,  $J = 9.08$  Hz, 1H), 3.79 (dd,  $J = 3.44$  Hz, 9.4 Hz, 1H). HRMS  $m/z$  Calcd for  $C_{42}H_{26}F_{17}NNaO_6$  ( $M+Na$ )<sup>+</sup> 986.13809, found 986.13824.

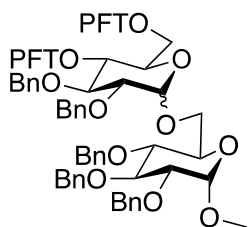
Synthesis of 2,3-di-O-benzyl-4,6-di-O-perfluorotolyl-D-glucopyranosyl 1-(N-phenyl)-2,2,2-trifluoroacetimidate **4.24**:



**4.22** (0.302 g, 0.379 mmol) was dissolved in a 10:1 mixture of acetone (10 mL) and water (1 mL). Cesium carbonate (0.247 g, 0.758 mmol) was added followed by 2,2,2-trifluoro-N-phenyl-acetimidoyl chloride (0.247 g, 0.758 mmol) at room temperature (18°C) and allowed to stir overnight (16 h). The reaction was quenched with triethylamine (0.34 mL) and concentrated. The crude material was purified by silica gel chromatography (isocratic run 8% EtOAc in hexanes) to afford 0.335 g (92%) of **4.24**. <sup>1</sup>H NMR (500 MHz, CDCl<sub>3</sub>)  $\delta$  7.34-7.27 (m, 10H), 7.23-7.19 (m, 4H), 7.16-7.09 (m, 2H), 6.93-6.90 (m, 3H), 6.79 (d,  $J = 7.8$  Hz, 1H), 6.74 (d, 7.75 Hz, 2H), 5.08 (d,  $J = 11.15$  Hz, 1H), 4.82- 4.60 (m, 7H), 4.41 (d,  $J = 11.15$  Hz, 1H), 4.36 (d,  $J = 11.3$  Hz, 1H), 4.19 (t, 7.36 Hz, 1H), 3.77 (s, 1H). <sup>13</sup>C NMR (126 MHz, CDCl<sub>3</sub>)  $\delta$  143.09, 142.99, 137.19, 136.98, 136.95, 136.90, 129.15, 128.87, 128.82, 128.69, 128.65, 128.29, 128.26, 128.25, 128.09, 127.86, 127.80, 127.76, 127.40, 126.44, 126.34, 124.70, 124.57, 120.64, 119.30, 119.14, 118.65, 115.97, 83.48, 80.44, 80.39, 79.17, 78.12, 75.36, 75.18, 74.96, 73.77, 73.36, 72.51, 71.95, 71.60, 53.38. <sup>19</sup>F NMR (471 MHz, CDCl<sub>3</sub>)  $\delta$  -56.27 (m, 3F), -141.84 (m, 2F), -155.20 (dd, 1F), -155.72 (dd, 1F). HRMS  $m/z$  Calcd for  $C_{42}H_{26}F_{17}NNaO_6$  ( $M+Na$ )<sup>+</sup> 986.13809, found 986.13824.

General glycosylation procedure A for Figure 4.3

To an oven dried 4 ml Wheaton vial with a stir bar, 0.7 equivalent of a hydroxyl bearing acceptor was added (0.105 mmol), followed by 1 equivalent of glycosyl imidate donor (0.15 mmol). 6 equivalence of  $\text{Ph}_3\text{PO}$  or 11.4 equivalence of  $(\text{CH}_3)_3\text{PO}_4$  was added. The vial was capped and with a septum then flushed with nitrogen gas then 2 mL of dichloromethane was added. The reaction was monitored by TLC and allowed to stir for 24h. Once all of the donor was consumed the reaction was diluted with dichloromethane (10 mL) and quenched with  $\text{Na}_2\text{S}_2\text{O}_3$ . Products were purified by silica gel chromatography (isocratic run of 10% EtOAc, 40% dichloromethane, 60% hexanes) of Methyl (2,3-di-O-benzyl-4,6-di-O-perfluorotolyl)-(1→6)-2,3,4-tri-O-benzyl-D-glucopyranoside **4.26**:



$^1\text{H}$  NMR (500 MHz,  $\text{CDCl}_3$ )  $\delta$  7.44 – 7.37 (m, 4H), 7.37 – 7.31 (m, 11H), 7.30 – 7.26 (m, 7H), 7.25 – 7.16 (m, 6H), 6.90 (ddd,  $J$  = 14.2, 7.2, 4.4 Hz, 3H), 5.07 – 4.96 (m, 4H), 4.90 (d,  $J$  = 3.3 Hz, 1H), 4.82 (d,  $J$  = 10.7 Hz, 1H), 4.77 – 4.62 (m, 4H), 4.62 – 4.55 (m, 5H), 4.52 (d,  $J$  = 3.5 Hz, 2H), 4.30 (d,  $J$  = 11.3 Hz, 1H), 4.18 (dt,  $J$  = 9.9, 3.3 Hz, 1H), 4.14 – 4.07 (m, 2H), 4.02 (t,  $J$  = 9.2 Hz, 1H), 3.86 – 3.79 (m, 2H), 3.68 (d,  $J$  = 10.2 Hz, 1H), 3.62 (t,  $J$  = 9.4 Hz, 1H), 3.53 (dd,  $J$  = 9.5, 3.4 Hz, 1H), 3.45 (dd,  $J$  = 9.6, 3.6 Hz, 1H), 3.41 (s, 3H), 3.31 (s, 3H).  $^{13}\text{C}$  NMR (126 MHz,  $\text{CDCl}_3$ )  $\delta$  145.87, 141.76, 139.70, 138.67, 138.46, 138.13, 138.09, 137.58, 137.50, 137.12, 136.39, 128.77, 128.74, 128.69, 128.56, 128.55, 128.52, 128.46, 128.45, 128.42, 128.40, 128.38, 128.31, 128.27, 128.23, 128.21, 128.17, 128.13, 128.10, 128.01, 128.00, 127.92, 127.89, 127.85, 127.72, 127.64, 127.57, 127.47,

126.51, 126.48, 126.41, 126.35, 118.65, 98.11, 96.71, 91.78, 82.70, 82.18, 80.58, 80.15, 79.90, 79.72, 79.03, 78.90, 77.76, 75.96, 75.85, 75.34, 75.08, 74.97, 73.43, 73.32, 73.00, 72.66, 72.39, 71.79, 70.26, 68.85, 66.51, 55.23, 29.72.  $^{19}\text{F}$  NMR (471 MHz,  $\text{CDCl}_3$ )  $\delta$  - 52.24 – -63.71 (m, 2F), -138.73 – -144.44 (m, 1F), -152.36 – -157.84 (m, 1F).

## CHAPTER 5. NEW STUDIES ON THE TOTAL SYNTHESIS OF AN ACINETOBACTER BAUMANNII LIPOOLIGOSACCHARIDE CORE PENTASACCHARIDE

### 5.1. Introduction

*Acinetobacter baumannii* is an aerobic, gram negative bacterium that affects those in healthcare settings.<sup>1</sup> Those who are at high risk are patients who require mechanical ventilation, burn victims, and victims of traumatic injury.<sup>2</sup> The bacteria forms robust biofilms on dry surfaces that can last several days and resists strong cleaning agents.<sup>4</sup> It is also one of the most common causes of infections in ICU patients.<sup>3</sup> *A. baumannii* causes sepsis, septicemia, pneumonia, urinary tract infections, and is associated with high mortality rates.<sup>5</sup> An issue of significant concern is the increased prevalence of *A. baumannii* isolates having resistance to commonly prescribed antibiotics.<sup>6</sup> Therefore, development of a preventative measure is of great interest.

Vaccines are an effective preventative measure. Vaccines often contain a weakened or killed disease-causing organism. The vaccine stimulates the body's immune system to build adaptive immunity. To contrast, glycoconjugate vaccines consist of synthetic carbohydrates conjugated to a carrier protein. The glycoconjugate vaccine enables T cells and B cells to participate in the development of robust adaptive immunity. *A. baumannii* has been the subject of numerous attempts at vaccine development. Targets include: k1 capsular polysaccharide (K1 CPS)<sup>7</sup>, outer membrane proteins (OmpA<sup>8</sup> and OmpW<sup>9</sup>), biofilm associated protein<sup>10</sup>, a whole cell vaccine<sup>11</sup>, and the poly-1→6-linked *N*-acetylglucosamine exopolysaccharide (PNAG)<sup>12</sup>. Although several targets for the prevention of *A. baumannii* infections have been explored, there are no FDA-

approved vaccines to date. The variability of *A. baumannii* strains have made it difficult to establish a target that will cover a significant portion of its population.

The lipopolysaccharide (LPS) and lipooligosaccharide (LOS), located on the outer membrane, have proven to be immunogenic in other gram negative bacteria.<sup>13</sup> LPS/LOS are located on the surface of gram negative bacteria and consist of a few components. A toxic lipid A portion anchors the molecule to the surface of the cell. Attached to the lipid A portion is the core oligosaccharide that consists of an inner core and an outer core. LOS consists of Lipid A, inner core, and outer core; LPS consists of Lipid A, inner core, outer core, and a polymeric O-antigen which is attached to the outer core.<sup>14</sup>

*A. baumannii* only contains LOS and not LPS.<sup>15</sup> Biosynthetic gene clusters associated with the *A. baumannii* outer core oligosaccharide of the LOS are located in the so-called OCL locus (OCL1)<sup>16</sup> in eight out of ten *A. baumannii* genomes.<sup>17</sup> As such, synthesis of a glycoconjugate vaccine that contains the core oligosaccharide of *A. baumannii*, leaving out the toxic lipid A portion, and a carrier protein has promise to be an effective and unexplored route.

The structure of the OCL1 associated LOS core oligosaccharide of *A. baumannii* isolate ATCC 19606 has been published<sup>18</sup> and consists of a decasaccharide attached to the lipid A portion (Figure 5.1). The pentasaccharide indicated with a black square consists of five sugar moieties: 3-deoxy-D-manno-oct-2-ulosonic acid (Kdo) (**A**), D-glucosamine (**B**), *N*-acetyl-D-glucosaminuronic acid (GlcNAcA) (**C**), D-galactosamine (**D**), and D-glucose (**E**). Moreover, three out of five sugars are not present, or are rare, in mammalian cells (**A**, **C**, and **D**) making it potentially a strong target for vaccine development.



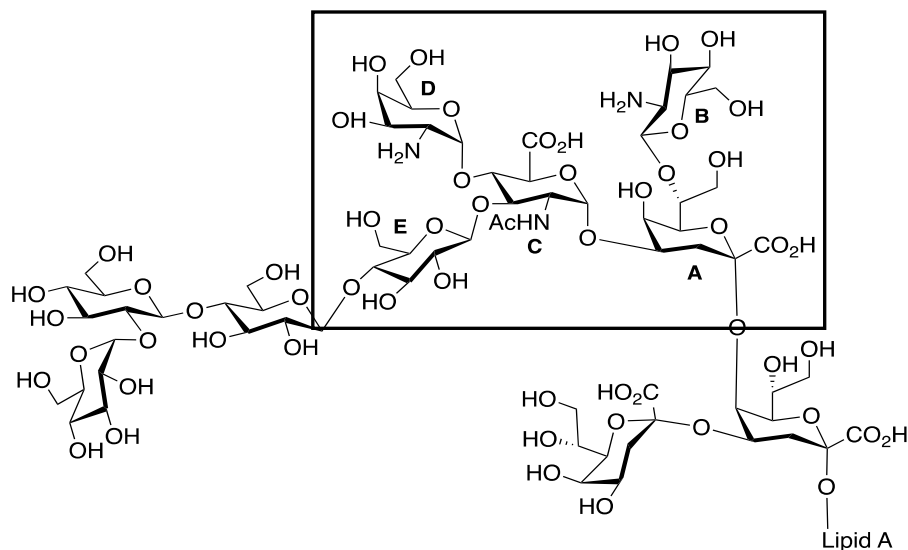


Figure 5.1. LOS Core Oligosaccharide of *A. baumannii*

Synthesis of this complex pentasaccharide first requires synthesis of the individual monosaccharides (Figure 5.2). The development of the proposed LOS-conjugate vaccine for prevention of *A. baumannii* infection will provide relief for those most vulnerable to the bacterium. Herein, chemical synthesis of the core pentasaccharide-based vaccine for the prevention of *A. baumannii* infection is being developed.

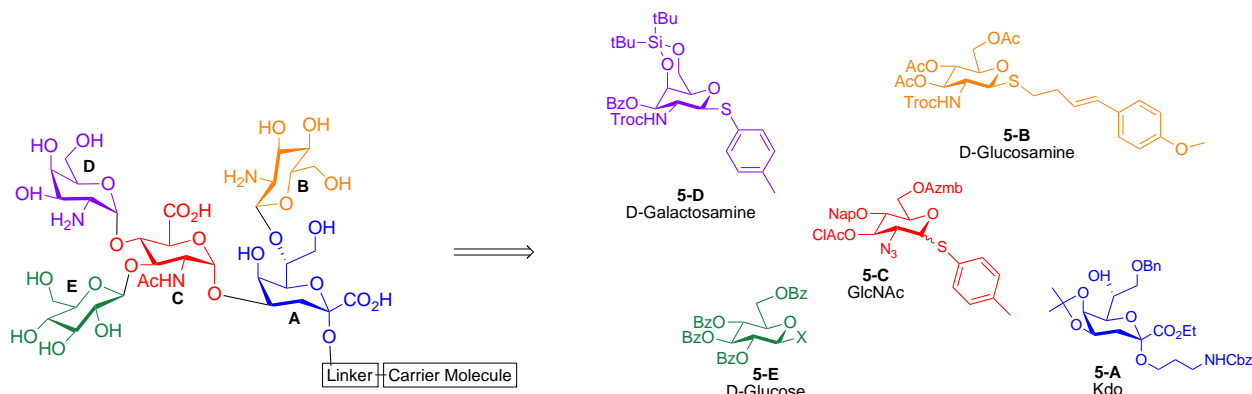


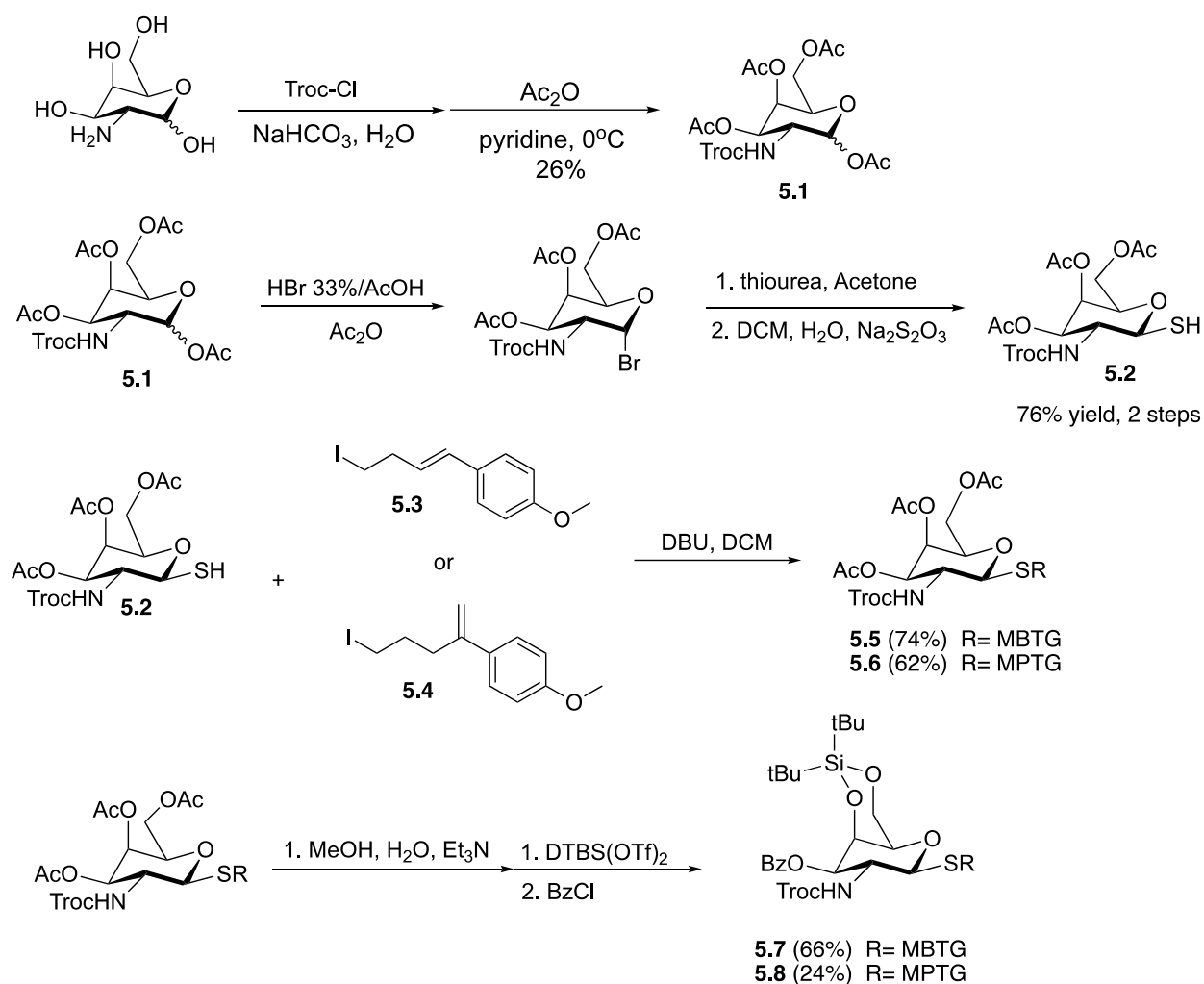
Figure 5.2 Retrosynthesis of LOS-Conjugate Vaccine

## 5.2. Results and Discussion

The complexity of the pentasaccharide core makes synthesis an arduous task. The structure has three alpha glycosidic linkages, two of which are connected to the **C** GlcNAcA core and are difficult to install. This requires strategic synthesis of the

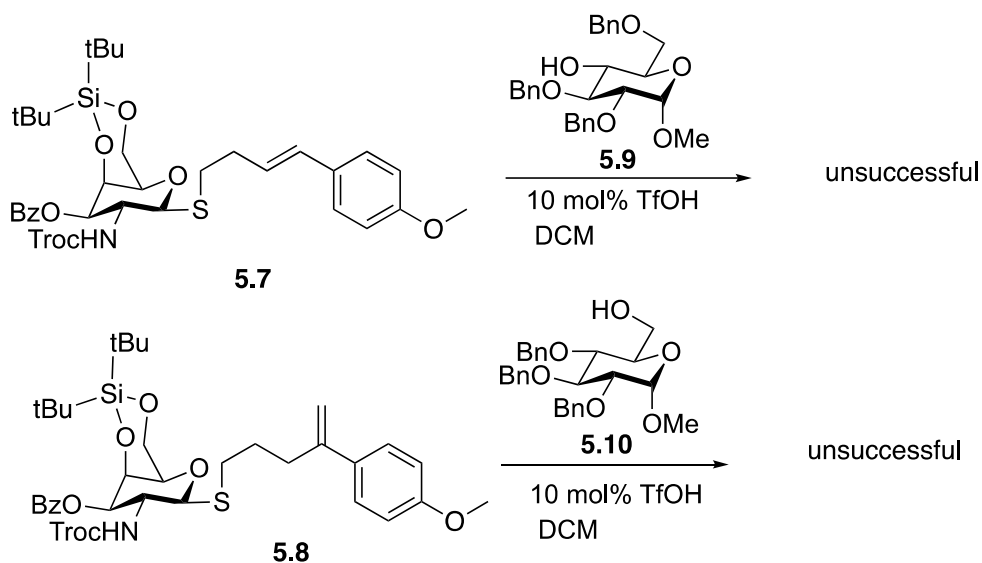
monosaccharide glycosidic units (Figure 5.2). I have been working on the synthesis of the galactosamine donor, GlcNAcA acceptor, and a disaccharide subunit of the pentasaccharide.

To synthesize **5-C**, I began with protecting the amino group of D-galactosamine with trichloroethyl chloroformate (Troc-Cl) followed by acetylation to give **5.1** (Scheme 5.1). The anomeric acetate was first displaced through bromination. Thiourea nucleophile attacks the anomeric carbon forming an isothiurea salt that is then hydrolyzed to form the thiol **5.2** (Scheme 5.1). Once the thiol was formed, installation of two different sidechains developed in the Ragains lab generated 4-(4-methoxyphenyl)-3-butenylthioglycoside **5.5** (MBTG) and 4-(4-methoxyphenyl)-4-pentenylthioglycoside (MPTG) **5.6**. Deacetylation was followed by di-*tert*-butylsilylsylene (DTBS) installation, to insure  $\alpha$ -selectivity in future glycosylations, subsequent benzylation afforded the desired galactosamine donors **5.7** and **5.8** (Scheme 5.1).



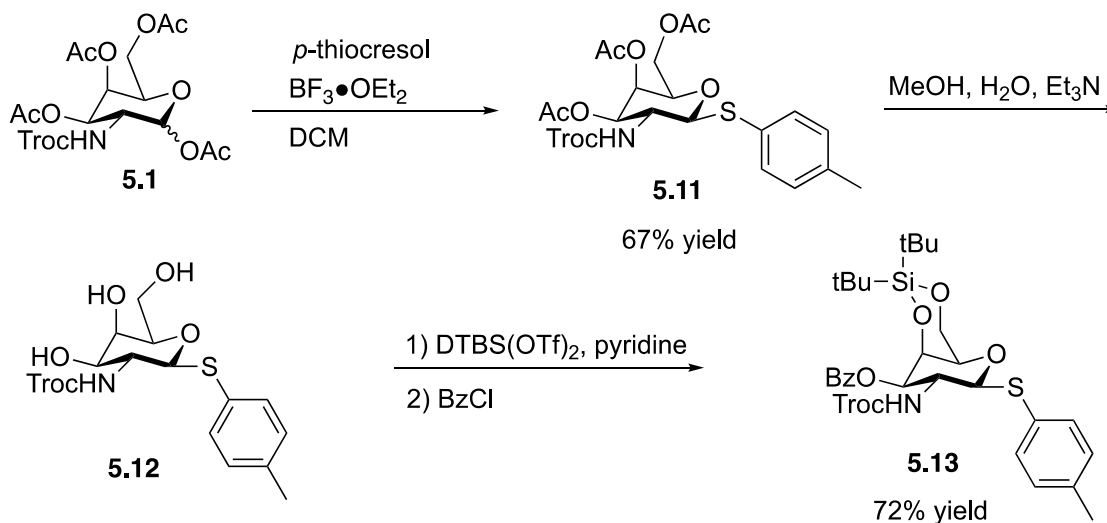
Scheme 5.1 Synthesis of Galactosamine Donors

Experiments were conducted to test the effectiveness of the donors. To approximate the reactivity of GlcNAcA, C<sub>4</sub> acceptor **5.9** was used in a glycosylation with MBTG donor **5.7** (Scheme 5.2). Unfortunately, the desired disaccharide was not achieved using this donor. MPTG has increased reactivity and was expected to give the desired disaccharide. Using the benzylated C<sub>6</sub> acceptor **5.10** and MPTG **5.8**, the desired disaccharide was not detected (Scheme 5.2).



Scheme 5.2 Pilot Glycosylations using MBTG and MPTG

To circumvent this obstacle, another thioglycoside was synthesized. DTBS protected galactosamine aryl thioglycosides are highly 1,2-*cis*-selective donors in *O*-glycosylation.<sup>19</sup> Synthesis of the thioglycoside began with **5.1**,  $\text{BF}_3 \bullet \text{OEt}_2$  promoted the installation of the *p*-thiocresyl affording the tri-acetyl thioglycoside **5.11** (Scheme 5.3). Deacetylation gave intermediate **5.12** followed by silyl and benzoyl protection to afford **5.13** (Scheme 5.3).



Scheme 5.3 Synthesis of Thioglycoside Donor

Pilot glycosylations with the thioglycoside donor **5.13** proved to be fruitful. Glycosylation with the C<sub>4</sub> acceptor was high-yielding and resulted in exclusive 1,2-*cis*-selectivity (entry 1, Figure 5.3). Using the same reaction conditions with the C<sub>4</sub> acceptor was low yielding (entry 2). Temperature plays a significant role in this reaction. Lowering the reaction to -20°C increased the yield significantly (entry 3). Donor concentration was shown to be an important factor as well. Entry 4 showed that increasing the donor concentration back to 0.06 M provided the desired disaccharide in 74% yield.

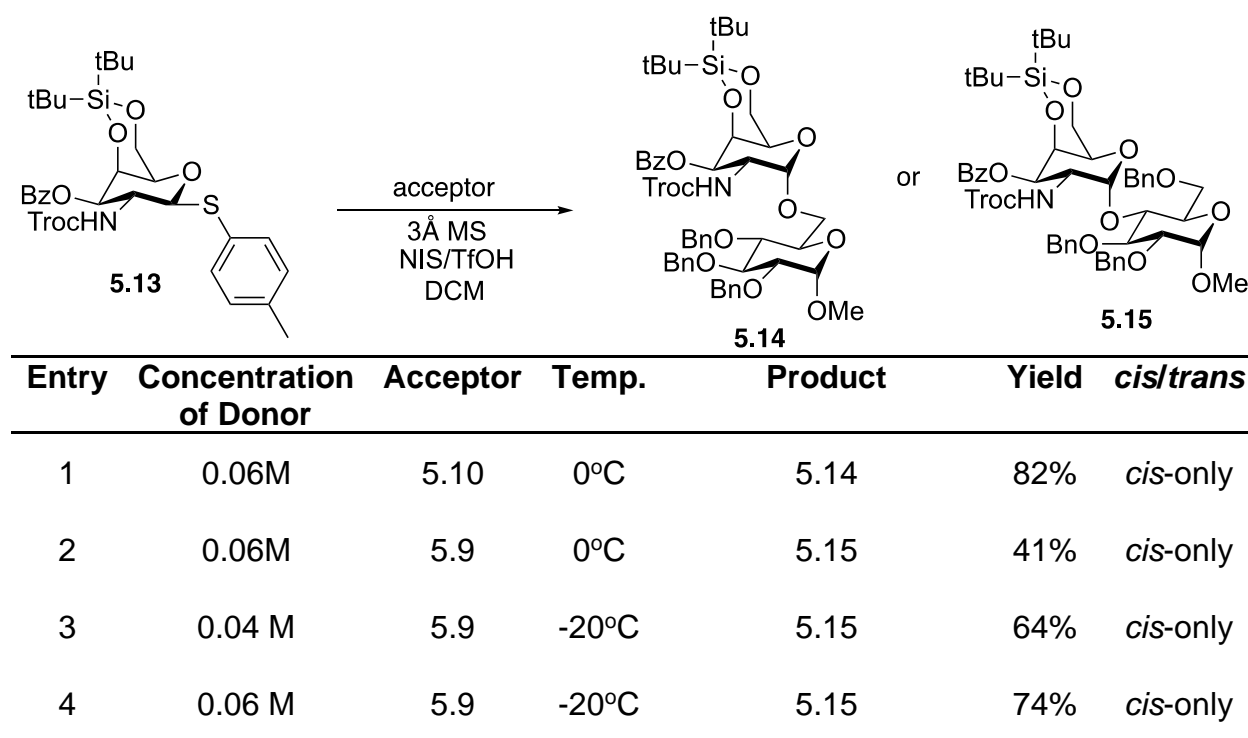


Figure 5.3 Optimization of Disaccharide Synthesis

Synthesis of glycosyl acceptor proved to be a difficult task. The orthogonally protected GlcNAcA unit **5.16** was completed by James Armstrong. I then needed to remove the 2-naphthylmethyl (Nap) group in the C<sub>4</sub> position to obtain the desired glycosyl acceptor, but this was not an easy undertaking. Nap has been shown to be selectively removed using 2,3-dichloro-5,6-dicyanobenzoquinone (DDQ).<sup>20</sup> In the first attempt of removal, only starting material was recovered (entry 1, Figure 5.4). Increasing the amount

of DDQ used only amounted to a 16% yield, starting material was recovered as well. To increase reactivity the temperature was raised to 80°C, but only a small increase in yield was afforded (entry 3). Due to the difficult synthesis of the GlcNAcA unit, I was unable to receive more material to study Nap removal. Glycosylation was attempted with available material.

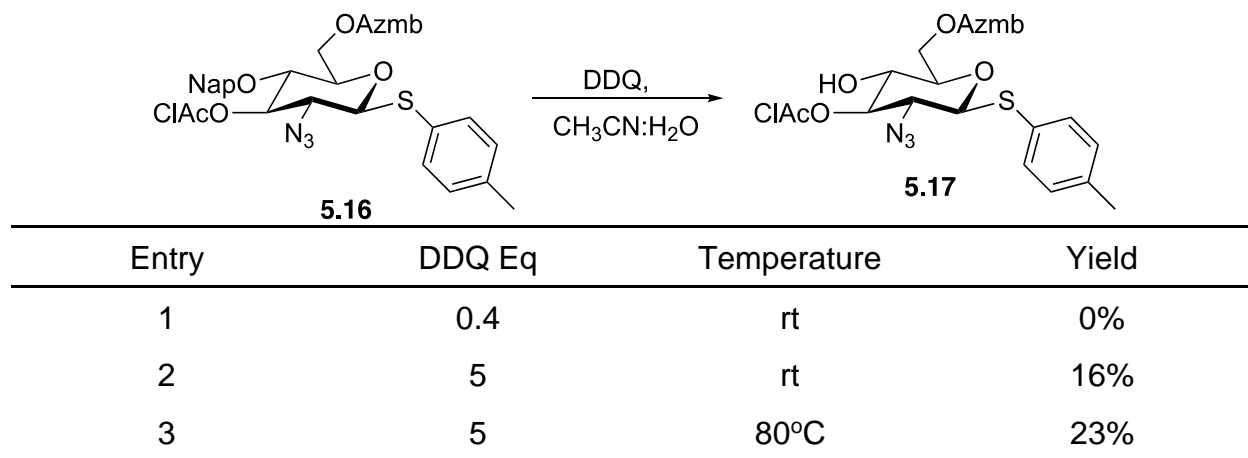
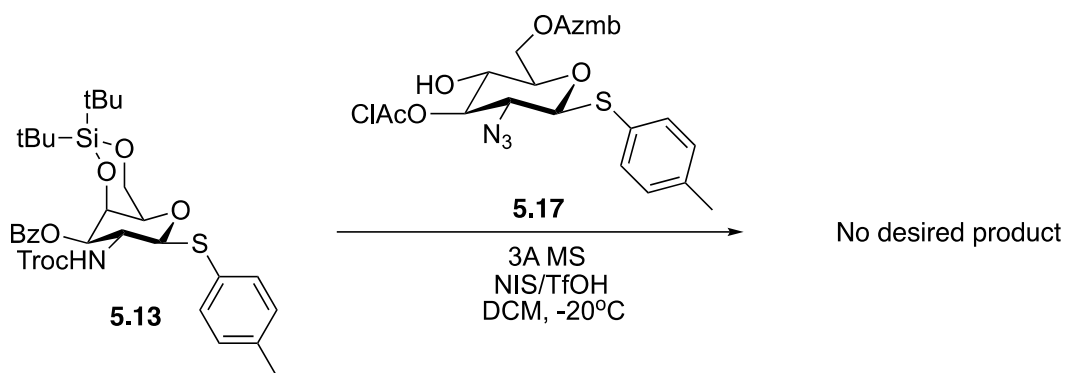


Figure 5.4 Nap Ether Cleavage

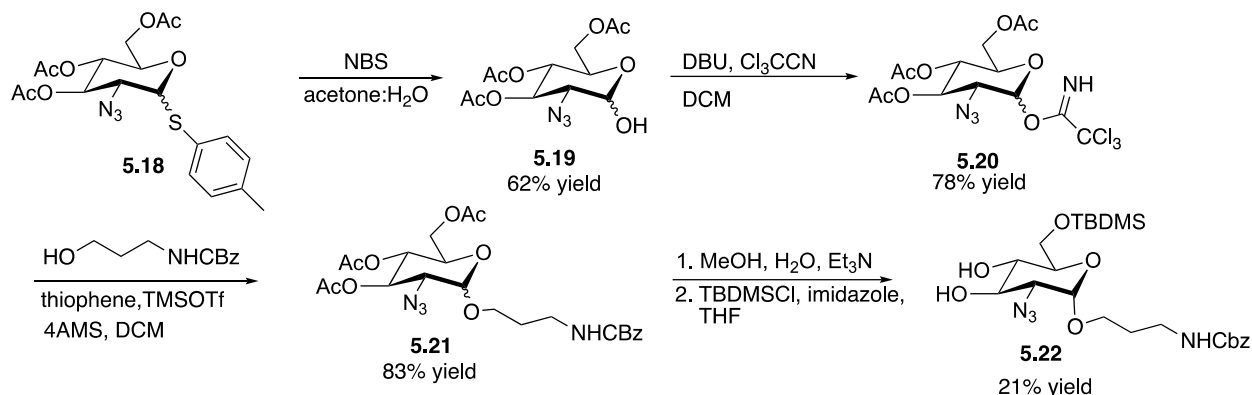
Glycosylation of acceptor **5.17** with donor **5.13** was attempted (Scheme 5.4). Unfortunately, the desired disaccharide was not obtained.



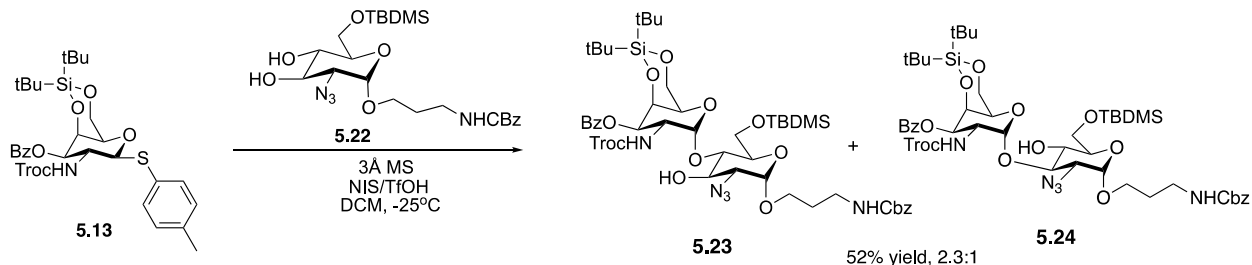
Scheme 5.4 Glycosylation of Disaccharide

Without more GlcNAcA intermediate **5.16** for synthesis, I tried a new route to achieve synthesis of the desired disaccharide. A less precious glycosyl acceptor was synthesized by first removing the *p*-thiocresyl group to afford the lactol **5.19** (Scheme 5.5).

The trichloroacetimidate donor **5.20** was synthesized and glycosylated with benzyl (3-hydroxypropyl) carbamate in the presence of thiophene in excess to promote 1,2-*cis*-selectivity. After deacetylation and installation of the silyl group, the anomers were identified and separated (Scheme 5.5). The 1,2-*cis* anomer was the desired one and was taken on to the next step.



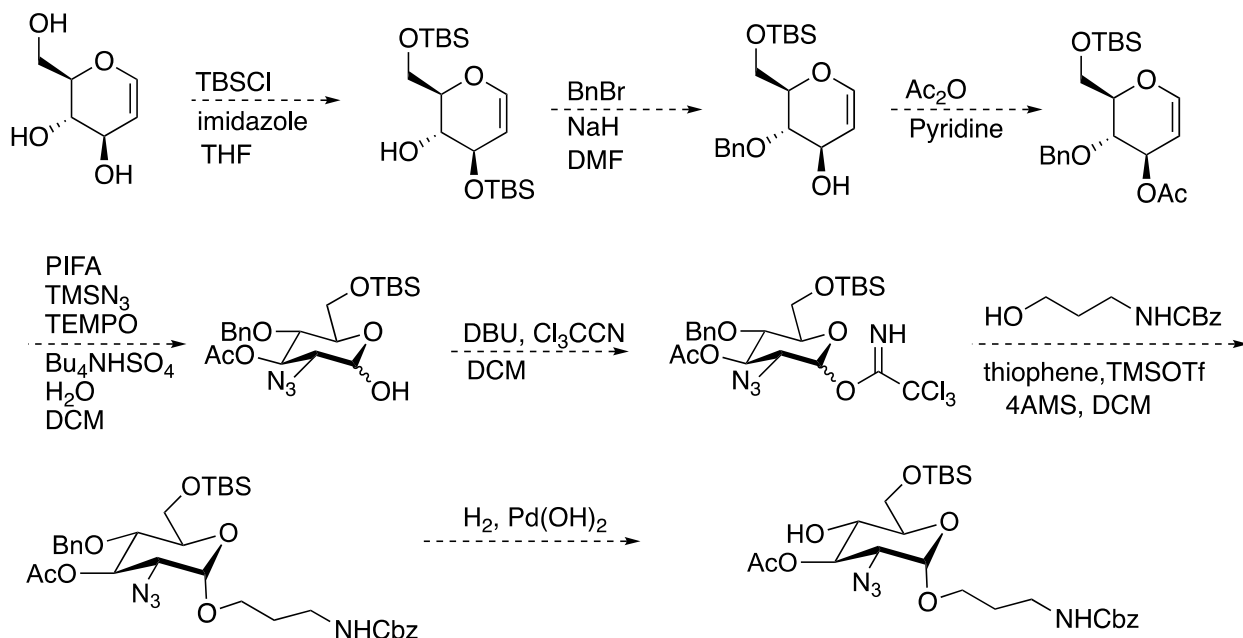
In glycosylations with C<sub>3</sub> and C<sub>4</sub> free hydroxyls the glycosylation is more likely to occur at the C<sub>4</sub> position. Glycosylation using the diol acceptor was undertaken using conditions gleaned from pilot experiments. The reaction proved to be poorly selective and gave moderate yield. The two products were inseparable (Scheme 5.6).



## 5.4. Future Work

To circumvent the selectivity issue shown in scheme 5.6, another route could be taken to synthesize the GlcNAcA unit (Scheme 5.7). Orthogonal protection is necessary

for the synthesis of this disaccharide. Synthesis of all sugar units for the pentasaccharide have been completed and optimizations are currently underway. Di- and trisaccharide components of the pentasaccharide will be synthesized and conjugated to a carrier molecule for animal study. Eventually, the completed pentasaccharide core will be synthesized, conjugated to a carrier molecule, and tested in mice for immunogenicity.



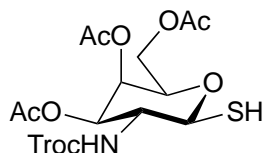
Scheme 5.7 Future Route to Glycosyl Acceptor

## 5.5. Experimental

$^1\text{H}$  NMR and  $^{13}\text{C}$  NMR spectroscopy were conducted using a Bruker AV-400 spectrometer or a Bruker AV-500 spectrometer. Mass spectra were attained using an Agilent 6210 electrospray time-of-flight mass spectrometer. All materials were received from commercial suppliers and used without further purification. Flash column chromatography was accomplished using high purity grade 60 Å silica gel (Fluka® Analytical). Qualitative TLC was performed on aluminum sheets (Merck, silica gel, F254) and observed via UV absorption (254 nm) and staining with anisaldehyde.



3,4,6-tri-*O*-acetyl-2-deoxy-1-mercapto-2-(2,2,2-trichloroethoxycarbonylamino)- $\beta$ -D-galactopyranose **5.2**

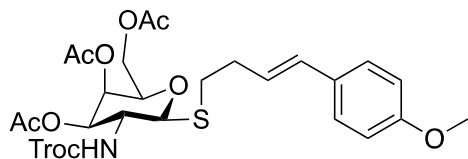


D-galactosamine hydrochloride (6.01 g, 27.8 mmol) was dissolved in 60 mL of H<sub>2</sub>O and cooled to 0°C. NaHCO<sub>3</sub> (5.84 g, 69.5 mmol) was added and allowed to stir for 10 min. 2,2,2-trichloroethyl chloroformate (5.1 g, 37 mmol) was added and allowed to stir at room temperature (17°C overnight (10 hrs)). The reaction mixture was then cooled to 0°C and acidified with 1 M HCl (110 mL), then filtered and the filter cake was washed with Et<sub>2</sub>O (200 mL). The resulting solid was then placed on high vacuum to remove remaining solvent. A mixture of Ac<sub>2</sub>O (60 mL) and pyridine (60 mL) was prepared and cooled to 0°C and the solid was added to mixture. The reaction was allowed to stir at room temperature (17°C) overnight (16 hrs). Upon completion, the reaction was concentrated and then redissolved in EtOAc (300 mL). The organic layer was washed with H<sub>2</sub>O (3 x 150mL), 1 N HCl (150 mL), sat. NaHCO<sub>3</sub> (150 mL), and sat. brine (150 mL). The organic layer was then dried over Na<sub>2</sub>SO<sub>4</sub>, filtered, and concentrated. The resulting crude material was purified using flash chromatography with an isocratic solvent system of 20% EtOAc in hexanes to afford 3.78 g (26%) 1,2,3,6-tri-*O*-acetyl-2-deoxy-2-(2,2,2-trichloroethoxycarbonylamino)-D-galactopyranose **5.1** as a white solid. Spectral data matched that previously reported in the literature.<sup>21</sup>

**5.1** (5.03 g, 9.57 mmol) was dissolved in 35.0 mL of dichloromethane and cooled to 0°C. 26.0 mL 33% HBr/HOAc was added to the solution and the reaction was allowed to warm to room temperature (17°C) and stirred for 3 h. 50 mL cold water was added to the

reaction. The aqueous layer was extracted with dichloromethane (2 x 30 mL) and the combined organic layers were washed with sat.  $\text{NaHCO}_3$  (30 mL), and sat. brine (30 mL). The organic layer was dried over  $\text{Na}_2\text{SO}_4$ , concentrated to a white foam, and carried on without further purification. The resulting white foam was dissolved in 15 mL acetone, and thiourea (1.09 g, 14.4 mmol) was added. The reaction was heated to reflux overnight (16 h) and then concentrated. The resulting material was then dissolved in dichloromethane (30 mL). A solution of water (15 mL) and  $\text{Na}_2\text{S}_2\text{O}_3$  (1.71 g) was prepared and heated to reflux for 3 h. The organic layer was separated and the aqueous layer was extracted with DCM (2 x 20 mL). The combined organic layers were then dried over  $\text{Na}_2\text{SO}_4$  and concentrated. The resulting crude material was purified by silica gel chromatography using a gradient solvent system starting at 100% hexanes and ending at 25% ethyl acetate in hexanes to afford 4.21 g (89%) 3,4,6-tri-*O*-acetyl-2-deoxy-1-mercapto-2-(2,2,2-trichloroethoxycarbonylamino)- $\beta$ -D-galactopyranose (**5.2**) as a white powder.  $^1\text{H}$  NMR (400 MHz,  $\text{CDCl}_3$ )  $\delta$  5.41(d,  $J$  = 3.28 Hz, 1H), 5.15-5.08 (m, 2H), 4.80-4.65 (m, 3H), 4.13 (d,  $J$  = 6.6 Hz, 2H), 3.98-3.91 (m, 2H), 2.51 (d,  $J$  = 9 Hz, 1H), 2.18 (s, 3H), 2.06 (s, 3H), 2.01(s, 3H).  $^{13}\text{C}$  NMR (101 MHz,  $\text{CDCl}_3$ )  $\delta$  170.57, 170.26, 154.58, 95.40, 80.40, 74.87, 74.52, 70.87, 66.92, 61.72, 55.19, 20.71, 20.63.

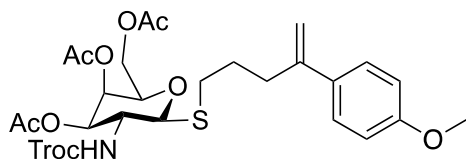
Synthesis of 4-(4-methoxyphenyl)-3-butenyl-3,4,6-tri-*O*-acetyl-2-deoxy-2-(2,2,2-trichloroethoxycarbonylamino)-1-thio- $\beta$ -D-galactopyranoside **5.5**



At room temperature, **5.2** (0.495 g, 1.01 mmol) was dissolved in dichloromethane (15 mL). 1-iodo-4-(4-methoxyphenyl)-3-butene **5.3** (0.401 g, 1.21 mmol) was added and

stirred until dissolution had occurred. DBU (0.20 mL, 1.3 mmol) was added to the solution dropwise and the reaction was allowed to stir until complete according to TLC analysis (15 min) and concentrated. The crude material was then purified via flash chromatography with a gradient solvent system of 20% to 40% EtOAc in hexanes affording 0.49 g (74%) of white solid **5.5**.  $^1\text{H}$  NMR (400 MHz,  $\text{CDCl}_3$ )  $\delta$  7.27 (d,  $J$  = 8.8 Hz, 2H), 6.84 (d,  $J$  = 8.8 Hz, 2H), 6.38 (d,  $J$  = 15.8 Hz, 2H), 6.09-6.02 (m, 1H), 5.41 (d,  $J$  = 2.92 Hz, 1H), 5.20-5.12 (m, 2H), 4.77 (d,  $J$  = 12.04 Hz, 1H), 4.67 (t,  $J$  = 10.92 Hz, 2H) 4.20-4.10 (m, 2H), 3.98-3.91 (m, 2H), 3.80 (s, 1H), 2.91-2.79 (m, 2H), 2.52 (q, 2H), 2.16 (s, 3H), 2.04 (s, 3H), 1.99 (s, 3H).  $^{13}\text{C}$  NMR (101 MHz,  $\text{CDCl}_3$ )  $\delta$  170.45, 170.41, 170.22, 159.01, 154.15, 131.02, 130.03, 127.20, 125.75, 114.03, 95.46, 85.03, 74.49, 71.04, 66.96, 61.67, 55.30, 51.60, 33.39, 30.25, 20.69, 20.62.

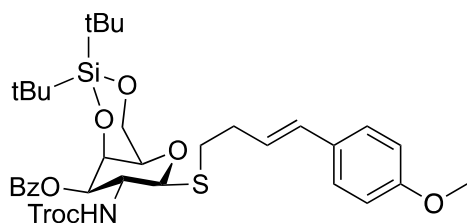
Synthesis of 4-(*p*-methoxyphenyl)-4-pentenyl-3,4,6-tri-*O*-acetyl-2-deoxy-2-(2,2,2-trichloroethoxycarbonylamino)-1-thio- $\beta$ -D-galactopyranoside **5.6**:



At room temperature **5.2** (1.75 g, 3.53 mmol) was dissolved in dichloromethane (20 mL). 1-iodo-4-(*p*-methoxyphenyl)-4-pentene **5.4** (1.28 g, 4.24 mmol) was added and stirred until dissolution occurred. DBU (0.69 mL, 4.6 mmol) was added to the solution dropwise and the reaction was allowed to stir until complete according to TLC analysis (15 min) and concentrated. The crude material was then purified via flash chromatography with a gradient solvent system of 20% to 40% EtOAc in hexanes affording 1.46 g (62%) of **5.6**.  $^1\text{H}$  NMR (400 MHz,  $\text{CDCl}_3$ )  $\delta$  7.37 – 7.24 (m, 2H), 6.88 (d,  $J$  = 2.2 Hz, 1H), 6.87 – 6.80 (m, 1H), 5.58 (dd,  $J$  = 18.8, 9.5 Hz, 1H), 5.47 – 5.36 (m, 1H), 5.23 (d,  $J$  = 1.5 Hz, 1H),

5.13 (td,  $J = 12.0, 10.8, 3.3$  Hz, 1H), 5.02 – 4.91 (m, 1H), 4.84 – 4.53 (m, 3H), 4.23 – 4.03 (m, 3H), 4.03 – 3.85 (m, 2H), 3.80 (d,  $J = 2.9$  Hz, 3H), 2.90 – 2.64 (m, 2H), 2.59 (d,  $J = 7.3$  Hz, 1H), 2.58 – 2.47 (m, 1H), 2.20 – 2.09 (m, 4H), 2.09 – 1.97 (m, 8H), 1.86 – 1.72 (m, 2H), 1.25 (t,  $J = 7.2$  Hz, 3H).

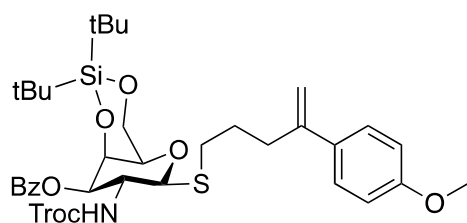
Synthesis of 4-(4-methoxyphenyl)-3-butenyl 2-deoxy-4,6-*O*-di-*tert*-butylsilylene-1-thio-2-(2,2,2-trichloroethoxycarbonylamino)-3-*O*-benzoyl- $\beta$ -D-galactopyranoside **5.7**:



**5.5** (0.49 g, 0.75 mmol) was dissolved in a solution of MeOH (5 mL), H<sub>2</sub>O (0.63 mL), and Et<sub>3</sub>N (0.63 mL) and allowed to stir overnight (16h). After completion, the reaction was concentrated and coevaporated with toluene (3 x 10 mL) to remove remaining H<sub>2</sub>O to afford the deacetylated thioglycoside. (0.211 g, 0.377 mmol) of the intermediate material was used and dissolved in pyridine (7.5 mL). The reaction was cooled to 0°C and DTBS(OTf)<sub>2</sub> (0.14 mL, 0.42 mmol) was added in one portion. The reaction was allowed to stir at room temperature until starting material was consumed according to TLC analysis. Benzoyl chloride (0.07 mL, 0.6 mmol) was then added, and the reaction was allowed to stir until complete according to TLC analysis (1 hr). The reaction was coevaporated with toluene and redissolved in chloroform (20 mL). The organic phase was then washed with 1 M HCl (15 mL), H<sub>2</sub>O (15 mL), sat. NaHCO<sub>3</sub> (15 mL), and brine (15 mL). The organic layer was then dried over Na<sub>2</sub>SO<sub>4</sub> and concentrated. The resulting crude material was then purified by silica gel chromatography (gradient run from 10% to 30% EtOAc in hexanes) to afford 0.191 g (66%) of **5.7** as a white solid. <sup>1</sup>H NMR (400 MHz, EtOAc in hexanes) to afford 0.191 g (66%) of **5.7** as a white solid. <sup>1</sup>H NMR (400 MHz,

CDCl<sub>3</sub>)  $\delta$  8.08 – 8.01 (m, 2H), 7.55 (d,  $J$  = 7.5 Hz, 1H), 7.43 (t,  $J$  = 7.8 Hz, 2H), 7.27 (dd,  $J$  = 9.2, 2.5 Hz, 2H), 6.87 – 6.80 (m, 2H), 6.38 (d,  $J$  = 15.8 Hz, 1H), 6.07 (dt,  $J$  = 15.8, 6.9 Hz, 1H), 5.30 (d,  $J$  = 9.4 Hz, 1H), 5.21 – 5.14 (m, 1H), 4.72 (d,  $J$  = 11.5 Hz, 3H), 4.28 (s, 2H), 3.79 (s, 3H), 2.85 (dd,  $J$  = 7.5, 2.5 Hz, 2H), 2.51 (td,  $J$  = 7.1, 1.4 Hz, 2H), 1.13 (s, 9H), 1.05 (s, 2H), 0.97 (s, 9H). <sup>13</sup>C NMR (101 MHz, CDCl<sub>3</sub>)  $\delta$  166.45, 158.94, 154.26, 133.45, 130.79, 130.22, 129.88, 129.75, 129.54, 128.48, 127.22, 126.08, 114.02, 95.45, 84.91, 75.21, 74.35, 70.19, 67.28, 55.30, 51.19, 33.41, 30.45, 27.55, 27.30, 23.26, 20.71, 19.81, 14.20.

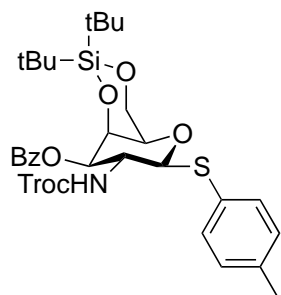
Synthesis of 4-(*p*-methoxyphenyl)-4-pentenyl-2-deoxy-4,6-*O*-di-*tert*-butylsilylene-1-thio-2-(2,2,2-trichloroethoxycarbonylamino)-3-*O*-benzoyl- $\beta$ -D-galactopyranoside **5.8**:



**5.6** (1.02 g, 1.86 mmol) was dissolved in a solution of MeOH (12.5 mL), H<sub>2</sub>O (1.6 mL), and Et<sub>3</sub>N (1.6 mL) and allowed to stir at room temperature (16°C) overnight (16h). After completion, the reaction was concentrated and coevaporated with toluene (3 x 10 mL) to remove remaining H<sub>2</sub>O to afford the deacetylated thioglycoside. 0.50 g (0.918 mmol) of the intermediate material was dissolved in pyridine (15 mL). The reaction mixture was cooled to 0°C and DTBS(OTf)<sub>2</sub> (0.33 mL, 1.01 mmol) was added in one portion. The reaction was allowed to stir at room temperature until starting material was consumed according to TLC analysis. Benzoyl chloride (0.16 mL, 1.4 mmol) was then added and the reaction was allowed to stir until complete according to TLC analysis (1 hr). The reaction was coevaporated with toluene and redissolved in chloroform (20 mL). The

organic phase was then washed with 1 M HCl, H<sub>2</sub>O, sat. NaHCO<sub>3</sub>, and brine. The organic layer was then dried over Na<sub>2</sub>SO<sub>4</sub> and concentrated. The crude material was then purified by silica gel chromatography (gradient run from 10% to 30% EtOAc in hexanes) to afford 0.17 g (24%) of **5.8** as a white solid.

Synthesis of 4-Tolyl-2-deoxy-4,6-*O*-di-*tert*-butylsilylene-1-thio-2-(2,2,2-trichloroethoxycarbonylamino)-3-*O*-benzoyl- $\beta$ -D-galactopyranoside **5.13**:

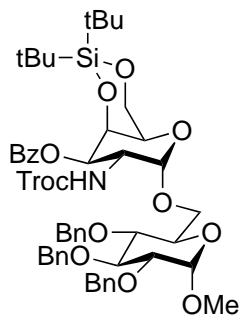


Tetraacetyl glycoside **5.1** (1.01 g, 1.91 mmol) and *p*-thiocresol (0.284 g, 2.29 mmol) were dissolved in dichloromethane (10 mL) and cooled to 0°C. Boron trifluoride diethyletherate (0.94 mL, 7.64 mmol) was added to the reaction solution dropwise. The reaction was then allowed to warm to room temperature (18°C) and stir overnight (18 hrs). The reaction was then quenched with sat. NaHCO<sub>3</sub> (30 mL) and then diluted with dichloromethane (30 mL). The organic layer was separated and the aqueous layer was extracted (3 x 10 mL) with dichloromethane. The combined organic layers were dried over Na<sub>2</sub>SO<sub>4</sub> and concentrated. The crude material was then purified using silica gel chromatography (gradient run of 15% to 40% EtOAc in Hexanes) to afford 0.85 g (76%) of **5.11**. The spectral data matched that previously reported in literature.<sup>22</sup>

The triacetyl thioglycoside **5.11** (9.76 g, 16.6 mmol) was dissolved in a mixture of MeOH (133 mL), H<sub>2</sub>O (16 mL), and Et<sub>3</sub>N (16 mL) and allowed to stir at room temperature overnight (16h). The solution was then concentrated and coevaporated with toluene (3 x

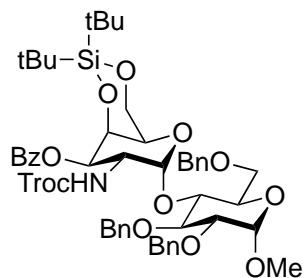
15 mL). The solid was then rinsed with dichloromethane and then dried under high vacuum to afford 5.34 g of deacetylated thioglycoside. The material was used in the next step without further purification. The intermediate (1.01 g, 2.19 mmol) was dissolved in pyridine (65 mL) and cooled to 0°C. DTBS(OTf)<sub>2</sub> (0.89 mL, 2.71 mmol) was added in one portion. The reaction was allowed to stir at room temperature until starting material was consumed via TLC. Benzoyl chloride (0.43 mL, 3.71 mmol) was then added and the reaction was allowed to stir until complete according to TLC analysis (4hr). The reaction was coevaporated with toluene (10 mL) and dissolved in chloroform (15 mL). The organic phase was then washed with 1 M HCl (30 mL), H<sub>2</sub>O (30 mL), sat. NaHCO<sub>3</sub> (30 mL), and brine (30 mL). The organic layer was then dried over Na<sub>2</sub>SO<sub>4</sub> and concentrated. The crude material was then purified by silica gel chromatography (gradient run from 10% to 30% EtOAc in hexanes) to afford 1.25 g (72%) of pure **5.13**. <sup>1</sup>H NMR (400 MHz, CDCl<sub>3</sub>) δ 8.05 (dd, *J* = 8.4, 1.4 Hz, 2H), 7.62 – 7.53 (m, 1H), 7.44 (dd, *J* = 7.9, 5.9 Hz, 4H), 7.26 (s, 1H), 7.11 (d, *J* = 7.8 Hz, 2H), 5.18 (d, *J* = 9.3 Hz, 2H), 4.85 (d, *J* = 10.4 Hz, 1H), 4.78 – 4.69 (m, 2H), 4.62 (d, *J* = 12.2 Hz, 1H), 4.26 (s, 2H), 3.52 (s, 1H), 2.34 (s, 3H), 1.15 (s, 9H), 0.98 (s, 9H).

Synthesis of Methyl (2-deoxy-4,6-*O*-di-*tert*-butylsilylene-1-thio-2-(2,2,2-trichloroethoxycarbonylamino)-3-*O*-benzoyl)-(1→6)-2,3,4-tri-*O*-benzyl-D-glucopyranoside **5.14**:



**5.13** (50.2 mg, 0.071 mmol), **5.10** (21.8 mg, 0.047 mmol), and 3Å molecular sieves (82.6 mg) were added to a dry reaction flask. Dichloromethane (1 mL) was added and the reaction were allowed to stir for 1 hr then cooled to 0°C. *N*-iodosuccinimide (31.7 mg, 0.141 mmol) and triflic acid (0.4 µL, 0.0047 mmol) was added to the mixture and allowed to stir for 30 min. Upon completion according to TLC analysis, the reaction mixture was filtered through celite using dichloromethane (15 mL). The organic layer was then washed with NaHCO<sub>3</sub> (10 mL), Na<sub>2</sub>S<sub>2</sub>O<sub>3</sub> (10 mL), and brine (10 mL). The organic layer was dried over Na<sub>2</sub>SO<sub>4</sub> and concentrated. The crude material was purified via silica gel chromatography (gradient run 5% to 20% EtOAc in Hexanes) to afford 40.1 mg (82%) of **5.14**. <sup>1</sup>H NMR (400 MHz, CDCl<sub>3</sub>) δ 8.09 – 8.02 (m, 3H), 7.61 – 7.51 (m, 2H), 7.43 (dd, *J* = 9.0, 6.5 Hz, 3H), 7.37 – 7.33 (m, 6H), 7.33 – 7.24 (m, 18H), 5.35 – 5.27 (m, 2H), 5.15 – 5.03 (m, 2H), 5.03 – 5.00 (m, 2H), 5.00 – 4.90 (m, 3H), 4.86 – 4.69 (m, 6H), 4.69 – 4.58 (m, 6H), 4.58 – 4.45 (m, 2H), 4.11 (qd, *J* = 12.6, 2.5 Hz, 3H), 4.01 (t, *J* = 9.2 Hz, 2H), 3.87 (dd, *J* = 11.1, 4.7 Hz, 1H), 3.83 – 3.74 (m, 2H), 3.72 – 3.66 (m, 2H), 3.56 (dd, *J* = 9.5, 3.7 Hz, 2H), 3.45 (dd, *J* = 10.1, 8.8 Hz, 2H), 3.40 (s, 3H), 3.37 (s, 1H), 1.26 (s, 2H), 1.07 (d, *J* = 10.8 Hz, 14H), 0.95 (d, *J* = 2.6 Hz, 13H).

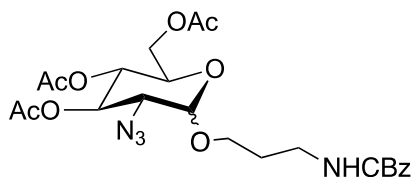
Synthesis of Methyl (2-deoxy-4,6-*O*-di-*tert*-butylsilylene-1-thio-2-(2,2,2-trichloroethoxycarbamoyl)-3-*O*-benzoyl)-(1→4)-2,3,6-tri-*O*-benzyl-D-glucopyranoside





**5.13** (101.8 mg, 0.142 mmol), **5.9** (44.1 mg, 0.095 mmol), and 3Å molecular sieves (180 mg) were added to a dry reaction flask. Dichloromethane (1.6 mL) was added and reaction was allowed to stir for 1 hr then cooled to -20°C. *N*-iodosuccinimide (64.1 mg, 0.285 mmol) and triflic acid (1.67 µL, 0.019 mmol) were added to the mixture and allowed to stir for 30 min. Upon completion via TLC, the reaction mixture was filtered through celite using dichloromethane (15 mL). The organic layer was then washed with NaHCO<sub>3</sub> (10 mL), Na<sub>2</sub>S<sub>2</sub>O<sub>3</sub> (10 mL), and brine (10 mL). The organic layer was dried over Na<sub>2</sub>SO<sub>4</sub> and concentrated. The crude material was purified via silica gel chromatography (gradient run 10% to 20% EtOAc in hexanes) to afford 73.5 mg (74%) of **5.16**. <sup>1</sup>H NMR (400 MHz, CDCl<sub>3</sub>) δ 8.09 – 8.01 (m, 2H), 7.63 – 7.51 (m, 1H), 7.46 – 7.36 (m, 2H), 7.36 – 7.31 (m, 6H), 7.31 – 7.20 (m, 6H), 7.20 – 7.10 (m, 2H), 6.09 (d, *J* = 10.3 Hz, 1H), 5.52 (d, *J* = 3.6 Hz, 1H), 5.05 (d, *J* = 11.1 Hz, 1H), 4.95 (dd, *J* = 11.1, 2.8 Hz, 1H), 4.81 – 4.40 (m, 10H), 4.05 – 3.85 (m, 4H), 3.82 (dd, *J* = 10.9, 3.7 Hz, 1H), 3.70 (dq, *J* = 9.7, 1.7 Hz, 2H), 3.61 (ddd, *J* = 14.7, 10.1, 2.7 Hz, 2H), 3.38 (s, 3H), 1.60 (s, 1H), 1.29 – 1.24 (m, 4H), 1.24 – 1.19 (m, 1H), 1.14 – 1.09 (m, 1H), 1.06 (s, 7H), 1.02 (d, *J* = 14.4 Hz, 3H), 0.93 (s, 8H), 0.91 – 0.79 (m, 3H).

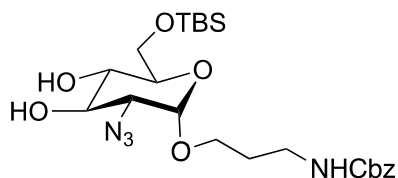
Synthesis of *N*-(benzyloxycarbonyl)aminopropyl 2-azido-3,4,6-tri-*O*-acetyl-2-deoxy-D-glucopyranoside



A mixture of **5.20** (101.4 mg, 0.2104 mmol), benzyl (3-hydroxypropyl) carbamate (65.9 mg, 0.315 mmol), 4Å molecular sieves (159.4 mg), thiophene (0.17 mL, 2.10 mmol), and

dichloromethane (2 mL) was allowed to stir for 20 minutes under nitrogen and then cooled to 0°C. TMSOTf (3.8  $\mu$ L, 0.021 mmol) was added and the reaction was allowed to warm to room temperature. Once complete by TLC (5 hr), the reaction was quenched by sat. NaHCO<sub>3</sub> (10 mL). The organic phase was separated, dried by Na<sub>2</sub>SO<sub>4</sub>, and concentrated. The crude material was purified using silica chromatography (gradient run 20% to 40% EtOAc in hexanes) to afford 91.1 mg (83%) of **5.21**. <sup>1</sup>H NMR (400 MHz, CDCl<sub>3</sub>)  $\delta$  7.35 (d,  $J$  = 4.6 Hz, 7H), 7.32 (tt,  $J$  = 5.1, 3.0 Hz, 2H), 5.46 (dd,  $J$  = 10.6, 9.2 Hz, 1H), 5.10 (d,  $J$  = 2.4 Hz, 5H), 5.07 – 4.98 (m, 2H), 4.97 (dd,  $J$  = 8.4, 3.1 Hz, 2H), 4.26 (td,  $J$  = 12.5, 4.7 Hz, 2H), 4.09 (ddd,  $J$  = 23.4, 12.2, 2.3 Hz, 2H), 3.83 (dt,  $J$  = 11.6, 5.9 Hz, 1H), 3.73 – 3.43 (m, 4H), 3.41 – 3.25 (m, 5H), 2.09 – 1.99 (m, 16H).

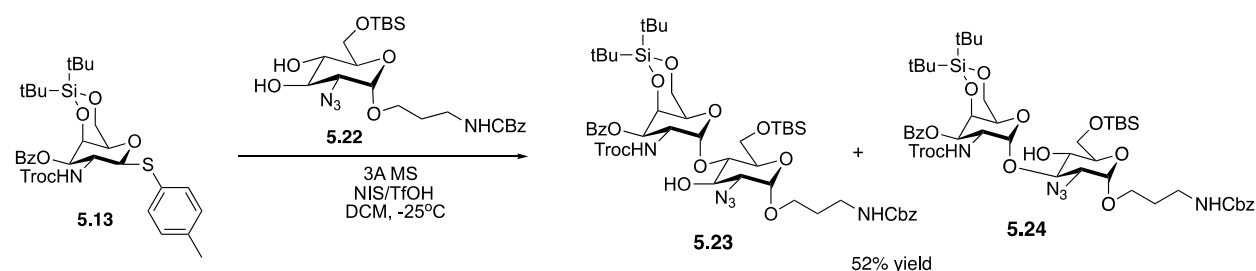
Synthesis of N-(benzyloxycarbonyl)aminopropyl 2-azido-6-O-acetyl-2-deoxy- $\alpha$ -D-glucopyranoside **5.22**:



**5.21** (0.31 g, 0.574 mmol) was dissolved in a mixture MeOH (3.8 mL), H<sub>2</sub>O (0.47 mL), and Et<sub>3</sub>N (0.47 mL) and allowed to stir at room temperature overnight (14 h). The reaction was concentrated and coevaporated with toluene (2 x 10 mL). The intermediate was dried and taken on to the next step without further purification. The intermediate was dissolved in THF (5 mL) and stirred at room temperature (18°C) under nitrogen. TBSCl (0.246 g, 1.63 mmol) followed by imidazole (0.185 g, 2.72 mmol) was added and the reaction mixture was allowed to stir overnight (16 h). The reaction was then diluted with EtOAc (10 mL) and then washed with H<sub>2</sub>O (2 x 10 mL), dried over Na<sub>2</sub>SO<sub>4</sub>, and concentrated. The

crude material was purified by silica gel chromatography (gradient run 20% to 40% EtOAc in Hexanes) to afford 58.7 mg (21%) of **5.22**.  $^1\text{H}$  NMR (400 MHz,  $\text{CDCl}_3$ )  $\delta$  7.38 – 7.32 (m, 5H), 7.28 (d,  $J$  = 17.5 Hz, 2H), 5.10 (s, 3H), 4.30 (d,  $J$  = 7.9 Hz, 1H), 3.97 – 3.88 (m, 2H), 3.81 (dd,  $J$  = 10.4, 6.2 Hz, 1H), 3.67 – 3.52 (m, 2H), 3.46 (d,  $J$  = 1.8 Hz, 1H), 3.38 – 3.23 (m, 4H), 2.84 (d,  $J$  = 2.7 Hz, 1H), 2.10 – 1.99 (m, 2H), 1.85 (q,  $J$  = 6.4 Hz, 2H), 0.90 (s, 9H), 0.09 (d,  $J$  = 2.0 Hz, 6H).  $^{13}\text{C}$  NMR (101 MHz,  $\text{CDCl}_3$ )  $\delta$  156.58, 128.52, 128.09, 97.70, 73.30, 71.98, 70.46, 66.66, 64.20, 62.76, 38.90, 29.31, 25.85, 18.27, -5.45, -5.47.



### Synthesis of **5.23** and **5.24**




**5.13** (101.7 mg, 0.142 mmol), **5.22** (48.5 mg, 0.095 mmol), and 3Å molecular sieves (174.3 mg) were added to a dry reaction flask. Dichloromethane (1.6 mL) was added and the reaction was allowed to stir for 1 hr then cooled to -25°C. *N*-iodosuccinimide (64.1 mg, 0.285 mmol) and triflic acid (1.6  $\mu\text{L}$ , 0.019 mmol) were added to the mixture and allowed to stir for 40 min. Upon completion by TLC analysis the reaction mixture was filtered through celite and extracted with chloroform. The organic layer was then washed with  $\text{NaHCO}_3$ ,  $\text{Na}_2\text{S}_2\text{O}_3$ , and brine. The organic layer was dried over  $\text{Na}_2\text{SO}_4$  and concentrated. The crude material was purified via silica gel chromatography (gradient run 10% to 20% EtOAc in Hexanes) to afford 50.8 mg (52%) of **5.23** and **5.24** as a sticky solid.  $^1\text{H}$  NMR (500 MHz,  $\text{CDCl}_3$ )  $\delta$  8.13 – 8.05 (m, 3H), 7.61 – 7.54 (m, 1H), 7.45 (t,  $J$  = 7.6 Hz, 3H), 7.42 – 7.30 (m, 7H), 5.34 – 5.23 (m, 2H), 5.12 (d,  $J$  = 4.4 Hz, 3H), 5.03 (d,  $J$

= 6.2 Hz, 1H), 4.93 (d,  $J$  = 3.5 Hz, 1H), 4.77 (s, 1H), 4.77 – 4.68 (m, 2H), 4.33 – 4.26 (m, 2H), 4.23 – 4.06 (m, 3H), 3.99 – 3.90 (m, 2H), 3.86 – 3.71 (m, 5H), 3.67 (t,  $J$  = 5.6 Hz, 2H), 3.63 – 3.50 (m, 2H), 3.44 – 3.31 (m, Hz, 3H), 3.03 – 2.94 (m, 1H), 1.96 – 1.82 (m, 3H), 1.28 (s, 2H), 1.12 (d,  $J$  = 3.4 Hz, 13H), 0.99 (s, 12H), 0.91 (d,  $J$  = 4.2 Hz, 13H), 0.14 – 0.06 (m, 8H).  $^{13}\text{C}$  NMR (126 MHz,  $\text{CDCl}_3$ )  $\delta$  166.62, 156.53, 154.65, 133.20, 129.96, 129.76, 128.56, 128.54, 128.41, 128.39, 128.15, 128.11, 100.57, 98.41, 95.56, 77.92, 75.56, 74.26, 74.16, 72.06, 70.66, 69.33, 68.38, 67.99, 67.21, 66.72, 66.09, 65.39, 63.92, 49.68, 38.52, 29.71, 29.61, 29.45, 27.51, 27.48, 27.34, 27.31, 25.90, 25.85, 25.62, 23.29, 23.28, 20.80, 18.38, 18.23, 0.01, -5.19, -5.30, -5.52, -5.54.

## APPENDIX A. COPYRIGHT RELEASE FOR CHAPTER 3



[Home](#) [Help](#) [Email Support](#) [Sign in](#) [Create Account](#)



**Acid-Catalyzed O-Glycosylation with Stable Thioglycoside Donors**  
Author: Kristina D. Lacey, Rashaniqua D. Quarels, Shaofu Du, et al  
Publication: Organic Letters  
Publisher: American Chemical Society  
Date: Sep 1, 2018  
*Copyright © 2018, American Chemical Society*

**PERMISSION/LICENSE IS GRANTED FOR YOUR ORDER AT NO CHARGE**

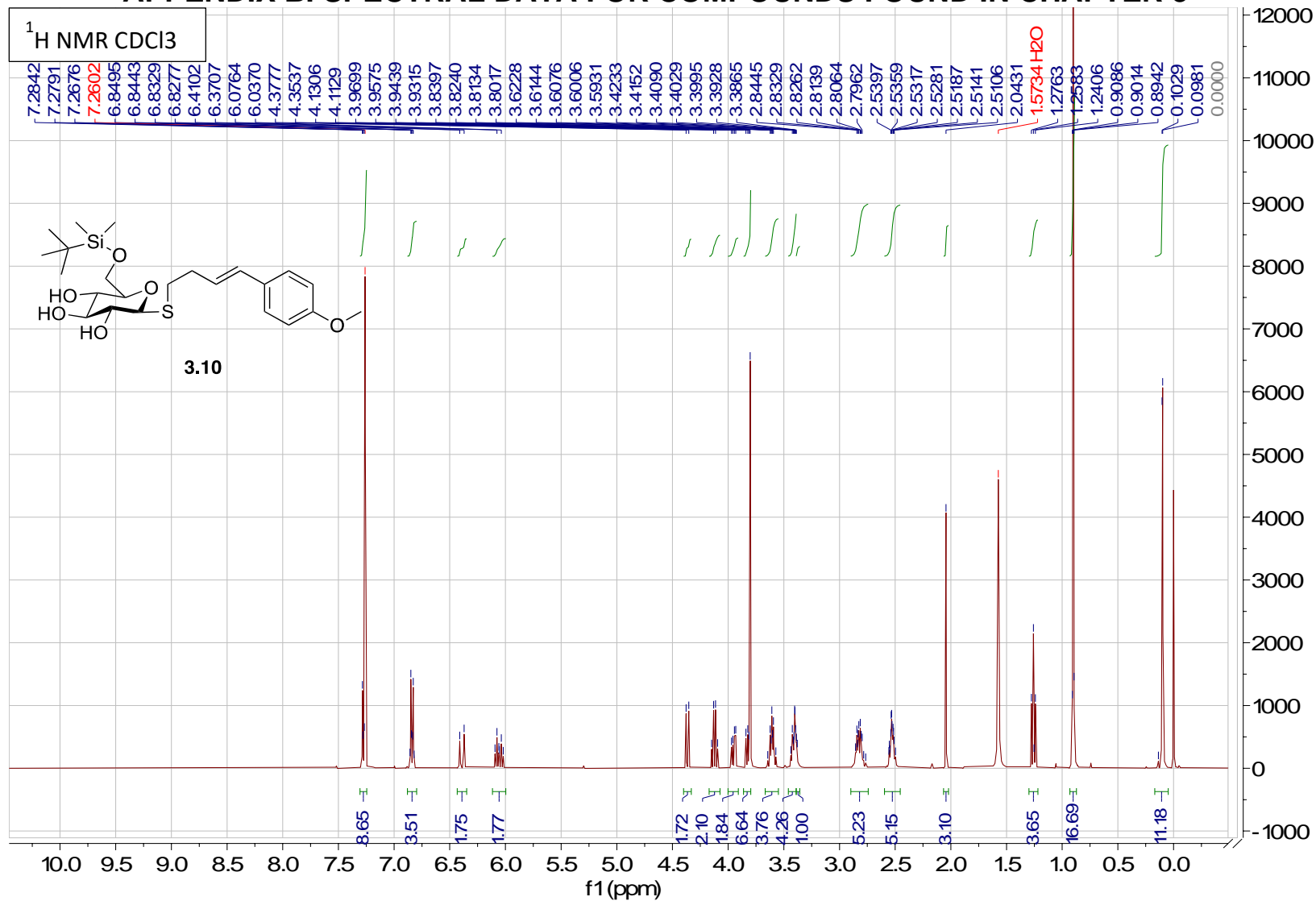
This type of permission/license, instead of the standard Terms & Conditions, is sent to you because no fee is being charged for your order. Please note the following:

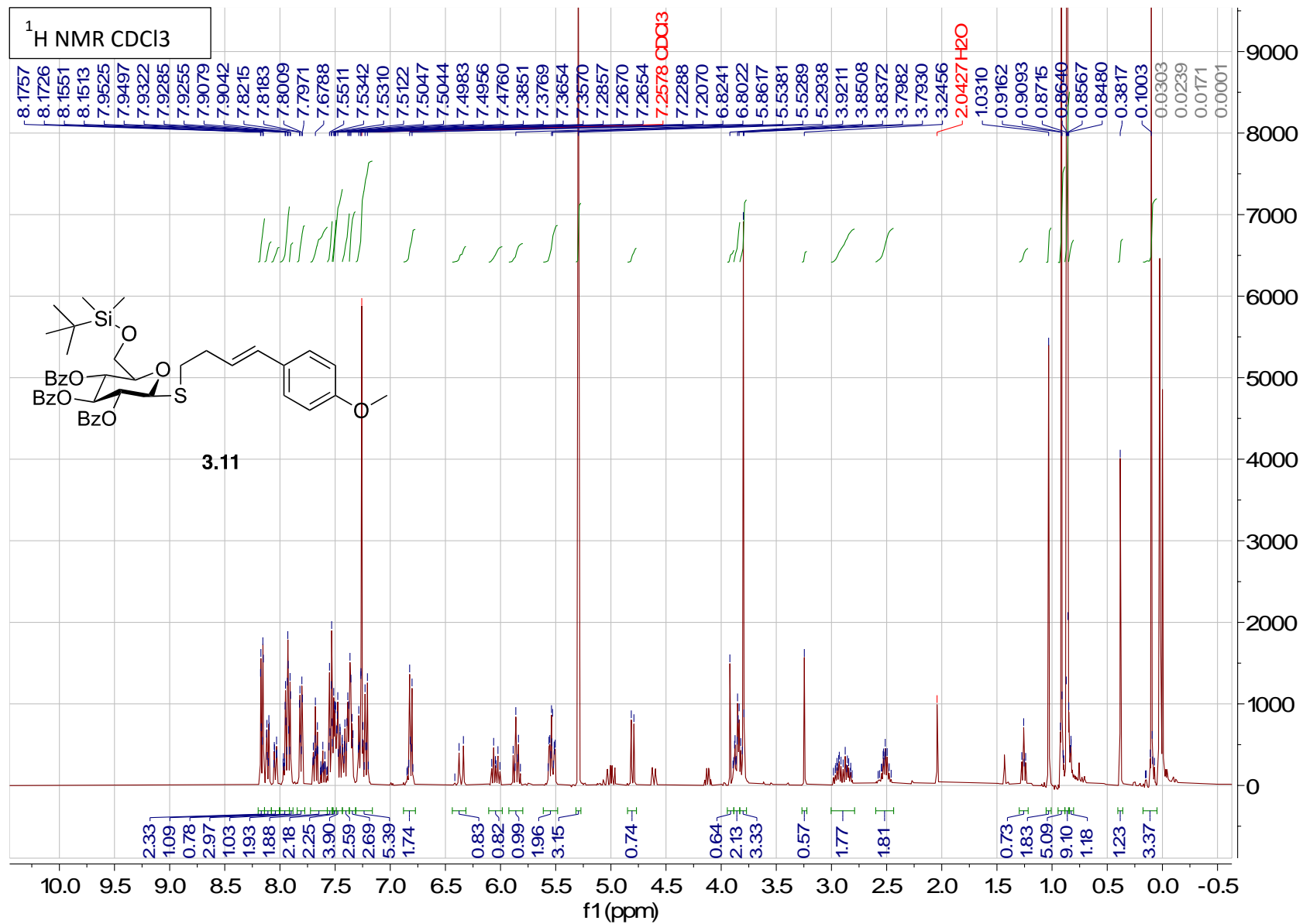
- Permission is granted for your request in both print and electronic formats, and translations.
- If figures and/or tables were requested, they may be adapted or used in part.
- Please print this page for your records and send a copy of it to your publisher/graduate school.
- Appropriate credit for the requested material should be given as follows: "Reprinted (adapted) with permission from (COMPLETE REFERENCE CITATION). Copyright (YEAR) American Chemical Society." Insert appropriate information in place of the capitalized words.
- One-time permission is granted only for the use specified in your request. No additional uses are granted (such as derivative works or other editions). For any other uses, please submit a new request.

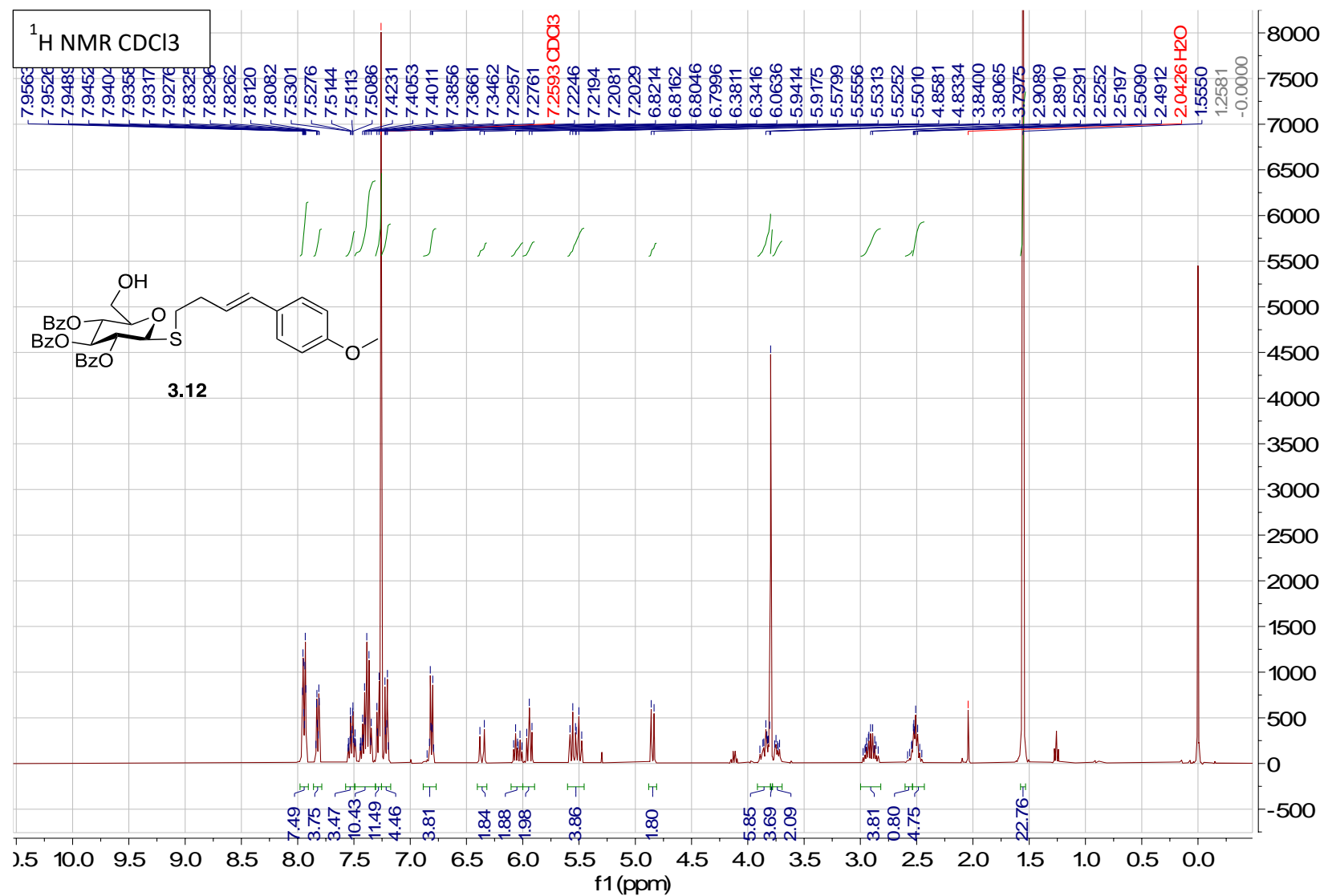
[BACK](#) [CLOSE WINDOW](#)

© 2020 Copyright - All Rights Reserved | Copyright Clearance Center, Inc. | [Privacy statement](#) | [Terms and Conditions](#)  
Comments? We would like to hear from you. E-mail us at [customer@copyright.com](mailto:customer@copyright.com)

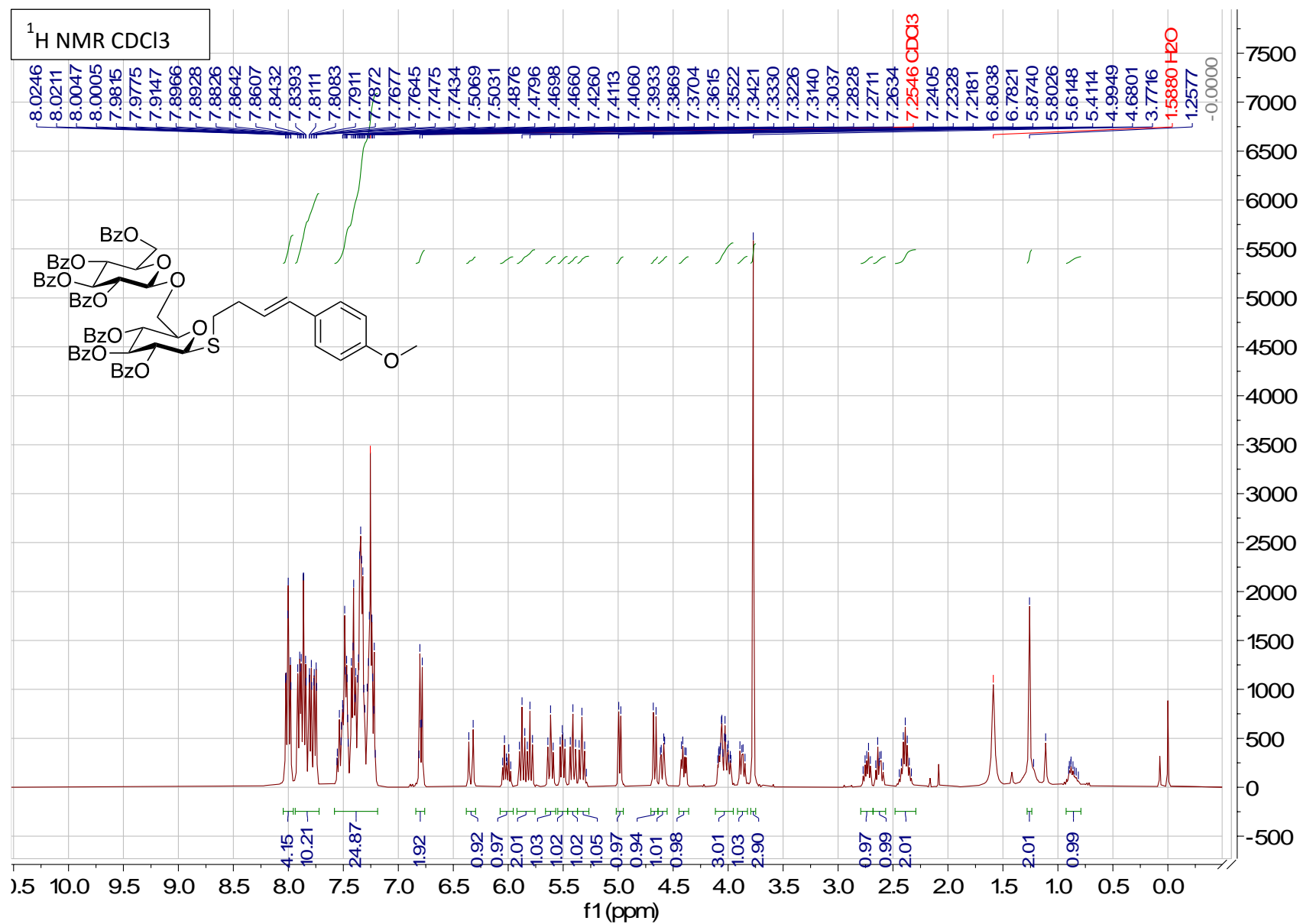
## APPENDIX B. SPECTRAL DATA FOR COMPOUNDS FOUND IN CHAPTER 3

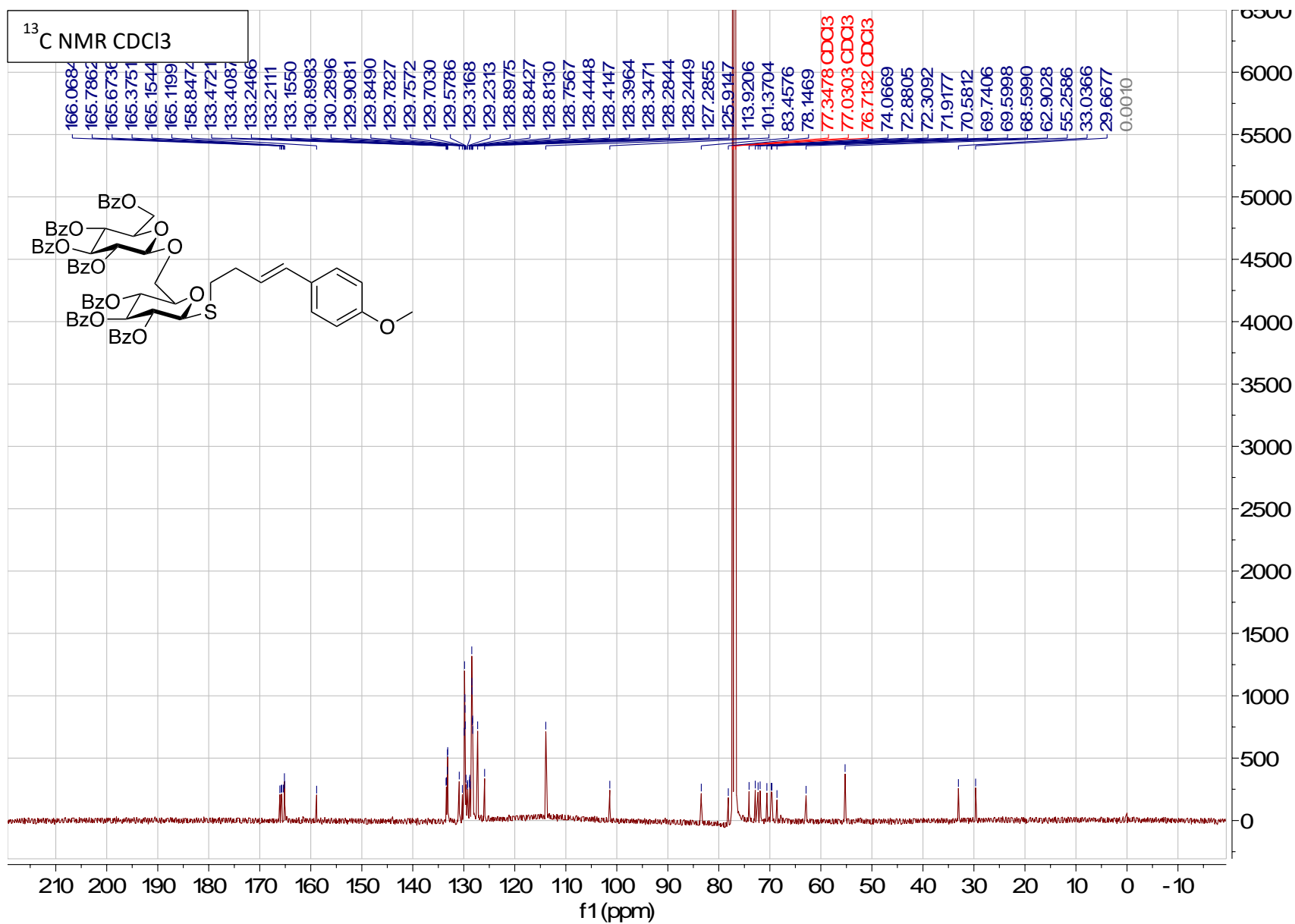


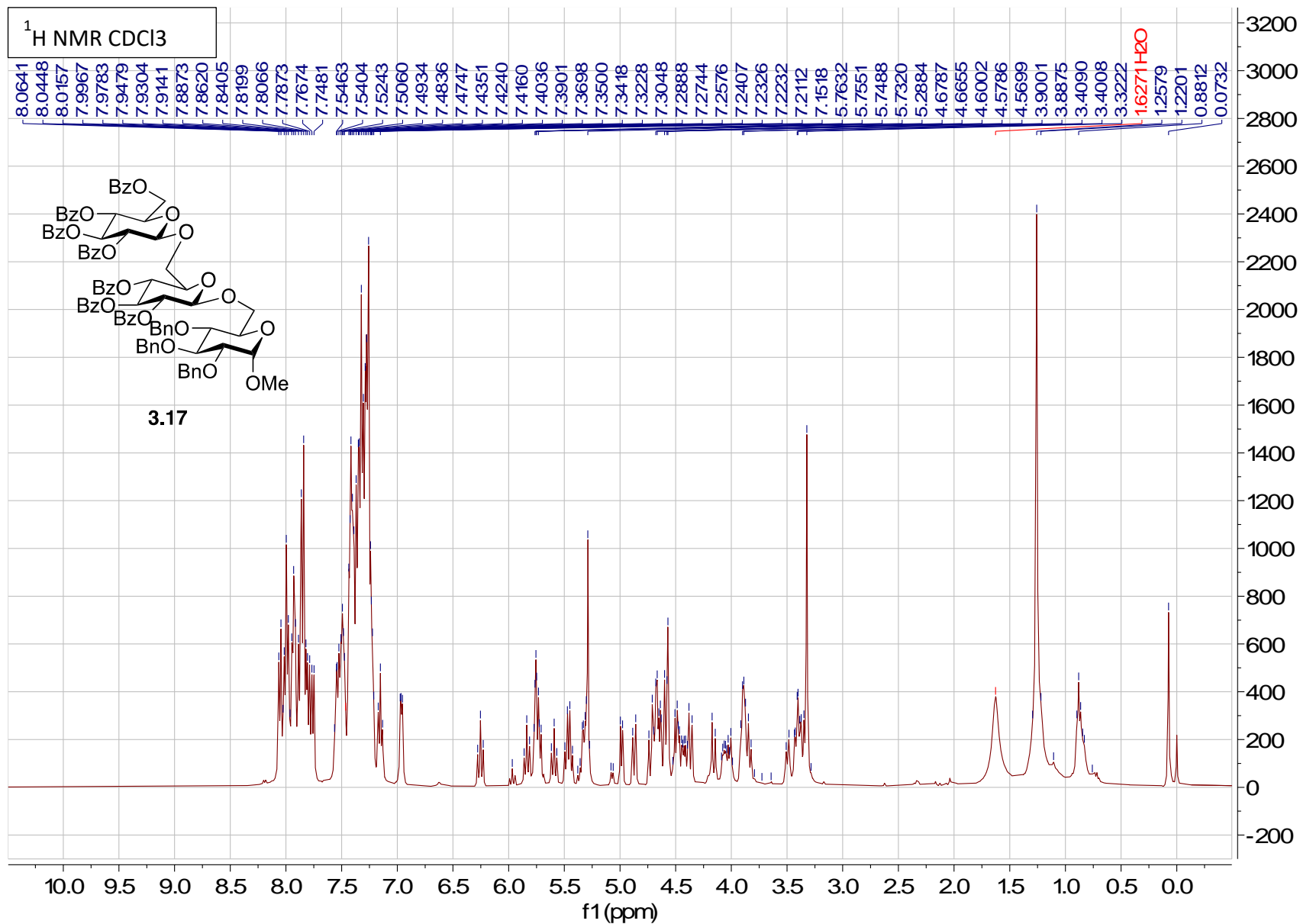


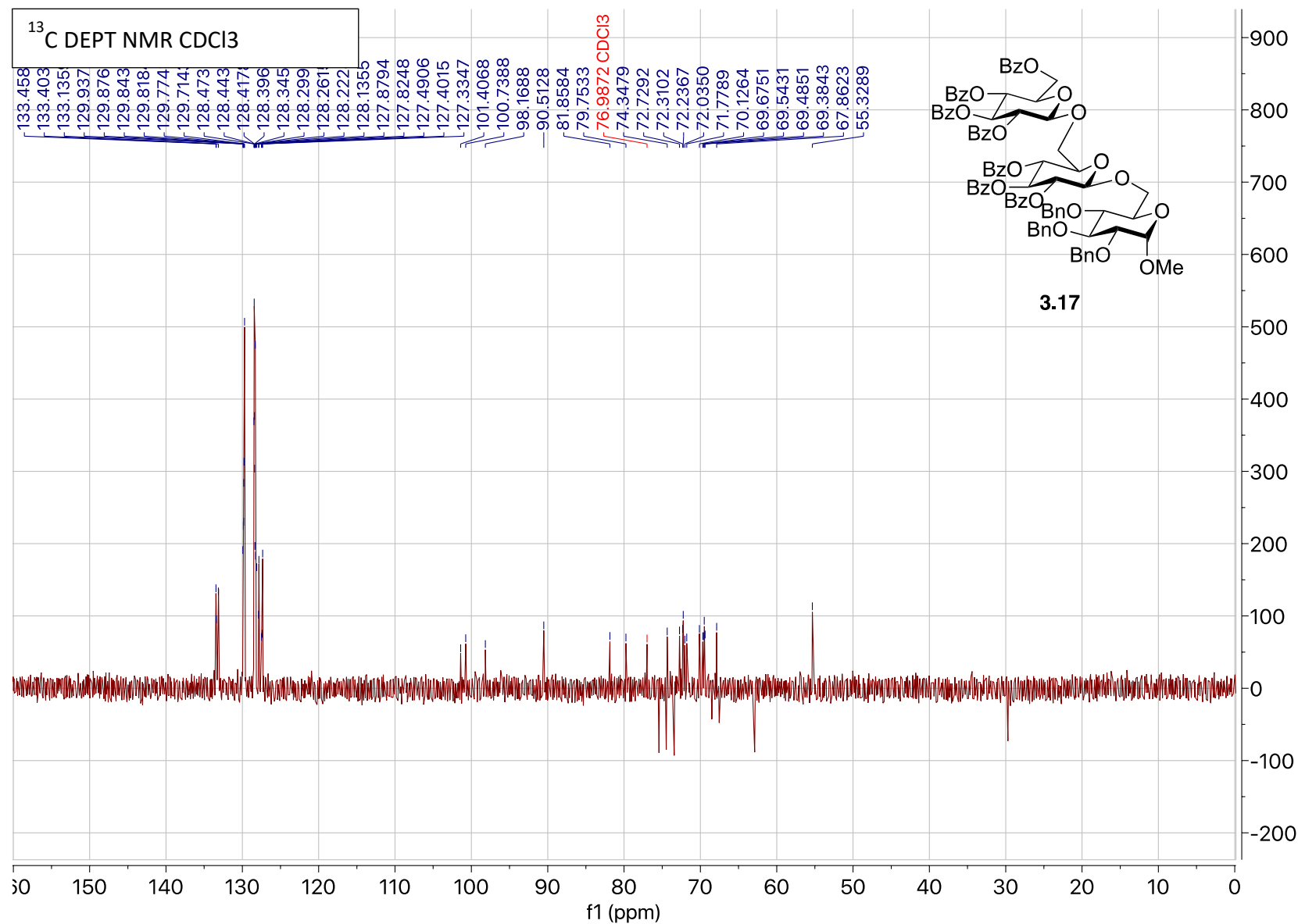




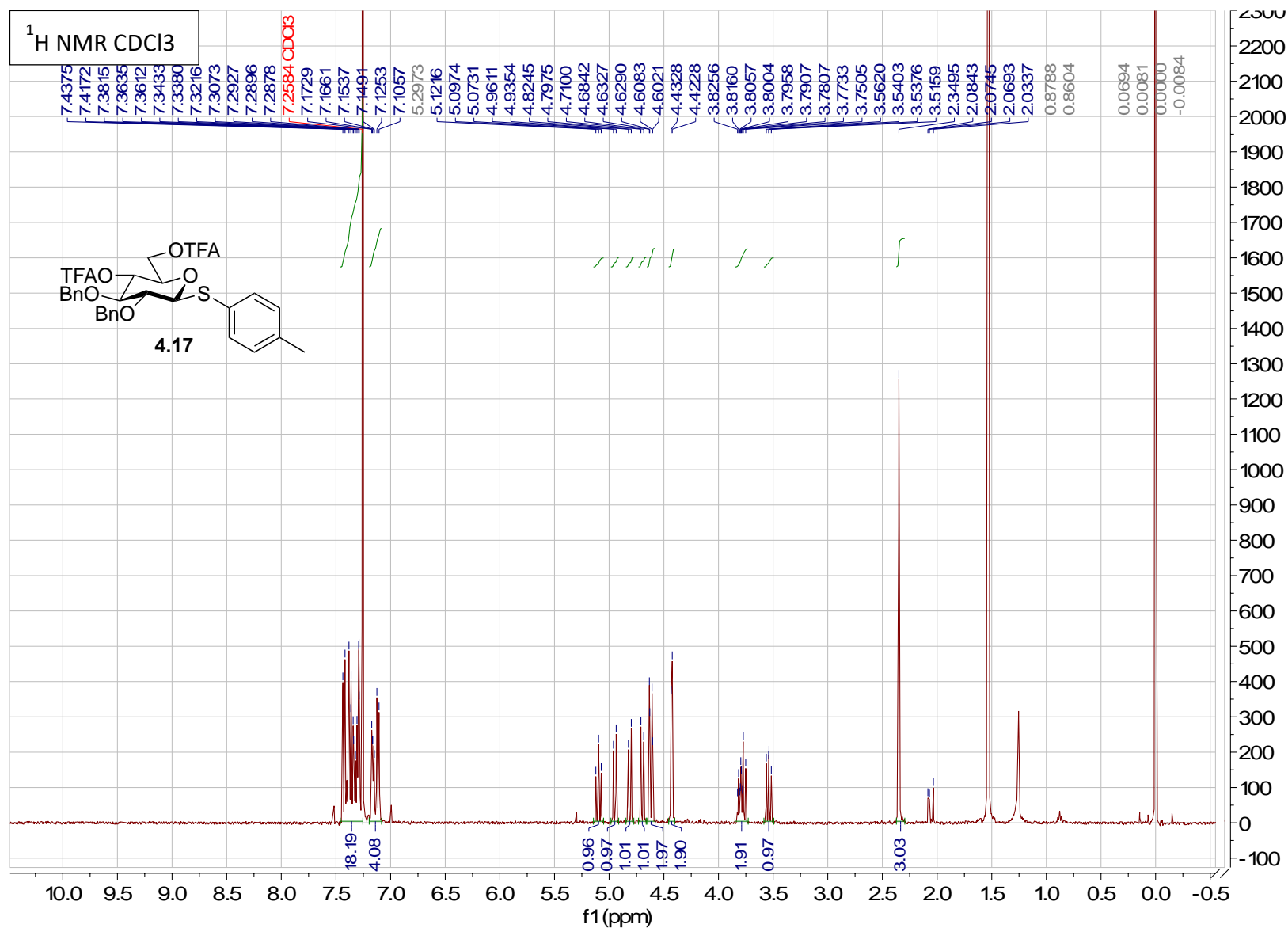


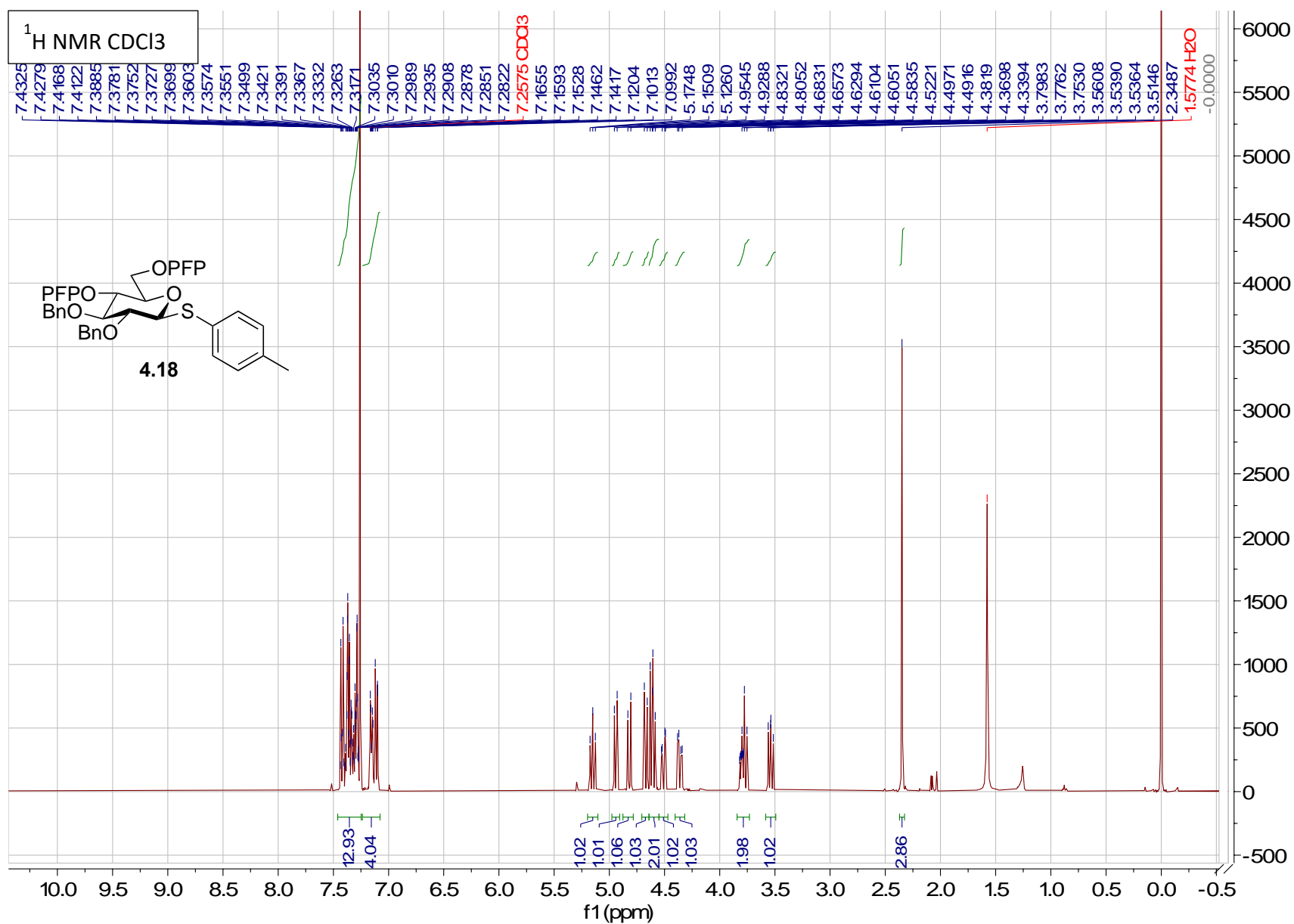


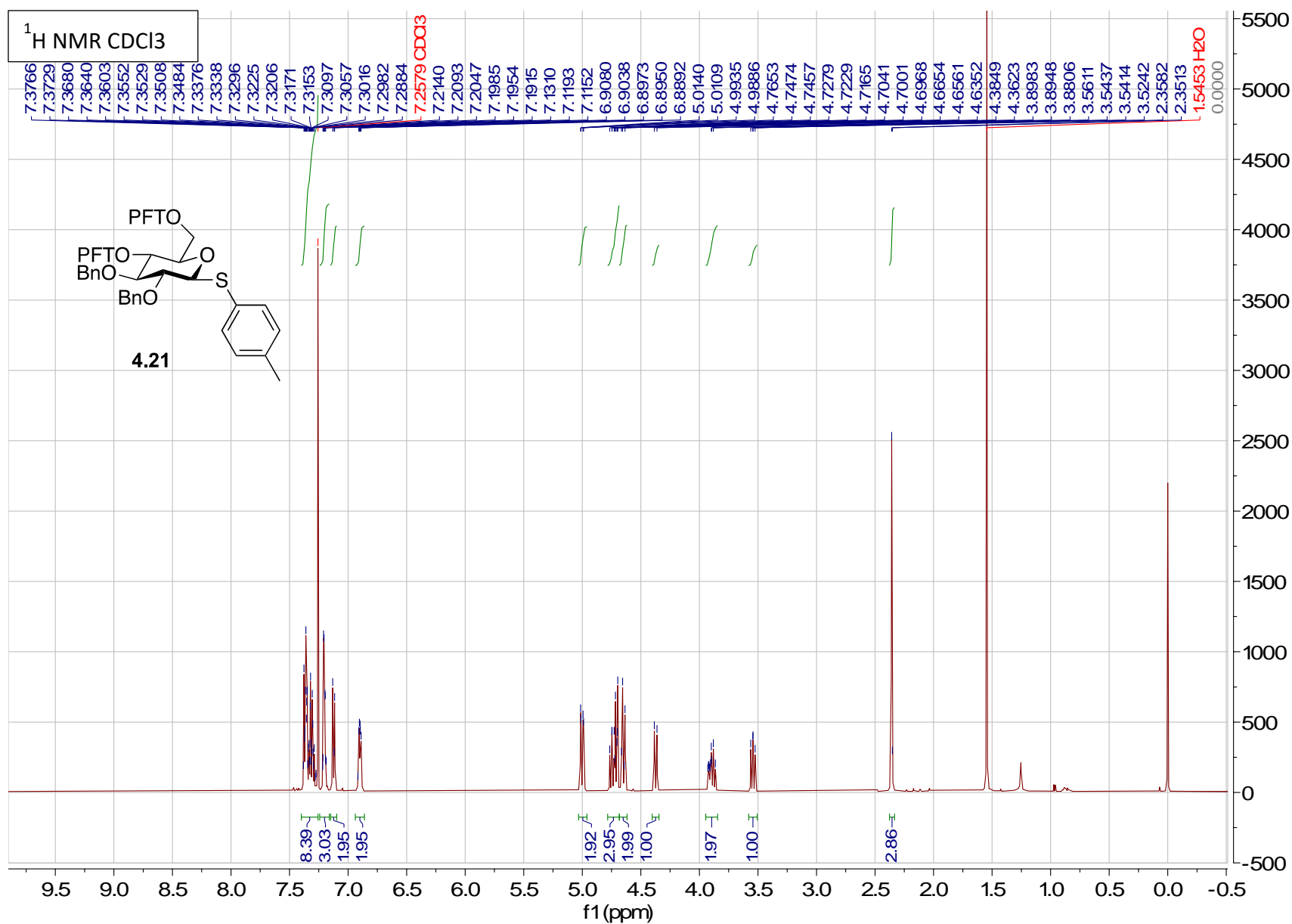


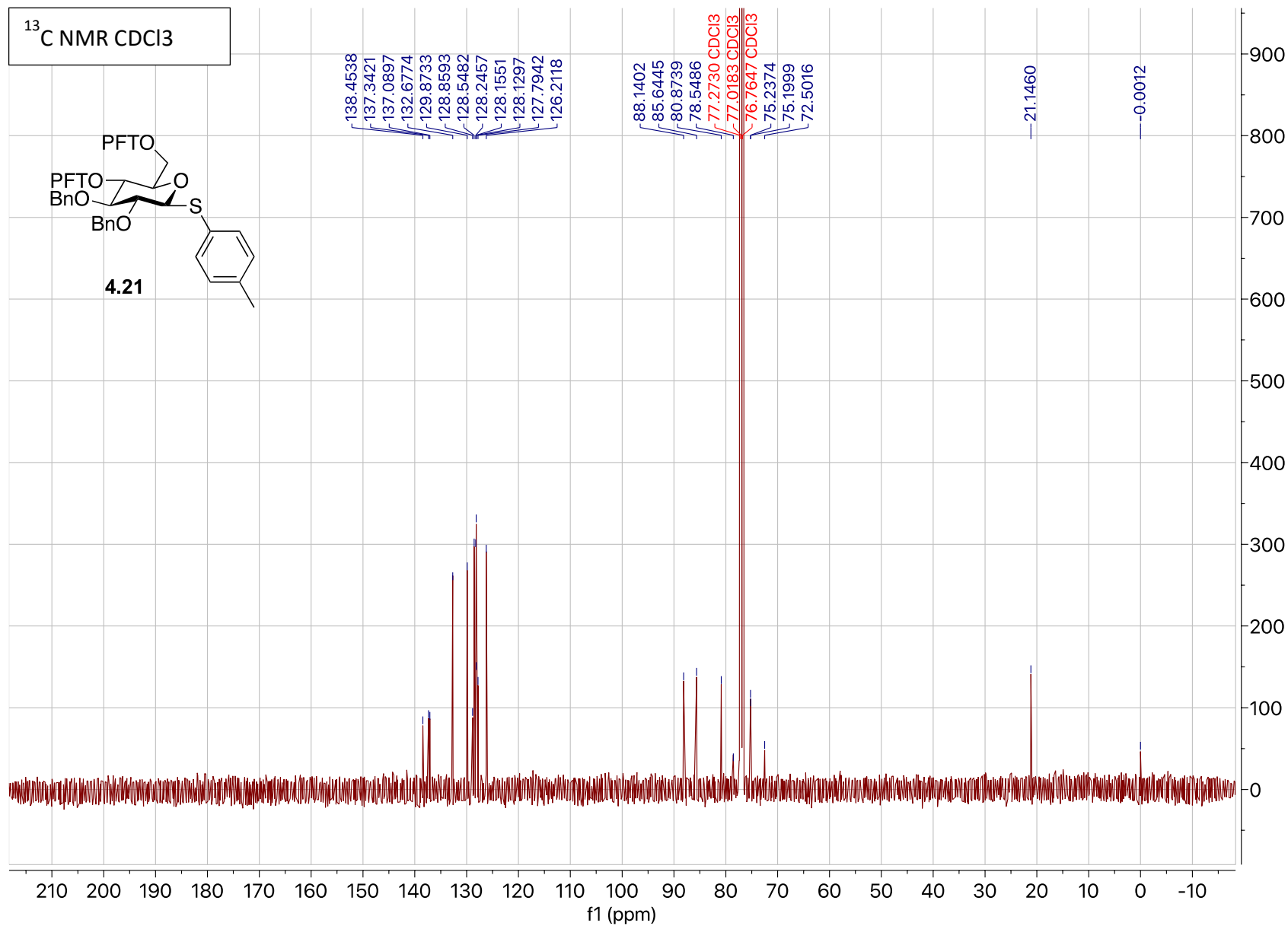


# APPENDIX C. SPECTRAL DATA FOR COMPOUNDS FOUND IN CHAPTER 4

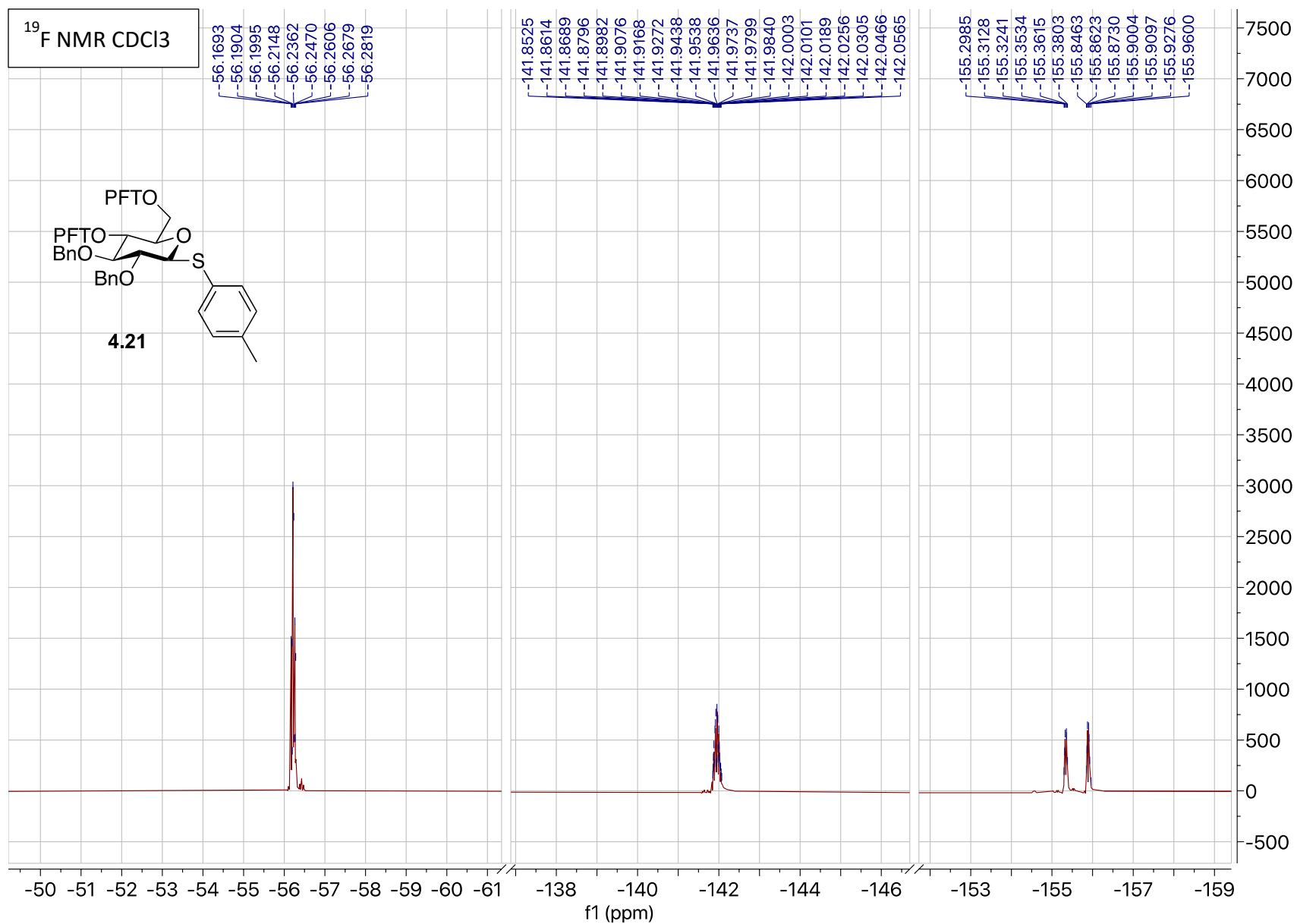


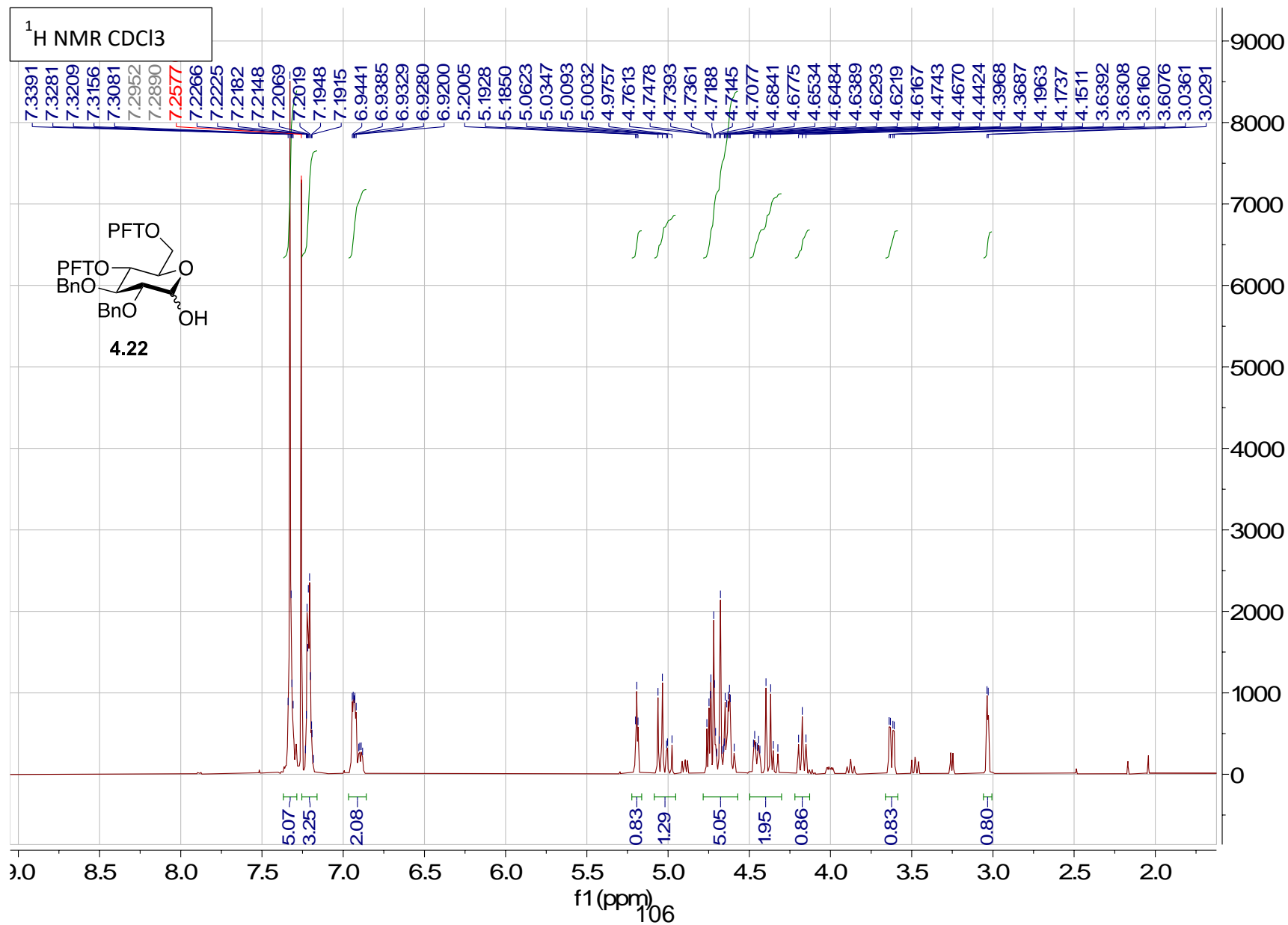


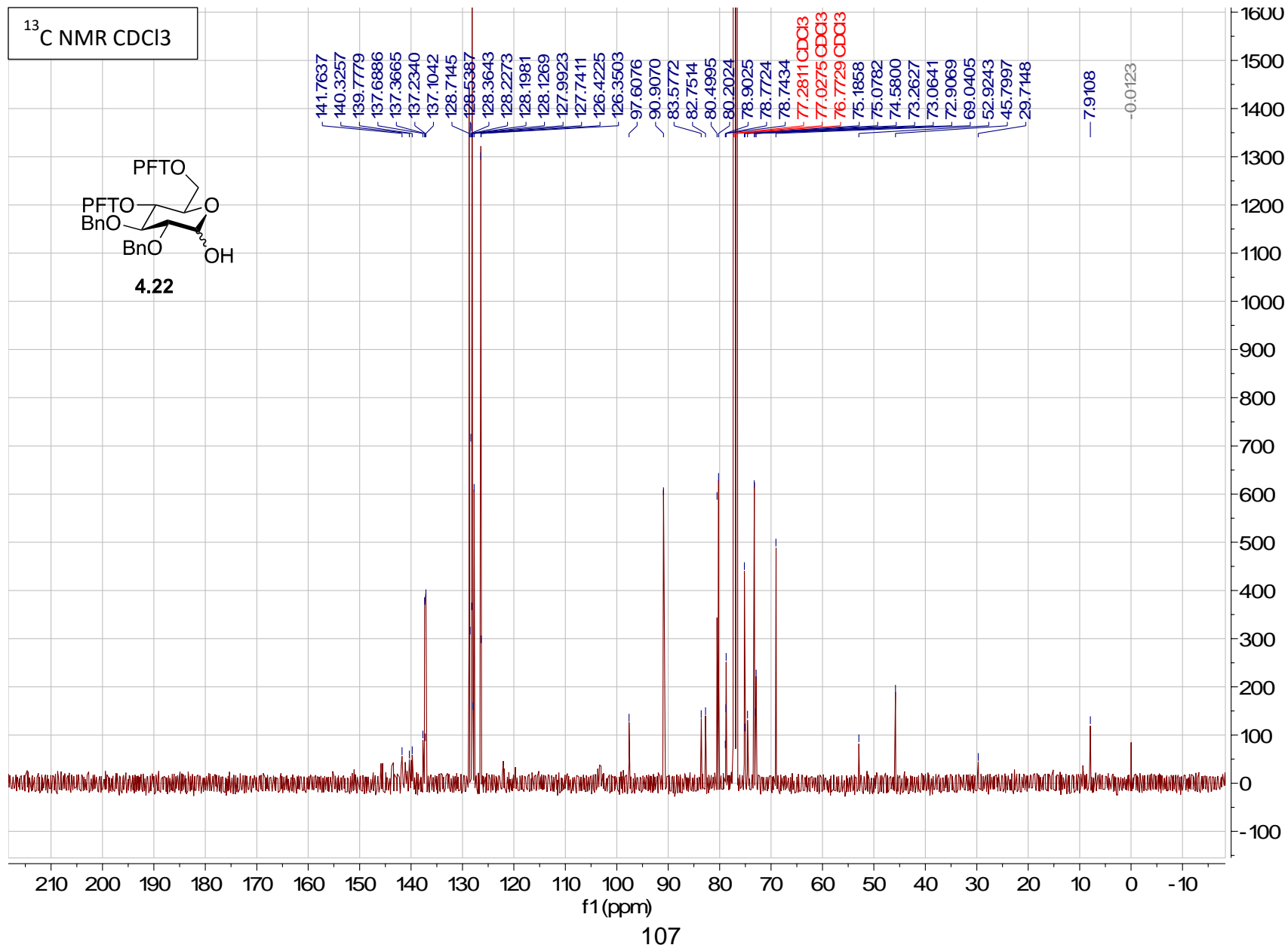


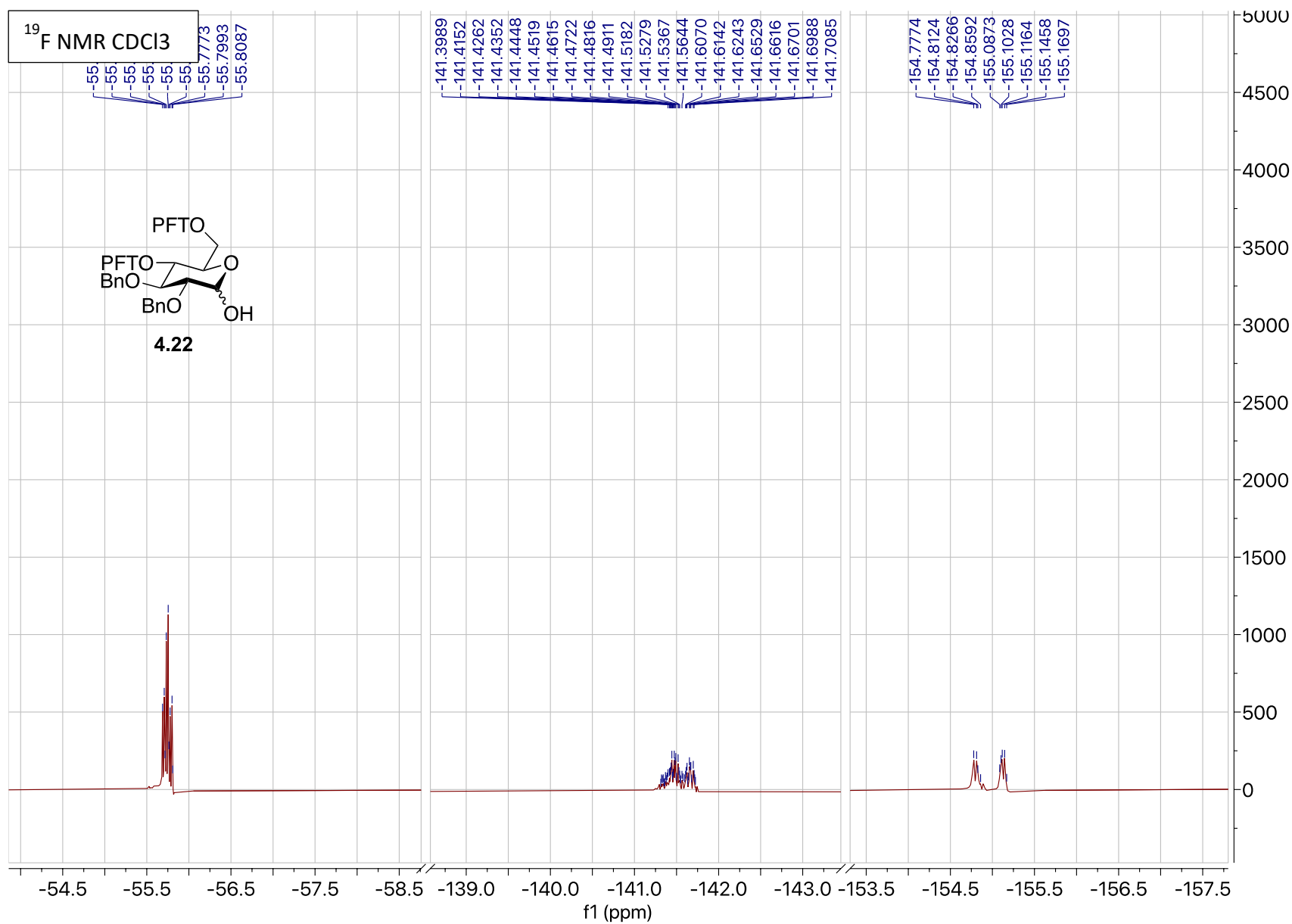


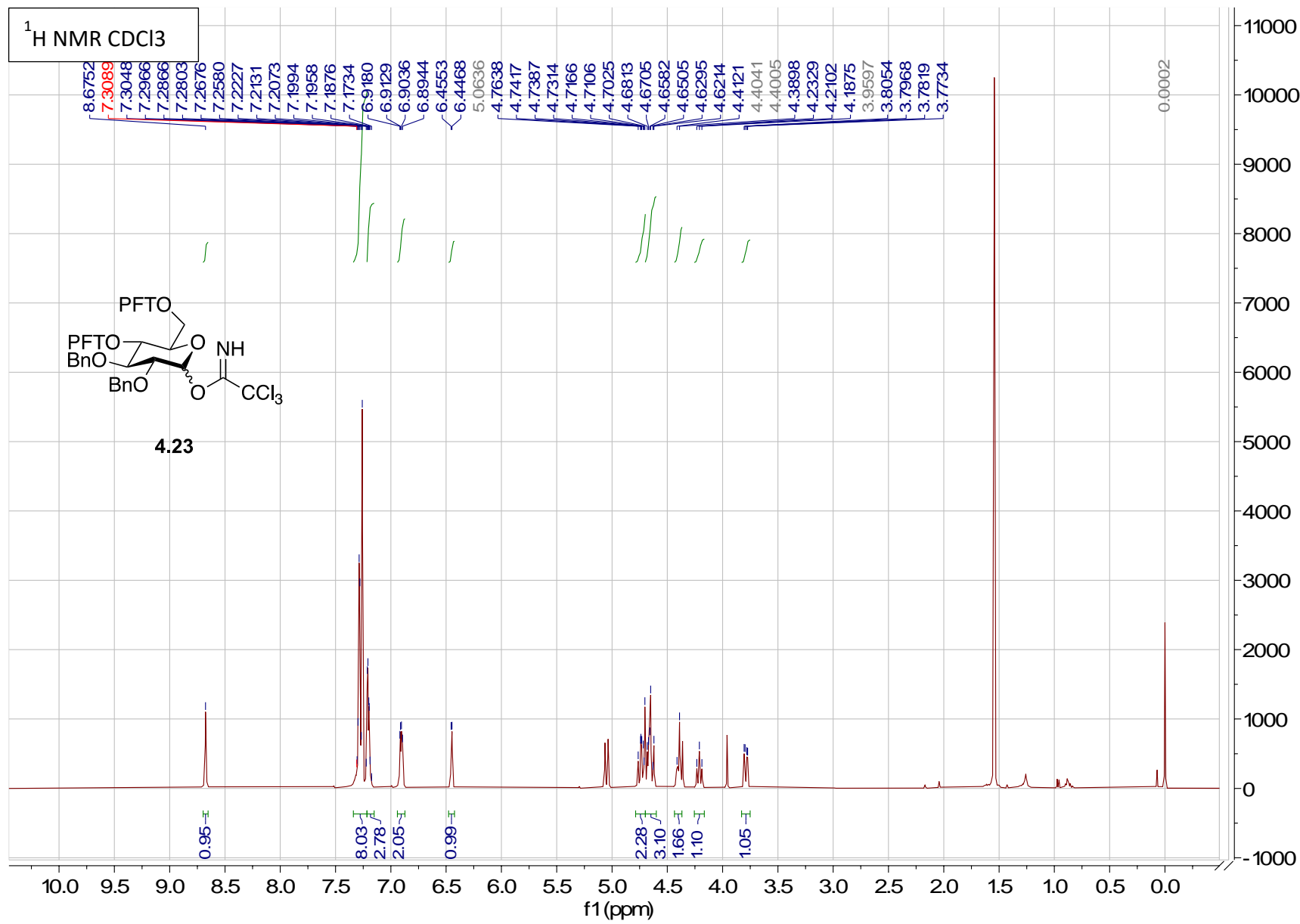


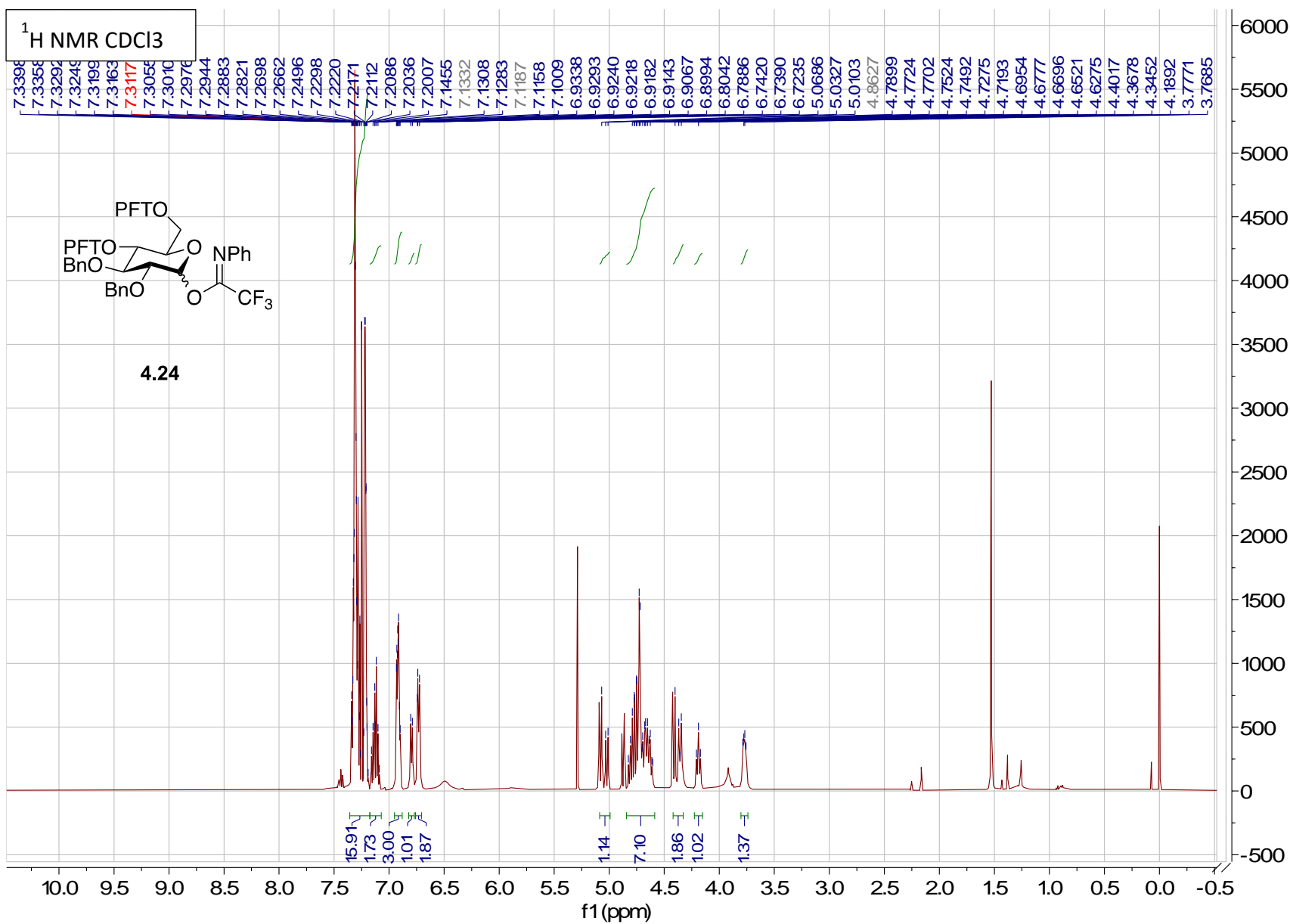


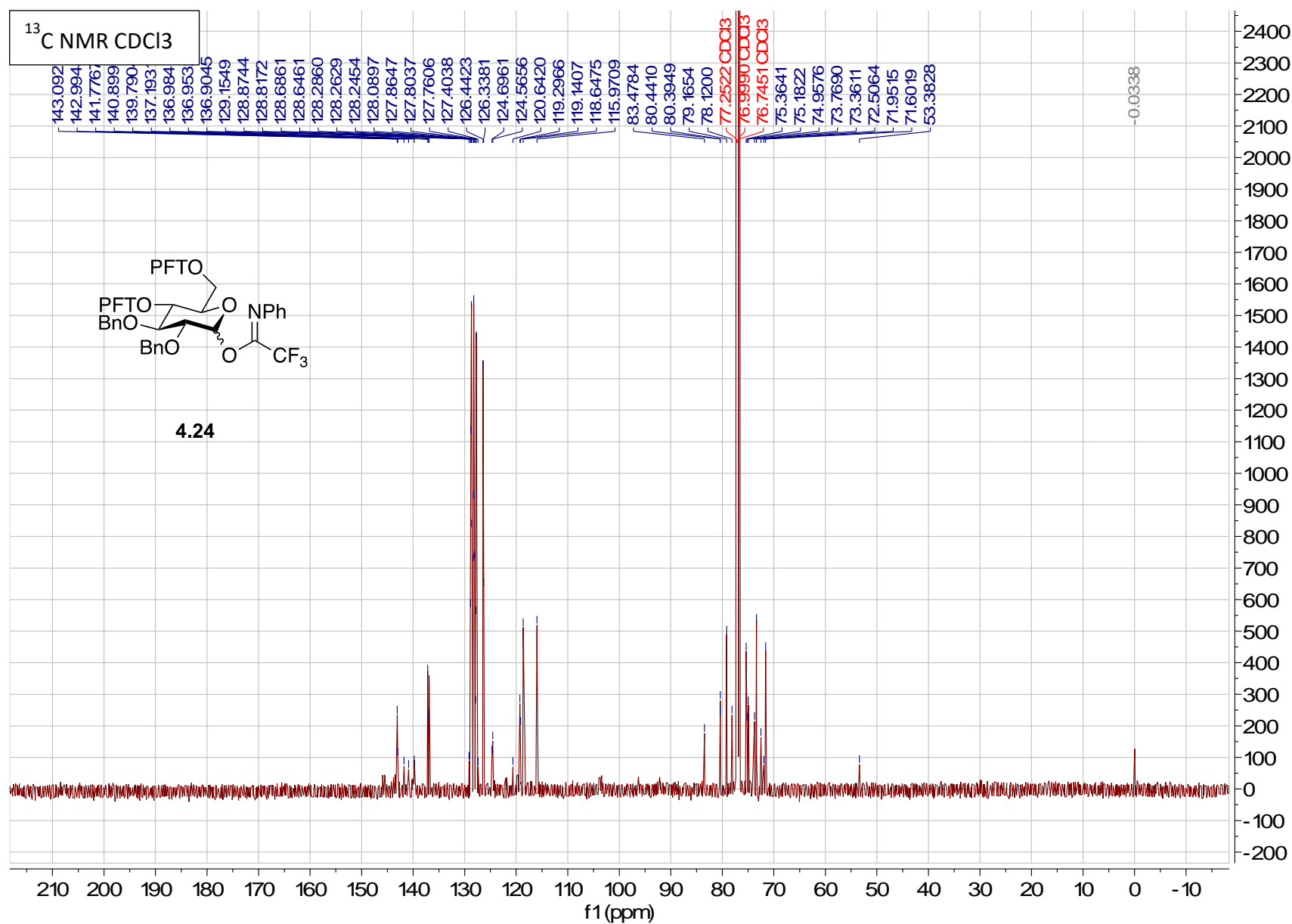


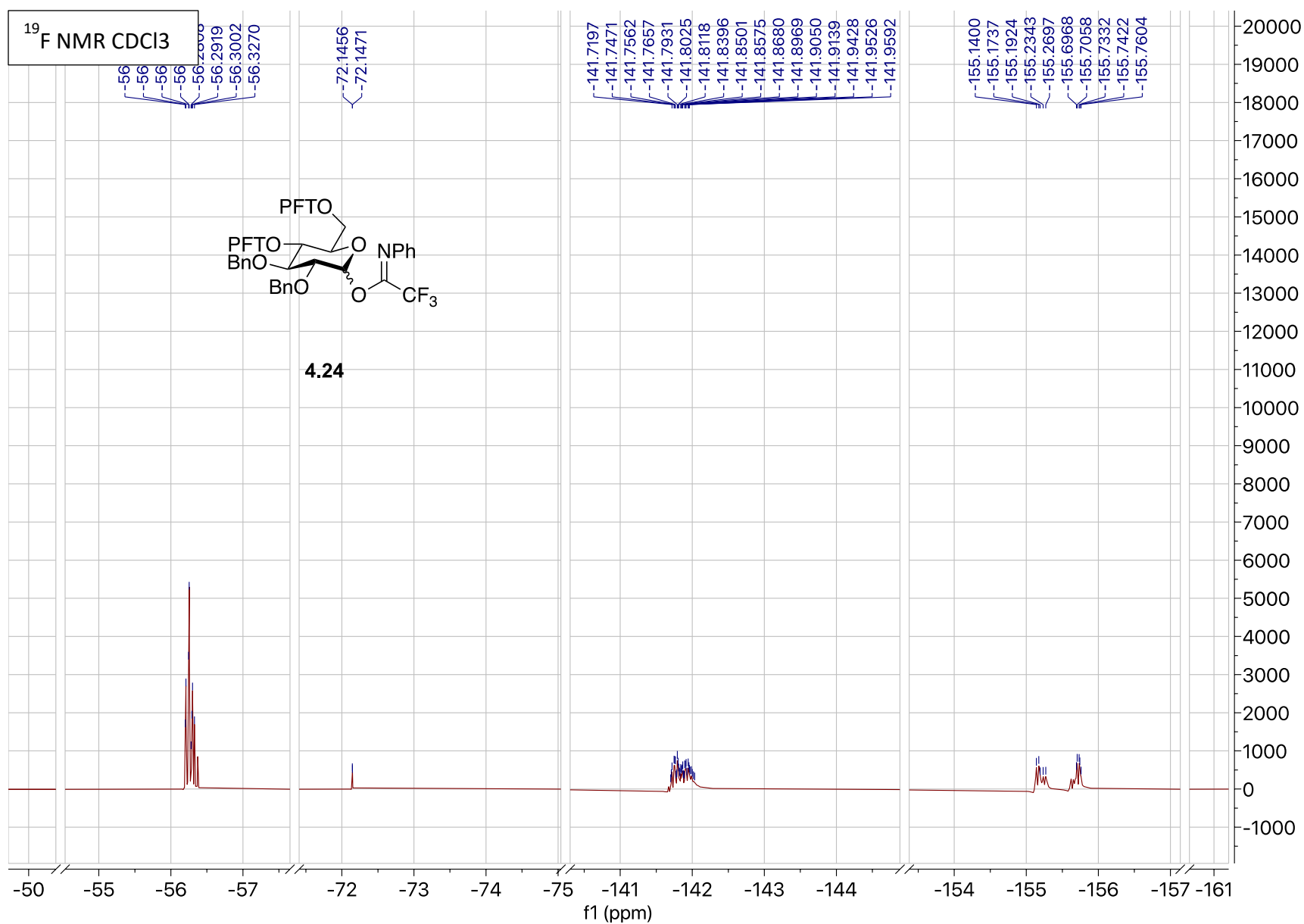




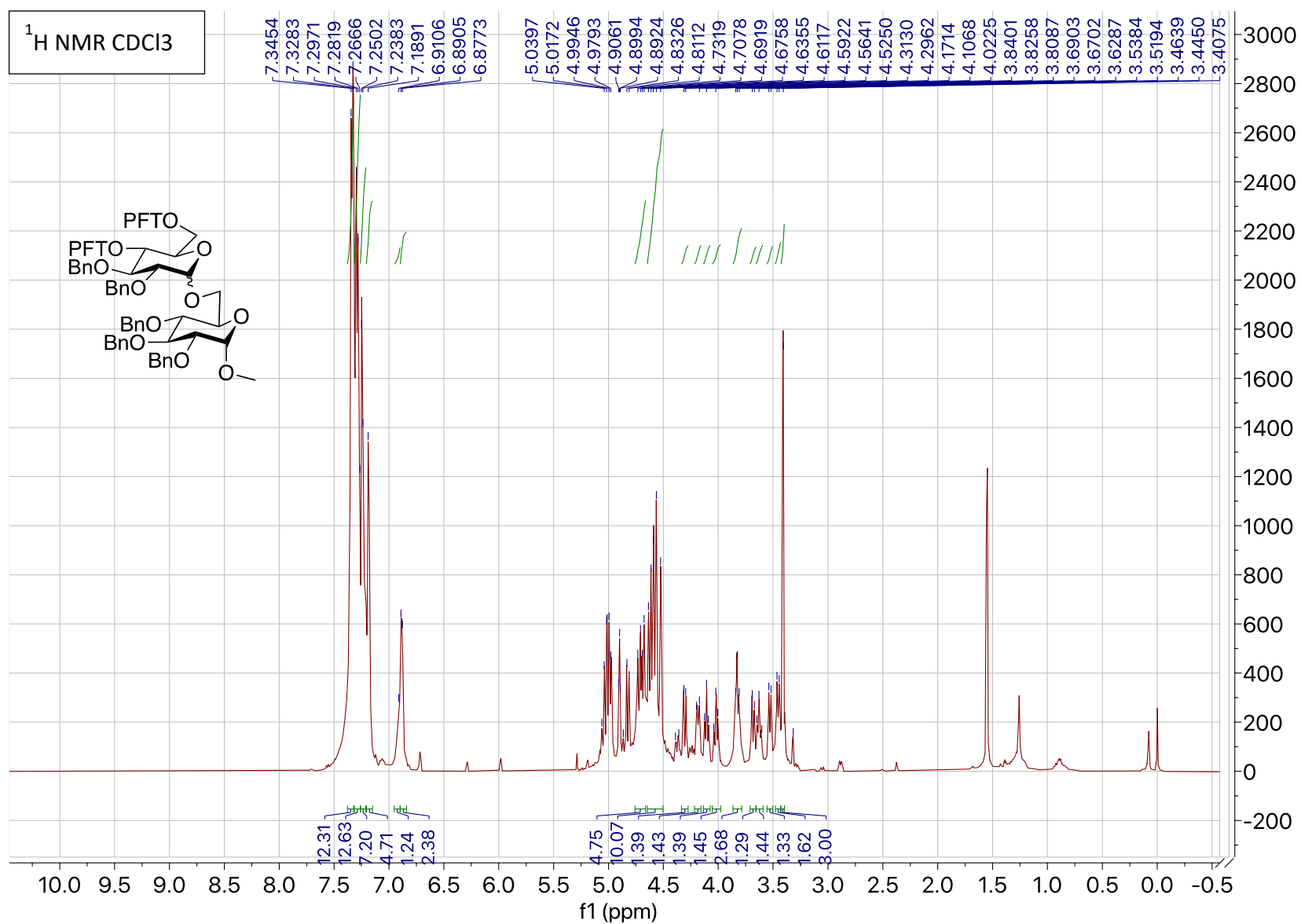




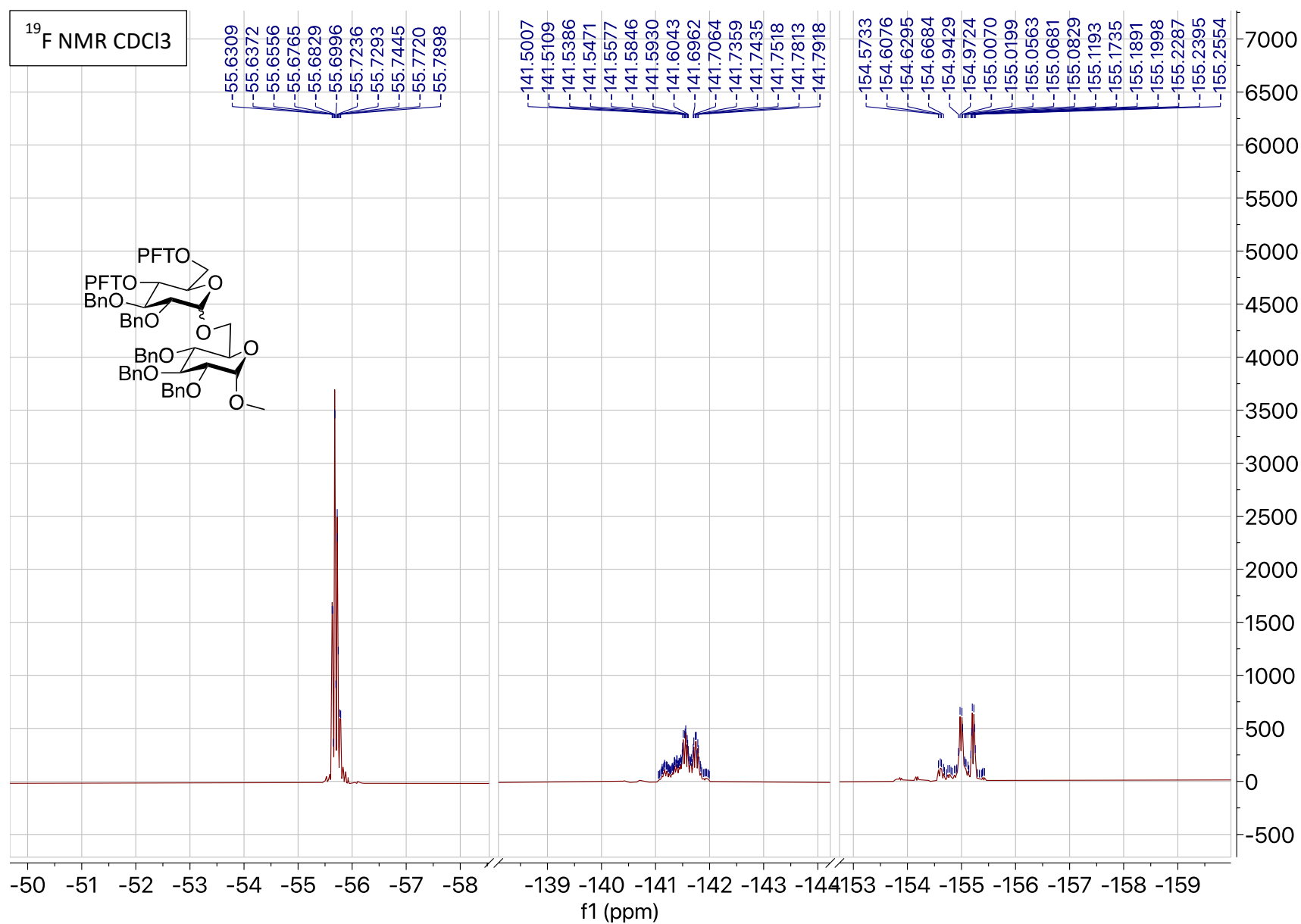




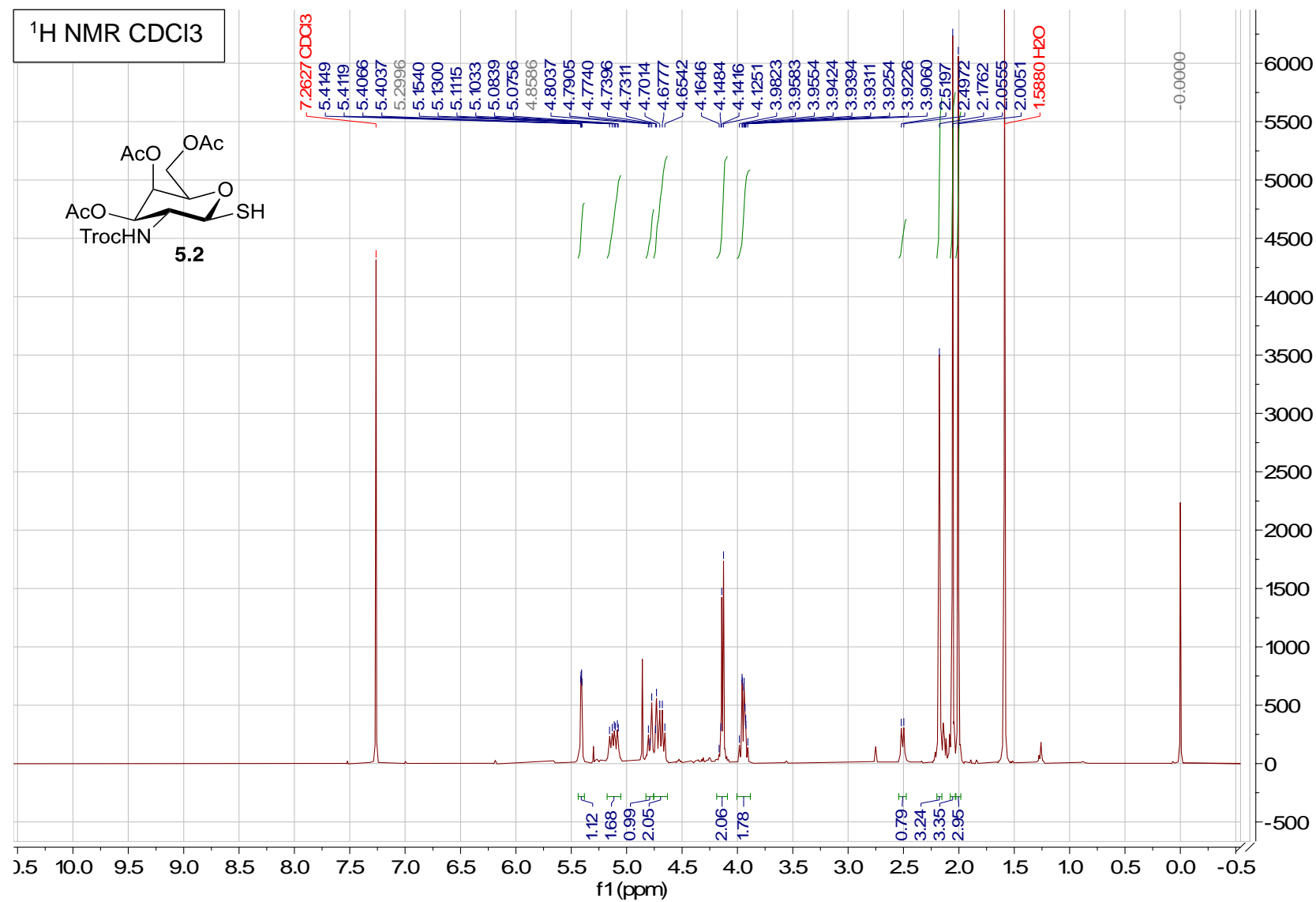


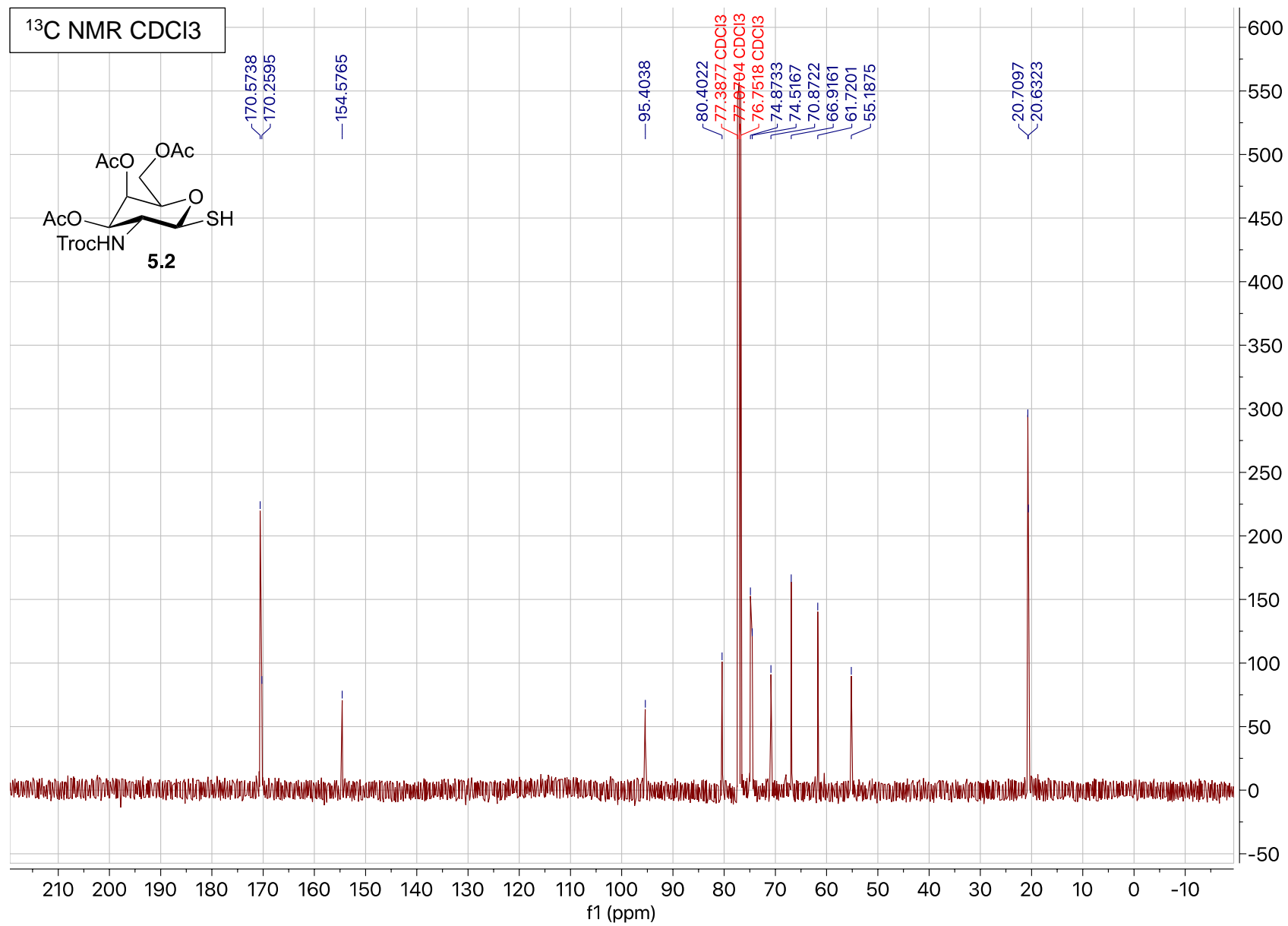


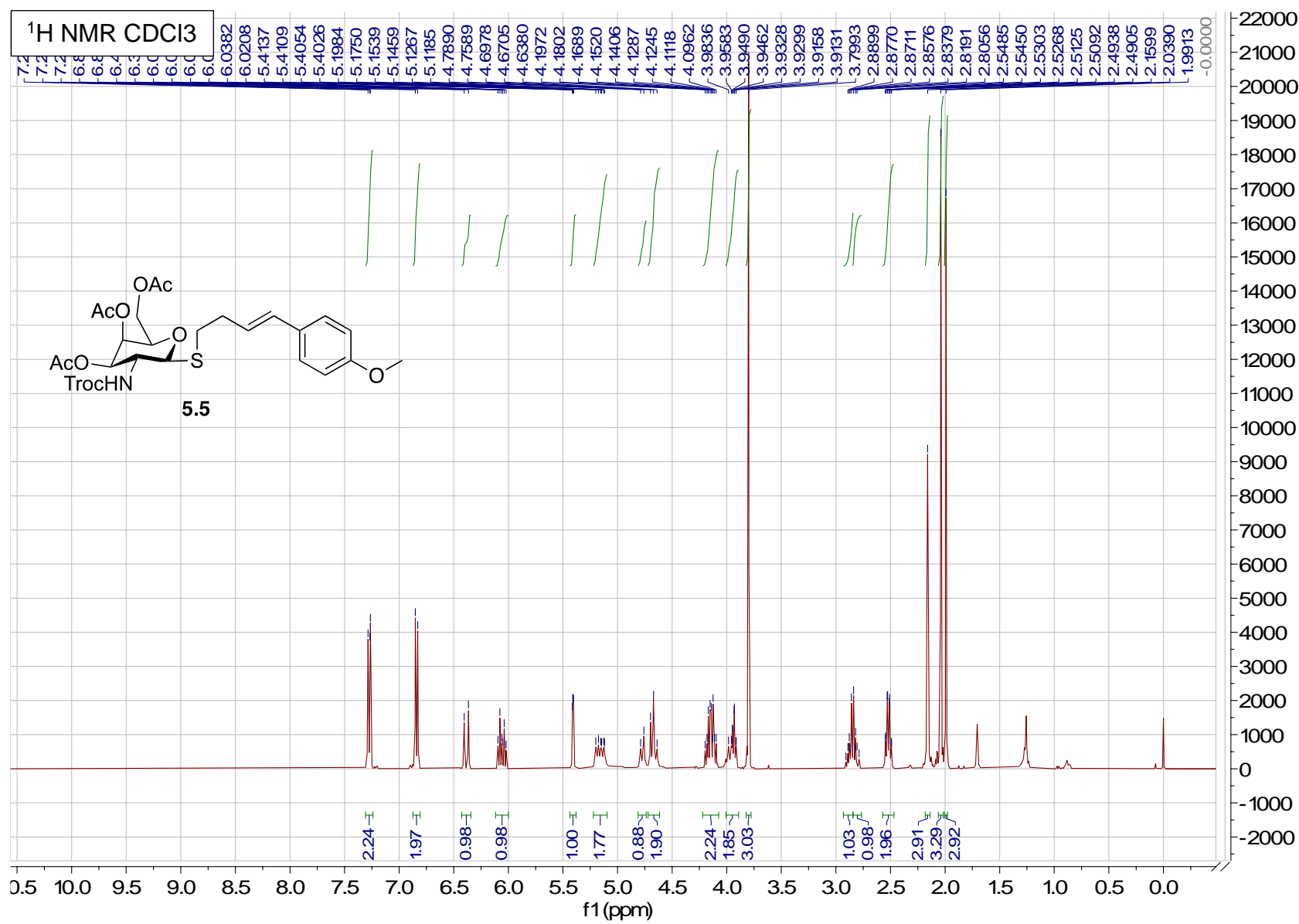


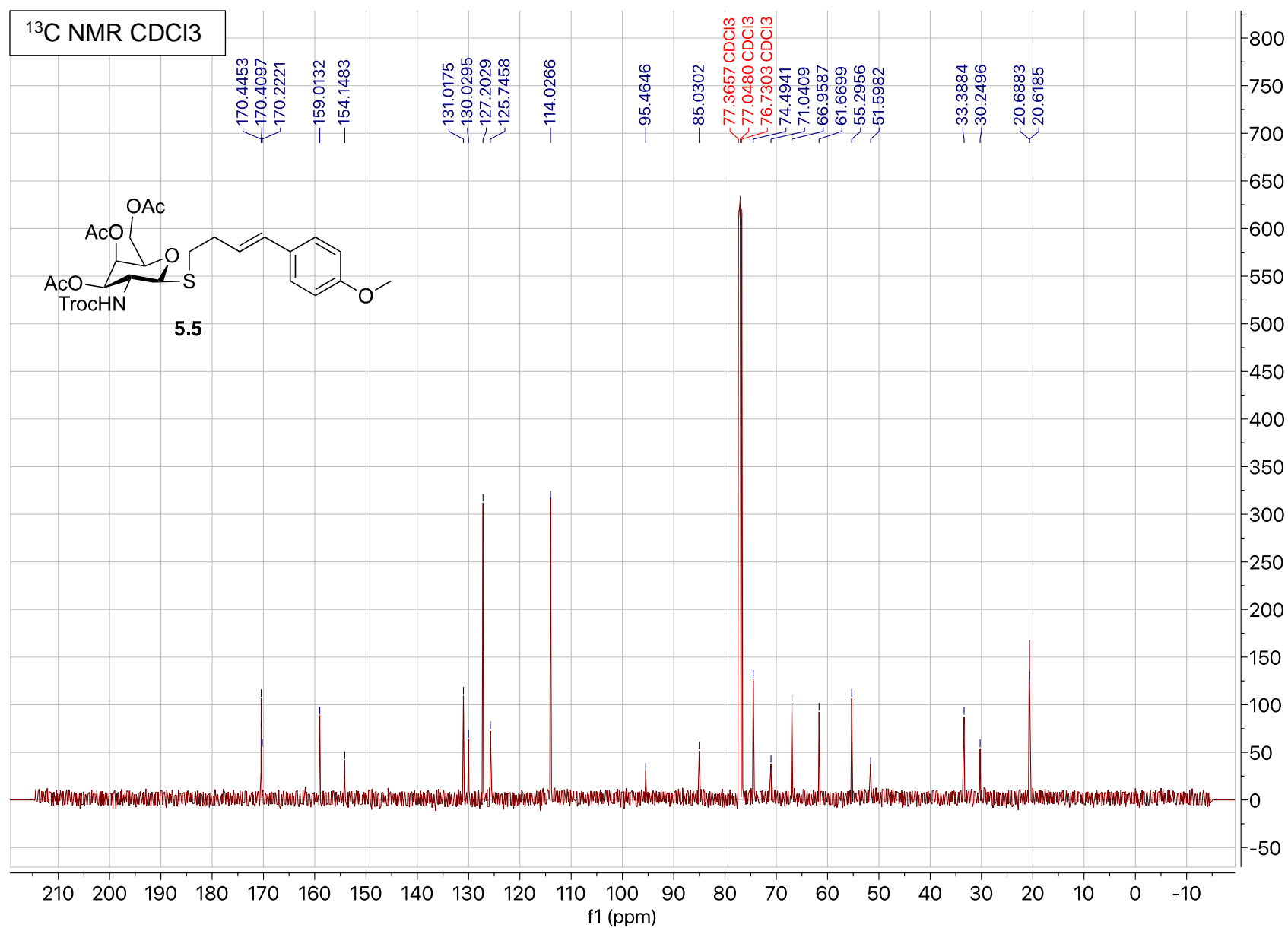


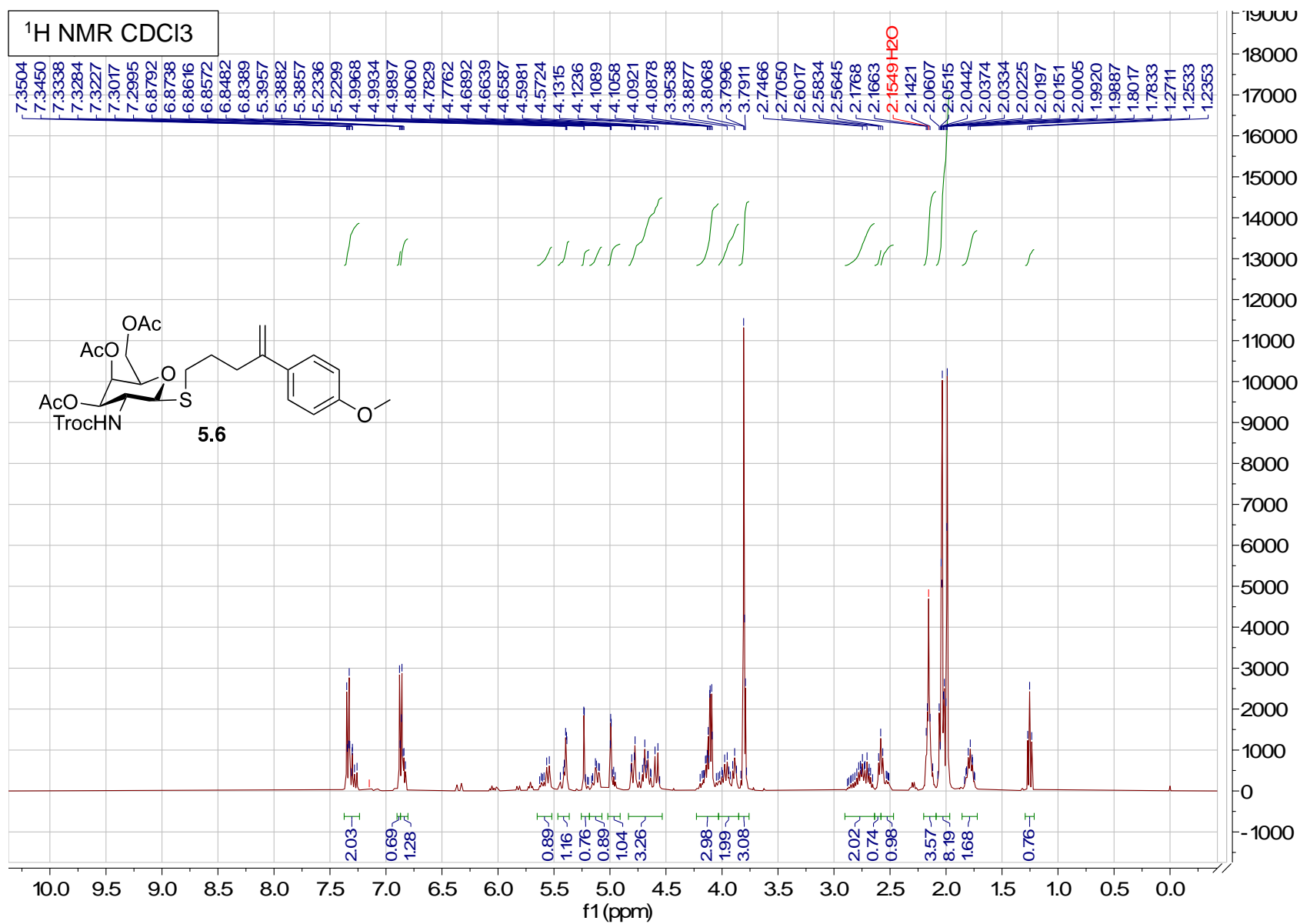
# APPENDIX D. SPECTRAL DATA FOR COMPOUNDS FOUND IN CHAPTER 5



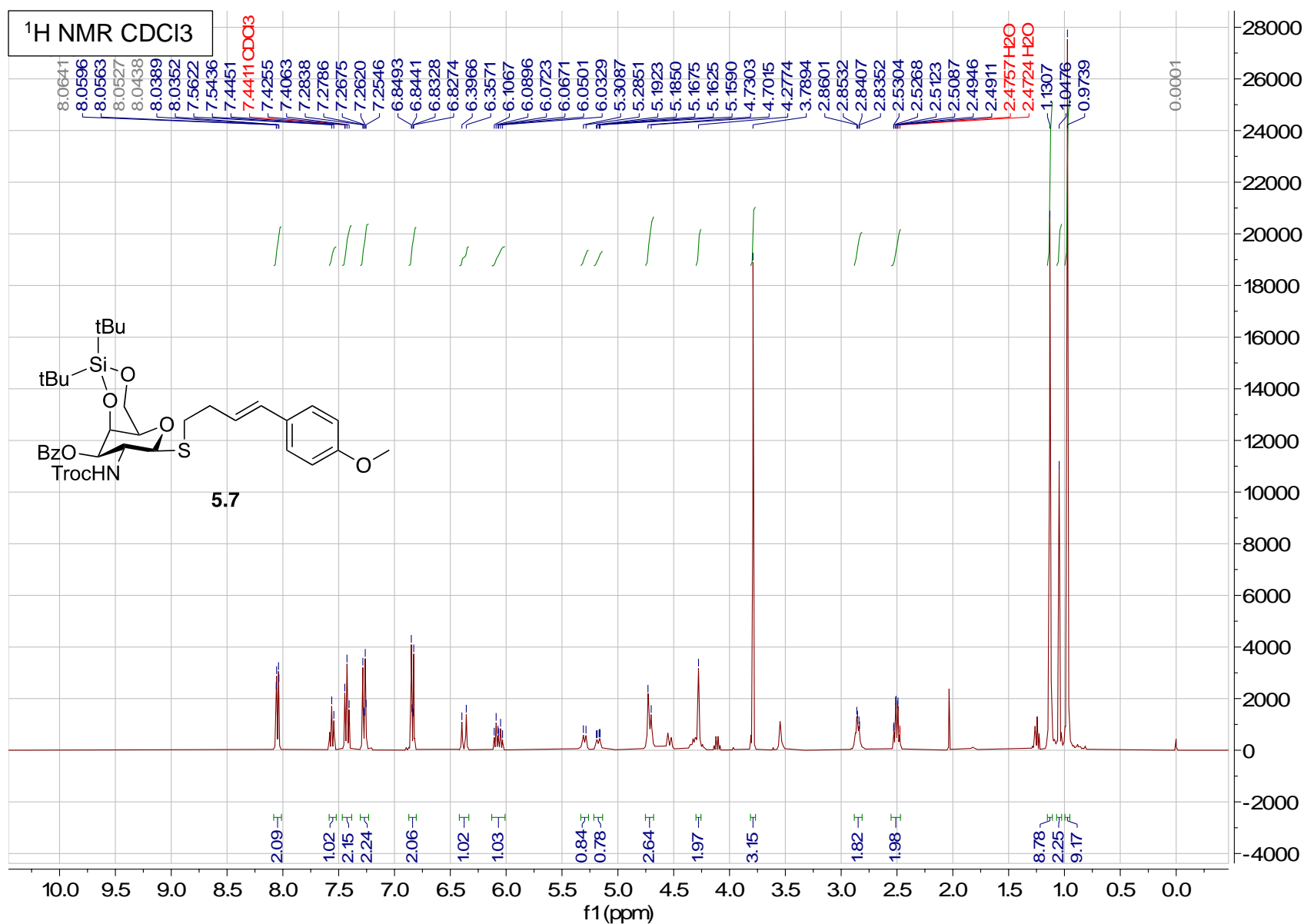


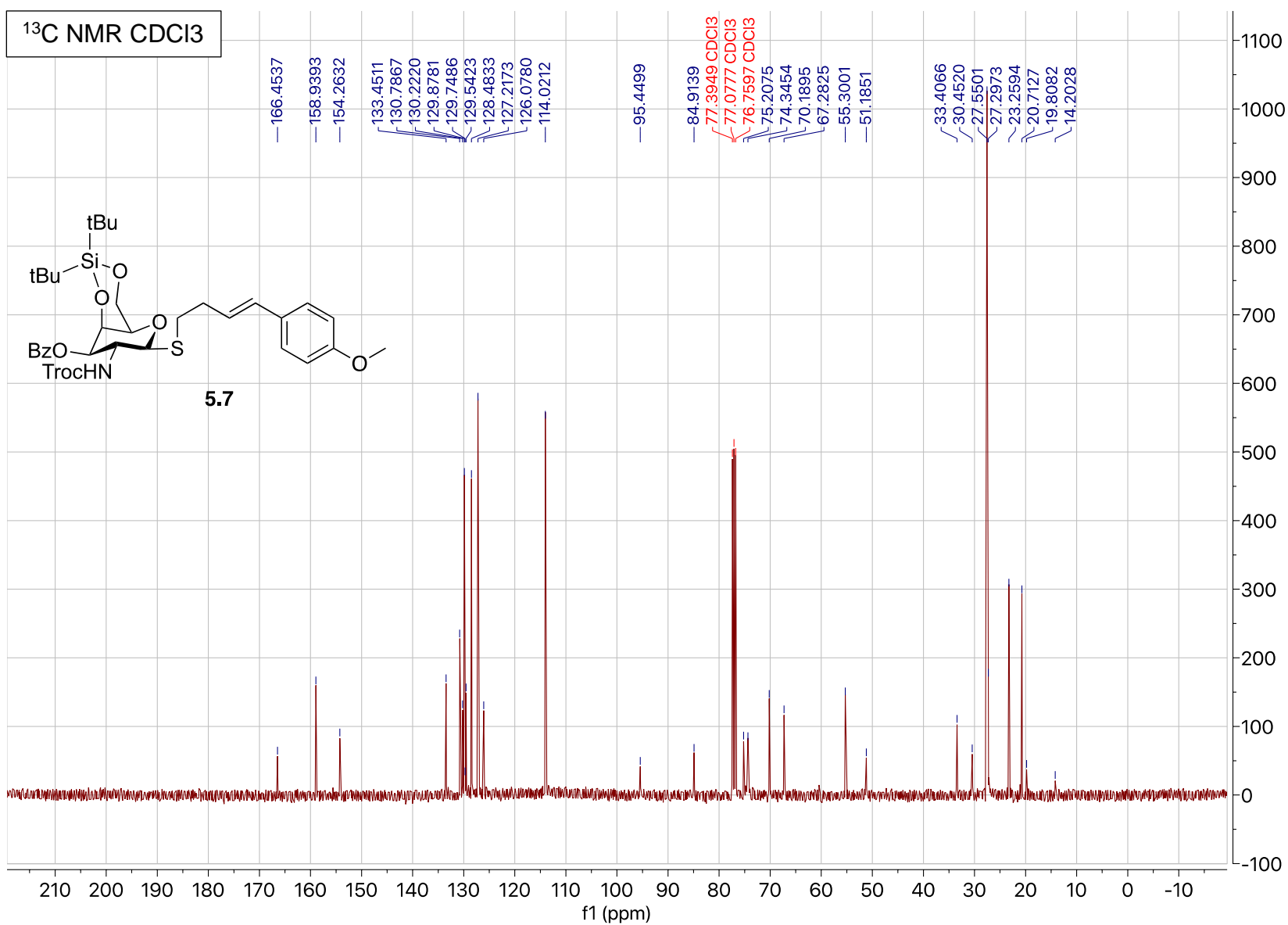


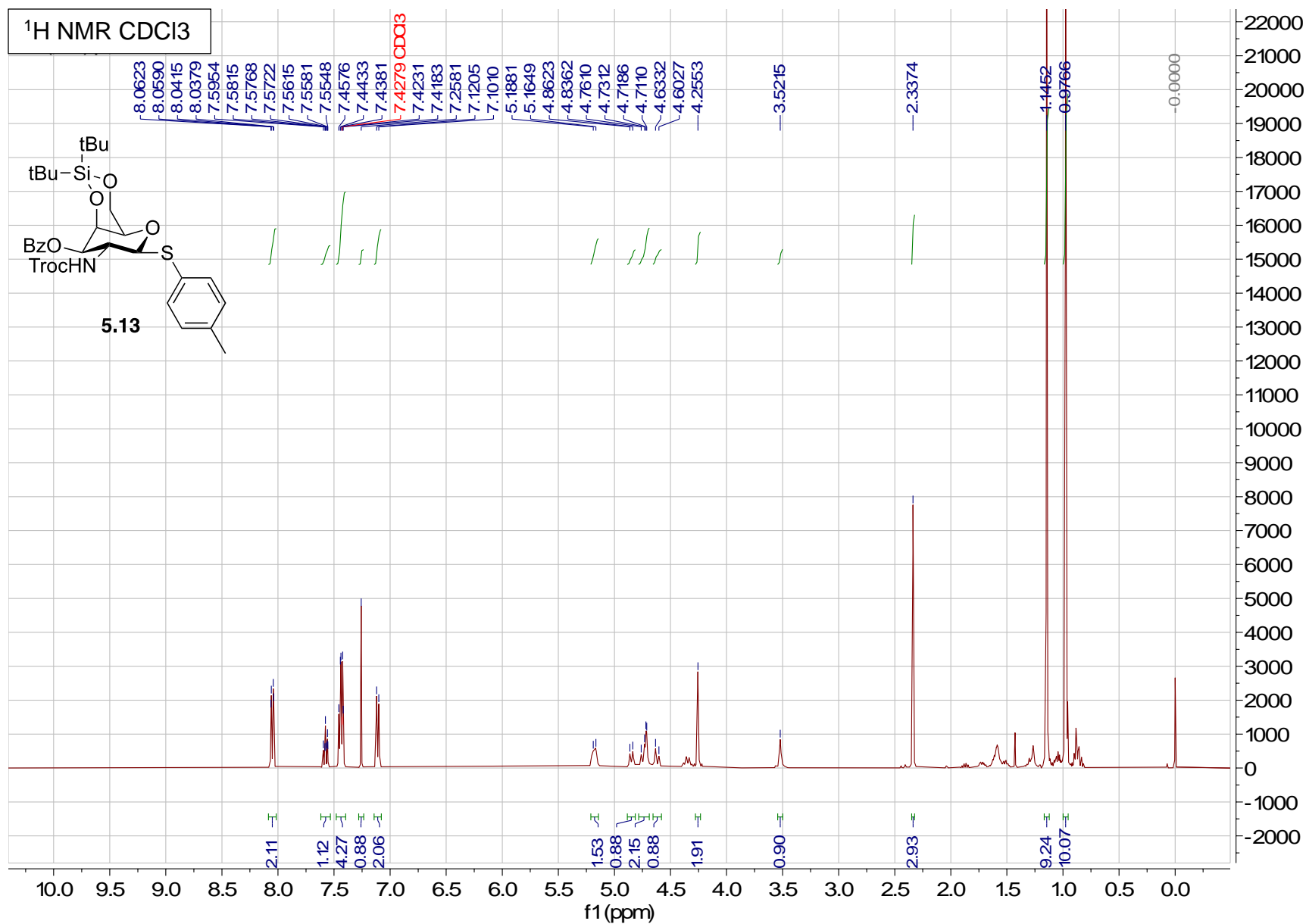


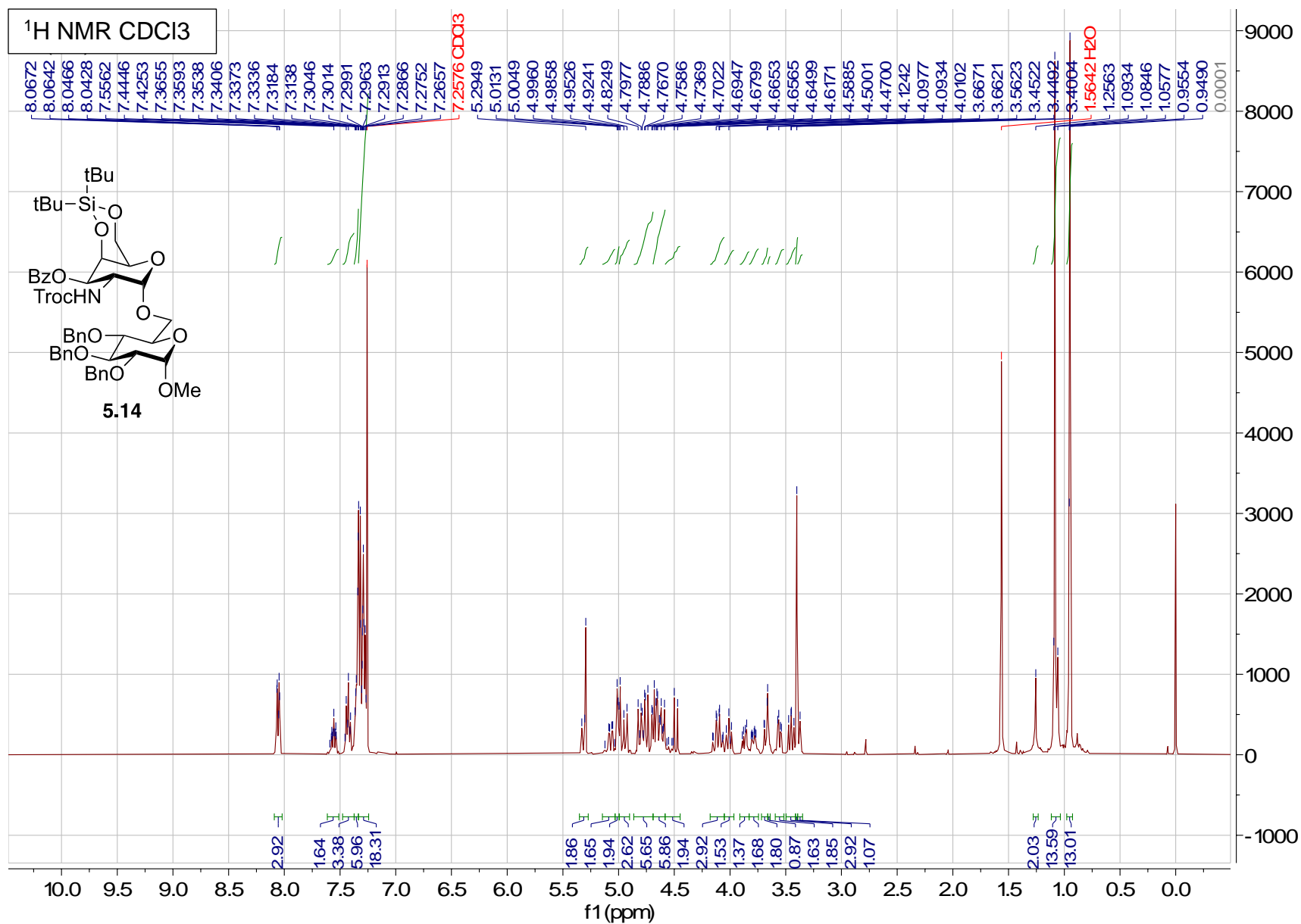


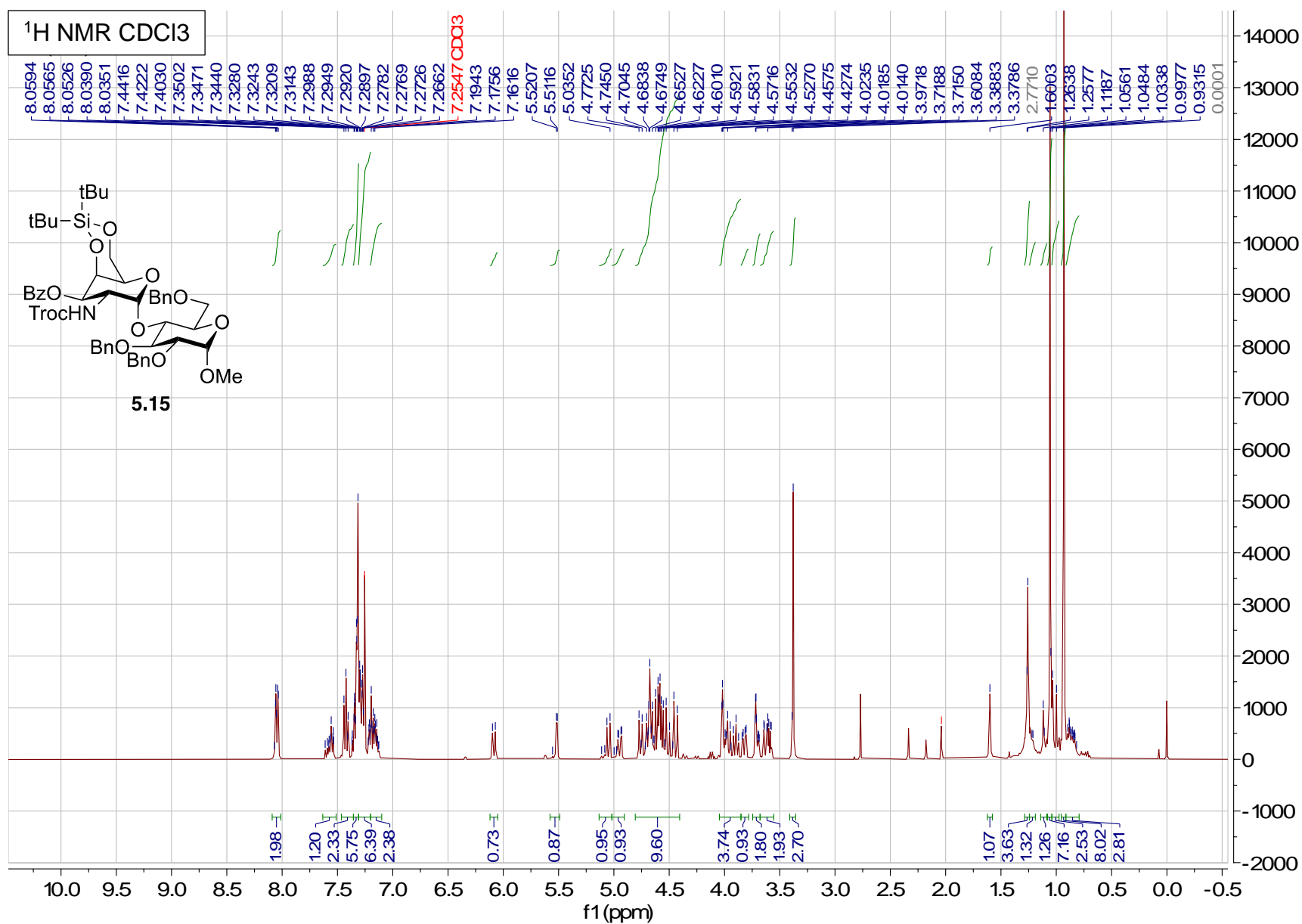


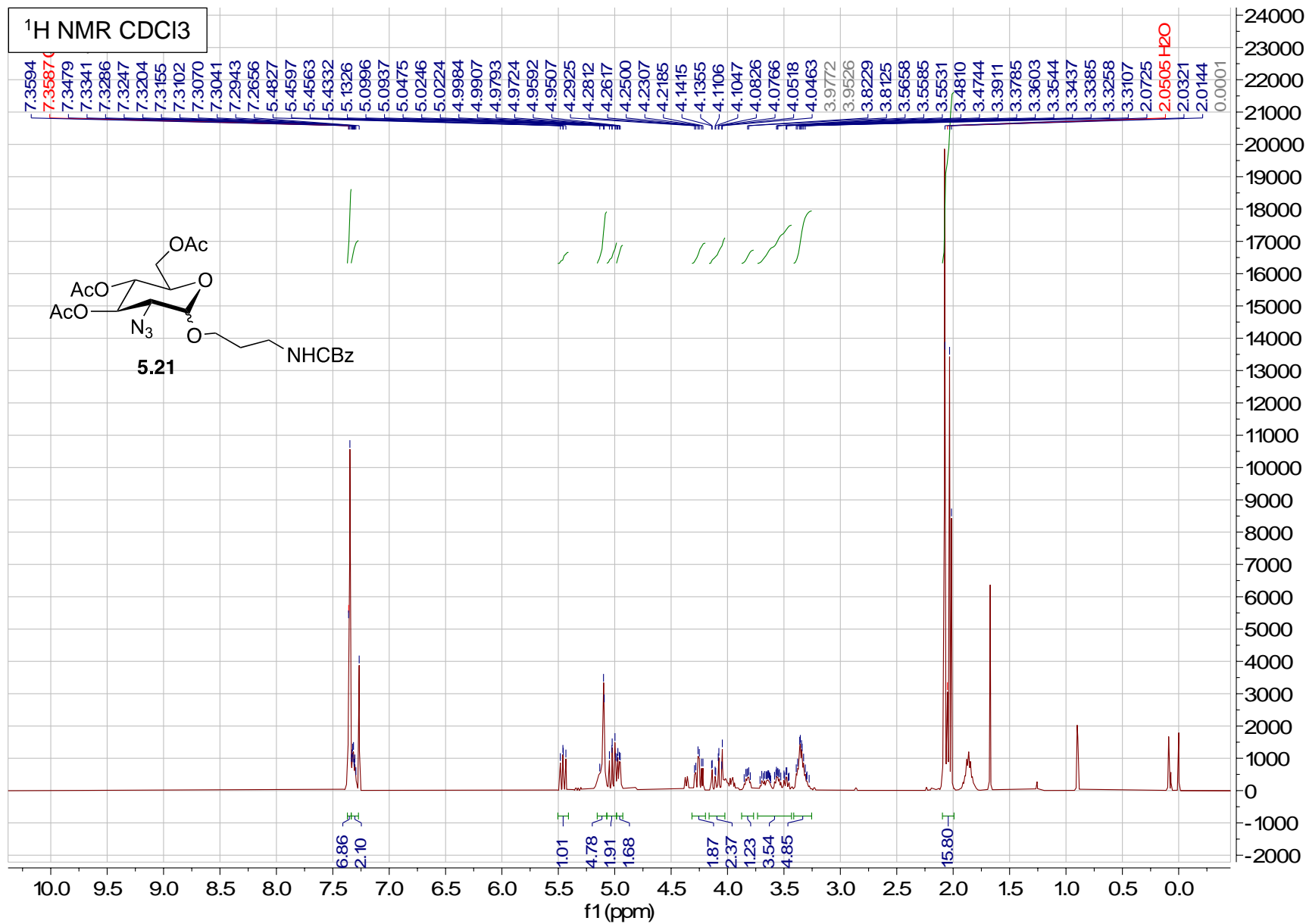


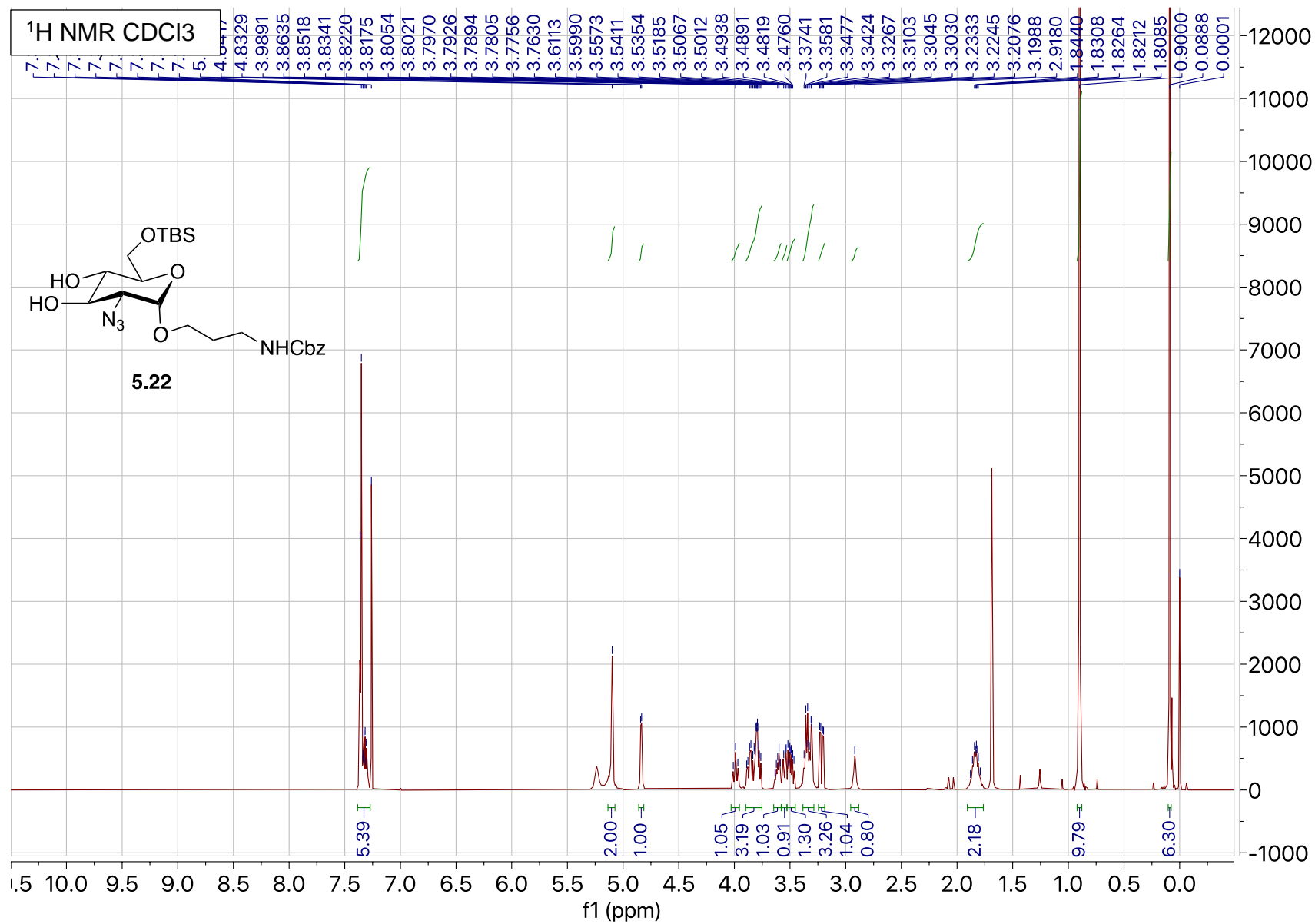


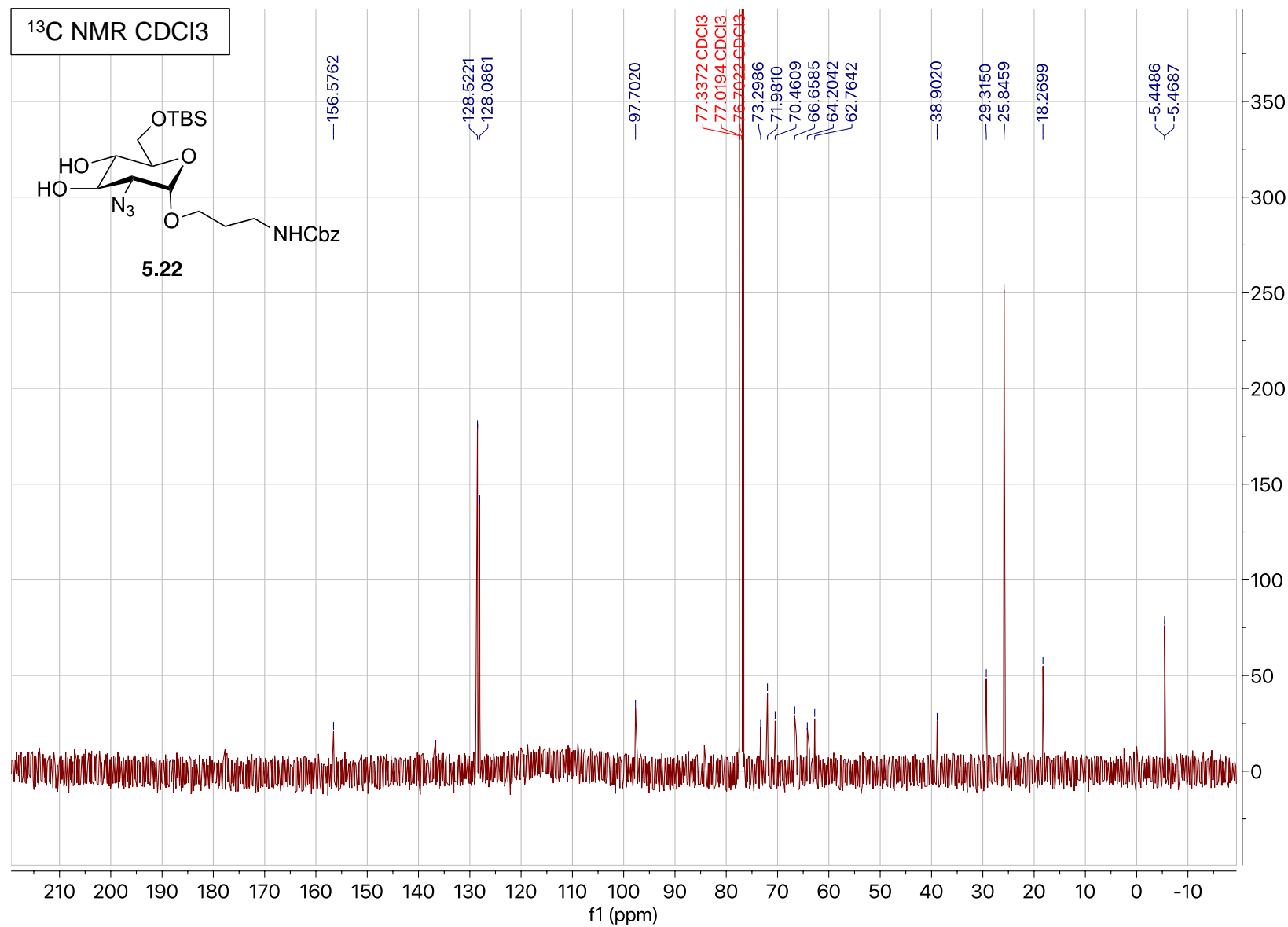




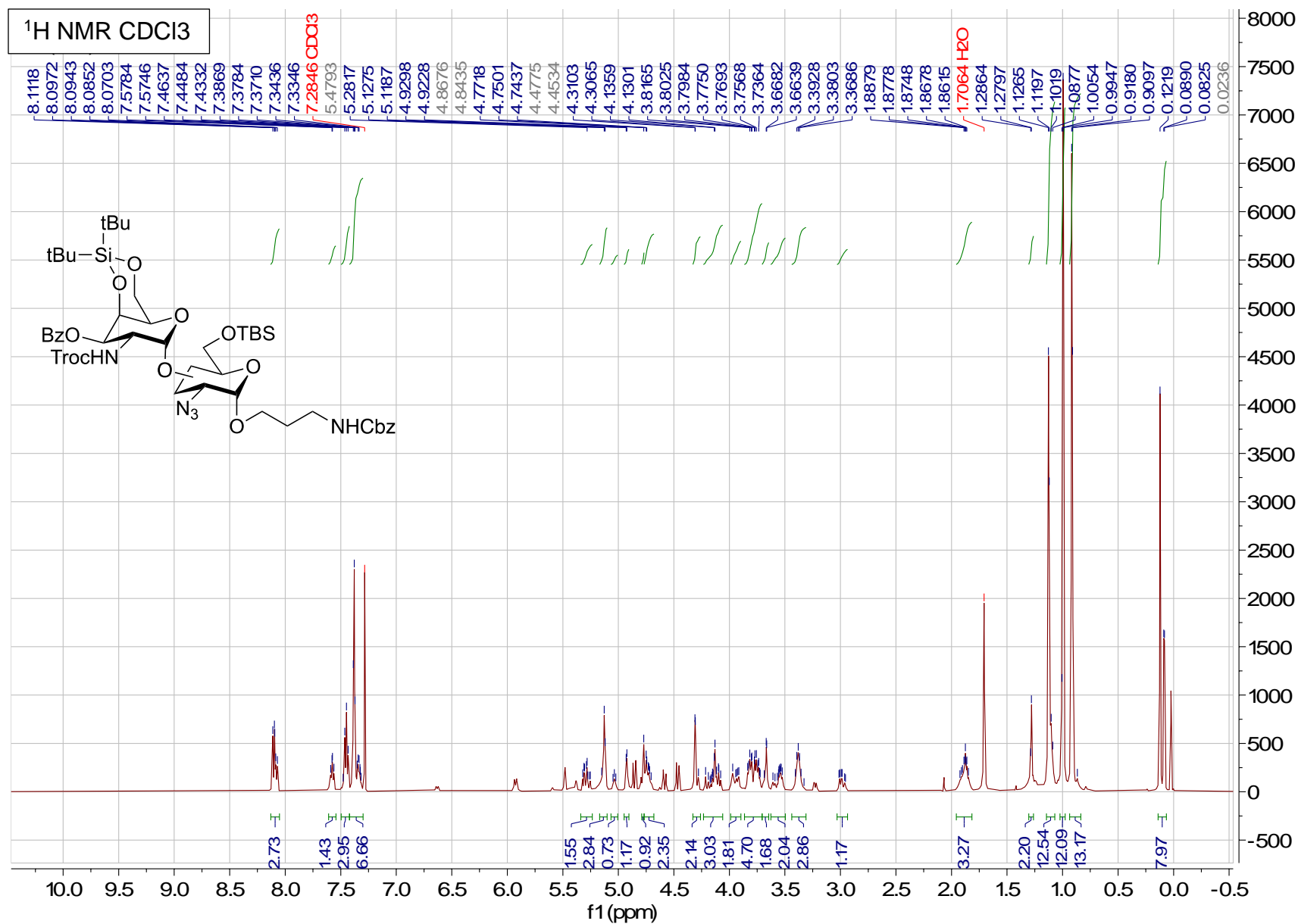


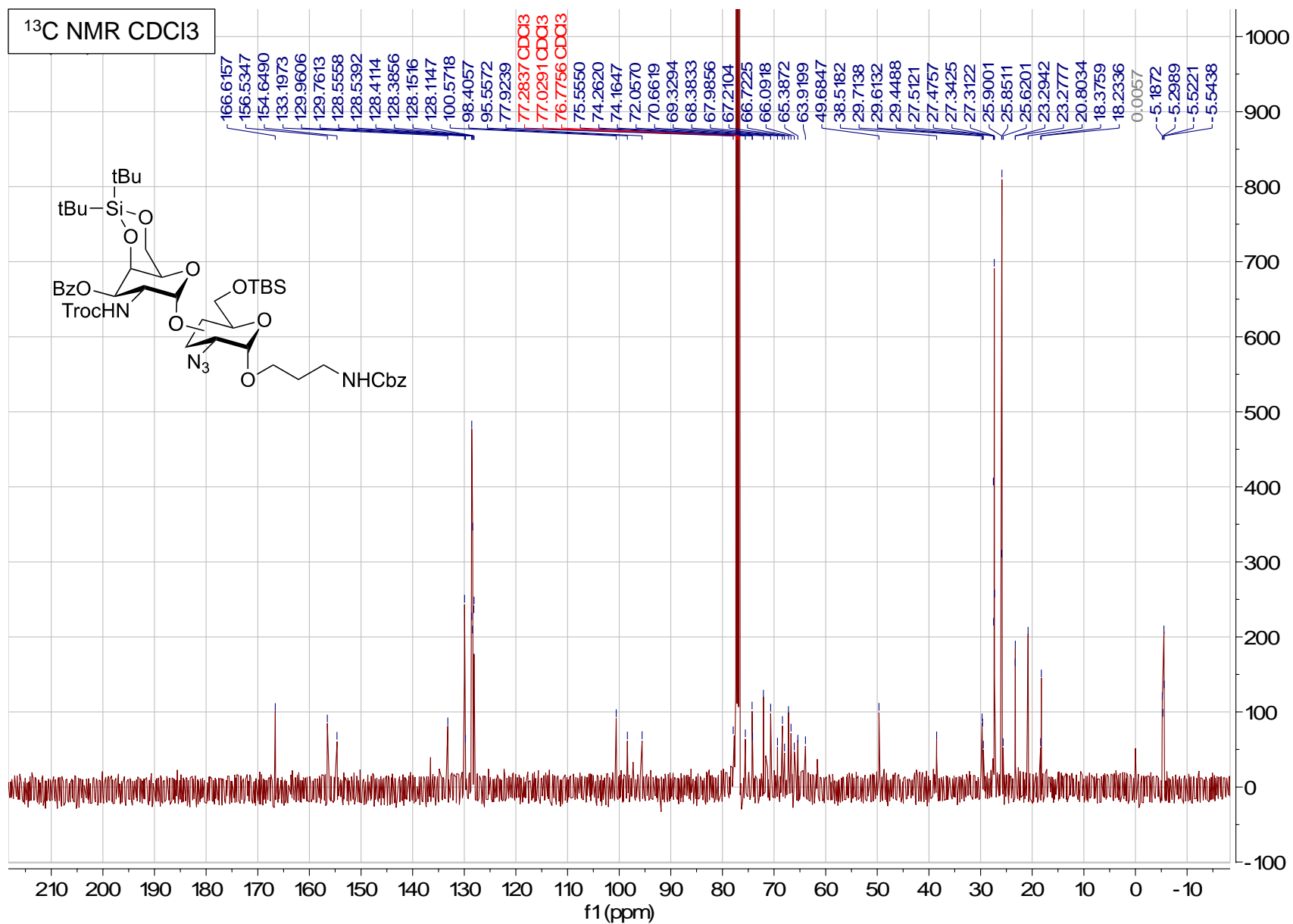


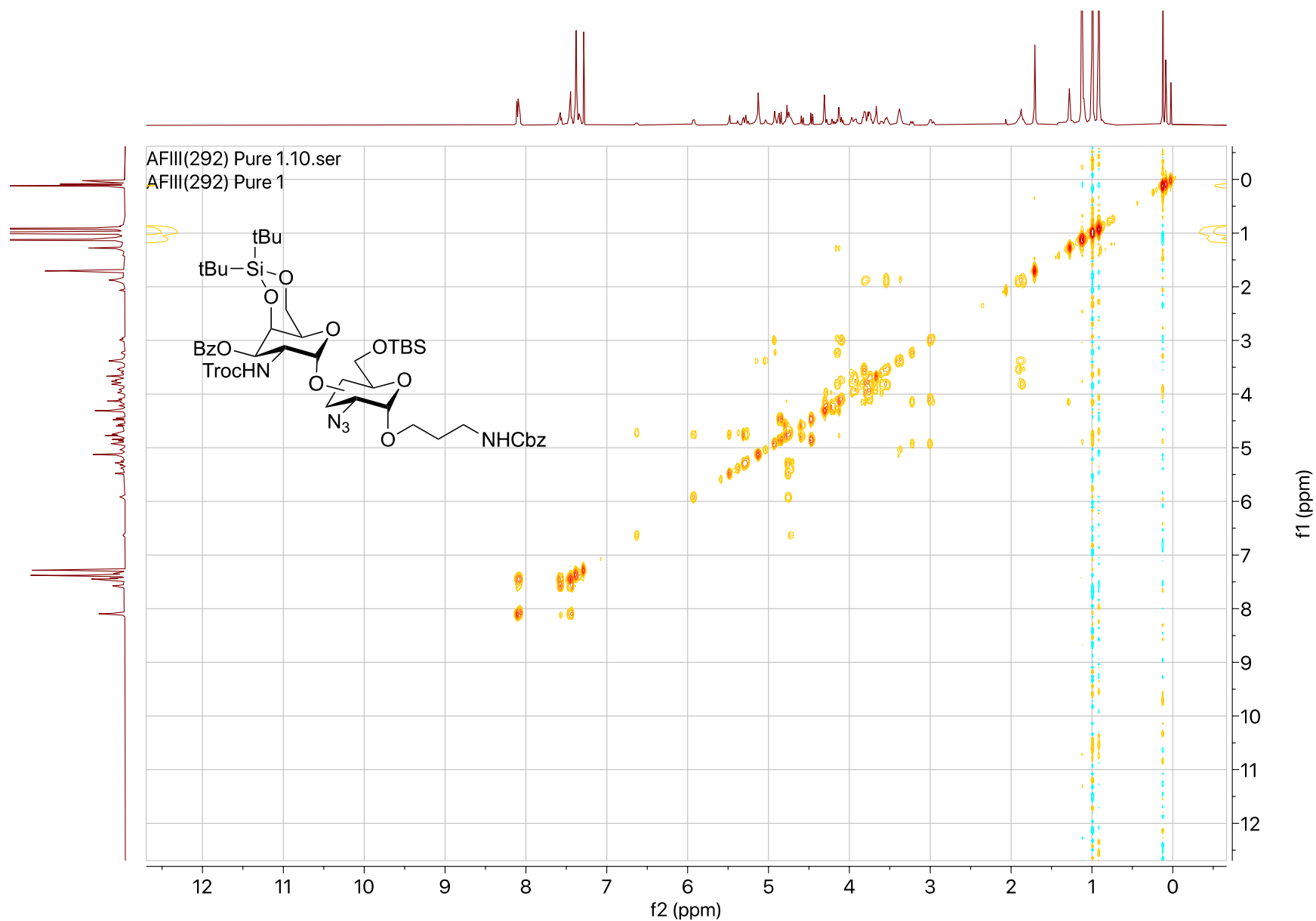


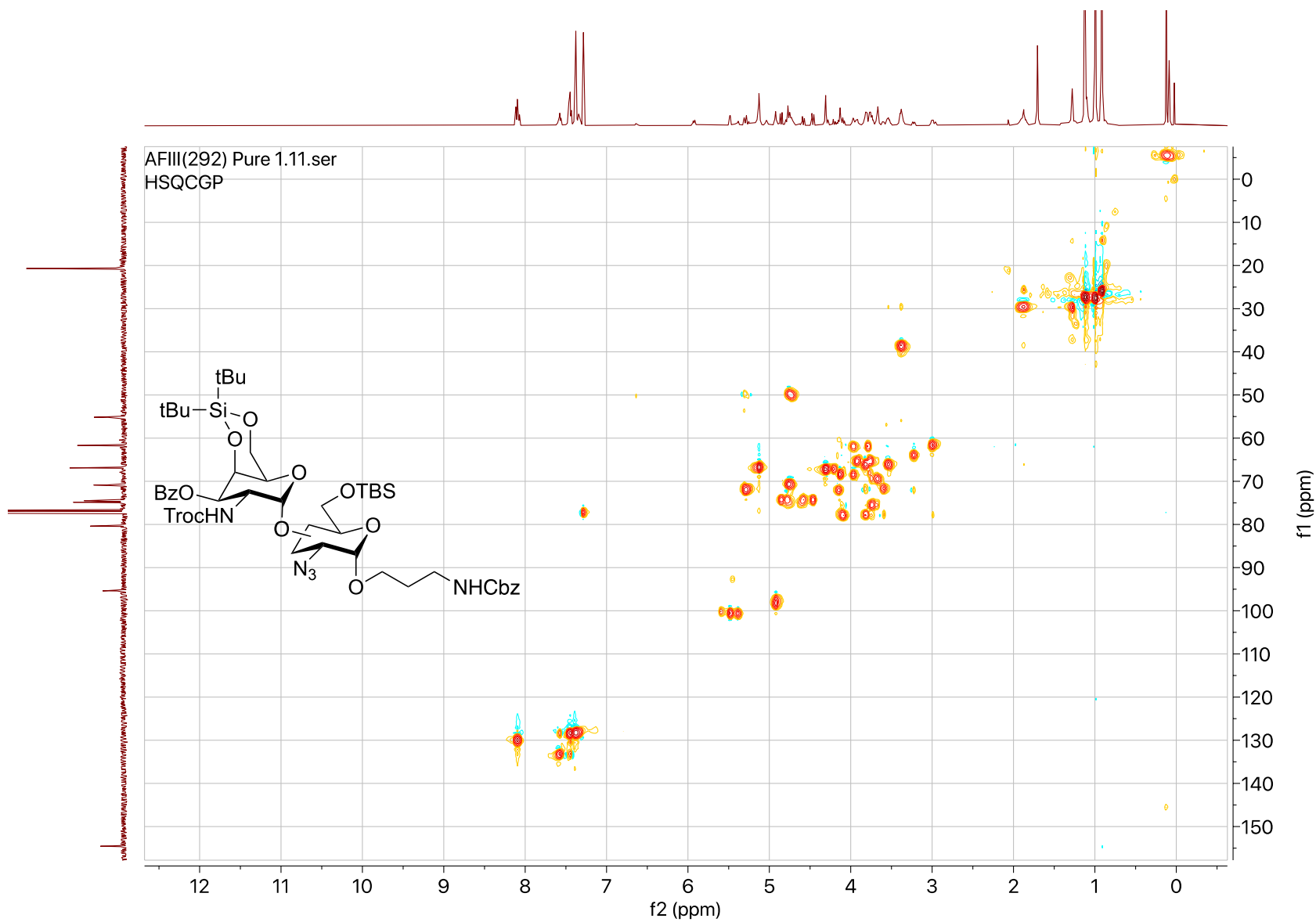


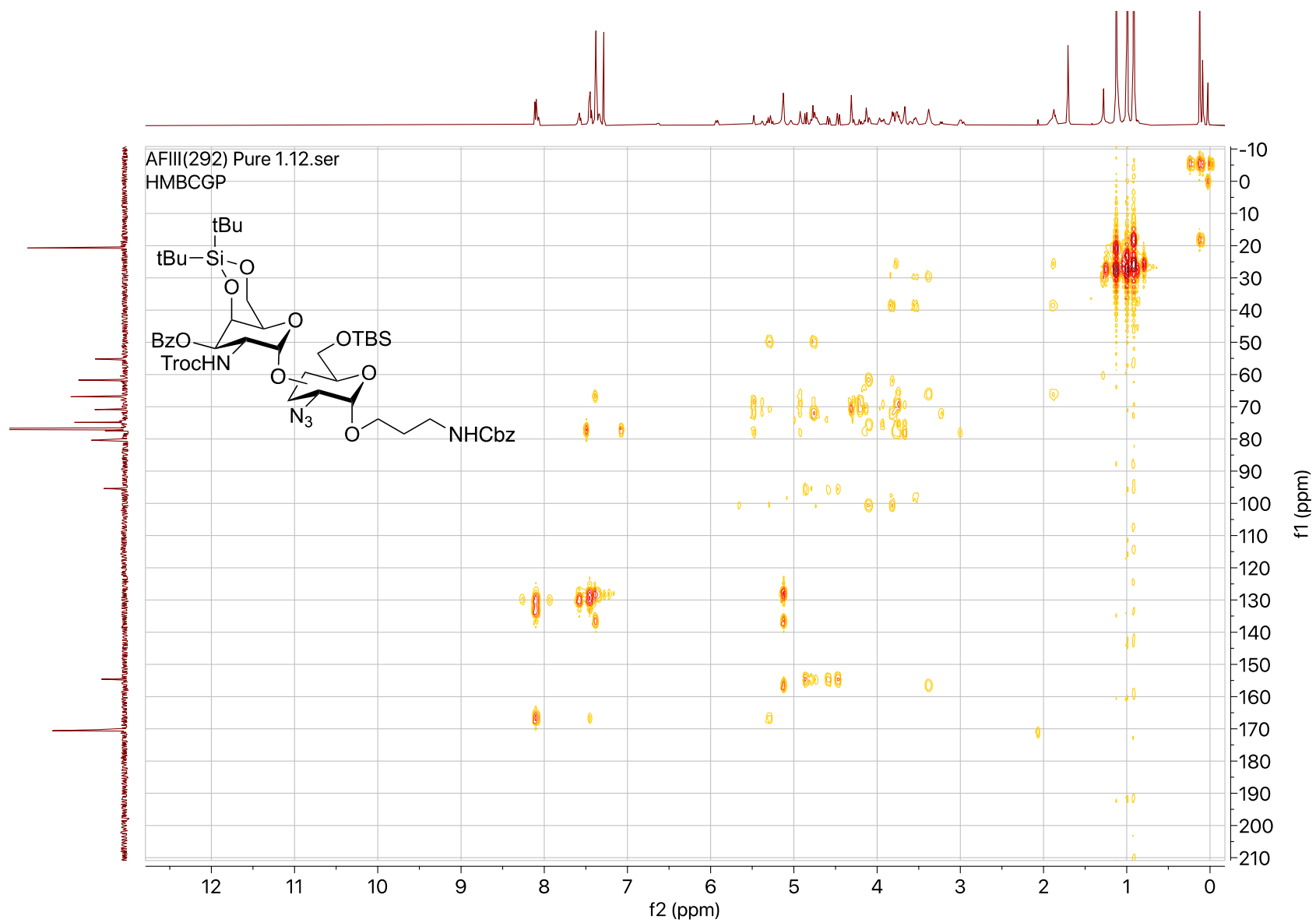












## LIST OF REFERENCES

### Chapter 1 References

1. Belanger, D.; Pinson, J., Electrografting: a powerful method for surface modification. *Chemical Society Reviews* **2011**, 40 (7), 3995-4048.
2. Weitemeyer, C.; Kropac, V.; Priesch, M., Preparation for the adhesive coating of baking tins, cake tins, frying pans, metal pots, and the like. Google Patents: 1981.
3. Schoenfisch, M. H.; Pemberton, J. E., Air stability of alkanethiol self-assembled monolayers on silver and gold surfaces. *Journal of the American Chemical Society* **1998**, 120 (18), 4502-4513.
4. Bandyopadhyay, D.; Prashar, D.; Luk, Y.-Y., Anti-fouling chemistry of chiral monolayers: enhancing biofilm resistance on racemic surface. *Langmuir* **2011**, 27 (10), 6124-6131.
5. Delamar, M.; Combellas, C.; Kanoufi, F. r.; Pinson, J.; Podvorica; ´ de, F. I., Spontaneous grafting of iron surfaces by reduction of aryldiazonium salts in acidic or neutral aqueous solution. *Chem Mater* **2005**, 17, 3968-3975.
6. Chaki, N. K.; Vijayamohanan, K., Self-assembled monolayers as a tunable platform for biosensor applications. *Biosensors and Bioelectronics* **2002**, 17 (1-2), 1-12.
7. Yu, P.; Zhou, H.; Cheng, H.; Qian, Q.; Mao, L., Rational Design and One-Step Formation of Multifunctional Gel Transducer for Simple Fabrication of Integrated Electrochemical Biosensors. *Analytical Chemistry* **2011**, 83 (14), 5715-5720.
8. Bouriga, M.; Chehimi, M. M.; Combellas, C.; Decorse, P.; Kanoufi, F. d. r.; Deronzier, A.; Pinson, J., Sensitized Photografting of Diazonium Salts by Visible Light. *Chemistry of Materials* **2013**, 25 (1), 90-97.
9. Wink, T.; Van Zuilen, S.; Bult, A.; Van Bennekom, W., Self-assembled monolayers for biosensors. *Analyst* **1997**, 122 (4), 43R-50R.
10. Lüssem, B.; Müller-Meskamp, L.; Karthäuser, S.; Waser, R.; Homberger, M.; Simon, U., STM study of mixed alkanethiol/biphenylthiol self-assembled monolayers on Au (111). *Langmuir* **2006**, 22 (7), 3021-3027.
11. Bigelow, W.; Pickett, D.; Zisman, W., Oleophobic monolayers: I. Films adsorbed from solution in non-polar liquids. *Journal of Colloid Science* **1946**, 1 (6), 513-538.
12. Ulman, A., Formation and structure of self-assembled monolayers. *Chemical reviews* **1996**, 96 (4), 1533-1554.

13. Shaw, M. H.; Twilton, J.; MacMillan, D. W., Photoredox catalysis in organic chemistry. *The Journal of organic chemistry* **2016**, *81* (16), 6898-6926.
14. Hermes, S.; Schröder, F.; Chelkowski, R.; Wöll, C.; Fischer, R. A., Selective nucleation and growth of metal- organic open framework thin films on patterned COOH/CF<sub>3</sub>-terminated self-assembled monolayers on Au (111). *Journal of the American Chemical Society* **2005**, *127* (40), 13744-13745.
15. Verberne-Sutton, S. D.; Quarels, R. D.; Zhai, X.; Garno, J. C.; Ragains, J. R., Application of visible light photocatalysis with particle lithography to generate polynitrophenylene nanostructures. *Journal of the American Chemical Society* **2014**, *136* (41), 14438-14444.
16. Elofson, R., The polarographic reduction of diazotized aromatic amines. *Canadian Journal of Chemistry* **1958**, *36* (8), 1207-1210.
17. Senaweera, S. M.; Singh, A.; Weaver, J. D., Photocatalytic hydrodefluorination: facile access to partially fluorinated aromatics. *Journal of the American Chemical Society* **2014**, *136* (8), 3002-3005.
18. Kim, H.; Lee, C., Visible-light-induced photocatalytic reductive transformations of organohalides. *Angewandte Chemie International Edition* **2012**, *51* (49), 12303-12306.
19. Laforgue, A.; Addou, T.; Bélanger, D., Characterization of the deposition of organic molecules at the surface of gold by the electrochemical reduction of aryldiazonium cations. *Langmuir* **2005**, *21* (15), 6855-6865.
20. Wagner, M.; Graham, D.; Ratner, B.; Castner, D. G., Maximizing information obtained from secondary ion mass spectra of organic thin films using multivariate analysis. *Surface Science* **2004**, *570* (1-2), 78-97.
21. Gross, L.; Mohn, F.; Moll, N.; Liljeroth, P.; Meyer, G., The chemical structure of a molecule resolved by atomic force microscopy. *Science* **2009**, *325* (5944), 1110-1114.
22. Smith, R. K.; Lewis, P. A.; Weiss, P. S., Patterning self-assembled monolayers. *Progress in surface science* **2004**, *75* (1-2), 1-68.
23. Gates, B. D.; Xu, Q.; Stewart, M.; Ryan, D.; Willson, C. G.; Whitesides, G. M., New approaches to nanofabrication: molding, printing, and other techniques. *Chemical reviews* **2005**, *105* (4), 1171-1196.
24. Binnig, G.; Quate, C. F.; Gerber, C., Atomic force microscope. *Physical review letters* **1986**, *56* (9), 930.

25. Zhong, Q.; Inniss, D.; Kjoller, K.; Elings, V., Fractured polymer/silica fiber surface studied by tapping mode atomic force microscopy. *Surface Science Letters* **1993**, 290 (1-2), L688-L692.
26. Liu, G.-y.; Salmeron, M. B., Reversible displacement of chemisorbed n-alkanethiol molecules on Au (111) surface: an atomic force microscopy study. *Langmuir* **1994**, 10 (2), 367-370.
27. Rosa, L. G.; Jiang, J.; Lima, O. V.; Xiao, J.; Utreras, E.; Dowben, P. A.; Tan, L., Selective nanoshaving of self-assembled monolayers of 2-(4-pyridylethyl) triethoxysilane. *Materials Letters* **2009**, 63 (12), 961-964.
28. Xiao, X.-D.; Liu, G.-Y.; Charych, D. H.; Salmeron, M., Preparation, structure, and mechanical stability of alkylsilane monolayers on mica. *Langmuir* **1995**, 11 (5), 1600-1604.
29. Wagner, P.; Zaugg, F.; Kernen, P.; Hegner, M.; Semenza, G.,  $\omega$ -functionalized self-assembled monolayers chemisorbed on ultraflat Au (111) surfaces for biological scanning probe microscopy in aqueous buffers. *Journal of Vacuum Science & Technology B: Microelectronics and Nanometer Structures Processing, Measurement, and Phenomena* **1996**, 14 (2), 1466-1471.

## Chapter 2 References

1. Merry, A. H.; Merry, C. L. R., Glycoscience finally comes of age. *EMBO reports* **2005**, 6 (10), 900-903.
2. Sharon, N., Glycoproteins. *Scientific American* **1974**, 230 (5), 78-87.
3. Sears, P. W., C.-H., Enzyme Action Glycoprotein Synthesis. *Cellular and Molecular Life Sciences CMLS* **1998**, 54, 223-252.
4. Li, Y.-T.; Li, S.-C., Biosynthesis and catabolism of glycosphingolipids. In *Advances in carbohydrate chemistry and biochemistry*, Elsevier: 1982; Vol. 40, pp 235-286.
5. Varki, A., Biological roles of oligosaccharides: all of the theories are correct. *Glycobiology* **1993**, 3 (2), 97-130.
6. Koeller, K. M.; Wong, C.-H., Synthesis of complex carbohydrates and glycoconjugates: enzyme-based and programmable one-pot strategies. *Chemical Reviews* **2000**, 100 (12), 4465-4494.
7. Schmidt, R. R., New Methods for the Synthesis of Glycosides and Oligosaccharides—Are There Alternatives to the Koenigs-Knorr Method?[New Synthetic Methods (56)]. *Angewandte Chemie International Edition in English* **1986**, 25 (3), 212-235.



8. Kim, J.-H.; Yang, H.; Park, J.; Boons, G.-J., A General Strategy for Stereoselective Glycosylations. *Journal of the American Chemical Society* **2005**, 127 (34), 12090-12097.
9. Juaristi, E.; Cuevas, G., *The anomeric effect*. CRC press: 1994.
10. Romers, C.; Altona, C.; Buys, H.; Havinga, E., Geometry and conformational properties of some five-and six-membered heterocyclic compounds containing oxygen or sulfur. *Topics in Stereochemistry* **1969**, 39-97.
11. Edward, J. T., Anomeric Effect: How It Came To Be Postulated. ACS Publications: 1993.
12. Walkinshaw, M. D., Variation in the hydrophilicity of hexapyranose sugars explains features of the anomeric effect. *Journal of the Chemical Society, Perkin Transactions 2* **1987**, (12), 1903-1906.
13. Wulff, G.; Röhle, G., Results and problems of O-glycoside synthesis. *Angewandte Chemie International Edition in English* **1974**, 13 (3), 157-170.
14. Demchenko, A.; Stauch, T.; Boons, G.-J., Solvent and other effects on the stereoselectivity of thioglycoside glycosidations. *Synlett* **1997**, 1997, 818-820.
15. Demchenko, A. V., *Handbook of chemical glycosylation: advances in stereoselectivity and therapeutic relevance*. John Wiley & Sons: 2008.
16. Ratcliffe, A. J.; Fraser-Reid, B., Generation of  $\alpha$ -D-glucopyranosylacetonitrilium ions. Concerning the reverse anomeric effect. *Journal of the Chemical Society, Perkin Transactions 1* **1990**, (3), 747-750.
17. Schmidt, R. R.; Behrendt, M.; Toepfer, A., Nitriles as solvents in glycosylation reactions: highly selective  $\beta$ -glycoside synthesis<sup>1</sup>. *Synlett* **1990**, 1990 (11), 694-696.
18. Satoh, H.; Hansen, H. S.; Manabe, S.; van Gunsteren, W. F.; Hünenberger, P. H., Theoretical Investigation of Solvent Effects on Glycosylation Reactions: Stereoselectivity Controlled by Preferential Conformations of the Intermediate Oxacarbenium-Counterion Complex. *Journal of Chemical Theory and Computation* **2010**, 6 (6), 1783-1797.
19. Sasaki, K.; Nagai, H.; Matsumura, S.; Toshima, K., A novel greener glycosidation using an acid-ionic liquid containing a protic acid. *Tetrahedron letters* **2003**, 44 (30), 5605-5608.

20. Van der Vorm, S.; Hansen, T.; Overkleeft, H.; Van der Marel, G.; Codee, J., The influence of acceptor nucleophilicity on the glycosylation reaction mechanism. *Chemical science* **2017**, 8 (3), 1867-1875.
21. Fraser-Reid, B.; Jayaprakash, K.; López, J. C.; Gómez, A.; Uriel, C., *Frontiers in Modern Carbohydrate Chemistry*. **2007**.
22. Goodman, L., Neighboring-group participation in sugars. In *Advances in Carbohydrate Chemistry*, Elsevier: 1967; Vol. 22, pp 109-175.
23. Mootoo, D. R.; Konradsson, P.; Udodong, U.; Fraser-Reid, B., Armed and disarmed n-pentenyl glycosides in saccharide couplings leading to oligosaccharides. *Journal of the American Chemical Society* **1988**, 110 (16), 5583-5584.
24. Pedersen, C. M.; Marinescu, L. G.; Bols, M., Glycosyl donors in "unusual" conformations – influence on reactivity and selectivity. *Comptes Rendus Chimie* **2011**, 14 (1), 17-43.
25. Pedersen, C. M.; Nordstrøm, L. U.; Bols, M., "Super armed" glycosyl donors: Conformational arming of thioglycosides by silylation. *Journal of the American Chemical Society* **2007**, 129 (29), 9222-9235.
26. Haynes, L.; Newth, F., The glycosyl halides and their derivatives. In *Advances in carbohydrate chemistry*, Elsevier: 1955; Vol. 10, pp 207-256.
27. Koenigs, W.; Knorr, E., Ueber einige Derivate des Traubenzuckers und der Galactose. *Berichte der deutschen chemischen Gesellschaft* **1901**, 34 (1), 957-981.
28. Bock, K.; Meldal, M., Mercury iodide as a catalyst in oligosaccharide synthesis. *Acta Chem. Scand. B* **1983**, 37 (9).
29. Paulsen, H., Haworth Memorial Lecture. Synthesis of complex oligosaccharide chains of glycoproteins. *Chemical Society Reviews* **1984**, 13 (1), 15-45.
30. Lemieux, R.; Hendriks, K.; Stick, R.; James, K., Halide ion catalyzed glycosidation reactions. Syntheses of. alpha.-linked disaccharides. *Journal of the American Chemical Society* **1975**, 97 (14), 4056-4062.
31. Gervay-Hague, J., Taming the reactivity of glycosyl iodides to achieve stereoselective glycosidation. *Accounts of chemical research* **2016**, 49 (1), 35-47.
32. van Well, R. M.; Ravindranathan Kartha, K.; Field, R. A., Iodine Promoted Glycosylation with Glycosyl Iodides:  $\alpha$ -Glycoside Synthesis. *Journal of carbohydrate chemistry* **2005**, 24 (4-6), 463-474.

33. Perrie, J. A.; Harding, J. R.; King, C.; Sinnott, D.; Stachulski, A. V., Glycosidation with a disarmed glycosyl iodide: promotion and scope. *Organic letters* **2003**, 5(24), 4545-4548.
34. Mukaiyama, T.; Murai, Y.; Shoda, S.-i., An efficient method for glucosylation of hydroxy compounds using glucopyranosyl fluoride. *Chemistry Letters* **1981**, 10(3), 431-432.
35. Toshima, K., Glycosyl fluorides in glycosidations. *Carbohydrate research* **2000**, 327(1-2), 15-26.
36. Schmidt, R. R.; Michel, J., Facile Synthesis of  $\alpha$ - and  $\beta$ -O-Glycosyl Imidates; Preparation of Glycosides and Disaccharides. *Angewandte Chemie International Edition in English* **1980**, 19(9), 731-732.
37. Schmidt, R. R.; Michel, J., O-( $\alpha$ -D-Glucopyranosyl)trichloroacetimidate as a Glucosyl Donor. *Journal of Carbohydrate Chemistry* **1985**, 4(2), 141-169.
38. Schaubach, R.; Hemberger, J.; Kinzy, W., Tumor-associated antigen synthesis synthesis of the gal- $\alpha$ -(1 $\rightarrow$ 3)-gal- $\beta$ -(1 $\rightarrow$ 4)-GlcNAc epitope a specific determinant for metastatic progression? *Liebigs Annalen der Chemie* **1991**, 1991(7), 607-614.
39. Zimmermann, P.; Sommer, R.; Bär, T.; Schmidt, R. R., Azidosphingosine glycosylation in glycosphingolipid synthesis. *Journal of Carbohydrate Chemistry* **1988**, 7(2), 435-452.
40. Li, Y.; Mo, H.; Lian, G.; Yu, B., Revisit of the phenol O-glycosylation with glycosyl imidates, BF<sub>3</sub>·OEt<sub>2</sub> is a better catalyst than TMSOTf. *Carbohydrate Research* **2012**, 363, 14-22.
41. Adinolfi, M.; Iadonisi, A.; Ravidà, A., Tunable activation of glycosyl trichloro- and (N-phenyl) trifluoroacetimidates with ytterbium (III) triflate: One-pot synthesis of trisaccharides under catalytic conditions. *Synlett* **2006**, 2006(04), 0583-0586.
42. Pornsuriyasak, P.; Demchenko, A. V., Glycosyl thioimidates in a highly convergent one-pot strategy for oligosaccharide synthesis. *Tetrahedron: Asymmetry* **2005**, 16(2), 433-439.
43. Garegg, P. J.; Henrichson, C.; Norberg, T., A reinvestigation of glycosidation reactions using 1-thioglycosides as glycosyl donors and thiophilic cations as promoters. *Carbohydrate Research* **1983**, 116(1), 162-165.
44. Konradsson, P.; Udodong, U. E.; Fraser-Reid, B., Iodonium promoted reactions of disarmed thioglycosides. *Tetrahedron letters* **1990**, 31(30), 4313-4316.
45. Konradsson, P.; Mootoo, D. R.; McDevitt, R. E.; Fraser-Reid, B., Iodonium ion generated in situ from N-iodosuccinimide and trifluoromethanesulphonic acid

- promotes direct linkage of 'disarmed' pent-4-enyl glycosides. *Journal of the Chemical Society, Chemical Communications* **1990**, (3), 270-272.
46. Spell, M.; Wang, X.; Wahba, A. E.; Conner, E.; Ragains, J., An  $\alpha$ -selective, visible light photocatalytic glycosylation of alcohols with selenoglycosides. *Carbohydrate Research* **2013**, 369, 42-47.
  47. Ferrier, R.; Hay, R.; Vethaviyasar, N.] A potentially versatile synthesis of glycosides. *Carbohydrate Research* **1973**, 27 (1), 55-61.
  48. Levy, D. E.; Fügedi, P., *The organic chemistry of sugars*. CRC Press: 2005.
  49. Lönn, H., Glycosylation Using a Thioglycoside and Methyl Trifluoromethanesulfonate. A New and Efficient Method for CIS and Trans Glycoside Formation. *Journal of Carbohydrate Chemistry* **1987**, 6 (2), 301-306.
  50. Amatore, C.; Jutand, A.; Mallet, J.-M.; Meyer, G.; Sinay, P., Electrochemical glycosylation using phenyl S-glycosides. *Journal of the Chemical Society, Chemical Communications* **1990**, (9), 718-719.
  51. Spell, M. L.; Deveau, K.; Bresnahan, C. G.; Bernard, B. L.; Sheffield, W.; Kumar, R.; Ragains, J. R., A Visible-Light-Promoted O-Glycosylation with a Thioglycoside Donor. *Angewandte Chemie International Edition* **2016**, 55 (22), 6515-6519.
  52. Lacey, K. D.; Quarels, R. D.; Du, S.; Fulton, A.; Reid, N. J.; Firesheets, A.; Ragains, J. R., Acid-Catalyzed O-Glycosylation with Stable Thioglycoside Donors. *Organic letters* **2018**, 20 (17), 5181-5185.
  53. Crich, D.; Sun, S., Direct synthesis of  $\beta$ -mannopyranosides by the sulfoxide method. *The Journal of Organic Chemistry* **1997**, 62 (5), 1198-1199.
  54. Crich, D.; Li, L., Stereocontrolled Synthesis of d- and l- $\beta$ -Rhamnopyranosides with 4-O-6-S- $\alpha$ -Cyanobenzylidene-Protected 6-Thiorhamnopyranosyl Thioglycosides. *The Journal of organic chemistry* **2009**, 74 (2), 773-781.

### Chapter 3 References

1. Merry, A. H.; Merry, C. L. R., Glycoscience finally comes of age. *EMBO reports* **2005**, 6 (10), 900-903.
2. Mootoo, D. R.; Konradsson, P.; Udodong, U.; Fraser-Reid, B., Armed and disarmed n-pentenyl glycosides in saccharide couplings leading to oligosaccharides. *Journal of the American Chemical Society* **1988**, 110 (16), 5583-5584.

3. Roy, R.; Andersson, F. O.; Letellier, M., "Active" and "latent" thioglycosyl donors in oligosaccharide synthesis. Application to the synthesis of  $\alpha$ -sialosides. *Tetrahedron letters* **1992**, 33 (41), 6053-6056.
4. Wang, Y.; Ye, X.-S.; Zhang, L.-H., Oligosaccharide assembly by one-pot multi-step strategy. *Organic & biomolecular chemistry* **2007**, 5 (14), 2189-2200.
5. Demchenko, A. V.; De Meo, C., Semi-orthogonality of O-pentenyl and S-ethyl glycosides: application for the oligosaccharide synthesis. *Tetrahedron letters* **2002**, 43 (49), 8819-8822.
6. Kanie, O.; Ito, Y.; Ogawa, T., Orthogonal glycosylation strategy in oligosaccharide synthesis. *Journal of the American Chemical Society* **1994**, 116 (26), 12073-12074.
7. Schaubach, R.; Hemberger, J.; Kinzy, W., Tumor-associated antigen synthesis synthesis of the gal- $\alpha$ -(1 $\rightarrow$ 3)-gal- $\beta$ -(1 $\rightarrow$ 4)-GlcNAc epitope a specific determinant for metastatic progression? *Liebigs Annalen der Chemie* **1991**, 1991 (7), 607-614.
8. Ferrier, R.; Hay, R.; Vethaviasar, N.] A potentially versatile synthesis of glycosides. *Carbohydrate Research* **1973**, 27 (1), 55-61.
9. Lacey, K. D.; Quarels, R. D.; Du, S.; Fulton, A.; Reid, N. J.; Firesheets, A.; Ragains, J. R., Acid-Catalyzed O-Glycosylation with Stable Thioglycoside Donors. *Organic letters* **2018**, 20 (17), 5181-5185.
10. Spell, M.; Wang, X.; Wahba, A. E.; Conner, E.; Ragains, J., An  $\alpha$ -selective, visible light photocatalytic glycosylation of alcohols with selenoglycosides. *Carbohydrate research* **2013**, 369, 42-47.
11. Spell, M. L.; Deveau, K.; Bresnahan, C. G.; Bernard, B. L.; Sheffield, W.; Kumar, R.; Ragains, J. R., A Visible-Light-Promoted O-Glycosylation with a Thioglycoside Donor. *Angewandte Chemie International Edition* **2016**, 55 (22), 6515-6519.
12. Perlman, N.; Livneh, M.; Albeck, A., Epoxidation of peptidyl olefin isosteres. Stereochemical induction effect of chiral centers at four adjacent C $\alpha$  positions. *Tetrahedron* **2000**, 56 (11), 1505-1516.
13. Zeng, X.; Miao, C.; Wang, S.; Xia, C.; Sun, W., Asymmetric 5-endo chloroetherification of homoallylic alcohols toward the synthesis of chiral  $\beta$ -chlorotetrahydrofurans. *Chemical Communications* **2013**, 49 (24), 2418-2420.
14. Grzywacz, P.; Plum, L. A.; Clagett-Dame, M.; DeLuca, H. F., 26-and 27-Methyl groups of 2-substituted, 19-nor-1 $\alpha$ , 25-dihydroxylated vitamin D compounds are essential for calcium mobilization in vivo. *Bioorganic chemistry* **2013**, 47, 9-16.

15. Luo, G.; Lin, L.; Ibrahim, A. S.; Baquir, B.; Pantapalangkoor, P.; Bonomo, R. A.; Doi, Y.; Adams, M. D.; Russo, T. A.; Spellberg, B., Active and passive immunization protects against lethal, extreme drug resistant-Acinetobacter baumannii infection. *PloS one* **2012**, 7 (1), e29446.
16. Schmidt, R. R.; Michel, J., O-( $\alpha$ -D-Glucopyranosyl)trichloroacetimidate as a Glucosyl Donor. *Journal of Carbohydrate Chemistry* **1985**, 4 (2), 141-169.
17. Iversen, T.; Bundle, D. R., Benzyl trichloroacetimidate, a versatile reagent for acid-catalysed benzylation of hydroxy-groups. *Journal of the Chemical Society, Chemical Communications* **1981**, (23), 1240-1241.

#### Chapter 4 References

1. Demchenko, A. V., *Handbook of chemical glycosylation: advances in stereoselectivity and therapeutic relevance*. John Wiley & Sons: 2008.
2. Codée, J. D.; Litjens, R. E.; van den Bos, L. J.; Overkleeft, H. S.; van der Marel, G. A., Thioglycosides in sequential glycosylation strategies. *Chemical Society Reviews* **2005**, 34 (9), 769-782.
3. Nigudkar, S. S.; Demchenko, A. V., Stereocontrolled 1, 2-cis glycosylation as the driving force of progress in synthetic carbohydrate chemistry. *Chemical science* **2015**, 6 (5), 2687-2704.
4. Kim, J.-H.; Yang, H.; Boons, G.-J., Stereoselective Glycosylation Reactions with Chiral Auxiliaries. *Angewandte Chemie International Edition* **2005**, 44 (6), 947-949.
5. Chu, A.-H. A.; Nguyen, S. H.; Sisel, J. A.; Minciunescu, A.; Bennett, C. S., Selective Synthesis of 1,2-cis- $\alpha$ -Glycosides without Directing Groups. Application to Iterative Oligosaccharide Synthesis. *Organic Letters* **2013**, 15 (10), 2566-2569.
6. Geng, Y.; Qin, Q.; Ye, X.-S., Lewis Acids as  $\alpha$ -Directing Additives in Glycosylations by Using 2,3-O-Carbonate-Protected Glucose and Galactose Thioglycoside Donors Based on Preactivation Protocol. *The Journal of Organic Chemistry* **2012**, 77 (12), 5255-5270.
7. Whitfield, D.; Douglas, S., Glycosylation reactions—present status future directions. *Glycoconjugate journal* **1996**, 13 (1), 5-17.
8. Spell, M. L.; Deveau, K.; Bresnahan, C. G.; Bernard, B. L.; Sheffield, W.; Kumar, R.; Ragains, J. R., A Visible-Light-Promoted O-Glycosylation with a Thioglycoside Donor. *Angewandte Chemie International Edition* **2016**, 55 (22), 6515-6519.

9. Lacey, K. D.; Quarels, R. D.; Du, S.; Fulton, A.; Reid, N. J.; Firesheets, A.; Ragains, J. R., Acid-Catalyzed O-Glycosylation with Stable Thioglycoside Donors. *Organic letters* **2018**, 20 (17), 5181-5185.
10. Komarova, B. S.; Orekhova, M. V.; Tsvetkov, Y. E.; Nifantiev, N. E., Is an acyl group at O-3 in glucosyl donors able to control  $\alpha$ -stereoselectivity of glycosylation? The role of conformational mobility and the protecting group at O-6. *Carbohydrate Research* **2014**, 384, 70-86.
11. Wang, L.; Overkleeft, H. S.; van der Marel, G. A.; Codée, J. D., Reagent Controlled stereoselective synthesis of  $\alpha$ -glucans. *Journal of the American Chemical Society* **2018**, 140 (13), 4632-4638.
12. Lu, S. R.; Lai, Y. H.; Chen, J. H.; Liu, C. Y.; Mong, K. K. T., Dimethylformamide: an unusual glycosylation modulator. *Angewandte Chemie International Edition* **2011**, 50 (32), 7315-7320.
13. Park, J.; Kawatkar, S.; Kim, J.-H.; Boons, G.-J., Stereoselective glycosylations of 2-azido-2-deoxy-glucosides using intermediate sulfonium ions. *Organic letters* **2007**, 9 (10), 1959-1962.
14. Pelletier, G.; Zwicker, A.; Allen, C. L.; Schepartz, A.; Miller, S. J., Aqueous glycosylation of unprotected sucrose employing glycosyl fluorides in the presence of calcium ion and trimethylamine. *Journal of the American Chemical Society* **2016**, 138 (9), 3175-3182.

## Chapter 5 References

1. Zarrilli, R.; Casillo, R.; Di Popolo, A.; Tripodi, M.-F.; Bagattini, M.; Cuccurullo, S.; Crivaro, V.; Ragone, E.; Mattei, A.; Galdieri, N., Molecular epidemiology of a clonal outbreak of multidrug-resistant *Acinetobacter baumannii* in a university hospital in Italy. *Clinical Microbiology and Infection* **2007**, 13 (5), 481-489.
2. Huang, W.; Yao, Y.; Long, Q.; Yang, X.; Sun, W.; Liu, C.; Jin, X.; Chu, X.; Chen, B.; Ma, Y., Immunization against multidrug-resistant *Acinetobacter baumannii* effectively protects mice in both pneumonia and sepsis models. *PloS one* **2014**, 9 (6), e100727.
3. Lăzureanu, V.; Poroșnicu, M.; Gândac, C.; Moisil, T.; Bădițoiu, L.; Laza, R.; Musta, V.; Crișan, A.; Marinescu, A.-R., Infection with *Acinetobacter baumannii* in an intensive care unit in the Western part of Romania. *BMC Infectious Diseases* **2016**, 16 (1), 95.
4. Tillery, L. M.; Barrett, K. F.; Dranow, D. M.; Craig, J.; Shek, R.; Chun, I.; Barrett, L. K.; Phan, I. Q.; Subramanian, S.; Abendroth, J., Toward a structome of *Acinetobacter baumannii* drug targets. *Protein Science* **2020**, 29 (3), 789-802.

5. Chen, H.-P.; Chen, T.-L.; Lai, C.-H.; Fung, C.-P.; Wong, W.-W.; Yu, K.-W.; Liu, C.-Y., Predictors of mortality in *Acinetobacter baumannii* bacteremia. *Journal of microbiology, immunology, and infection= Wei mian yu gan ran za zhi* **2005**, *38* (2), 127-136.
6. Lee, N.-Y.; Lee, H.-C.; Ko, N.-Y.; Chang, C.-M.; Shih, H.-I.; Wu, C.-J.; Ko, W.-C., Clinical and economic impact of multidrug resistance in nosocomial *Acinetobacter baumannii* bacteremia. *Infection control and hospital epidemiology* **2007**, *28* (6), 713-719.
7. Russo, T. A.; Beanan, J. M.; Olson, R.; MacDonald, U.; Cox, A. D.; Michael, F. S.; Vinogradov, E. V.; Spellberg, B.; Luke-Marshall, N. R.; Campagnari, A. A., The K1 capsular polysaccharide from *Acinetobacter baumannii* is a potential therapeutic target via passive immunization. *Infection and immunity* **2013**, *81* (3), 915-922.
8. Nie, D.; Hu, Y.; Chen, Z.; Li, M.; Hou, Z.; Luo, X.; Mao, X.; Xue, X., Outer membrane protein A (OmpA) as a potential therapeutic target for *Acinetobacter baumannii* infection. *Journal of Biomedical Science* **2020**, *27* (1), 26.
9. Huang, W.; Wang, S.; Yao, Y.; Xia, Y.; Yang, X.; Long, Q.; Sun, W.; Liu, C.; Li, Y.; Ma, Y., OmpW is a potential target for eliciting protective immunity against *Acinetobacter baumannii* infections. *Vaccine* **2015**, *33* (36), 4479-4485.
10. Saipriya, K.; Swathi, C.; Ratnakar, K.; Sritharan, V., Quorum-sensing system in *Acinetobacter baumannii*: a potential target for new drug development. *Journal of applied microbiology* **2020**, *128* (1), 15-27.
11. McConnell, M. J.; Pachón, J., Active and passive immunization against *Acinetobacter baumannii* using an inactivated whole cell vaccine. *Vaccine* **2010**, *29* (1), 1-5.
12. Bentancor, L. V.; O'Malley, J. M.; Bozkurt-Guzel, C.; Pier, G. B.; Maira-Litrán, T., Poly-N-acetyl- $\beta$ -(1-6)-glucosamine is a target for protective immunity against *Acinetobacter baumannii* infections. *Infection and immunity* **2012**, *80* (2), 651-656.
13. Heumann, D.; Roger, T., Initial responses to endotoxins and Gram-negative bacteria. *Clinica chimica acta* **2002**, *323* (1-2), 59-72.
14. Raetz, C. R. H.; Whitfield, C., Lipopolysaccharide Endotoxins. *Annual Review of Biochemistry* **2002**, *71* (1), 635-700.
15. Wyres, K. L.; Cahill, S. M.; Holt, K. E.; Hall, R. M.; Kenyon, J. J., Identification of *Acinetobacter baumannii* loci for capsular polysaccharide (KL) and lipooligosaccharide outer core (OCL) synthesis in genome assemblies using curated reference databases compatible with Kaptive. *Microbial Genomics* **2020**, *6* (3).



16. Kenyon, J. J.; Holt, K. E.; Pickard, D.; Dougan, G.; Hall, R. M., Insertions in the OCL1 locus of *Acinetobacter baumannii* lead to shortened lipooligosaccharides. *Res Microbiol* **2014**, 165 (6), 472-5.
17. Kenyon, J. J.; Nigro, S. J.; Hall, R. M., Variation in the OC locus of *Acinetobacter baumannii* genomes predicts extensive structural diversity in the lipooligosaccharide. *PLoS One* **2014**, 9 (9), e107833.
18. Vinogradov, E. V.; Duus, J. Ø.; Brade, H.; Holst, O., The structure of the carbohydrate backbone of the lipopolysaccharide from *Acinetobacter baumannii* strain ATCC 19606. *European journal of biochemistry* **2002**, 269 (2), 422-430.
19. Imamura, A.; Kimura, A.; Ando, H.; Ishida, H.; Kiso, M., Extended Applications of Di-tert-butylsilylene-Directed  $\alpha$ -Predominant Galactosylation Compatible with C2-Participating Groups toward the Assembly of Various Glycosides. *Chemistry—A European Journal* **2006**, 12 (34), 8862-8870.
20. Wright, J. A.; Yu, J.; Spencer, J. B., Sequential removal of the benzyl-type protecting groups PMB and NAP by oxidative cleavage using CAN and DDQ. *Tetrahedron Letters* **2001**, 42 (24), 4033-4036.
21. Wrodnigg, T. M.; Lundt, I.; Stütz, A. E., Synthesis of N-Protected Galactosamine Building Blocks from d-Tagatose via the Heyns Rearrangement. *Journal of Carbohydrate Chemistry* **2006**, 25 (1), 33-41.
22. Wang, Z.; Zhou, L.; El-Boubbou, K.; Ye, X.-s.; Huang, X., Multi-Component One-Pot Synthesis of the Tumor-Associated Carbohydrate Antigen Globo-H Based on Preactivation of Thioglycosyl Donors. *The Journal of Organic Chemistry* **2007**, 72 (17), 6409-6420.

## **VITA**

Ashley Fulton was born in Chicago, Illinois but considers herself a Houstonian since living in Houston, Texas from childhood. She attended George Bush High School and graduated in the top 5% of her 2007 class. Ashley attended Xavier University of Louisiana where she graduated with her Bachelors of Science cum laude in May 2011. After taking some time off, Ashley began her studies at Louisiana State University in August 2015. She joined the Ragains' research group in spring of 2016 with her research focusing on oligosaccharide synthesis. While at LSU, Ashley obtained one fellowship, NSF LS-AMP Bridge to the Doctorate, and has published one peer-reviewed manuscript. Currently, Ashley is a PhD Candidate in chemistry. She anticipates graduating with her Doctor of Philosophy from LSU in December 2020.